TECHNISCHE
UNIVERSITÄT
WIEN

VIENNA
UNIVERSITY OF
TECHNOLOGY

Dissertation

Development of Titanium based composites via Powder Metallurgy

ausgeführt zum Zwecke der Erlangung des akademischen Grades eines
Doktors der technischen Wissenschaften unter der Leitung von

Univ.Prof. Dr. Herbert Danninger
E164
Institut für Chemische Technologien und Analytik

eingereicht an der Technischen Universität Wien
Fakultät für Technische Chemie

von

Dipl.-Ing. Isabel Montealegre Meléndez
Matrikelnummer: 0326557
Ziegelofengasse 9/13, 1050 Wien

Wien, 23. März 2009

Danksagung (Agradecimientos)

Besonderer Dank gilt dem FWF, der das Projekt finanziert hat (Projektnummer: P18952-N19).

Ich bedanke mich herzlichst bei meinen Betreuern Dr. Erich Neubauer (ARC), Prof. Herbert Danninger (TU Wien) und Prof. Jose Manuel Torralba (UC3M). Sie haben mich ständig unterstützt und auch in schwierigen Zeiten stets aufgemuntert.

Des Weiteren möchte ich mich bei allen Mitarbeiten aus den Arbeitsbereichen Pulvermetallurgie, Advanced Materials und Aerospace Technologies für ihre Geduld und Hilfe bedanken. Speziellen Dank gilt auch Dr. Rudolf Zauner für die Hilfe vor allem zu Beginn meiner Ausbildung in der Pulvermetallurgie.

Gracias a mis amigos y compañeros de Seibersdorf, aquellos que en su día me animaron y me siguen apoyando en todo momento. Gracias a ellos, estos años de trabajo han sido mucho más llevaderos. Contar con ellos cuando los he necesitado es algo que siempre les agradeceré.

En la Universidad Carlos III de Madrid me he sentido muy bien acogida y arropada por todos. A mi tutor el Profesor Torralba, a todos mis compañeros y amigos les quiero dar también las gracias. Ellos me han soportado y ayudado en todo momento durante mis diversas estancias. Siempre que lo he necesitado, me han echado una mano y, a veces, las dos.

Me siento muy agradecida y afortunada por el ánimo que durante estos años me han ido dando todos mis amigos. Sin ellos no hubiera podido llevar a cabo esta tesis. Cada uno de ellos ha contribuido de una forma especial a que poco a poco haya superado mil y una de las dificultades que se me han presentado en el camino.

Mis padres son los primeros que no han dejado de ayudarme y fortalecerme en ningún momento, al igual que mi hermana. Mi abuela, mis titas y primos han sido otro punto de apoyo para mí durante este tiempo. Ellos me han dado muchas energías y fuerzas, las cuales he necesitado en los momentos difíciles de estos últimos años.

Quien realmente me ha soportado día tras día y a quien le debo este trabajo es a Manu. Gracias por estar siempre ahí y por tu infinita paciencia.

Kurzfassung

Die Nachfrage und auch die Ansprüche an Materialien für verschiedene Anwendungsgebiete wie Raumfahrtindustrie, Biomedizintechnik, Hochbau oder Transport steigen fortwährend. Diese Tatsache ist die treibende Kraft für die Entwicklung von neuen Materialien, die nach den Anforderungen der Anwender hergestellt werden.

Die vorliegende Arbeit zielte auf die Entwicklung von Metal Matrix Composite-Materialien auf der Basis von Titan, d.h. Titanium Metal Matrix Composites (TiMMCs), über pulvermetallurgische Techniken. Die Titan-Pulvermetallurgie ermöglicht die Erzeugung von Bauteilen ohne nennenswerte Materialverluste und ohne den hohen Kostenaufwand, der mit der Verarbeitung von Ti über konventionelle Techniken vom Schmiedemetall verbunden ist, vor allem weegen der sehr schlechten Zerspanbarkeit von Titanwerkstoffen.

Es wurden Titanbasis-Matrices ausgewählt, die mit verschiedenen Materialien - TiB, Nano-Bor, Carbon nanofibers (CNFs) und Nano-Diamanten - verstärkt werden.

Zunächst wurden Ti-basierte Pulver (entweder Rein-Ti oder Titaniumhydride und Ti-6A1-4V) durch Kaltpressen und Sintern konsolidiert und die erhaltenen Körper charakterisiert (Härte, Dichte, Sauerstoff- und Stickstoffgehalt und Mikrostruktur), um das Sinterverhalten zu bewerten und die geeignetsten Pulver für die Erzeugung von TiMMCs auszuwählen. Das erarbeitete Sinterregime brachte saubere, sauerstoff- und stickstoffarme Produkte, sofern die interstitials nicht bereits über die Ausgangspulver eingeschleppt wurden; in diesem Fall kann der Gehalt während der Verarbeitung nicht nennenswert vermindert werden.

Danach wurden aus diesen Pulvern Ti-Basis-Verbundwerkstoffe über Kaltpressen und Sintern sowie zwei weitere Konsolidierungsmethoden (Konventionelles Axialheißpressen und Induktivheißpressen) hergestellt. Die Probekörper wurden wie oben beschrieben charakterisiert; in einigen Fällen wurden auch Zug- bzw. Biegeversuche durchgeführt und die Bruchflächen fraktographisch untersucht.

Die Versuche zeigten, dass der Zusatz von Verstärkungsphasen die Verdichtung im allgemeinen behindert, d.h. in den MMCs verbleibt mehr Restporosität als in den monolithischen Matrixwerkstoffen. Zusatz von Nanobor mit Konsolidierung durch Heißpressen ergab z.T. überraschend gute, aber nicht eindeutig erklärbare mechanische Eigenschaften. Bei den CNFs erwies sich die Dispergierung als gravierendes Problem; bei allen Nanophasen ist die lokale Anreicherung an den ursprünglichen Partikelgrenzen ein Hindernis. Hier wäre die Verwendung entsprechend feiner Matrixpulver vorteilhaft, die aber wiederum mehr Sauerstoff einbringen würden. Die Reaktion der Verstärkungsphasen, vor allem CNFs und Nanodiamanten, war außer beim

Hochtemperatursintern im Bereich 1200-1300°C kein Problem; im genannten Fall bildeten sich TiC-Phasen, die zwar ebenfalls verstärkend wirken, für die aber sehr viel kostengünstigere C-Träger verwendet werden können. Wenn die Konsolidierungstemperatur unter 920°C gehalten wird, bleiben die Verstärkungsphasen erhalten.

Insgesamt zeigte sich, dass wie generell in der Ti-Pulvermetallurgie, der Schlüssel zur Herstellung von Ti-MMCs in der Verfügbarkeit entsprechend hochwertiger, d.h. feiner und gleichzeitig chemisch reiner, Titanpulver liegt.

Abstract

Nowadays the demands and requirements in the aerospace, biomedical, structural and transport industry, etc. to materials are increasing. This fact is closely related to the development of new materials which are conceived to present outstanding properties and to achieve the needs required for the final user.

The research into new materials in this work is focused on the development of metal matrix composite materials, in particular titanium metal matrix composite (TiMMCs). Here, powder metallurgy (PM) offers the possibility of creating net-shape parts without the material loss and cost associated with machining intricate components from wrought stock material, Ti being notoriously difficult to machine.

This work is centred on the search for suitable titanium based metal matrices which are reinforced by different materials (boron and carbon based reinforcements).

Firstly, different titanium based powders (either pure titanium or titanium hydride and Ti-6Al-4V) were consolidated as metal matrix via cold pressing and sintering. In order to study the sintering behaviour of these materials and to select several of them for the fabrication of TiMMCs, a characterisation of all of them took place, involving measurements of hardness, density, oxygen content and microstructural analysis.

Secondly, after the selection of the most adequate matrix powders, the conventional cold pressing and sintering process in addition to two hot consolidation methods (Conventional Hot Pressing and Inductive Hot Pressing) were employed for the manufacturing of the composites. After their fabrication, a rigorous characterisation took place. Next, several comparisons of the obtained results were carried out.

The aim of this work, i.e. fabrication via PM of new TiMMCs improving the properties of the pure metal matrices, was not totally achieved because the reinforcement material in general did not improve the mechanical properties. There was a marked decrease of densification at higher reinforcement contenst (i.e. 20 mass% of TiB_2). The incorporation of interstitials into the titanium based matrix from the reinforcement material was observed for the boron based reinforcements (10 mass% of oxygen in nano-boron particles). The carbonaceous reinforcement, in particular CNFs, was not effective because its dispersion in the titanium based matrix was not optimal. On another side, nano-diamond particles at high concentration caused the effect of particle boundary decoration; it might be avoided using finer starting matrix powders. Additionally, admixed nano-diamonds reacted with the titanium of the matrix at higher sintering temperatures. For that reason the more suitable processing for this reinforcement is hot pressing below 900ºC.

Generally, it was confirmed that for Ti MMCs, as with Ti PM as a whole, the key to success is the availablility of high quality, i.e. fine and chemically pure, matrix powders.

Resumen

En la actualidad, las demandas y los requisitos exigidos por diferentes sectores de aplicación como el aeroespacial, el biomédico, el estructural y la industria del transporten están en aumento. Este hecho está my relacionado con el desarrollo de nuevos materiales, los cuales son concebidos para presentar excelentes propiedades y alcanzar las necesidades del usuario final.

La investigación de nuevos materiales en este trabajo está focalizada en el desarrollo de materiales compuestos de matriz metálica, en particular material compuesto de matriz de titanio (TiMMCs). Además, la pulvimetalurgia de titanio (PM) ofrece la posibilidad de crear componentes “near net shape”, esto es, próximos a su forma final, sin perdida de material ni coste de mecanizado asociados.

Este trabajo se centra en la búsqueda de matrices metálicas adecuadas de base titanio, las cuales se reforzarán con diferentes materiales (materiales de refuerzo base boro y carbono). En primer lugar, distintos polvos de titanio como base (titanio puro CPTi, e hidruro de titanio TiH2) fueron consolidados como matrices metálicas via compactación uniaxial en frío y sinterización. Para estudiar las propiedades y comportamiento de sinterización de estos materiales y con el fin de seleccionar alguno de ellos para la fabricación de materiales metálicos de titanio reforzado, la caracterización de todos ellos tuvo lugar a través de medidas de dureza, densidad, contenido de oxigeno y el estudio de su microestructuras. En segundo lugar, tras la selección de los polvos para la matriz más adecuados, se emplearon para la fabricación de los materiales compuestos los métodos de compactación uniaxial en frío y sinterizado, además de las dos técnicas de consolidación en caliente, convencional e inductiva. A continuación, todas las muestras fueron rigurosamente caracterizadas.

En resumen, el fin de este trabajo es la fabricación, a través de técnicas pulvimetalurgicas, de nuevos materiales compuestos de matriz metálica de titanio reforzados, mejorando sus propiedades respecto a la matriz metálica pura y evaluando las influencias de algunos factores como el polvo de partida, tipo de material de refuerzo y parámetros del procesado. Este objetivo no fue totalmente alcanzado ya que los materiales de refuerzo no mejoraron las propiedades mecánicas. El estudio del comportamiento de distintos materiales compuestos mostró una acusada disminución de la densificación del material a altas concentraciones de refuerzo (20 % en masa de TiB2). La incorporación de diversas impurezas del material de refuerzo a la matriz de titanio, se observó para los materiales de refuerzo base boro (10 % en masa de oxigeno en las nano-partículas de boro). Los refuerzos carbonosos, en particular las nano-fibras de carbono (CNFs) no fueron adecuados como material de refuerzo debido a que su dispersión en la matriz de titanio no fue óptima. Por otro lado, las nano-partículas de diamante a altas concentraciones originaron el fenómeno de “decoración en borde de

grano”; el cual se podría haber evitado mediante el uso de polvos de partida mas finos. Además, a altas temperaturas de sinterización, los nano-diamantes reaccionaron con la matriz de titanio. Por esta razón, para este tipo de refuerzo el procedimiento de procesado más adecuado es compactación en caliente por debajo de 900ºC.

En general, fue conformado que para Ti MMCs, como con Ti PM, la calve para alcanzar resultados exitosos, es la disponibilidad de alta cualidad, fineza y pureza química del polvo de matriz.

Contents

Preface

This work is intended for obtaining knowledge about the titanium and titanium composites, and the manufacturing process of powder metallurgy used to fabricate these interesting materials.

The Chapter 1 will deal with a general overview about the properties of titanium and its alloys, also a brief description of metal matrix composites and several manufacturing processes for them. In particular the fabrication route of powder metallurgy will be described in more detail in this part. Here, an overview of titanium as metal matrix and the different reinforcement materials used will be carried out. Moreover, the description of possible fabrication routes for the manufacturing of TiMMCs will be presented in this section of the work.

In the Chapter 2 the investigated powder metallurgical fabrication routes will be presented. Furthermore in the Chapter 2, the characterization techniques used for the study of the starting materials and for the specimens will be described.

The starting materials used in this work will be reported in the Chapter 3. The results of the characterization of all the starting materials will be presented.

The Chapter 4 will summarize the experimental work. The description of each test will be carried out in this chapter. Additionally the results obtained after the characterization of the produced specimens will be reported in this chapter.

The summary will be presented in the Chapter 5. Finally, in the Chapter 6 the general conclusions will be listed.

Motivation of this work

There has been a growing interest in MMCs for use in the automotive industries, aerospace, and other structural applications over the past 25 years as a result of several processing routes being developed and due to the availability of reinforcements. Additionally the attractive properties that titanium and its alloy (Ti6Al4V) offer as metal matrix for the composite manufacturing industry are widely known. The combination of these interesting properties and the advantages of the powder metallurgical process are the starting point of this work.

The motivation of this work is the fabrication of different titanium based composites through powder metallurgical processes, i.e. cold pressing and sintering, and hot pressing technique (conventional and inductive HP) in order to improve the final properties of the specimens for demanding applications.

Objectives

The major objective of this research work is the development of TiMMCs via Powder Metallurgy (PM) in order to achieve new and interesting materials which present attractive and suitable properties applicable to the sectors of aerospace, biomedical and transport industries.

Moreover, the evaluation of the sintering behaviour of titanium based powder materials is considered an important aspect which is described in the first part of the experimental part of the work. Also in this first section, the effect of the starting materials (impurities, particle size, etc.) on the final properties of the specimens is carefully examined in order to carry out the selection of the starting matrix powders for the manufacturing of the TiMMCs.

Furthermore, the determination of suitable processing parameters depending on the powder metallurgy methods (cold pressing and sintering, and two hot consolidation processes) employed will be another interesting topic to be studied. Thus, considering the results obtained after the characterisation of the compacts, the evaluation of the influence of the process parameters can be carried out.

The characterisation of the titanium based composite (matrices from CPTi, TiH_2 and Ti6Al4V), including density and hardness measurements, microstructural studies in addition to chemical analysis and mechanical properties will be carried out; their results being a important contribution to the objectives of this research work.

Development of the work

The present work can be explained and summarised through the following Figure 0-1.

In that diagram, the different steps of the development of the work are represented. Firstly, the search of the most suitable titanium based starting powders takes place. The reinforcement materials, boron and carbon based particles and fibres, are selected to reinforce the titanium and Ti6Al4V matrices. Moreover, the characterisation of all these starting materials is also carried out in this first step.

In the second step, optimisation and study of the different manufacturing techniques is realised in order to produce pure matrices and the composites. By varying the operational parameters and conditions, a successful fabrication route for the composite is acquired.

Next, the characterisation of all the produced specimens is performed. Measurements of density, hardness and mechanical properties are done. Additionally, the chemical analysis and microstructural study are realised. The discussions of this work are reported using and comparing the results obtained.

Finally, conclusions are drawn out in order to meet the objectives of this present work.

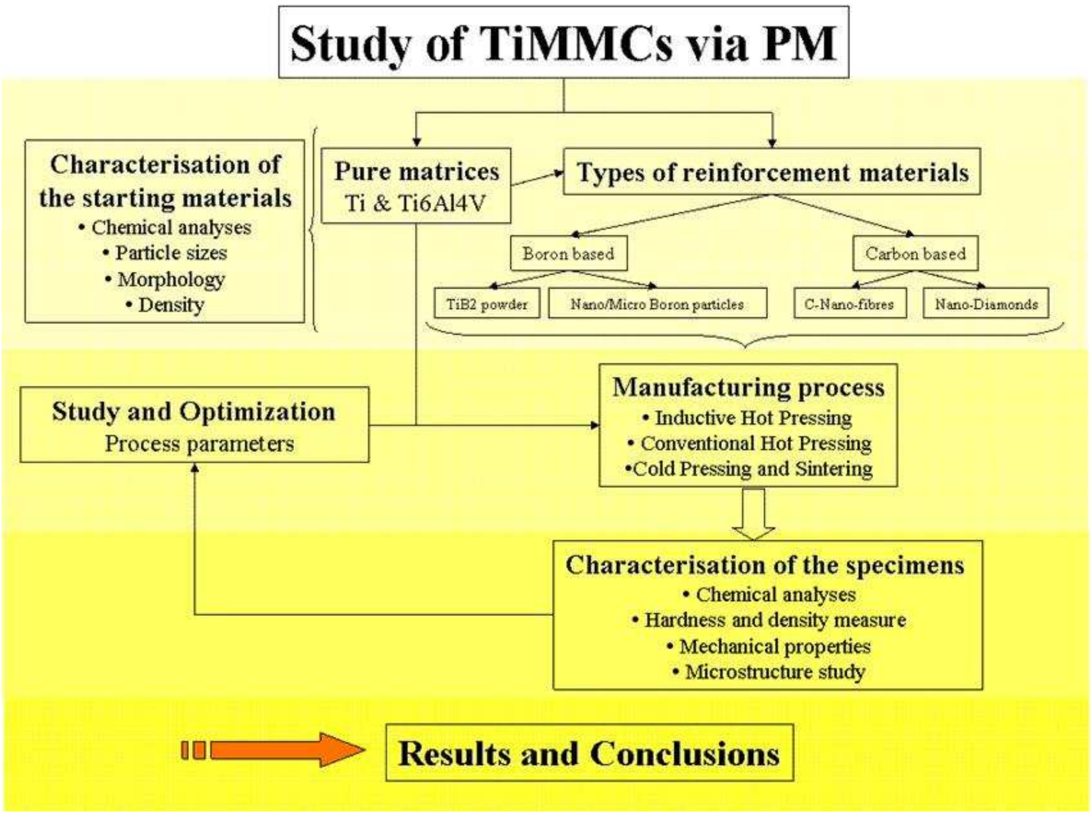

Figure 0-1. Flow sheet for the present study of TiMMCs manufactured via PM.

1 Introduction

1.1 Titanium and its alloys [1-5]

1.1.1 History of Titanium

Titanium was first discovered in an impure form by William Gregor in England, 1791. He isolated “black sand”, now know as “ilminita” (ilmenite, $FeTiO_3$).

The term “titanium” was named in 1795 by the German chemist Martin Heinrich Klaproth who also discovered this element to exist in the ore rutile.

In 1910, pure titanium was manufactured by M.A. Hunter, an American chemist. Hunter was able to extract the metal from the ores and developed the process of mixing rutile ore (TiO_2) with chlorine and coke, then applying extreme heat, producing titanium tetrachloride ($TiCl_4$), which was further reduced with sodium to form titanium in a steel bomb. The Hunter process successfully produced high quality titanium (99% purity).

Finally, Wilhelm Justin Kroll from Luxembourg is recognized as father of the titanium industry.

In 1946, he developed the process currently used for producing titanium commercially. This process reduces titanium tetrachloride ($TiCl_4$) with magnesium. Today, this is still the most widely used method and is known as the "Kroll process".

1.1.2 Basic properties

Titanium is the fourth most abundant metallic element on the planet after aluminium, iron and magnesium; it makes up approximately 0.6% of the earth's crust. It occurs in nature only in chemical compounds, usually with oxygen and iron.

The present mineral sources of titanium are rutile (TiO_2), ilmenite ($FeTiO_3$), and leucoxene, which is not a valid mineral species and consists mainly of rutile or anatase (it is an alteration product and mixture of Fe-Ti oxides). Ti is also extracted from minerals such as perovskite, brookite, sphene, and anatase [6]. The high price of titanium is due to the solubility of interstitials in Ti, which makes it tricky to produce in sufficient purity.

As compared to other metallic structural materials (Al, Fe and Ni), titanium and its alloys present the highest strength-to-density ratio [7]. Its coefficient of thermal expansion is somewhat lower than that of steel's and less than half that of aluminium. Moreover, titanium has a much higher melting temperature compared to aluminium, the main competitor in lightweight structural applications.

The Table 1-1 shows the comparison of Ti in between the elements as Al, Fe and Ni.

Table 1-1. Some of the important basic characteristics of titanium and titanium based alloys as compared to other structural metallic materials based on Al, Fe, and Ni [2].

Basic characteristics	Ti	Al	Fe	Ni
Density [g/cm^3]	4.5	2.71	7.86	8.9
Melting Temperature [°C]	1670	660	1538	1455
Allotropic Transformation [°C] (during cooling)	β→α [882°]		γ→α [912°]	
Crystal Structure	bcc → hex	fcc	fcc → bcc	fcc
E modulus at RT [GPa]	115	72	215	200
Yield Stress [MPa]	1000	500	1000	1000
Comparative Corrosion Resistance	Very High	High	Low	Medium
Comparative Reactivity with Oxygen	Very High	High	Low	Low
Comparative Price of Metal	Very High	Medium	Low	High

1.1.3 Metallurgy of Titanium

1.1.3.1 Crystal structure and α/β transformation

Titanium is an element which presents allotropy; it exists in more than one crystallographic modification. At 882°C, pure titanium exhibits its allotropic phase transformation, changing from a hexagonal close-packed crystal structure (hcp) (α phase) at lower temperatures (see Figure 1-2. Unit cells of β phase) to a body-centred cubic crystal structure (bcc) (β phase) at higher temperatures (up to 882ºC) (see Figure 1-1). This transformation temperature is the β-transus temperature. Its exact value is influenced by interstitial and substitutional elements – there are α and β stabilizers, respectively - and therefore depends on the purity of the metal.

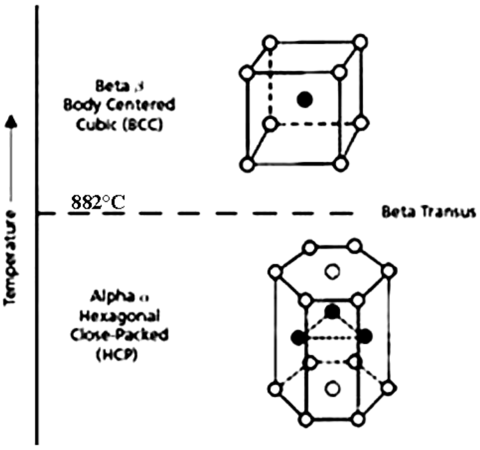

Figure 1-1. Beta transus temperature [4].

The basis for the large variety of properties achieved by titanium alloys reside in the existence of these two crystal structures. On one hand, the intrinsically anisotropic character of the hexagonal crystal structure of α phase has important consequences for the elastic properties of titanium and its alloys (see Figure 1-3).

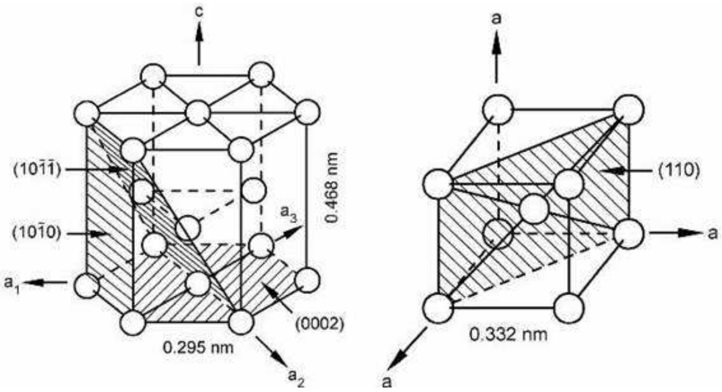

Figure 1-2. Unit cells of β phase (left) and α phase (right) [2].

The modulus of elasticity E varies between 145 GPa (stress axis parallel to the c-axis) and 100 GPa (stress axis perpendicular to the c-axis). In general, commercial β titanium alloys have lower E values than α and α + β. The modulus of elasticity for the β phase at room temperature cannot be measured for pure titanium due to its instability at room temperature.

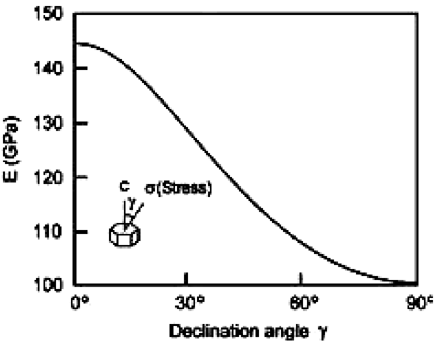

Figure 1-3. Modulus of elasticity E of alpha titanium single crystals vs. declination angle γ to the c axis [2].

On the other hand, the study of the plastic deformation of both phases shows the limited plastic deformability of the hcp α-phase compared to the bcc β titanium. The plastic deformability increases from the hcp to the bcc structure. In Table 1-2, the two crystal structures applicable to the titanium metal are summarised. The number of slip systems is only 3 for the α phase (hcp) while it is 12 for the β phase (bcc). The planes and directions of highly dense packed atoms of the β phase (bcc) are energetically more favourable for the plastic deformation than the planes of α phase (hcp)

The distance between the basal planes in the α phase (hcp) is slightly larger than the corresponding distance in β (see Table 1-2 $_{bmin}$/a), therefore the β/α transformation produces a slight lattice distortion.

Macroscopically, a slight increase in the volume is observed during cooling through the β/α transformation temperature (start from high temperatures). Then this phase transformation results in a expansion of volume of 0,1% approximately [8, 9].

Table 1-2. Characteristic parameters of the metallic structure types for titanium [5].

Structure Type	**N**	**CN**	**P**	**Slip planes;** Slip directions		**Slip system per unit cell**	**Atom density of slip plane**	**b_{min}/a**
				Indices	Nr.			
hcp (c/a=1.633)	6	12	74%	{0001} {1120}	1 3	1x3=3	≈91%	1
bcc	2	8	68%	{110} {111}	6 2	6x2=12	≈83%	1/2 √3 ≈0.87

N: Number of the atoms per unit cell
CN: Coordination Number
P: Packing density
b_{min}/a: Minimal slip component

In general, the properties of titanium and its alloys are determined by the volume fractions of the two phases (see Table 1-3). Compared with the β phase (bcc), the α phase (hcp) is more densely packed and presents an anisotropic crystal structure. Examining both phases, the hexagonal α phase has higher resistance to plastic deformation, reduced ductility and higher creep resistance than the cubic β phase. Furthermore, the α phase exhibits anisotropic mechanical and physical properties, in addition to lower self diffusion rate compared to the β phase.

Table 1-3. Properties of α, α+β and β titanium alloys.

Properties	**α**	**α + β**	**β**
Density	+	+	–
Strength	–	+	++
Ductility	–/+	+	+/–
Fracture toughness	+	–/+	+/–
Creep strength	+	+/–	–
Corrosion behaviour	++	+	+/–
Oxidation behaviour	++	+/–	–
Weldability	+	+/–	–
Cold formability	– –	–	–/+

- - = lowest
- = lower
-/+ = low- medium

+/- = medium-high
+ = higher
++ = highest

1.1.3.2 Titanium Alloys [3]

Depending on their influence on the β-transus temperature (882°C with pure titanium), the alloying elements in titanium are usually classified into neutral, α or β stabilizers. Their additions increase (α–stabilizer) or decrease (β–stabilizer) this α/β transformation temperature. The neutral elements have only minor influence on this β-transus temperature (see Figure 1-4)

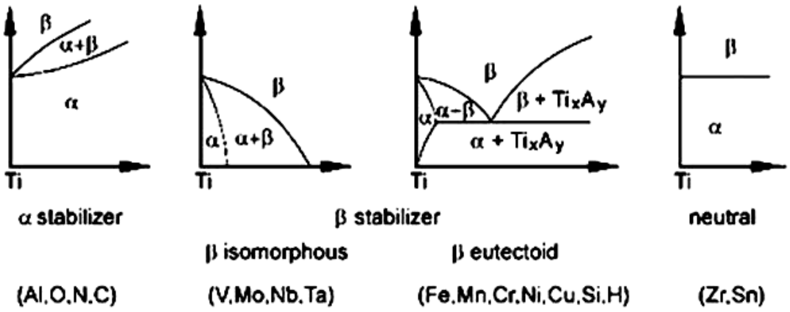

Figure 1-4. Influence of alloying elements on phase diagrams of titanium alloys (schematically).

In the group of α-stabilizing elements are the interstitial elements such as oxygen, nitrogen, and carbon. The β-stabilizing elements are subdivided into two categories, β-isomorphous and β-eutectoid elements. As neutral elements, Sn and Zr are considered since they have (nearly) no influence on the β/α phase boundary. Considering the previous classification, titanium and its alloys are divided into three important groups: α, α+β and β alloys:

α and near-α alloys group:

The α alloys are exclusively alloyed with α-stabilizing and/or neutral elements, and commercially pure titanium (CPTi) is also included here which is subdivided into four different grades depending on the oxygen content. Aluminium is the main alloying element apart from Zr and Sn. The alpha titanium alloys contain essentially a single phase at room temperature, similar to that of unalloyed titanium.

The alloys with a fraction of β-stabilizing elements less than 10% vol. are known as *near-α alloys*. These types of alloys have principally an all-alpha structure but contain small quantities of a beta phase because the composition contains some beta stabilizing elements. In this alloy type, alpha phase is stabilized by aluminium, tin, and zirconium. These elements, especially aluminium, contribute greatly to strength and also reduce the density [10]. This class of alloys was developed for higher operating temperatures in the compressor section of aircraft gas turbine engines. They present higher tensile strength at room temperature than the fully α alloys. Above approximately 400ºC, they possess the best creep resistance of all the titanium alloys. The final microstructure of the near α alloys consists of equiaxed primary-α grains, Widmanstätten α plates separated by the β-phase.

The α and near-α alloys are not heat treatable, have medium formability, are weldable, have medium strength and good creep resistance in the range of 316ºC - 590ºC.

The use of pure α alloy is in cryogenic applications because it retains its ductility and fracture toughness down the cryogenic temperatures.

In the next Table 1-4 the different grades of commercially pure titanium and several α alloys are listed in addition to their chemical composition and minimum yield stress (MPa).

Table 1-4. Chemical composition and minimum yield stress for CP titanium and α titanium Alloys [2, 11].

Grade or Alloy	**O, mass% (max.)**	**Fe, mass% (max.)**	**Other Additives**	**$\sigma_{0.2}$ (MPa)**
CP Titanium				
CP Titanium Grade 1	0.18	0.20		170
CP Titanium Grade 2	0.25	0.30		275
CP Titanium Grade 3	0.35	0.30		380
CP Titanium Grade 4	0.40	0.50		480
Ti-0.2Pd (Grade 7)	0.25	0.30	0.12-0.25Pd	275
Ti-0.2Pd (Grade 11)	0.18	0.20	0.12-0.25Pd	170
Ti-0.05Pd (Grade 16)	0.25	0.30	0.04-0.08Pd	275
Ti-0.05Pd (Grade 17)	0.18	0.20	0.04-0.08Pd	170
Ti-0.1Ru (Grade 26)	0.25	0.30	0.08-0.14Ru	275
α Titanium Alloys				
Ti-0.3Mo-0.9Ni (Grade 12)	0.25	0.30	0.2-0.4Mo, 0.6-0.9Ni	345
Ti-3Al-2.5V (Grade 9)	0.15	0.25	2.5-3.5Al, 2.0-3.0V	485
Ti-3Al-2.5V-0.05Pd (Grade 18)	0.15	0.25	2.5-3.5Al, 2.0-3.0V, (+Pd)	485
Ti-3Al-2.5V-0.1Ru (Grade 28)	0.15	0.25	2.5-3.5Al, 2.0-3.0V, (+Ru)	485
Ti-5Al-2.5Sn (Grade 6)	0.20	0.50	4.0-6.0Al, 2.0-3.0Sn	795
Ti-5Al-2.5Sn ELI	0.15	0.25	4.75-5.75Al, 2.0-3.0Sn	725

α+β alloys group:

This group of alloys has a range in the following phase diagram from the near- α alloys to the intersection of the Ms-line (Martensitic start temperature) with room temperature. The α+β alloys, at room temperature, present a volume fraction of β-phase between 5% - 40%. The chemical compositions of the α and β phases change in the two-phase field with decreasing temperature under equilibrium conditions.

The alpha-beta titanium alloys contain both alpha and beta phases at room temperature. The alpha phase is similar to that of unalloyed titanium but is strengthened by alpha stabilizing additions (e.g. aluminium). The beta phase is the high-temperature phase of titanium but is stabilized to room temperature by sufficient quantities of beta stabilizing elements such as vanadium, molybdenum, iron, or chromium. In addition to strengthening of titanium by the alloying additions, alpha-beta alloys may be further strengthened by heat treatment. The alpha-beta alloys have good strength at room temperature and for short times at elevated temperature. They are not noted for long-time creep strength. With the exception of annealed Ti-6Al-4V, these alloys are not recommended for cryogenic applications. The weldability of many of these alloys is poor because of the two-phase microstructure. As Figure 1-5 shows, Vanadium is a strong stabiliser of the β phase even at lower temperature.

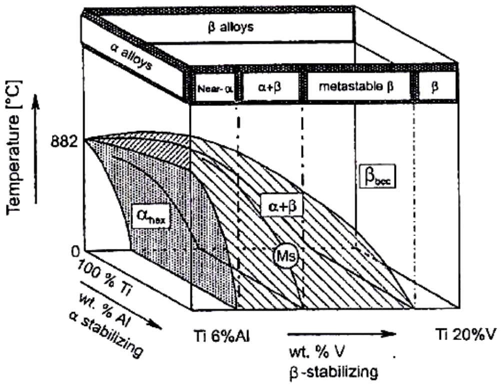

Figure 1-5. Schematically three-dimensional phase diagram of the titanium alloys [12].

β-alloys group:

The metastable β alloys have a volume fraction of more than 50% of β phase and finally, the single β-alloys end the classification of the titanium alloys (see Figure 1-5). These alloys contain high percentages of bcc phase that greatly increases their response to heat treatment. It provides higher ductility in the annealed condition, and much better formability than the α and α+β alloys. Their creep properties are limited to about 371ºC. In general they present good weldability and high fracture toughness. Some mechanical properties of selected titanium alloys are listed in the next table (see Table 1-5).

Table 1-5. Composition and properties of some commercial titanium alloys at room temperature [5].

Alloy	**Chemical composition (mass %)**	**T_β (°C)**	**Hardness (HV)**	**E (GPa)**	**Ys (MPa)**	**TS (MPa)**	**ε (%)**	**K_{IC} ($MPam^{1/2}$)**
α alloys								
high purity Ti	99.98 Ti	882	100	100-145	140	235	50	
Grade1	(cpTi: 0.2Fe,0.180)	890	120		170-310	>240	24	
Grade 4	(cpTi: 0.5Fe-0.40O)	950	260	100-120	480-655	>550	15	
Grade 6	(Ti-5Al-2.5Sn)	1040	300	109	827	861	15	70
Near α alloys								
Ti-6-2-4-2-S	Ti-6A1-2Sn-4Zr-2Mo-0.1Si	995	340	114	990	1010	13	70
TIMETAL 1100	Ti6A1-2.7Sn-4Zr-0.4Mo0.4si	1010		112	900-950	1010-1050	10-16	60-75
TIMETAL 685	Ti.6Al-5Zr-0.5Mo-0.25Si	1020		120	850-910	990-1020	6-11	68
TIMETAL 834	Ti-5.8Al4Sn-3.52r-0.5Mo-0.7Nb-0.35Si0.06C	1045	350	120	910	1030	6-12	45
α +β Titanium Alloys								
Ti64	Ti-4V-6Al	995	300-400	110-140	800-1100	900-1200	13-16	33-110
Ti.6-6.2	Ti-6Al-6V-2Sn	945	300-400	110-117	950-1050	1000-1100	10-19	30-70
Ti-6-2-2-2-2	Ti-6Al-2Sn-2Zr-2Mo2C,r-0.25Si			110-120	1000-1200	1100-1300	8-15	65-110

Ti-6-24-6	Ti-6Al-2Sn-4Zr-6Mo	940	330-400	114	1000-1100	1100-1200	13-16	30-60
Ti-17	Ti-5Al-2Sn-2Zr-4Mo-4Cr	890	400	112	1050	1100-1250	8-15	30-80
Metastable β alloys								
SP 700	Ti.4.5Al-3V-2Mo-2Fe	900	300-500	110	900	960	8-20	60-90
Beta III	Ti.11.5Mo-6Zr-4.5Sn	760	250-450	83-103	800-1200	900	1300	50-100
Beta C	Ti.3A1.8V-6G-4Mo-4Zr	79s	300-450	86-115	800-1200	900	1300	50-90
Ti-10-2.3	Ti.l0V.2Fe-3Al	800	300-470	110	1000-1200	1000	140	30-100
Ti-15-3	Ti-15V.3Cr-3Al.3Sn	760	300-450	80-100	800-1000	800	1100	40-100

1.1.3.3 Reactivity of titanium

The chemical reactivity of titanium is dependent upon temperature. The reaction of the metal with other substances proceeds more readily at elevated temperatures. This property is especially exemplified by the extreme reactivity of the metal to the atmospheric constituents at high temperatures. Thereafter, the use of inert atmospheres is necessary for hot working and for high temperature applications. The next diagram (**Richardson-Ellingham diagram)** is used to predict the equilibrium temperature between the titanium, its oxide and oxygen. This diagram is useful in attempting to predict at which conditions TiO_2 can be reduced, but only to a metal highly contaminated with oxygen (and carbon, in case of carbothermic reduction). As is well known, Titanium has a strong chemical affinity to oxygen, and it forms a tight microscopic oxide film on freshly prepared surfaces at room temperature (similar to magnesium and aluminium). The oxide film makes titanium passive to further reactivity. This accounts in part for the excellent corrosion resistance of titanium in aqueous salt or oxidizing acid solutions as well as its above-average corrosion resistance to mineral acids. This holds however only at and near room temperature; at higher temperatures oxygen is easily dissolved in the lattice, embrittling the metal.

Pure titanium is quite ductile (15 to 25% elongation see in Table 1-5), and it has a relatively low ultimate tensile strength (207 MPa) at room temperature. The ductility of the α-phase in unalloyed Ti is very sensitive to interstitial elements (such as C, O, N and H)[13].

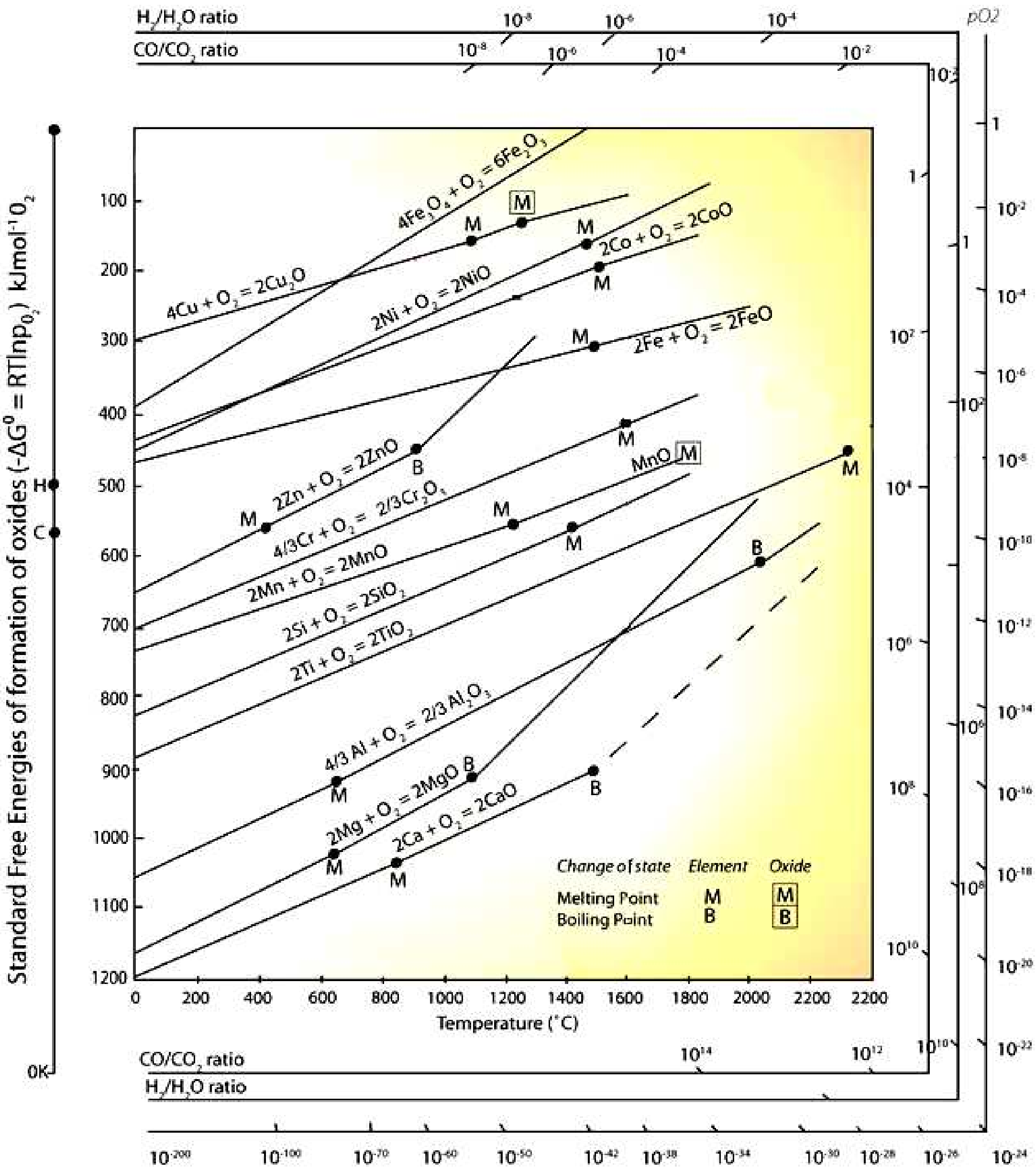

Figure 1-6. Rivhardson-Ellingham diagram.

These interstitial elements can be absorbed during the different processing stages carried out at elevated temperatures [14]. These elements are known to adversely affect the ductility of titanium. In the following graphics (Figure 1-7 to Figure 1-10), binary phase diagrams of titanium and the different interstitials are shown. The very high solubility of oxygen (up to >30 at%) and nitrogen (up to >20 at%) is evident; this effect is typical for the IVa and Va elements (Ti, Zr, Hf; V, Nb, Ta) but rather uncommon for other metals. Limited amounts of oxygen and nitrogen in solid solution will strengthen titanium; however they will embrittle the metal if present in excessive quantity. In any case, careful control of the O and N levels are of decisive importance for technical practice. Carbon exerts a similar but less intense effect on titanium, because of its much lower solubility.

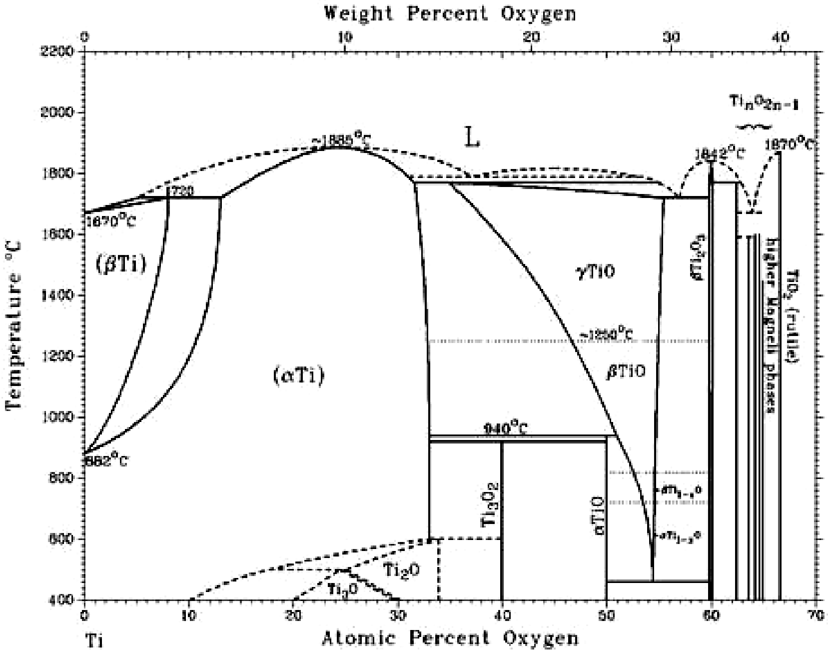

Figure 1-7. Binary phase diagram Ti - oxygen.

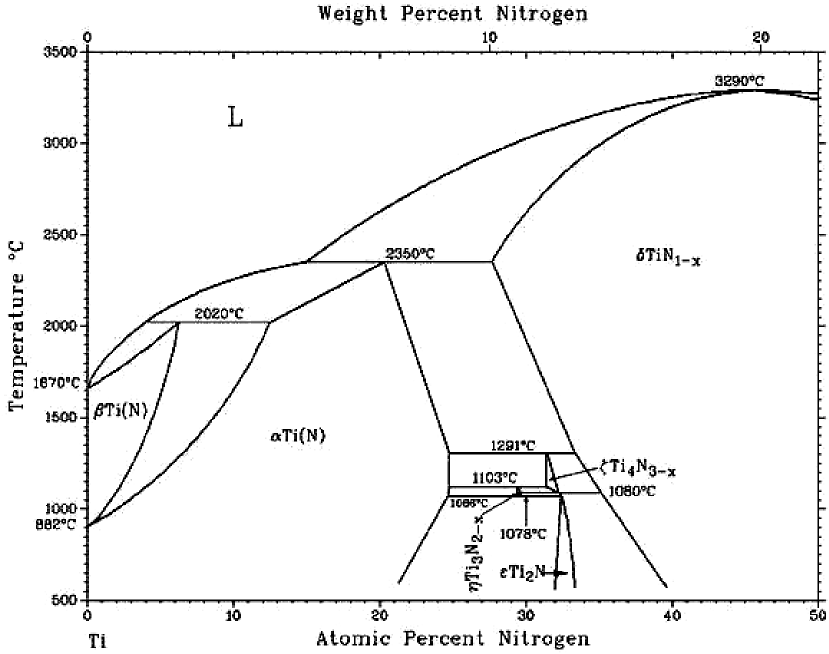

Figure 1-8. Binary phase diagram Ti - nitrogen.

Hydrogen also promotes embrittlement when present above specified limits but, in contrast to the other interstitials, can be easily removed e.g. by annealing in high vacuum [15, 16].

The atomic radius of titanium is the cause of the solubility of the different interstitials. Titanium has an atomic radius of 0.147 nm; if the solute atomic radius is less than 0.088 nm the atoms occupy interstitial sites and have high solubility and low activation energy for diffusion in a-titanium (see in Table 1-6).

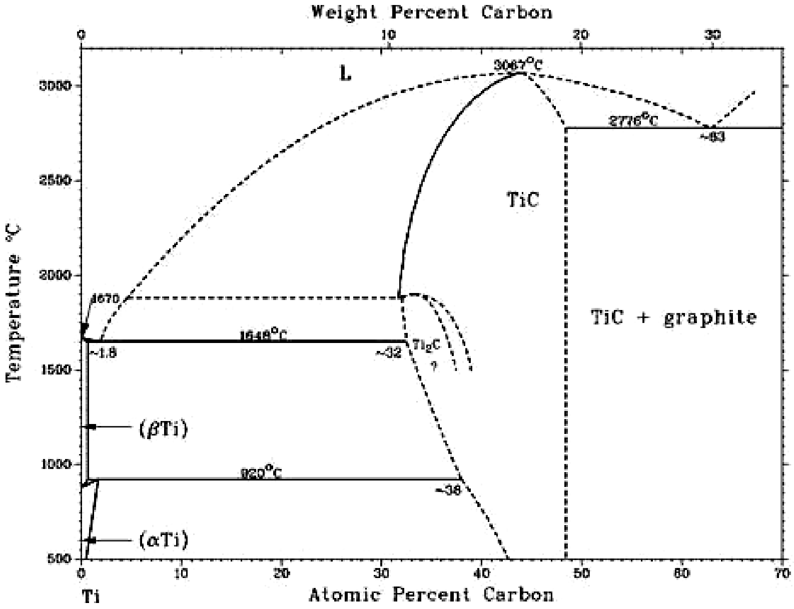

Figure 1-9. Binary phase diagram Ti - carbon.

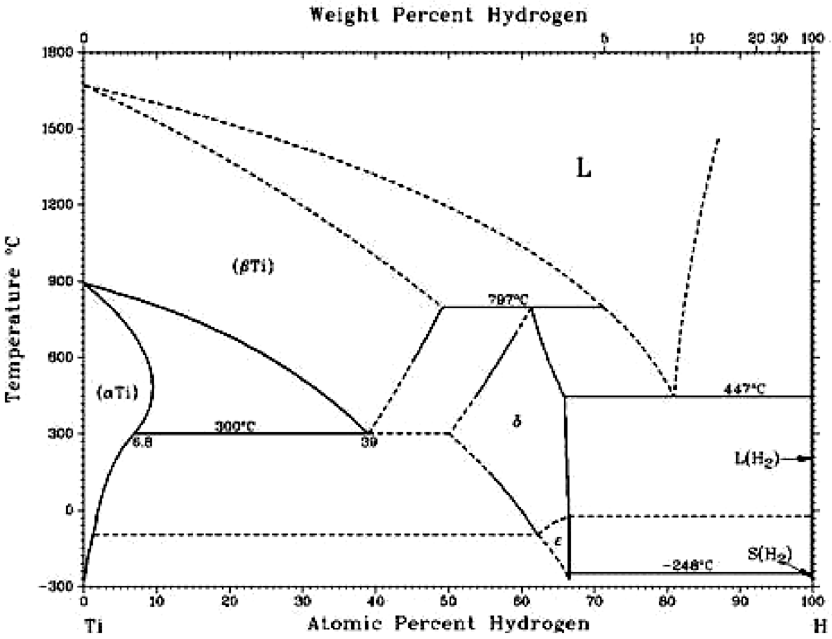

Figure 1-10. Binary phase diagram Ti – hydrogen.

Moreover, the activation energy for the diffusion of the interstitial increases from carbon, nitrogen to oxygen, with values for oxygen and nitrogen similar to those for titanium self diffusion (182 KJ/mole [17] for carbon and 258 KJ/mol for Ti self diffusion) (see in Figure 1-11). However in the literature, differing data can be found for the diffusion of interstitials in Ti [18]. In the next Figure 1-12 and Figure 1-13, the influence of these interstitial elements on the alpha titanium crystal (see Figure 1-12) and on the hardness of titanium (see Figure 1-13) specimens is shown.

Table 1-6. Interstitial solute diameter and maximum solubility in alpha-titanium at room temperature [19].

Element	Atomic Diameter (nm)	Maximum solubility (mass%)
O	0.120	12.5
N	0.142	6.4
C	0.154	0.25

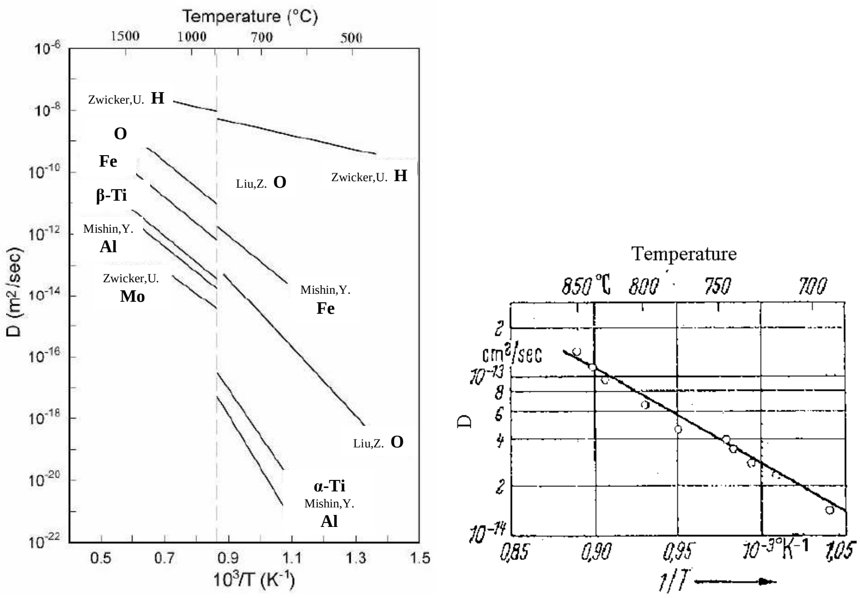

Figure 1-11. (Left) Arrhenius diagram of titanium self-diffusion and various alloying elements in the beta and alpha phases of titanium (dashed line: beta to alpha transformation temperature) [2]. (Right) Self diffusion of Ti in alpha phase[18].

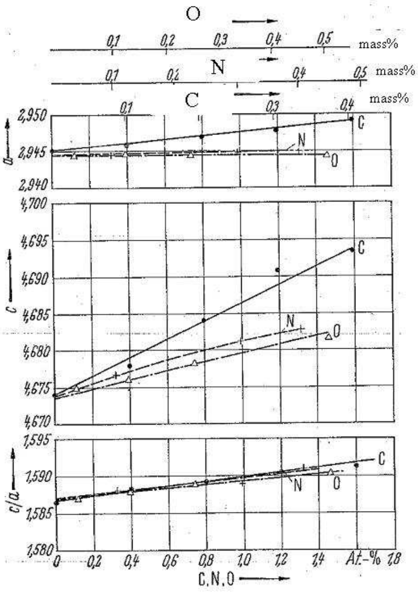

Figure 1-12. Influence of the interstitial element (C, N, and O) in the crystal of alpha titanium[18].

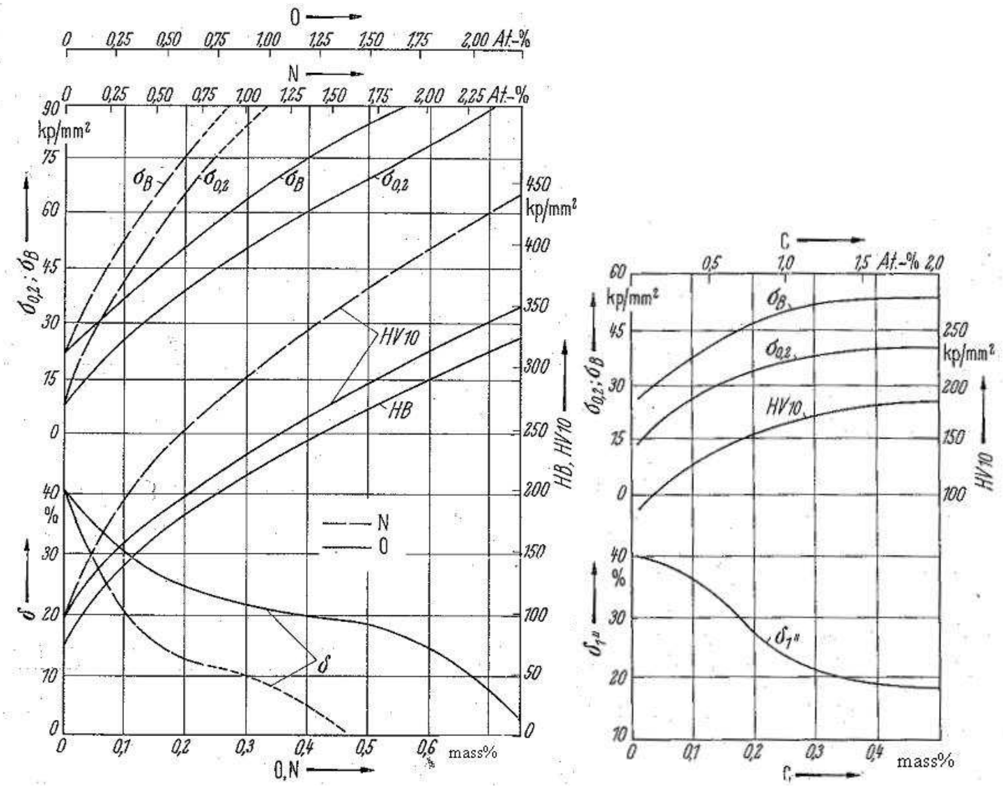

Figure 1-13. Influence of the interstitials (left: O and N; right: C) in the hardness of titanium at RT[18].

Finally, in order to explain the high affinity of titanium metal and the interstitial elements (e.g. H, N, O, C) previous studies were carried out [19, 20].

Concluding, because of the strong influence of interstitial elements on the mechanical properties of titanium, chemical requirements have been established for different applications. Due to the high affinity of titanium for oxygen and the inevitable presence of oxygen in manufacturing processes of titanium and TiMMCs, oxygen has to be an important element to control.

1.2 Powder Metallurgy

1.2.1 Introduction: Overview of PM [21]

Powder metallurgy (PM) is a processing route of metallic materials from metal powders, including the processing of metal powders, the production, characterization, and conversion of metal powders into useful engineering components. The Figure 1-14 shows the three main steps of PM processing.

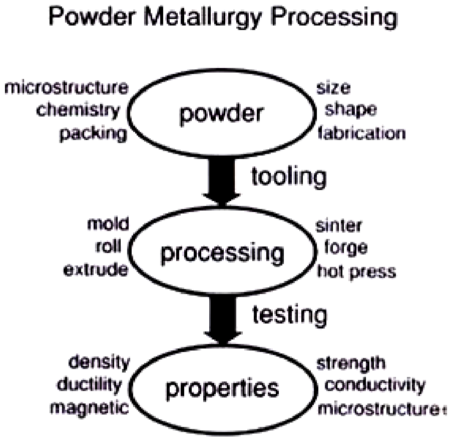

Figure 1-14. Conceptual flow for powder metallurgy from powder through the processing to the final product.

Here, firstly the fabrication, characterization, classification and handling of the powder are described. In addition, also the sampling, packaging, safety and transportation of the powder are shown in this first section. Next follows the processing step which comprises the forming and densification of the powders. Concluding, the properties of the final product are studied. It involves microstructural study and measurements of density, hardness, mechanical properties, etc.

The final properties depend on the relationship between the starting powder and the consolidation procedure.

1.2.2 Powder production, preparation and characterization [22]

1.2.2.1 Powder production

The method selected for fabricating a powder depends on specific material properties. The fabrication techniques are divided into four main categories based on mechanical reduction to powders, chemical reactions, electrolytic deposition, and liquid metal atomization.

Mechanical fabrication techniques:

Machining, milling, other impaction techniques and mechanical alloying are included in this group of mechanical production techniques. By transfer of energy of mechanical movement to the material, the mechanical disintegration takes place.

Electrolytic fabrication techniques:

In this type of techniques the electric current is the reducing agent. The metal is separated from the melt salt or from aqueous electrolytes depending on the material. An important application of this technique is for the production of tantalum. The purity of the powder obtained is considerably high. However, these methods present some disadvantages such as high energy cost, the generation of residues from the electrolytes and the limitation of the process to produce the metal powders only in their elemental form.

Chemical fabrication techniques:

Decomposition of a solid by a gas, thermal decomposition, precipitation from a liquid and from a gas, solid-solid reactive systems and reduction processes are included in this group of chemical fabrication techniques.

Generally, as reducing agents carbon and hydrogen are used, in gaseous compounds or mixture, or in their elemental form.

Commonly, the production of powder of hard materials is carried out via thermo-chemical reactions in solid, liquid, and gaseous states.

Atomisation techniques:

These techniques involve mechanical disintegration with phase change. The production of powders by disintegration of molten material is used in different variants. Several methods such as gas atomisation, water atomization, centrifugal atomization and other atomisation approaches are included in this group In these processes a melt is disintegrated into droplets by using a high pressure gas or liquid. The solidification of the droplets produces the powdered material.

1.2.2.2 Powder preparation

After the production, in most cases, raw powder as manufactured is not suitable for powder-metallurgical use directly. It requires to be further processed. The main series of operations performed are: Classification by the particle size, heating for purification or softening, the addition of pressing agents, mixing of different particle fractions or powder types, mechanical alloying and granulation.

The powder classification:

By screening in addition to sedimentation and counting methods the particle size can be determined.

Heat treatments:

Thermal treatments like thermochemical treatment are eventually needed, if the powder are superficially oxidised. This happens if the powders have been produced by water atomization or if its storage is done under unfavourable conditions or for prolonged periods, although the reduced powder presents higher reactivity to oxidise. For superficially oxidized Ti powder, however, a reducing heat treatment is not effective since it results in irreversible dissolution of oxygen in the bulk material, with resulting embrittlement.

Lubricant agent additions:

To reduce friction between the powder and the wall of the die during pressing or to decrease the wear of the tools, *lubricant agents* are often mixed with the powders. The addition of pressing agents should not exceed 0.2 to 1 mass% since large quantities can cause disintegration of the green part if the lubricant is still present.

Mixing:

This is necessary to achieve a uniform powder from different powder fractions or to process different powder components into a homogenised powder mixture.

For the production of sintered alloys and compound materials, mixing of powders with different chemical compositions is frequently used. This is one of the most widely used powder-metallurgical alloying techniques.

The design of the mixers employed in the industry is very different, according to forces used to get up particle movement. This classification of mixers is: a) Units using gravity, b) Using mechanical forces, c) using flow forces.

Diffusion-alloying, coating and mechanical alloying:

Diffusion-alloying, coating and mechanical alloying of powder are techniques to produce pre-alloyed powder with desired compositions.

The sintered alloys can be produced using fully pre-alloyed powder, if the components of the alloy are mutually soluble.

- The *diffusion alloying* is the technique where powders with different chemical compositions are firstly mixed mechanically.

Then, this mixture is heated, forming a thin diffusion layer between the alloying element and the base powder which bonds both particles together, thus preventing segregation. The diffusion alloying process is used in industrial practice to produce steel powders and bronze powders.

- The *coating* of the powder particles consists in a measure to coat each particle with a layer the thickness of which depends on the required alloy content and the base powder size. By using coated powder particles, a uniform distribution of the components in the powder can be achieved while simultaneously avoiding de-mixing. It is a important advantage of this type of powder.

- The *mechanical alloying* of the powders is the technique where high energy milling is employed. During the process, the high energy leads to strong deformation of the powders and a continuous sequence of welding, fracturing and re-welding. The homogenisation can be observed even at atomic level.
The high energy intensity during the milling due to the collision increases the temperature of the particles locally to several hundred degrees, in that cases the diffusion can take place. Its intensity increases with increasing milling. The mechanical alloying technique is widely used to produce super-alloys.

Granulation:

Powder granulation is a stage in which the primary particles of the original powder are agglomerated into larger secondary particles. It is employed to obtain better apparent density and flowability, also to avoid demixing.
The different types of preparing alloyed materials from powders can be observed in the Figure 1-15.

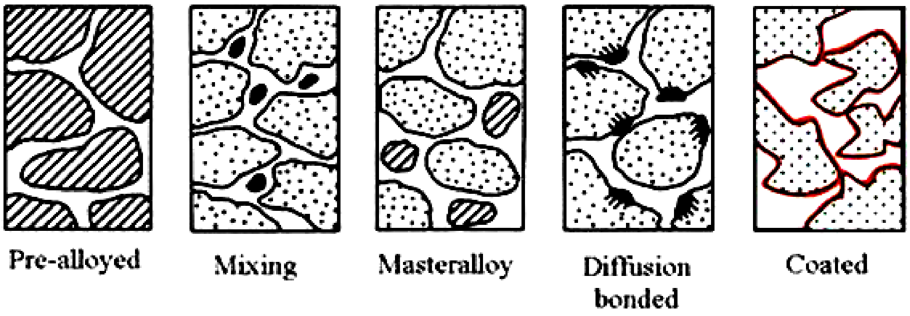

Figure 1-15. Alloying variants in powder metallurgy [23].

Additionally the advantages and problems of each one are listed in the next table (see Table 1-7).

Table 1-7. Advantages and disadvantages of the different alloying variants in powder metallurgy.

Powder variant	Advantage	Disadvantage
Pre-alloyed	- Equal distribution of alloy elements. - Good diffusion properties	- Poor compressibility - Low flexibility (limited variety of powders available)
Mixing	- Flexibility in the composition - Low cost	- Segregation - Demixing
Masteralloy	- Cheaper alloyed powder than the elemental component powder. (e.g. FeMo, FeMn)	- Segregation
Diffusion bounded	- Equal distribution of alloy elements. - No demixing, no segregation - Good compressibility	- Limited variety of powders (Distaloy)
Coated	- Very good distribution of alloy elements - No demixing	- Expensive powders

1.2.2.3 Testing and characterisation of the powders

A particle is defined as the smallest unit of a powder that cannot be easily subdivided. The properties of a single particle comprise size, shape, chemistry, microstructure, density and hardness.

The characterisation of a powder involves the knowledge of these properties in addition to the packing, flow and the characteristics of the surface.

Sufficient knowledge and control of properties of the starting materials result in more exact and narrower tolerance range of the properties of the final component.

Particle shape:

Particle shape is an important property, because it influences the specific surface area of the powder, its permeability and flow, and its density after compaction.

Depending on the method of production, metal powders exhibit a diversity of shapes (see Figure 1-16) from spherical to acicular.

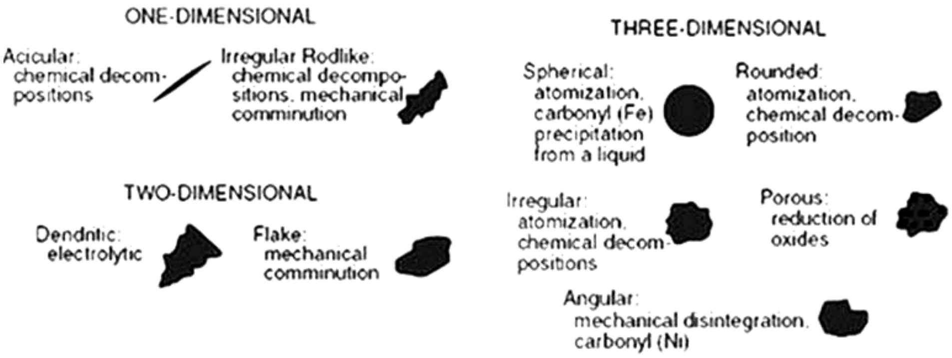

Figure 1-16. Powder particle shape as a function of the method of production [24].

Particle size:

The particle size could be defined by the determination of the dimensions of a particle. However, only spherical particles can be defined completely (by the diameter). Therefore, other quantifiable physical properties of the particles are used, such as mass, length, volume, setting velocity, or interaction with an electric field. From these properties, the equivalent spherical diameter can be determined.

The classification of the different methods for measuring the particle size comprises three groups:

a) Separation methods:

These methods are commonly used in the industry as sieving and air-elutriation. The different types of sieves used are vertically agitated, horizontal moved and stationary sieves. The particles size analysis (DIN ISO 4497 and DIN 66165) obtained with a normal sieve, shows usually a particle size > 20 µm, although there are special micro-sieves that can be used to retain particle size smaller than 5 µm.

b) Sedimentation methods:

The sedimentation method (DIN 66111) involves the calculation of the particle size and distribution of the particles in a stationary liquid.

After a pre-determined time, the particle concentration distributed over the height of the suspension changes (from C_0 to C_t). This concentration (C_t) is measured by different ways. In this way, the C_t calculated is proportional to undersize particle diameter (D).

c) Counting methods:

By examination of an image using metallographic methods or measuring interactions with electrical fields, the counting methods are carried out to obtain particle size and distribution. The laser beam methods are included in this classification group. The laser beam analysis of particle size is based on the principle of laser-light diffraction by particles. This method presents high speed of measurement. Nowadays it is very popular.

Surface area:

The surface area is an important property of particles. This factor influences the surface activity of the powder compacts during sintering. For that reason, it describes an important driving force for material transport during sintering. The specific surface area of a powder is the surface area of a 1 gram mass unit of this powder.

For measuring the surface area, two analysis techniques are employed: gas adsorption and gas permeability [21, 25, 26].

Interparticle friction, Flow and packing:

The friction between particles and the flow properties are closely related. They depend on the surface area, the surface roughness and particle size. A powder with large specific surface area presents higher interparticle friction, and its flowability is lower than that of a powder with smaller specific surface. Resistance to flow is the main distinctive aspect of friction. Therefore, the interparticle friction affects the flowability of the powder and consequently its packing properties. Also, fine powders have a tendency to the formation of bridges, in this way the particle flow is inhibited. The uniform filling of the die is an important requisite for mass production of sintering compacts. The flow properties of the powder influence the press speed and also the tool designs. Powders with very small particle size have poor flow properties, therefore these powders have to be granulated.

The fill or “apparent” density (ρ_0) is the density (mass/volume) of a powder when it is in loose state without agitation. Tap density (ρ_t) is the highest density that can be achieved by agitation of the powder without external pressure. The ratio of tap density to apparent density is called “Friction coefficient” which is an important factor for the mass production of sintered components. Concluding, packing properties of a powder are affected by the size, distribution and shape [21, 25].

Compressibility [27]:

Compressibility or compactibility is the ability to densify a powder under an applied load, i.e. to obtain maximum relative density at a given pressure. For the evaluation of the compactibility, the elasticity and plasticity of the particles have to be considered in addition to the particle shape and surface structure. The powder itself has significant influence on the compaction properties. That means that powders from ductile metals present better compactibility. The particle shape is another important factor. The powders with a wider particle range in the coarse range have the best compactibility. The addition of lubricant reduces the interparticle friction and favours the powder compaction, however inhibits the densification to higher density levels.

1.2.3 Powder Metallurgy Processing

There is a wide variety of forming processes to transform a mass of powder into a final compact. In most cases, firstly the consolidation stage in which inter-particle metallurgical bonds are formed takes place.

Following, an elevated temperature diffusion process referred to as sintering, sometimes assisted by external pressure, completes the manufacturing of the nearly full dense material. However, component production does not end with the sintering or densification. Frequently, additional finishing operations are necessary to achieve the final requisites of the application for the components.

Generally, the selected method for the fabrication of a components by powder metallurgy depends on the level of performance required from the part. Many components, i.e. ferrous precision parts, are adequate when produced at 85-90% of theoretical full density (T.D.), compared to other specimens which require full density for satisfactory performance, such as e.g. hardmetal tools. However, there are some components produced with significant and controlled levels of porosity, the porosity being subsequently filled with other components. Examples are self-lubricating bearings. The wide range of consolidation techniques can be structured depending on the temperature employed to carry out the compaction and shaping of the powder (see in Figure 1-17).

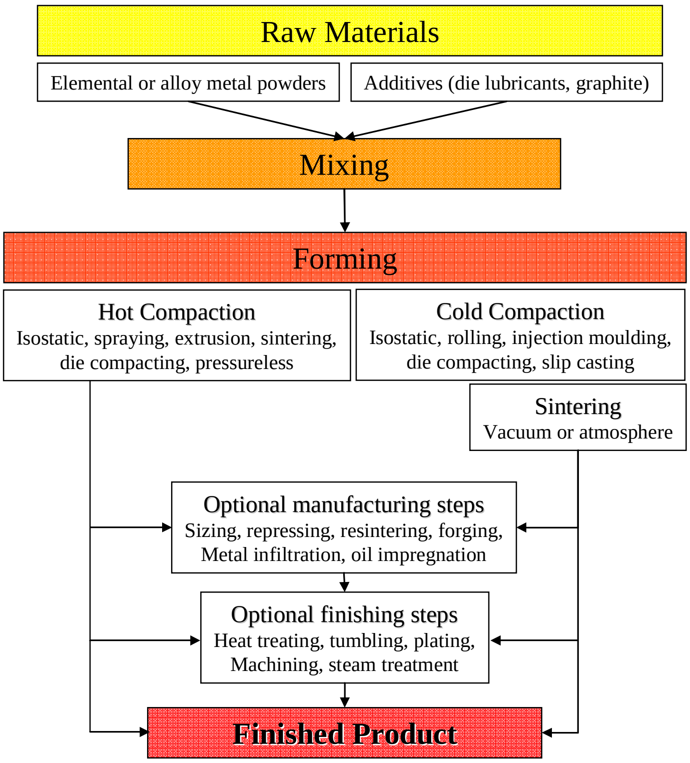

Figure 1-17. Powder Metallurgy Processing Variants [28].

1.2.3.1 Shaping and compaction of powders at room temperature:

Cold Uniaxial Pressing

The powder is mixed with a lubricant and axially pressed in a die. After the cold compaction, the ‘green’ component is dimensionally very accurate, as it is moulded precisely to the size and shape of the die. One disadvantage of this technique is the variation of pressed density that can occur in different parts of the component due to particle/particle and die wall/particle frictional effects, for that reason it is very necessary to employ lubricants.

Cold Isostatic Pressing (CIP)

The metal powders are contained in a deformable die (e.g. a rubber membrane) which is uniformly pressed in all directions by external (hydrostatic) pressure. Considering the media for transferring the isostatic pressure to the die, this process is divided into Wet-bag compaction process if this media is a liquid (typically oil) or Dry-bag compaction process where the pressure media may be a gas or also a liquid for dry-bag techniques. Here, liquids are mostly used since they generate high pressures at very slight volume changes. In this last technique the pressure is radial, and it is usually used for manufacturing of cylindrical parts. As the pressure is isostatic the as-pressed component is of uniform density. Irregularly shaped powder particles must be used to provide adequate green strength in the as-pressed component. This technique is normally used for semi-finished products.

High Velocity Compaction [29] (HVC)

This is a new manufacturing process for the consolidation of PM components. The developer of this technique is Höganäs AB (Sweden) and Hydropulsor-EPM AB (Sweden) [30]. The densification of the specimens is controlled by the impact energy. The powder is compacted in less than 20 milliseconds by high-energy impact. Further densification is possible by adding multiple impacts as short as 300 milliseconds after each other.

Powder Rolling

The densification of the powders is carried out by friction forces. Increasing the speed of rolling decreases the density of the compacted strip. One advantage of powder rolling is the few rolling passes required to produce a thin strip.

Slip casting

This is a forming process which does not use pressure. The powders are suspended in liquid, in this way the friction can be reduced. This liquid clay body slip is poured into plaster moulds and allowed to form a layer, the cast, on the inside cavity of the mould. The slip casting is a common process in the production of ceramics, and for the use in powder metallurgy for large-scale it is not usually suitable. Wet powder pouring is a variation of slip casting process. The powders are suspended in an organic liquid as carrier. It contains normally binding agents. After the liquid evaporation, the dried component is processed in similar way to MIM process.

Metal Injection Moulding (MIM)

Metal Injection Moulding (PIM) is a process derived from plastic injection moulding. This process comsists of four main steps: mixing (binder and powder), injection moulding, debinding and sintering.

In the mixing step, the powder is dispersed in an organic vehicle, called the binder, to form the feedstock. It is then granulated, transferred, and injected into the required shape by injection moulding.

In the debinding step, the binder in the molded part is removed, commonly by heat. Finally, the debinded part is sintered at high temperature to achieve the required mechanical properties. Usually, MIM is a forming process which does not use pressure during sintering [31].

1.2.3.2 Hot consolidation techniques

Hot Pressing (HP)

This process involves the simultaneous application of pressure and temperature. Hot pressing consists of loading loose powder into a die which is typically made of graphite. To reduce the reaction between the die and the powder to be consolidated, the graphite mould is lined with a thin foil of a low reactivity carbonaceous material, and/or a spray is used to apply a thin film of ceramic particles, e.g. BN, on the surface of the graphite mould. These measures prevent unwelcome reactions between powder and tool.

Hot Isostatic Pressing (HIP)

The powders are usually encapsulated in a metallic container but sometimes in glass. The container is evacuated; the powder is degassed, to avoid contamination of the materials by any residual gas during the consolidation stage, and sealed off. It is then heated and subjected to isostatic pressure sufficient to plastically deform both the container and the powder. As with cold isostatic pressing, mainly semifinished products are produced, either for subsequent working to smaller sizes, or for machining to finished dimensions. HIP is however also used to eliminate residual closed pores in sintered or cast components.

Pseudo HIP processes [22]

In order to obtain the same results as with HIP but at lower cost, variants of this manufacturing process appeared. STAMP-process, CAP-process, Ceracon-process, Electroconsolidation, and Rapid Omnidirectional compaction are examples of these pseudo HIP processes. Due to the high cost effectivity of HIP today, these processes have virtually disappeared.

Hot Forging (Powder Forging)

This technique combines drop forging and powder pressing. In powder forging, an as-pressed and then sintered component is heated to a forging temperature, usually below the sintering temperature of the material, and then forged in a closed die very similar to a powder pressing die. This produces a virtually fully dense component with the shape of the forging die and appropriate mechanical properties.

Powder Extrusion

This manufacturing process is not normally used as final forming technique. In cases where the appearance of oxide layers on the surface of the powder particles limits the sintering of the compact to full density, the use of the extrusion process is necessary. Also it is employed for the further consolidation of semi-finished components.

Spray-deposition

The production of the solid specimens is carried out by impacting of semi-solid powder particles onto a substrate surface. This process is normally used for manufacturing of semi-finished components where the high cooling rates can be used to produce advantage microstructures and material properties (Osprey process). It can be described as a gas atomization process in which the droplets are collected on a solid substrate before they have completely solidified.

Direct Metal Laser sintering [21]

The process basically starts with a computerized 3D solid model of a part, which the computer slices into extremely thin layers (0.0762 to 0.254mm). This cross sectional data is then sent to the selective laser sintering machine to selectively guide the laser beam over a correspondingly thin layer of powdered material. These powders fuse or “sinter” under the heat of the laser. Layer by layer and feature by feature the digital solid model is recreated into a real functional part. Direct Metal Laser Sintering (DMLS) is an evolving technique for the production of parts with complex geometry and unique microstructure. DMLS, generally, employs a mixture of high and low melting-point powders, denominated as structural and binder particles, respectively.

Selective Laser Sintering

Additionally, another laser sintering technique commonly used is the Selective Laser Sintering (SLS). It is a further rapid manufacturing technique that uses a high power laser (for example, a carbon dioxide laser) to fuse small particles of metal powders into a mass representing a desired 3-dimensional object. The laser selectively fuses powdered material by scanning cross-sections generated from a 3-D digital description of the part on the surface of a powder bed. After each cross-section is scanned, the powder bed is lowered by one layer thickness, a new layer of material is applied on top, and the process is repeated until the part is completed.

Electron Beam Sintering:

The electron beam sintering technology (EBM) involves higher power density and beam velocity. A suitable application of this method is for sintering high-tensile steel powder in an economic way [4, 32]. Comparatively to SLS and DMLS, EBM has a generally superior build rate because of its higher energy density and scanning method. A disadvantage is the necessity to operate in high vacuum.

As example for EBM technique is Arcam EBM. This method uses an electron beam gun to melt metal powders and build solid details with a homogeneous material structure. The parts are built by melting metal powder layer-by-layer with the EBM process, and the result is functional metal parts. The process uses standard biocompatible materials, such as Ti6Al4V ELI, Ti Grade 2 and Cobalt-Chrome. EBM is typically used in the medical, aerospace and automotive industries [33].

Spark Plasma Sintering (SPS)

The main characteristic of the Spark Plasma Sintering (SPS) is also known as plasma activated sintering. This technique is thought of a type of rapid hot pressing, implying that the application of a uniaxial pressure is essential for enhanced densification kinetic. A pulsed current directly passes through the graphite die, as well as the powder compact, in case of conductive samples.

The heat is generated internally, in contrast to the conventional hot pressing, where the heat is provided by external heating elements.

The general speed of the process ensures that it has the potential of densifying powders with nanosize or nanostructure while avoiding coarsening which accompanies standard densification routes. Whether plasma is generated has not been confirmed yet. It has, however, been experimentally verified that densification is enhanced by the use of a current or field [34].

1.2.3.3 Sintering [21, 22, 28]

ISO definition of "Sintering process":

"Thermal treatment of a powder or compact at a temperature below the melting point of the main constituent, for the purpose of increasing its strength by bonding together of the particles".

The bonding together of particles can occur at temperatures below the melting point by solid-state atomic transport. Depending on the sintered materials and the temperature, the sintering processes can be divided into two important groups: Solid phase sintering and liquid phase sintering (see Figure 1-18).

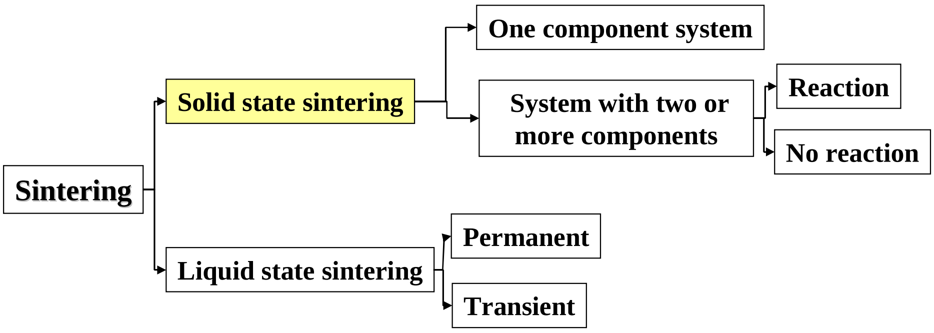

Figure 1-18. Sintering process variants.

The sintering process:

There is no definitive theory of sintering, consequently there is no specific formula to describe the sintering process, although "master sintering curves" have been drafted to describe the densification behaviour. However, there are several models which try to explain the different stages of the sintering process. An important model for the sintering study is "The Two Sphere Sintering Model" [35]. In this model, two spherical particles are considered. The bonds between contacting particles grow and consolidate as sintering progresses.

On a microstructural scale, the bonding is shown as a neck formation. This formation and growth causes the change of the properties. At the same time, inherent structural defects are eliminated by the bonding between adjacent powder particles. The sintering stages are represented in the following Figure 1-19. In the first and initial stage the particle bonding is initiated at contact points. Next, in the intermediate stage, the contact points grow into "necks". After that the pores are reduced. In the final stage, the grain boundaries develop in place of the necked regions.

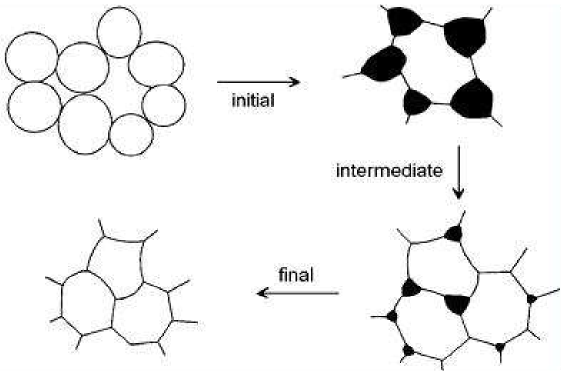

Figure 1-19. Descriptions of the different sintering stages [36].

During the sintering, the particle system which contains large amounts of free energy tends to a more stable state. The reduction of the surface free energy is the main driving force in the sintering process ($\Delta Gs < 0$), at least in the absence of solubility effects. The surface energy per unit volume roughly depends on the inverse of the particle diameters (see in Equation 1-1). Therefore, smaller particles have more energy and sinter faster.

$$\frac{E}{V} = \frac{6\gamma_{SV}}{D}$$

Equation 1-1

E/V = energy release per unit of solid volume
D = diameter
γ_{SV} = surface energy

On atomic scale, two other important factors force the atomic motion and consequently the growing of the necks (se Figure 1-20). On one side, on the convex areas the vapour pressure is much higher than on the concave. On another side, there is the effect of the high vacancy concentration in the neck areas.

The next Laplace Equation 1-2 gives the stress σ associated with a curved surface as:

$$\sigma = \gamma(\frac{1}{R_1} + \frac{1}{R_2})$$

Equation 1-2

Γ = surface tension (= specific surface energy)
R_1 and R_2 = principal radii of curvature for the surface.

Considering the basic concepts of the two-sphere model, in the sphere and in the neck the surface tension is:

In the sphere → $R \sim R_{1=}R_2$

$$\sigma \propto \frac{2\gamma}{R}$$

Equation 1-3. Stress in the sphere

Using a circle approximation to the neck shape with a radius r, where r is approximately equal to x^2/D, the curvature at the neck gives a stress as:
In the necks $R_1 = x/2$ and $R_2 = -r$

$$\sigma \propto \gamma\left(\frac{2}{x} - \frac{4D}{x^2}\right)$$

Equation 1-4. Stress in the neck

Therefore, within a small distance there is a strong driving force for mass flow to the neck (see in Figure 1-20). As the neck grows, the curvature gradient is relaxed and the process slows down.

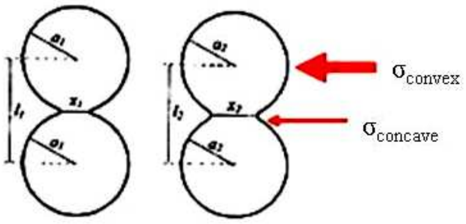

$x_2 > x_1$; $l_2 < l_1 < 2\alpha_2$ $\alpha_2 \leq \alpha_1$ $\sigma(\text{neck}) < \sigma(\text{sphere}) \rightarrow$ necks growing

Figure 1-20. Growth of necks during sintering [37].

Transport mechanisms determine how the mass flows in response to the driving forces. Two classes of transport mechanisms are the surface transport and bulk transport.
Surface transport involves neck growth without a change in the particle spacing (no shrinkage). However, bulk transport-controlled sintering causes shrinkage.
The surface transport includes surface diffusion and evaporation-condensation flow. The bulk transport mechanisms include volume diffusion, grain boundary diffusion, and plastic flow (see in Figure 1-21). Generally, bulk transport processes are more active at higher temperature.
Diffusion is thermally activated (see in Equation 1-5), meaning an activation energy has to be overcome for atomic movement. Both the formation of vacancies and the motion of atoms depend on the number of atoms with an energy equal to or above the activation energy.
The number of atoms with energy above the activation energy varies with the Arrhenius temperature relation.

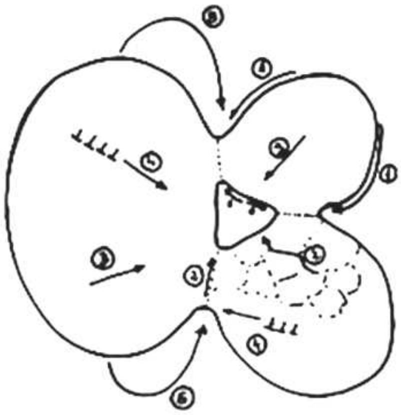

1. Surface diffusion 2. Volume diffusion 3.Grain boundary diffusion
4. Plastic creep 5. Evaporation- Condensation

Figure 1-21. Mass transfer mechanisms during sintering [37].

$$\frac{N}{N_0} = \exp\left(\frac{-E}{k * T}\right)$$

Equation 1-5. Arrhenius equation

N/N_0 : ratio of activated atoms to total atoms E: Activation energy
k: Boltznann´s constant T: Absolute temperature

The density of the specimens can also change during sintering, depending on the material and the sintering temperature. These dimensional changes can be controlled by an understanding and adjustment of the pressing and sintering parameters. Increase in density during sintering implies an overall shrinkage (see Equation 1-6, assuming that the mass does not change).

$$Vol_{shrinkage} = \frac{V_{\sin tered}}{V_{green}} = \frac{\rho_{green}}{\rho_{\sin tered}}$$

Equation 1-6

$V_{sintered}$: Volume of the sintered specimen $\rho_{sintered}$: Density of sintered specimen
V_{green} : Volume of the green specimen ρ_{green} : Density of green specimen

1.2.3.4 Finishing and secondary operations

To increase density and hardness, improve the properties and the accuracy or accomplish additional shaping of the sintered part, secondary operations are required such as heat treatments, re-pressing, re-sintering, machining, various surface treatments (Surface hardening), re-pressing, Sizing, machining, de-burring, impregnation, infiltration, electroplating, steam treatment etc.

1.3 Metal Matrix Composites

1.3.1 Description of Metal Matrix Composites

A metal matrix composite (MMC) is a composite material with at least two phases, one being a metal and the other/s non metallic material (usually). The metallic component is called matrix (continuous system) and the other components are known as reinforcement [38]. Reinforcement materials in MMCs are second phase additions to a metallic matrix that result in some property improvement, typical ones being an increase in strength and/or Young's modulus, improvement of the thermal, tribological or electrical properties. Generally, most reinforcement materials for MMCs can be fibres or discrete ceramic particles (oxides, carbides, nitrides, and so on) which are characterized by their high strength and stiffness both at ambient and elevated temperatures. Examples of common MMC reinforcements are: SiC, Al_2O_3, TiB_2, B_4C, and graphite in various types (long or short fibers, nano-tubes,...).

1.3.2 Manufacturing and forming methods [4, 39]

MMC manufacturing can be classified into three types: solid, liquid, and vapor.

Solid phase methods

- Powder blending and consolidation (powder metallurgy): Powdered metal and discontinuous reinforcement are mixed and then bonded through a process of compaction, degassing, and thermo-mechanical treatment (possibly via sintering, hot isostatic pressing (HIP) or extrusion).
- Foil diffusion bonding: Layers of metal foil are sandwiched with long fibres, and then (usually hot) pressed to form a matrix.

Fluid phase methods

- Stir casting: Discontinuous reinforcement is stirred into molten metal, which is then allowed to solidify (e.g. Al-SiC "Duralcan").
- Squeeze casting: Molten metal is injected into a form with fibres pre-placed inside it.
- Spray deposition: Molten metal is sprayed onto a continuous fibre substrate.
- Reactive processing: A chemical reaction occurs, with one of the reactants forming the matrix and the other the reinforcement.

1.4 Fabrication of Titanium Metal Matrix Composites via Powder Metallurgy

1.4.1 Introduction to TiMMCs

In the last decade, Titanium has become more important as metal matrix material due to its outstanding properties such as low density combined with resistance to fatigue, high temperature capability and resistance to corrosion, etc. Additionally, titanium metal matrix composites (TiMMCs) offer a number of advantages compared to its base metal and its alloys, such as higher specific strength and E-modulus, higher elevated temperature resistance, etc...[4]

However, they are more expensive than titanium base metal. Therefore Titanium powder metallurgy (PM) provides the possibility of creating net-shape or near-net-shape parts without the material loss and cost associated with machining intricate components from wrought billets [40-43].

Moreover, many efforts to lower the production cost of the titanium based powders contribute to promote the development of TiMMCs via PM techniques [44-48].

This part of the work consists in a review of the state-of-the-art of several types of TiMMCs reinforced by several types of materials and manufactured through powder metallurgy routes.

1.4.2 Applications and types of TiMMCs

The attractive physical and mechanical properties that can be obtained with Titanium Metal Matrix Composites (Ti-MMCs), such as high specific modulus, strength or wear resistance, have been documented extensively. Interest in MMCs for use in the automotive industries, aerospace, other structural applications, and biomedicine, has increased over the past 25 years as a result of several processing routes being developed and of availability of reinforcements. Additionally, Titanium powder metallurgy (P/M) offers the possibility of creating new compositions of materials, which could be competitive in front of the conventional material.

Furthermore, titanium based composites are often used to save weight by replacing heavier steel alloys in the airframe and superalloys in the low temperature part of gas turbines [49].

In the industry of transports, the use of light composites is increasing, and also the role of titanium composite materials [40].

The biocompatibility of the titanium and its alloys as matrices and their good corrosion properties, are suitable to employ these composite materials as implants [50].

Opportunities in wheelchair and sports goods such as bicycles, also for golf club and tennis rackets are attractive for the use of titanium composite materials [51]. Although the size of these sectors is limited, the customers are willing to pay excessively for these goods.

1.4.3 Types of TiMMCs

TiMMCs can be subdivided according to the type of reinforcement materials employed. Thus reinforcements can be particles (Micro/ Nano), high strength single crystal whiskers, short fibres (Micro/Nano) or long aligned multifilament or monofilament fibres [3, 4].

The continuously reinforced materials are expensive, for that reason the use of these composites is limited for commercial applications.

In the discontinuously reinforced metal matrix materials, powder metallurgy processing plays an important role. It is applicable to the manufacturing of TiMMCs. The cast metal matrix composites are often cheaper to produce than the powder metallurgy (PM). However PM presents advantage to prepare very different combinations of material properties. These properties of the reinforced materials can be tailored for specific applications.

In order to reduce cost and make the TiMMCs more competitive, previous works have been focused on the development of discontinuously reinforced titanium based composites. Thereby, the titanium matrices reinforced with particles, whiskers and short fibres are widely studied, in addition to their different manufacturing processes. Ceramic and carbonaceous reinforcement materials are frequently used (see Table 1-8).

More recently, the use of standard or near-standard metal working methods which are utilized to fabricate metal matrix composites with reproducible structure and properties are increasing the interest on the fabrication of TiMMCs.

On one hand, discontinuously reinforced composites have been traditionally produced by several processing routes. These techniques are based on the addition of the reinforcements to the matrix materials in molten or powder form. Thus, they can be considerate as “ex situ” or “conventional” techniques.

On another site, there are techniques in which the reinforcements are synthesised in the titanium matrix by chemical reactions between the compounds during the fabrication process. They are denominated “in situ” techniques [52, 53].

The properties of the composites are controlled by the size and volume fraction of the reinforcements as well as by the matrix-reinforcement interfaces.

Depending on the final application of the titanium based composites, the matrices can be reinforced by different materials to achieve the required needs.

On one hand, the materials reinforced by ceramic particles or whiskers present relatively favourable applications due to the low cost of their fabrication in comparison to the continuously reinforced matrices. Additionally, the properties of the materials reinforced with these types of discontinuous reinforcement present relatively isotropic properties (in comparison to the titanium matrices reinforced with long aligned multifilament or monofilament fibres) [54-56].

As an example, the addition of boron based particles as reinforcement (TiB_2) is widely known to improve the strength of the metal matrix [57, 58].

On the other hand, the use of nanofibres, in particular carbon nanofibres, considerably improves strength and stiffness of titanium and its alloys, in particular titanium matrix strengthened with nano-carbon reinforcements [59]. These types of reinforcement materials are extensively studied and documented [53].

The next shows some common reinforcement materials, particles or fibres used with matrices of titanium or its alloy Ti-6Al-4V, in addition to the powder metallurgical technique employed for fabrication. Furthermore, some applications of these composites materials are simultaneously listed.

The powder metallurgy processing commonly used for the manufacturing of TiMMCs and Ti6Al4V-MMCs are conventional Cold Pressing and Sintering (CP-S), Hot Pressing (HP) and Metal Injection Molding (MIM). Additionally, techniques as Spark Plasma Sintering (SPS), Hot Extrusion (HE), High Velocity Compaction (HVC) and Equal Channel Angular Pressing (ECAP) are occasionally used.

The specification of the type of reinforcement as particle or fibers is also reported in the next table. In the case of composites reinforced with nano-diamonds particles and carbon nano-fibers, their applications in the different industry sectors are not actually defined.

In the present work, the addition of different reinforcements to titanium and Ti6Al4V is studied and evaluated.

Firstly as ceramic particles, TiB_2 particles and nano-boron particles are used. In this way in-situ Titanium and Ti6Al4V composites are manufactured by admixing the element. Thereafter, possible reaction between the titanium based matrix and the boron reinforcement can take place at the different sintering and hot consolidation temperatures (see Figure 1-22).

In the same way, in-situ manufacturing of the titanium and Ti6Al4V matrices reinforced with carbon nano-fibres and nano-diamonds is carried out. The processing temperature is varied in order to study the reactivity of the titanium based matrix with the carbonaceous reinforcements (see Table 1-8).

Table 1-8. Reinforcements used for the fabrication of several types of TiMMCs and Ti6Al4V-MMCs.

Matrix	Reinforcement	Manufacturing	Applications	References
Ti	TiC/ TiN (particles)	HP MIM CP-S	Solving tribological fretting problems	[60-66]
Ti6Al4V				[67, 68]
Ti	SiC/ Si_3N_4 (particles)	ECAP SPS HE CIP	Aeronautic Wear resistence	[62, 65]
Ti	TiB_2 / TiB (whiskers)	CP-S	Aerospece Automotive Defense industry	[69-72]
Ti6Al4V				[58, 73]
Ti	Hydroxyapatite (HA- particles)	HVC MIM	Biomaterial for dental implants	[50, 74]
Ti6Al4V				[50, 74]
Ti	Boron (B- particles)	PM	Aerospece Automotive Defense industry	[71, 75-77]
Ti6Al4V				[71, 75-77]
Ti	Carbon Nanofibres (CNFs)	HP		[78, 79]
Ti	Carbon Nanotubes (CNTs)	HP		[78, 80]
Ti	Nanodiamonds (NDs- particles)	HP SPS	Wear resistance Tool applications	[81-83]

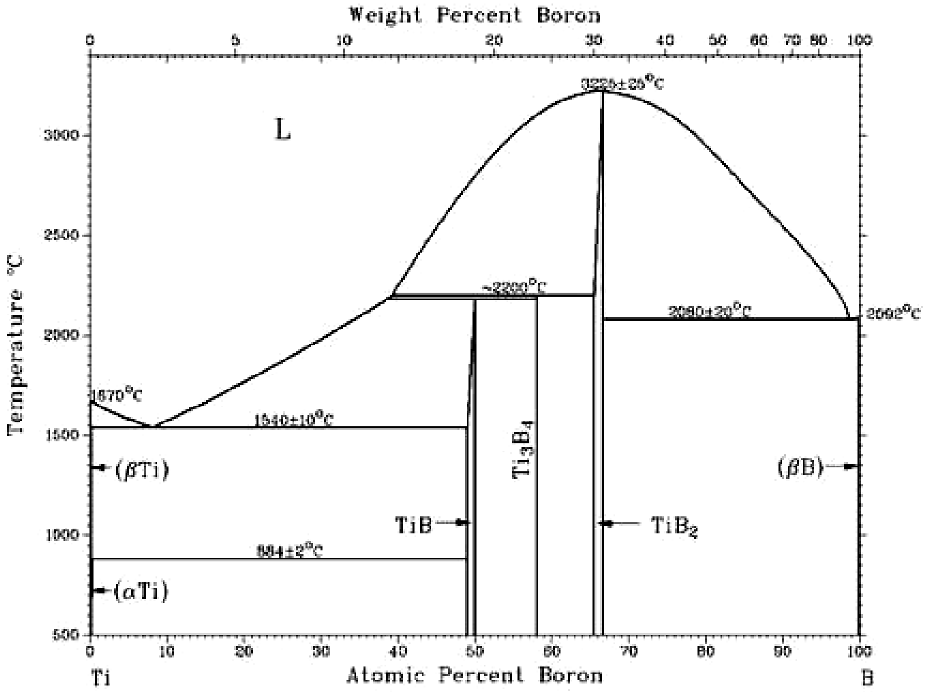

Figure 1-22. Binary phase diagram Titanium - Boron

2 Manufacturing Processes and Characterisation techniques

2.1 Manufacturing Equipment and Processes

The fabrication of the TiMMCs via powder metallurgy (PM) was previously documented in chapter 2 of this work.

Usually, the procedure to fabricate the composites involves different stages from the characterisation and selection of the raw materials to the final characterisation of the composites.

As an overall view for manufacturing of the titanium composites in this present work, the next Figure 2-1 shows the different stages of the fabrication process.

After the selection of the starting powder, the powder preparation and mixing processes took place here.

The powder metallurgical (PM) process used for the manufacturing of the compacts was not specified in the diagram, since three possible methods were employed. Depending on the reinforcement material and the starting matrix powders used, the PM techniques and processing parameters used were varied. That means, for each type of starting powder and reinforcement materials, different consolidation conditions were employed. Furthermore, the manufacturing of the composites via PM was only carried out by the three proposed techniques (CP-Sintering, HP and iHP) for the fabrication of specific composite materials (e.g. Titanium matrices reinforced with nano-diamonds).

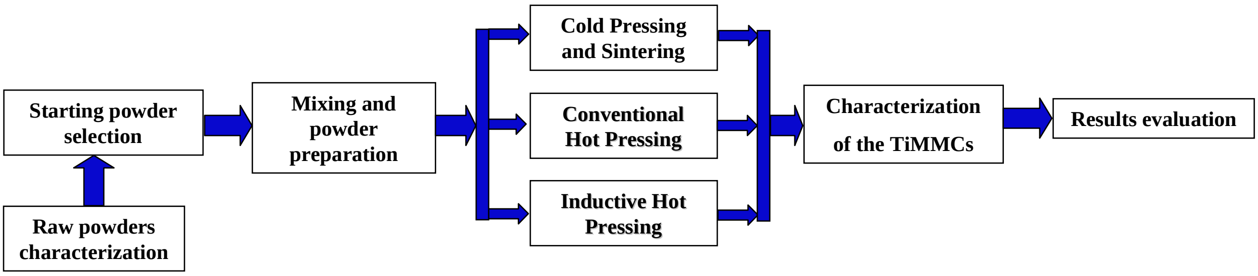

Figure 2-1. Overview of manufacturing routes of the TiMMCs.

The advantages/disadvantages of the three Powder Metallurgical (PM) techniques for the development of the titanium based composites are described.

The consolidation techniques employed for the fabrication of the composites were:

- Cold-Pressing and Sintering (CP+S).
- Conventional Hot Pressing (HP).
- Inductive Hot Pressing (iHP).

In this section, a general description of these processes is provided. The processing parameters and conditions are reported in the experimental part (Chapter 5).

2.1.1 Powder Treatment (Mixing)

The manufacturing process commenced with the powder preparation, mixing.

Basically the first stage is mixing of the powders in order to get a homogeneous mix.

For all the mixing, the tubular "Sintris mixer" was employed.

The use of cyclohexane as solvent to avoid powder agglomeration, supported by ceramic balls, was standard in all the experiment.

However, the amount, type and size of the ceramic balls (Al_2O_3 or ZrO_2) and the mixing time depend on the type of the titanium composite fabricated.

Qualitatively, the most common mixing procedure consists of weighing a given powder amount. The volume of this powder quantity should be the same volume as that of balls and solvent, respectively (see in Figure 2-2).

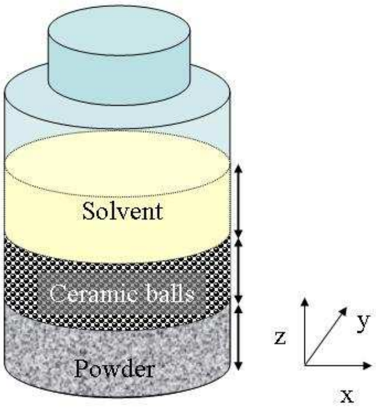

Figure 2-2. Qualitative sketch of the mixing assembly inta plastic bottle.

Next to the wet-mixing process, the powders were perfectly dried. The time for this stage was depending on the amount of solvent (from 6-16 hours).

Finally, the dried powder was blended for a certain period of time without the ceramic balls.

This blending time varied from 15 min to 1h depending on the characteristics and content of the mixing in order to avoid agglomeration of the reinforcement after the drying. After that the powders were ready to be compacted.

2.1.2 Powder Consolidation

2.1.2.1 Cold Pressing Process and Sintering

Cold Pressing

For the uni-axial cold pressing, a hydraulic press PE 50 from Jessernigg and Urban Co. was employed. In spite of its press capacity of 500 kN, the maximum force used was 68 kN only.

The starting powder was placed into a cylindrical die (12 mm inner diameter) or in a rectangular die (55 mm x 6.4 mm section), the wall of the die was lubricated with paraffin to facilitate the ejection of the compacted samples (“die wall lubrication”). The dies used are shown in the next Figure 2-3.

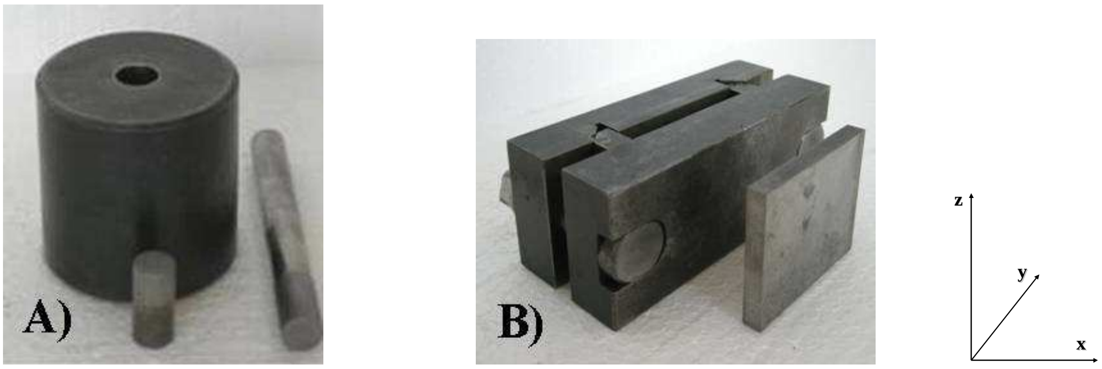

Figure 2-3. Cold pressing die and punches. A) Cylindrical die (12 mm inner diameter). B) Rectangular die (55 x 6.4 mm^2).

The geometrical dimensions of the green compacts were according to the die used, i.e. 12 mm diameter or 6.4 x 55mm^2, and 5mm of height approximately for both types of green compact (see in Figure 2-4). This height depends on the amount of powder used.

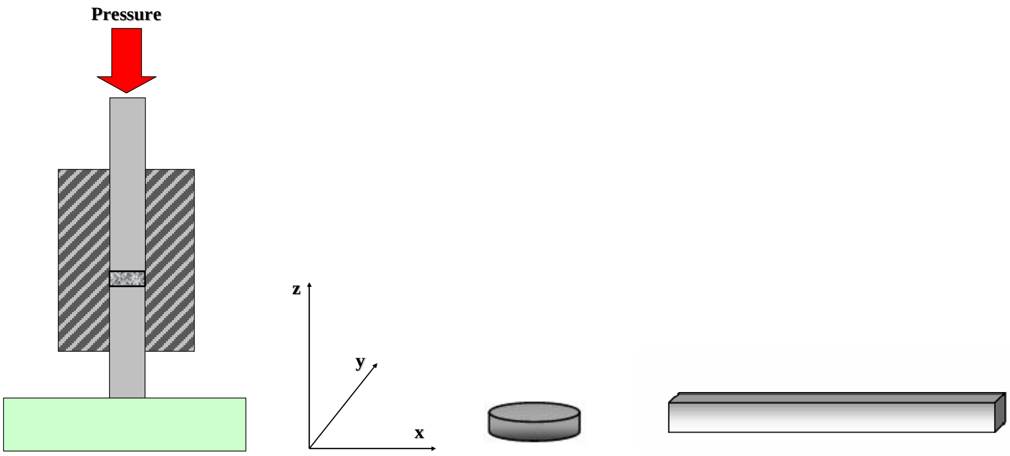

Figure 2-4. Cold Pressing set up and geometrical dimensions of the titanium green compacts.

Sintering process

All the sintering process was carried out in high vacuum using a Thermal Technology Inc. furnace model Astro. It can reach 10^{-6} mbar nominal vacuum and 1650ºC as maximum temperature. However the sintering temperatures employed here ranged between 1200º and 1300ºC.

2.1.2.2 Hot Consolidation Processes

As already mentioned in chapters 1 and 2, hot pressing is a consolidation process which requires the simultaneous application of pressure and temperature. In summary, hot pressing here consisted of loading loose powders into a die made of graphite. It was always lined with a thin graphite foil coated with boron nitride (BN). The die preparation was done in the same way for all the hot pressing processes to reduce reactions between the die and the titanium based powders that were consolidated. The die assembly was then loaded into the hot pressing equipment. The equipment (for HP and iHP processes, respectively) consisted of a vacuum chamber, heating elements for the furnaces and the press ram which supplied the required load (in the z-direction) to the punch in each process (HP and iHP).

The applied pressure was always uni-axial. A small amount of pressure was usually applied to the punch before the temperature was raised. Comparing conventional hot pressing to inductive hot pressing, some advantages and disadvantages of each one can be defined; they are reported in the next Table 2-1.

On one hand, inductive hot pressing presents short process cycles and a high heating rate in comparison to the conventional hot pressing. However at conventional hot pressing the load is quite superior to that allowed for the inductive hot pressing.

Table 2-1. Comparison between the two hot pressing technique used.

Process parameters	Conventional Hot Pressing	Inductive Hot Pressing
Heating rate	Low (<20 K/min)	High (<100 K/min)
Process cycle	Long (> 8 h)	Short (< 1 h)
Die dimensions	Variety of dies (up to 200mm Ø)	Limited (10 mm Ø)

Therefore, the limited dimension of the produced titanium composites made the study of their mechanical properties difficult (see Table 2-2). This restricted characterisation of the compacts; thus limited properties of the composites prepared by iHP could be measured which partially makes a comparison to other processes difficult. After hot pressing (HP and iHP), the specimens were removed from their respective dies. The graphite foils were completely separated from the compact surfaces by sand blasting. Their final dimensions varied according to the die used. The next Table 2-2 shows the different die geometries employed for the manufacturing of the titanium based specimens.

Table 2-2. Conventional and inductive hot pressing die geometries

Hot pressing technique	**Graphite matrix**		
	Section geometry	Dimensions (mm)	Filling height (mm)
Conventional HP	Square	13.5 x 13.5	4
	Circular	Ø 100 and 65	6
Inductive HP	Circular	Ø 10	4

The hot pressing atmosphere for the fabrication of titanium based compacts was vacuum 10^{-1} mbar for the conventional HP and to 10^{-5}- 10^{-6} mbar for the inductive HP. This was another advantage of the inductive HP .This vacuum level was achieved using a special turbomolecular pumping system.

2.1.2.3 Conventional Hot Pressing

The conventional hot pressing processes were carried out in a hot press HPW 315/400-2200-1000-PS (FCT, Rauenstein, Germany). The mechanical pressure applied was 30 MPa and the heating rate was 10 K/min. These conditions were fixed for all the experiments. Also the vacuum was for all the experiments close to 10^{-1} mbar. The vacuum used was the maximum allowed by the hot pressing equipment.

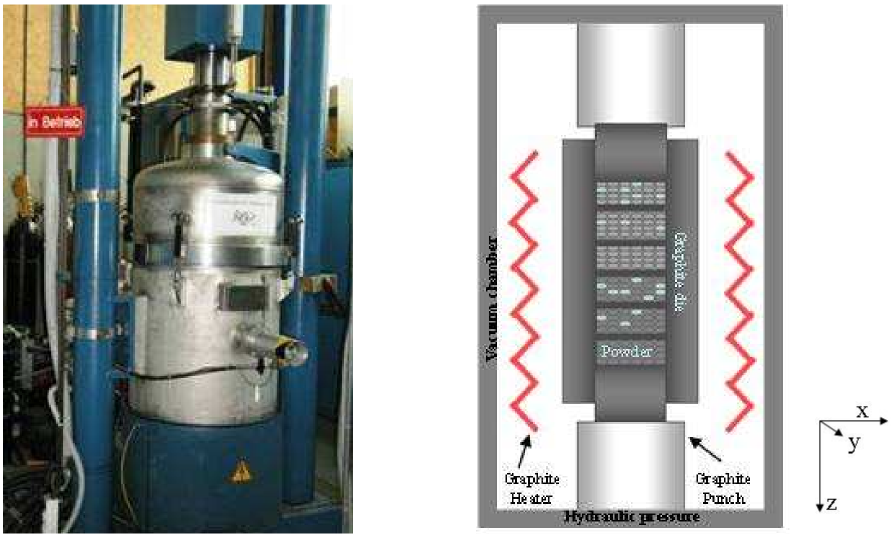

Figure 2-5. Conventional Hot Pressing equipment of Austrian Research Centers GmbH.

The composite geometry produced was varied depending on the die used in each fabrication procedure. The following images show the geometries of the dies used to perform the hot consolidations (see in Figure 2-6 and Figure 2-7).

Figure 2-6. Conventional hot pressing matrix with 12 square cavities used for the development of TiMMCs

In case of conventional HP, large plates could be produced with diameter of 100 mm and 5 mm in height (see Figure 2-7). From these discs, mechanical test specimens could be easily obtained.

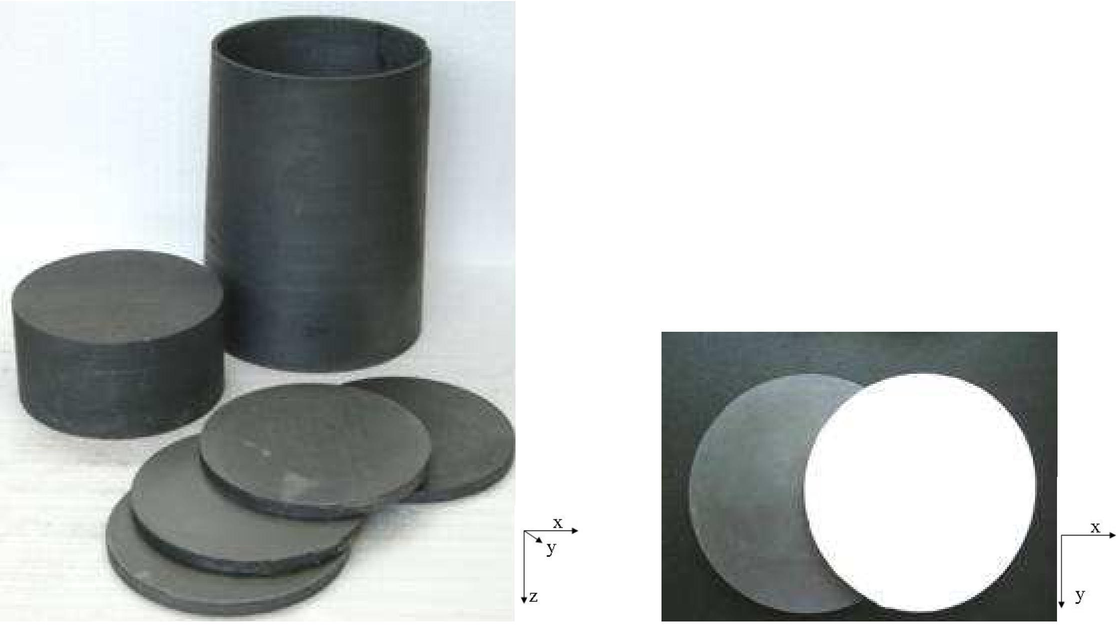

Figure 2-7. Conventional hot pressing die and plates from graphite in addition to graphite foil coated with boron nitride powder, used for the manufacturing of larger samples of TiMMCs

2.1.2.4 Inductive Hot Pressing

For this innovative hot pressing process, a self-made Inductive Hot Pressing machine was used.

The advantage is a high heating rate due to its special heating set up (see Figure 2-8)

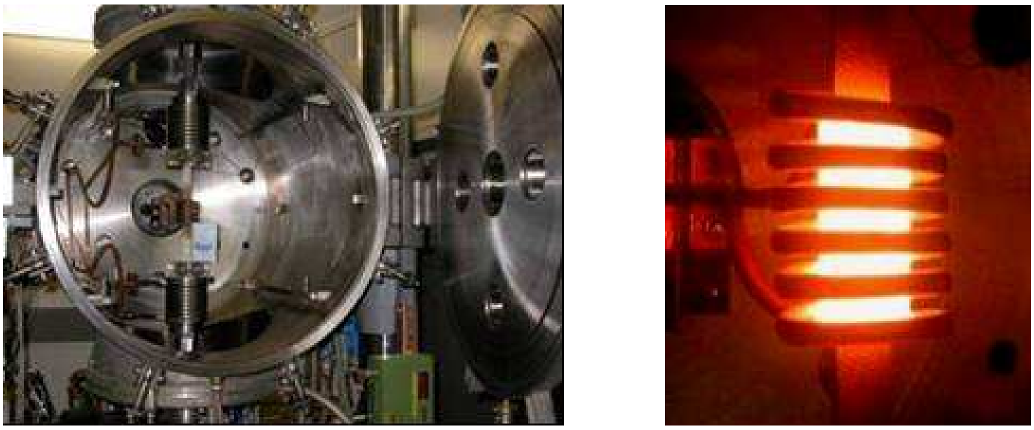

Figure 2-8. Inductive Hot Pressing equipment of Austrian Research Centers GmbH.

The die used for all the inductive hot pressing experiments is shown in the next Figure 2-9.

For each one of the inductive hot pressing tests the die was always lined with thin graphite. The number of samples produced was usually two specimens for one cycle (see in Figure 2-9).

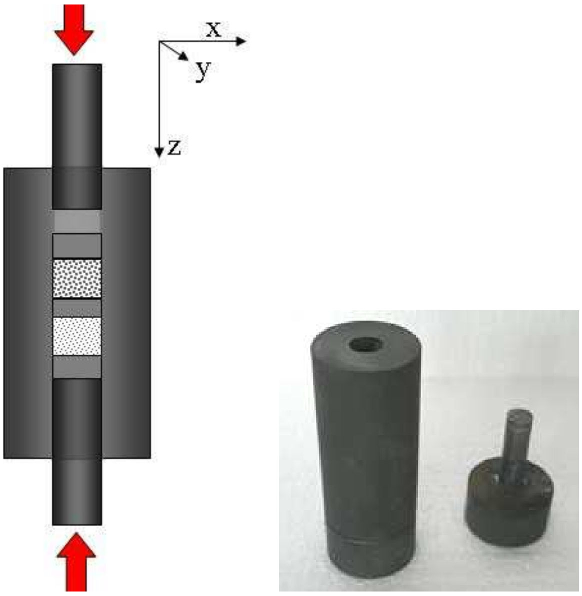

Figure 2-9. Inductive hot pressing die.

Hot pressing profiles:

The next Figure 2-10 shows qualitatively the typical temperature-time profiles for the conventional and inductive hot pressing cycles.

Additionally the difference of the isothermal holding time is also evident. Compared to the 15 min holding time for inductive hot pressing, the holding time of the conventional hot pressing can be varied from 60 min to 120 min, depending on the consolidation requirements.

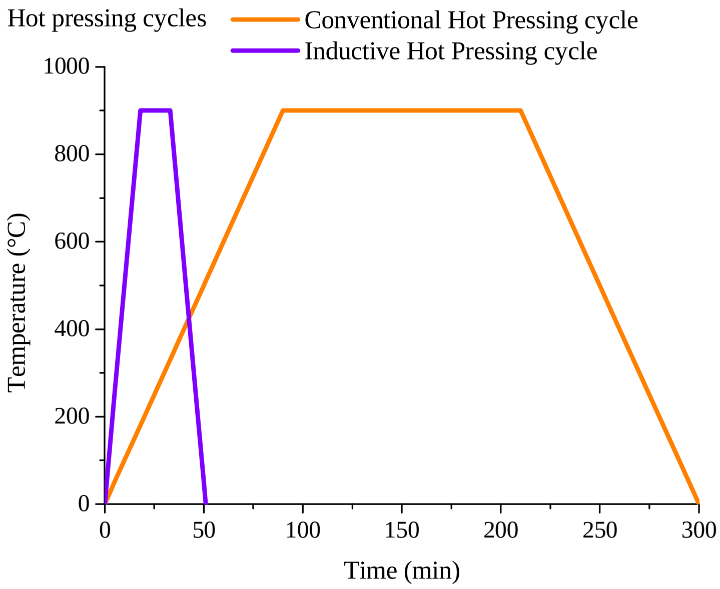

Figure 2-10. Profiles of the temperature (°C) vs. time during a conventional compared to inductive hot pressing operation.

2.2 Characterization techniques

2.2.1 Particle size analysis

The particle size analyser used was the Mastersizer2000. The measuring range of this equipment is nominally 0.02 to 2000 µm, depending on material properties.The used powders were in that range. Here, the measuring principle applied is sedimentation method. To start the analysis of the particle size of the powders, they were dispersed in a liquid. Generally it was distilled water. That equipment has incorporated a system of laser diffraction particle sizing. In this way, the particle size rage is calculated. The results of this characterisation technique are given in the chapter 3.

2.2.2 Density measurements

Density of the powders

In the pycnometer "AccuPyc 1330V3.3" (Helium pycnometer), the density of several powders was measured. The results of this characterisation are reported in the description of the starting materials (see Table 3-3 and Table 3-9 in chapter 3).

Density of the compacts

The results of all the density measurements are reported and listed in chapter 5.

- Geometrical density

In some cases (for the Cold pressing-Sintering process) it was possible to calculate the geometrical density before and after sintering from the dimensions and mass of the compacts (see Figure 2-11).

Figure 2-11. Green and sintered compacts

For the calculation of the geometrical density of the specimens, the Equation 2-1 was used.

$$\rho_g = \frac{m}{V}$$

Equation 2-1. Geometrical density.

ρ_g: geometrical density of the compact (green or sintered stage)
m: weight of the compact. V: volume of the compact = $d^2/4.\pi$

- Archimedes’ density:

It was measured in water, in some case using paraffin or water-stop spray coatings, and in other cases – if open porosity was definitely absent - without coatings.

a) The next Equation 2-2 was used for the calculation in water with the water-stop coating or without paraffin.

$$\rho = \frac{m_a * \left[\rho_{fl} - \rho_a \right]}{m_a - m_{fl}} + \rho_a$$

Equation 2-2. Archimedes’s equation for the calculation of the density.

ρ : density of the compact (sintered stage)

ρ_a : density of the air

m_a : weight in air with out paraffin

ρ_{fl} : density of the distilled water

m_{fl} : weight in distilled water

Firstly, the mass of the compact is measured in air. Afterwards, the water-stop spray is applied on the surface of the compact (just in the case in which the water-stop spray was used), and the specimens are then dried. Next, the mass of the compact mass is measured in water. If the temperature of the distilled water is 20ºC, its density is 0.998 g/cm^3. At the same temperature, the density of the air is around 1.204x10^{-3}g/cm^3. Since >>> ρ_a and ρ_{fl} is near 1, the previous Equation 2-4 is simplified to Equation 2-3.

$$\rho = \frac{m_a}{m_a - m_{fl}}$$

Equation 2-3. Archimedes equation simplified. Measurement without paraffine or with the water-stop spray.

b) The Equation 2-4 was employed for the calculation of the density in water and with paraffin.

$$\rho = \frac{m_a}{\left[\frac{m_p - m_w}{\rho_w} - \frac{m_p - m_a}{\rho_p} \right]}$$

Equation 2-4. Archimedes’s equation for the calculation of the density using paraffin

ρ : density of the compact (sintered stage)

m_a : weight in air without paraffin

m_p : weight in air with paraffin

m_w : weight in distilled water with paraffin

ρ_{fl} : density of the water (1g/cm^3 at RT)

ρ_p : density of the paraffin (0.9 g/cm^3 at RT)

The procedure is similar to the previously described method. In this technique, the application of the paraffin as coating takes place after the mass measurement in air. The mass of the coated compacts in air is measured. After that, the weight of the coated compacts is measured in the distilled water.

2.2.3 Hardness measurements

For the Vickers hardness (HV10), a tester model “Shimadzu HSV-30” was used.

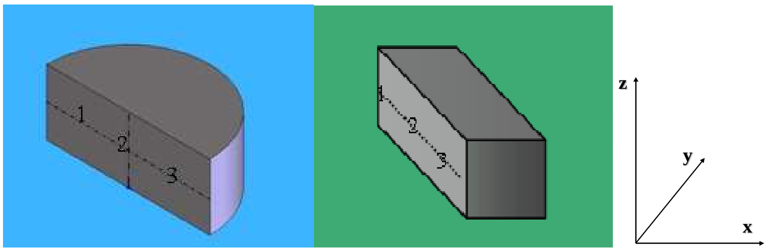

Figure 2-12. Schematic where in the sections of the compacts hardness measurements take place.

The hardness measurements were carried out on polished cross sections of the compacts (see in Figure 2-12). In general, the specimens were cut into several parts for their characterisation.

Afterwards, the cut surfaces were perfectly prepared, polished and cleaned, to carry out the hardness measurements.

Depending on the geometry of the specimens, the number of measurements varied. The normal number of hardness measurements was 3 along the cross section of the specimens. However, larger samples required a minimum of 9 measurements (see Figure 2-13).

The hardness measurement was used in several cases to check if the uni-axial compaction had resulted in homogeneous density or not (see chapter 5th).

2.2.4 Chemical analysis

Chemical analysis of the starting powders:

All the chemical analyses of the starting materials were carried out in a LECO TC 500. With the LECO TC 500 it is only possible to measure the oxygen and nitrogen content of the samples. When testing titanium based powder, the equipment has to be calibrated prior to measuring the oxygen and nitrogen contents.

The amount of powder tested is around 0.3 g.

Firstly, the starting powder is wrapped into a tin paper. Simultaneously, it is introduced into a tin-basket.

The sample is placed in the loading area. From that place it is pneumatically moved to the graphite crucible which is then set into a powerful electrode impulse furnace. In the crucible the reaction of the sample with the graphite of the crucible takes place. Through a Helium flow, the CO/CO_2 liberated is carried out of the furnace and quantified though an infrared detector.

Chemical analysis of the compacted samples:

The chemical analyses of several compacts were carried out in a LECO TC 500 and LECO TC 600, for oxygen, nitrogen and hydrogen contents.

The measuring procedure is similar to that used for the characterisation of the powders. After the calibration of the equipment the specimens are tested. For that, the maximum weight of the samples must not exceed 0.4g. The minimum weight of the samples has to be > 0.2g. To measure titanium specimens the use of the tin-basket is always necessary.

2.2.5 Microstructural study

Light Microscopy

For the determination of the titanium alpha phase, an optical microscope “LEICA DMI5000M” with polarised light for the observation of the hexagonal close-packed structure of this alpha phase was used. Additionally, another optical microscope “Reichert-Jung MeF3” was employed for the microstructural study of the specimens.

SEM/EDX

- Equipment used:

1) An SEM Zeiss Gemini Supra VP40 was employed firstly for the characterisation of many starting materials. The morphological studies on the powder materials and reinforcement particles were carried out using this equipment. Additionally, a chemical component mapping for the two Ti6Al4V powders was carried using this equipment. Secondly it was used for the characterisation of titanium and Ti6Al4V compacts.

2) Zeiss 1540XB crossbeam equipment was used just for the study of the composites: The Focused Ion Bean (FIB) technique was employed for the study of the interface between the reinforcement particle and the matrix in some of composites fabricated, e.g nano/micro boron particles in a titanium matrix.

2.2.6 Tensile tests

The tensile properties of some composites were measured in a tensile tester. The tested materials were titanium and Ti-6Al-4V matrices reinforced with nano/micro boron particles. Also pure matrices, without boron additions fabricated at the same conditions as the composites were tested.

The tensile tests were carried out in the “Shimadzu AG-10TC”. The test standard was DIN 10002-1 for measurements at room temperature (RT). The crosshead speed was is 0.5 mm/min. The initial fixing length of the sample was 80 mm.

Considering the standard dimensions for the tensile test, the plates were perfectly cut (see Figure 2-13) using an electro discharge machine.

In all these plates each cut piece was numbered in the same way; thus the samples “1” to “5” were employed for the measurements of tensile properties. Furthermore, the tensile properties of these materials were measured. For that reason the remaining parts of the plate were simultaneously cut according to the tensile test standard (it is described in the next part).

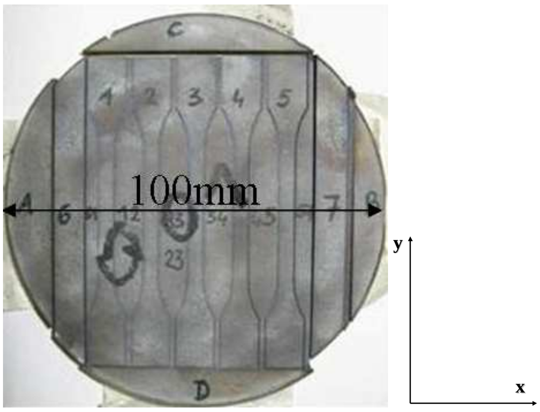

Figure 2-13. TiMMCs plates after conventional hot pressing (for 2h at 900°C, 30 MPa and vacuum 10^{-1} mbar).

Tensile test at high temperature

To study the tensile properties of the manufactured composites at higher temperature, additional tests were performed. At 250º and 450ºC, the tensile properties of the consolidated composites were measured and compared with the tensile properties of the titanium and its alloy (Ti-6Al-4V) at the same temperature. These matrices were manufactured on the same conditions as the composite plates. For measurement at 250º and 450ºC, the test standard DIN 10002-5 was employed. The test velocity was 0.5mm/min for both tests (at 250° and 450°C).

The setup for the tensile test at high temperature (250° and 450°C) is illustrated in the next Figure 2-4 (left). Also the special holder is represented Figure 2-4 (right)

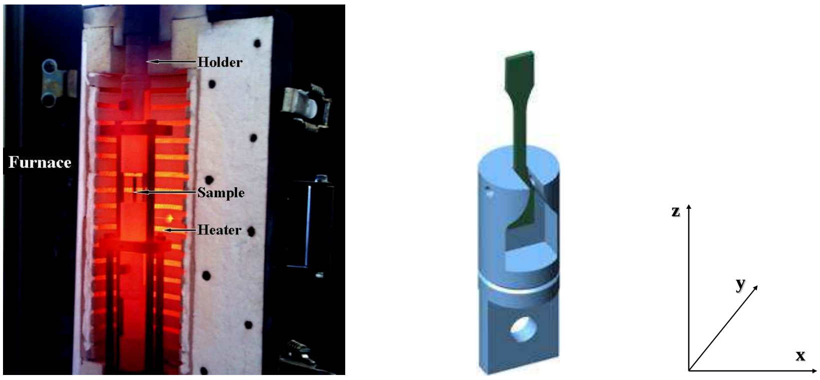

Figure 2-14. Tensile test setup at high temperature (left) and sample holder used (right).

2.2.7 Flexural tests

The flexural properties were measured using two different equipments. The specified dimensions of the compacts were varied according to the equipment employed.

First flexural tests:

As mentioned previously, the other samples “6”, “7” and “A” to “D”, from the fabricated plates (Ø 100mm), were also cut. They were employed for the bending test. Other pieces were used for the hardness measurements, e.g. 12 (between the sample “1” and “2”).

This can be seen in the Figure 2-13. The three point flexural test was employed as technique to measure the flexural properties of the specimens. As test standard used was EN 7438. The equipment employed was the machine “Shimadzu AG-10TC”. All the measurements were done at room temperature (approx.20°C). The crosshead speed was 0.1mm/min. According to the flexural test used and for rectangular cross section, the next equations were used to calculate the flexural strength and maximal deformation.

$$\sigma = F \cdot \frac{3 \cdot l_s}{2 \cdot b \cdot a^2} \left[MPa \right]$$

Equation 2-5. Flexural stress.

σ: flexural stress and strain; l_s: distance of support-dogs;

a: thickness; b:width;

$$\varepsilon = f \cdot \frac{600 \cdot a}{l_s^2} \left[\% \right]$$

Equation 2-6. Deformation after flexural test.

ε: deformation; f: deflection (for plastic deformation); a: thickness;

Bending tests carried out secondly:

A method to measure the flexural properties of the specimens was also the three point flexural test at room temperature. MPIF Standard 41: "Determination of Transverse Rupture Strength of Powder Metallurgy Materials" was the standard used for these bending tests. The equipment employed was a uni-axial hydraulic press “MICROTEST”. The crosshead speed was 0.4 mm/min.

The specimens used for the three-point flexural tests were produced through two different manufacturing processes: conventional hot pressing (HP), and cold-pressing and sintering process. On one hand, the hot consolidation produced plates with 65 mm diameter and approximately 4 mm thickness.

After consolidation, the cutting of these specimens was done using the “Discotom-6” for the large slide and „Accutom-50“ for the thick slices. On the other hand, some specimens were directly cold pressed and sintered in the rectangular cold-pressing die (see Figure 2-3). The final geometrical dimension exceeded the standard dimensions for the flexural test. For that reason, the specimens had to be cut ($6.4x3.5x24mm^3$ approx see in Figure 2-15.), using a conventional diamond-blade cutting machine.

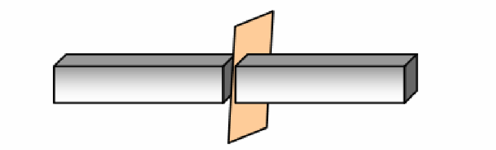

Figure 2-15. Geometrical dimensions for the specimens to measure the flexural properties, after cold-pressing and sintering ($6.4x3.5x24mm^3$ approx.).

To be sure that the dimensions of the compacts were suitable to carry out the test, the next Equation 2-7 was employed.

$$TRS = \frac{3 \cdot F \cdot L}{2 \cdot w \cdot t^2}$$

Equation 2-7. Transverse rupture strength calculation (3-point).

TRS: Transverse rupture strength (MPa) F_{max} = 5000 N (max. load of the equipment)

L = 23.8mm w = 6.4mm t : thickness

The calculations of the deformation and strength was carried out using the Equation 2-5 and Equation 2-6.

3 Starting Materials

In this chapter a detailed description of the materials (matrix powder and reinforcements) used in the experimental work is given. It is structured according to the type of raw materials described.

The characterisation of all of them has been performed in the same way. Firstly, the oxygen and nitrogen contents of the powders materials and reinforcement materials have been analysed by LECO TC500.

In the majority of the powder materials, the particle size has been measured by Mastersizer. Additionally, SEM images of all the materials have been taken by the Zeiss HRSEM, which is equipped with EDAX and EDS/EBSD Detectors.

Finally, the pycnometer AccuPyc 1330V3.3 has been used to determine the density of the powders.

3.1 Matrix powders

3.1.1 Commercial pure titanium (CPTi) and titanium hydride powders (TiH_2)

Occurrence and price:

Considering the previous works, commercial pure titanium (CPTi) and titanium hydride (TiH_2) powders [84, 85] were selected for the manufacturing of the titanium specimens.

The quality and price of these powders varied widely depending on supplier, particle size and fabrication process used for the powders. Additionally, their oxygen content and level of other impurities affects the price.

An intensive search of suppliers was done in order to evaluate the markets for titanium based powders and to achieve good relationship price/quality.

In the next Table 3-1, the origin and cost per kg of the titanium based powder are listed.

Table 3-1. Origin and price of the different titanium based powders (purchased in 2006).

Type of powder	Supplier	Country	Price (Purity >95%)
CPTi (1)	Phelly	USA	100-200 $/kg
CPTi (2)	Parameet	South Korea	
TiH_2 (3)	Phelly	USA	80-400 $/kg
TiH_2 (4)	Parameet	South Korea	
TiH_2 (5)	Toho	Japan	
TiH_2 (6)	Chemetal	Europe	

Important factors increasing the price are low oxygen content and high purity of the powder. These, in addition to the particle size, were considered for the selection of the starting powders. Thus, two commercial titanium powders and four titanium hydride powders were employed as starting powders for a detailed analysis.

Chemical composition, particle size distribution and density measurements:

All the CPTi powders were of grade 4; this means the theoretical content of oxygen is below 0.4 mass% (see specification for CPTi grade 4 in Table 1-4 and Table 1-5). However the results of the oxygen analysis were different. These values measured are reported in the following Table 3-2, in addition to the particle size measurements. In the case of the powder CPTi(1) its particle size, this data was be supplied by the manufacturer.

Table 3-2. Oxygen and nitrogen contents and particle size distribution of all the titanium based powders used. CPTi (1)*according to the manufacturer.

Type of powder	Particle size distribution			Impurity content	
	d_{10} (µm)	d_{50} (µm)	d_{90} (µm)	O (mass%)	N (mass%).
CPTi (1)*	3.33	9.99	30.00	0.59	0.01
CPTi (2)	6.65	13.75	25.63	0.45	0.01
TiH_2 (3)	4.60	10.12	19.61	0.77	0.15
TiH_2 (4)	3.97	7.82	21.73	0.62	0.11
TiH_2 (5)	3.77	7.19	13.48	0.62	n.d.
TiH_2 (6)	5.23	10.85	20.60	1.47	n.d.

Finally, the theoretical density values of the two different powder materials as obtained by pycnometry are given in Table 3-3.

Table 3-3. Theoretical density values obtained by the pycnometer and compared to the literature values.

Powder material	Measured density by pycnometer (g/cm^3)	Theoretical density (g/cm^3)
CPTi Grade 4	4.53± 0.04	4.50-4.54 [1, 18]
TiH_2	3.97± 0.08	3.9[86]

Powder morphology

The scanning electron microscope (SEM) was used to observe the morphology of all the starting powders. The SEM images of the powder were taken by the secondary electron detector.

In this way, a qualitative morphological study of the particle was performed.

The morphology of the different titanium based powders is shown in Figure 3-1 to Figure 3-6. The CPTi powders (CPTi(1) and CPTi(2)) have similar angular morphology. In the case of CPTi (1), finer particles are observed.

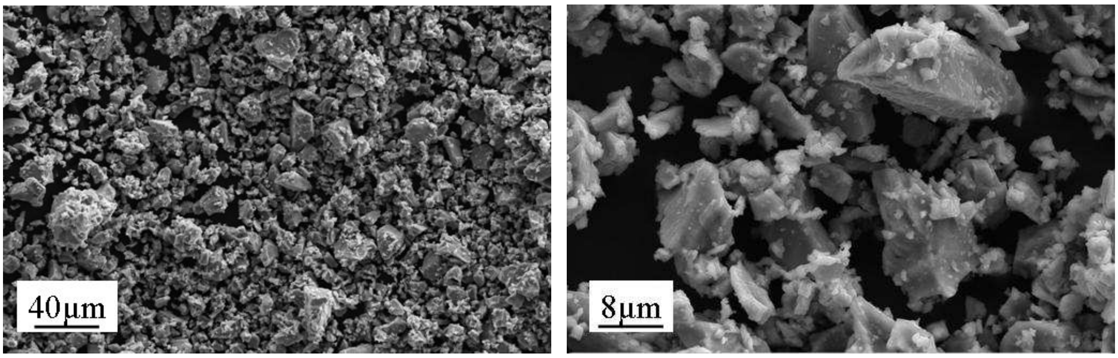

Figure 3-1. SEM images of CPTi(1) starting powder.

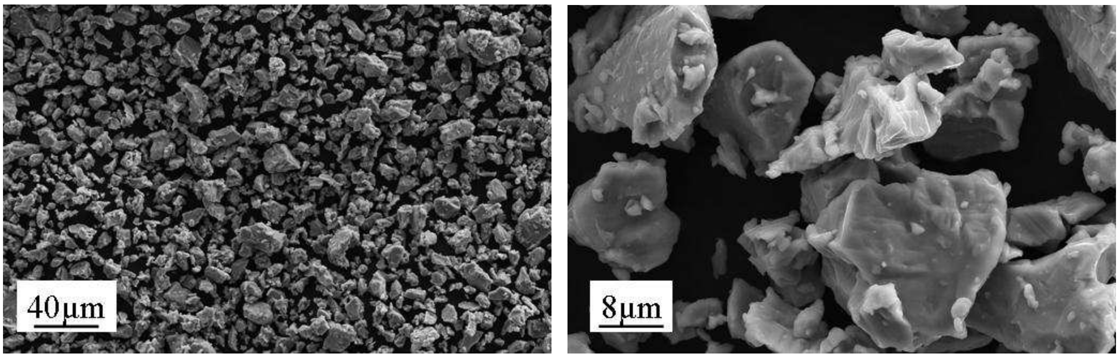

Figure 3-2. SEM images of CPTi(2) starting powder.

The TiH_2 powders (TiH_2(3), TiH_2(4), TiH_2(5) and TiH_2(6)) show a fine and irregular morphology.The TiH_2(3) and TiH_2(4) powders have similar particle size distribution (see Figure 3-3 and Figure 3-4). For both powders finer particles (~ 4µm) are observed in addition to some larger particles (~ 20µm).

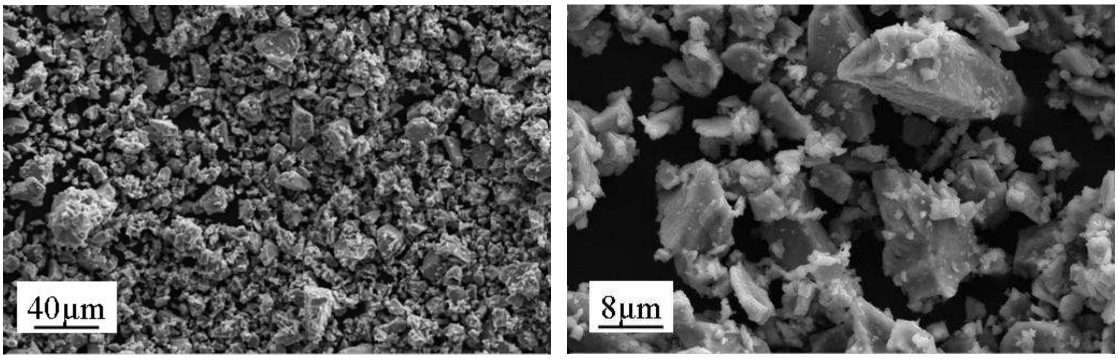

Figure 3-3. SEM images of TiH_2(3) starting powder.

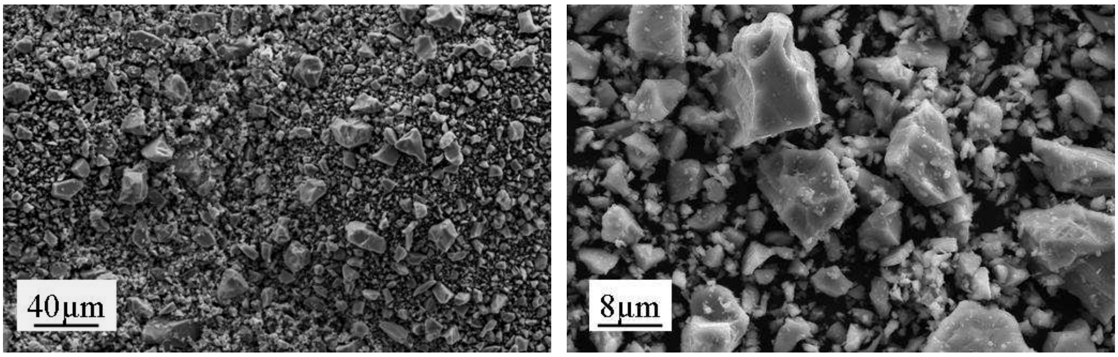

Figure 3-4. SEM images of TiH_2(4) starting powder.

The TiH_2(5) and TiH_2(6) are the finest starting powders. They also have an angular morphology. However, in the TiH_2(5) (see Figure 3-5), the particle size is within a narrower range (~ 3-7µm).

The TiH_2(6), in contrast, was supposed to be the finest powder (~2.7µm) of all of them; but also here larger particles (~ 20µm) are found as visible in Figure 3-6.

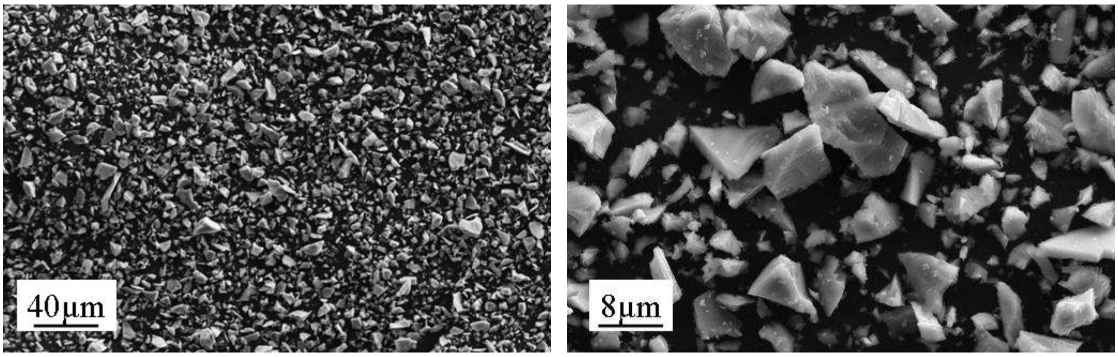

Figure 3-5. SEM images of TiH_2(5) starting powder.

Additionally, agglomerations of finer particles are present in the powder TiH_2(6) such as shown in Figure 3-6.

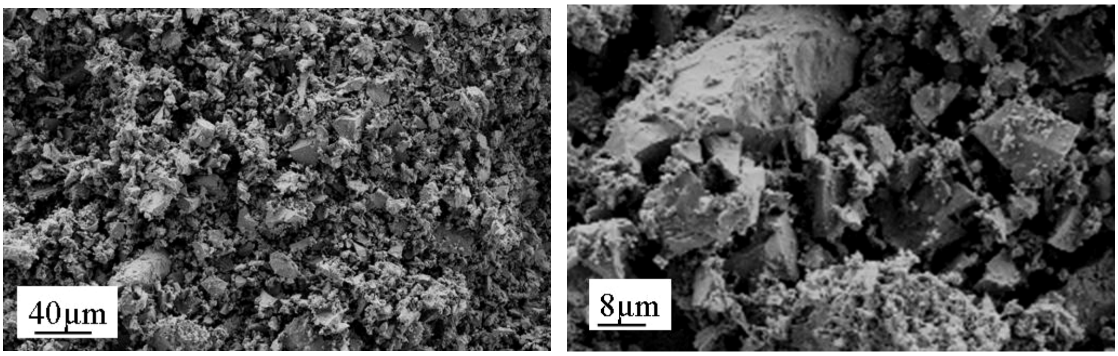

Figure 3-6. SEM images of TiH_2(6) starting powder.

Sintering behaviour:

The sintering behaviour was studied for the CPTi(1), CPTi(2), TiH_2(3), TiH_2(4) and TiH_2(5) starting powders. Due to its highest oxygen content, the TiH_2(6) powder was only used in the preliminary experimental part. For that reason its sintering behaviour was not measured. The other five titanium based powders were cold compacted at 560 MPa. The dimensions of these green samples were length 6.3 mm and diameter 6 mm.

This study of the sintering behavior of these five starting powder (CPTi(1) to TiH_2(5)) was carried out in a dilatometer “Bähr Thermo analyses DIL 802” with an Alumina tubular carrier. The heating rate was 5 K/min up to 1300ºC, after 2 h at 1300ºC in Ar.

The result of the geometrical density measurements is listed in the following Table 3-4.

Table 3-4. Geometrical density of titanium based green samples compacted at 560 MPa. ***(The data for T.D. are available from pycnometry*****)**

Type of starting powder	**Geometrical green density (g.cm^{-3})**	**Relative green density (%)**	**Density relative to T.D. of Ti (%)**
CPTi(1)	3.20	71	71
CPTi(2)	3.43	76	76
TiH_2 (3)	3.02	76	67
TiH_2 (4)	3.02	76	67
TiH_2 (5)	2.88	72	64

In Figure 3-7 and Figure 3-8 the sintering runs (studied in a dilatometer) of these compacts are presented.

The two CPTi powders show lower length change at the same temperature in comparison to the specimens from TiH_2 powders. The difference between the dimensional change with CPTi and TiH_2, respectively, are enormous.

On one side, between the two commercial pure titanium powders, the CPTi(2) was selected as matrix powder since it presents higher sintering activity (shrinkage) in comparison to CPTi(1). Up to 1000°C the length of the green compact from the CPTi(2) changes significantly.

Moreover, the initial oxygen content of the CPTi(2) is 0.45 mass% and thus lower than the 0.59 mass% oxygen in CPTi(1).

On the other side, the study of the sintering properties of the TiH_2 powders reveals that during holding at 1300°C the compacts from TiH_2 (3), TiH_2 (4) and TiH_2 (5) don’t change their dimensions significantly. It means that the sintering of these specimens takes place in the heating section of the sintering run below 1300°C.

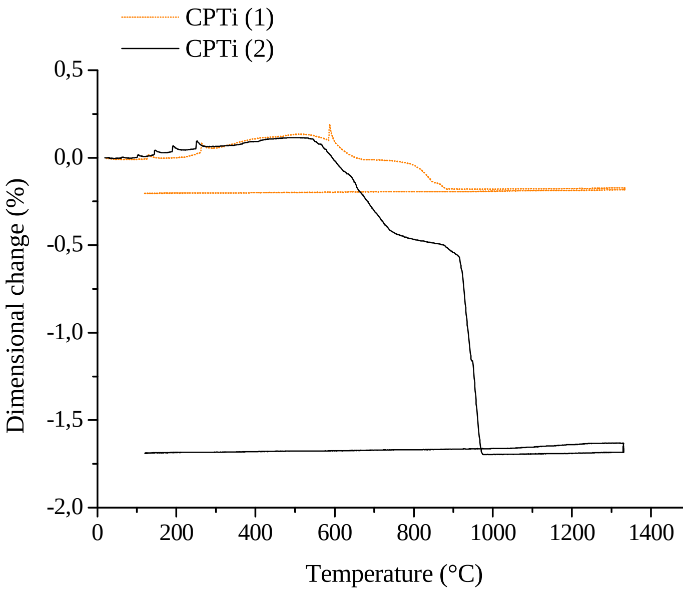

Figure 3-7. Dimensional change (%) vs temperature of the two commercial pure titanium starting powders.

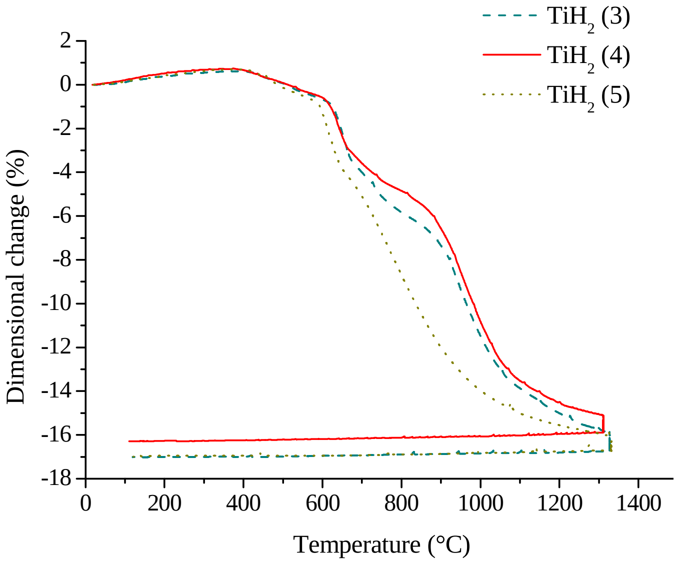

Figure 3-8. Dimensional change variation (%) vs temperature of the three TiH_2 starting powders.

After the sintering, measurement of Archimedes density of these five sintered specimens was carried out. The values of the density are represented and compared to the theoretical density in the next table. Specimens from TiH_2(4) and TiH_2(5) starting powder present values of relative density up to 98%. However, specimens from CPTi(1) and CPTi(2) show values of relative density below 95%. The agreement between the change of density (Table 3-4 / Table 3-5) and the dimensional change recorded in the dilatometer is acceptable for the TiH2 based materials but unsatisfactory for the CPTi based compacts; possibly there is anisotropic shrinkage perpendicular / parallel to the pressing direction. Furthermore, the oxygen content of the TiH_2 (3) exceeds 0.70mass%, for that reason this powder grade is not a suitable candidate for the production of metal matrix composites. The oxygen content after the sintering of the green compacts from the five titanium based powders is analysed in order to evaluate possible reduction of the oxygen content.

Table 3-5. Archimedes density of the sintered specimens.

Sample	**T.D (g/cm^3)**	**Arch. density (g/cm^3)**	**% Relative density**
CpTi(1)	4.54	4.30	94.7%
CpTi(2)	4.54	4.29	94.5%
TiH_2(3)	4.54	4.34	95.5%
TiH_2(4)	4.54	4.45	98.1%
TiH_2(5)	4.54	4.46	98.3%

3.1.2 Titanium alloy powders: Ti-6Al-4V

Oxygen content and particle size distribution:

After the search of suppliers for Ti-6Al-4V powder, the two most promising powders were ordered. The selection of the powder was done with respect to purity and particle size. Confirming that the previous results of the supplier's characterisation of the Ti-6Al-4V powders were reliable, chemical analysis and particle size measurements were carried out (see Table 3-6 Impurities).

Table 3-6 Impurities and Particle size distribution of the two Ti-6Al-4V powders used.

Type of Ti6Al4V powders (Supplier)	**Particle sizes) (µm)**			**Impurity**			
	d_{10} (µm)	d_{50} (µm)	d_{90} (µm)	O mass%	N mass%	C mass%	S mass%
Ti-6Al-4V (1) USA (Phelly)	20.92	43.03	78.36	0.50	0.044	0.043	0.0003
Ti-6Al-4V (2) Italy (MBN)	11.16	29.13	56.29	0.49	n.d.	n.d.	0.0022

Powder morphology:

The morphological study of these two Ti6Al4V powders was carried out. The SEM-images of the two grades Ti6Al4V(1) and Ti6Al4V(2) in addition to images from the optical microscope were used for such a morphological study. The SEM images of the two Ti-6Al-4V powders show the morphology of these powders (Figure 3-9). Both Ti6Al4V powder possess angular and irregular morphology. The Ti6Al4V(2) is finer than the Ti6Al4V(1), therefore it presents more particle agglomeration than Ti6Al4V(1).

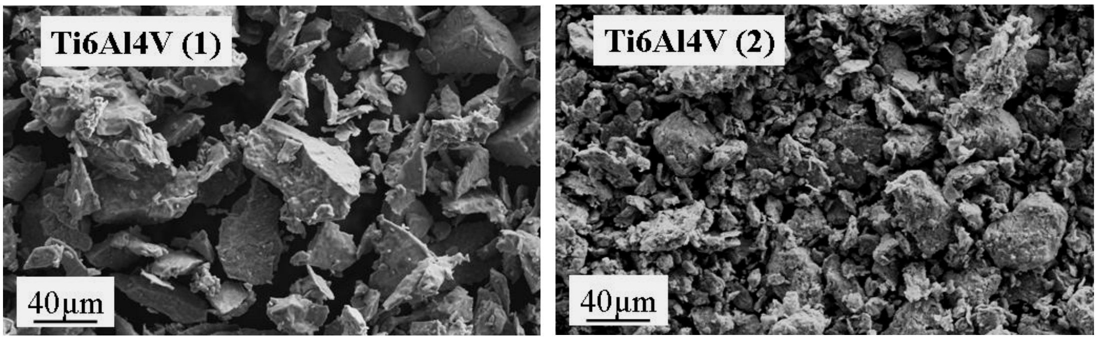

Figure 3-9. SEM images of the two Ti-6Al-4V powders.

Moreover, in order to analyse each Ti6Al4V powder, the technique of Energy Dispersive X-ray spectroscopy (EDS) as analytical technique is used. The chemical composition of the Ti6Al4V(1) and Ti6Al4V (2) powders was measured. Titanium, aluminium and vanadium as elements were detected. This technique was used as qualitative characterisation technique of the Ti6Al4V powder. To carry out this analysis, the powders were embedded in a resin. In this way, a section of the powder can be analysed. The main focus here was to check if all powder particles in fact consisted of Ti+Al+V (i.e. the powder was fully prealloyed) or if admixed components were visible. In the next Figure 3-10 and Figure 3-11 the aluminium, titanium and vanadium present in the Ti6Al4V powders are illustrated.

Furthermore, the following Table 3-7 shows the content of each element in the powders. Both powders have almost identical composition although a certain deviation from 6Al-4V can be found. This is related to an uncertainly of the EDS measurement.

Table 3-7. Chemical analysis of the Ti6Al4V (1) and Ti6Al4V (2) by the EDS detector (area scan).

Powder	**Ti6Al4V (1)**		**Ti6Al4V (2)**	
Element	mass%	At%	mass%	At%
Al	7.67	12.86	7.80	13.07
Ti	90.28	85.31	90.17	85.13
V	2.06	1.83	2.04	1.81

Each colour (red for Aluminium, green for Titanium and blue for Vanadium) represent a specific element. The location of each one informs about the type of powder and how the alloying has been done. The results of these investigations showed the Ti6Al4V(1) powder as Ti-Al-V prealloy with some TiV masteralloy. Additionally, the Ti6Al4V(2) powder was observed as TiV prealloyed powder mixing with Al powder.

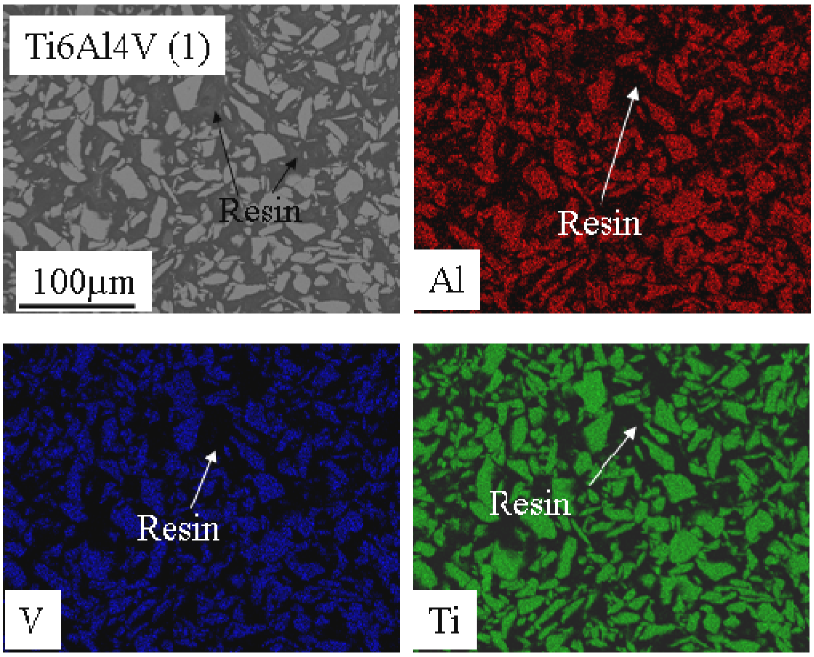

Figure 3-10. EDX-analyse of the starting powder Ti6Al4V(1). Up left it is the SEM image; Mapping of Aluminium (red colour image), Vanadium (blue); Titanium (green).

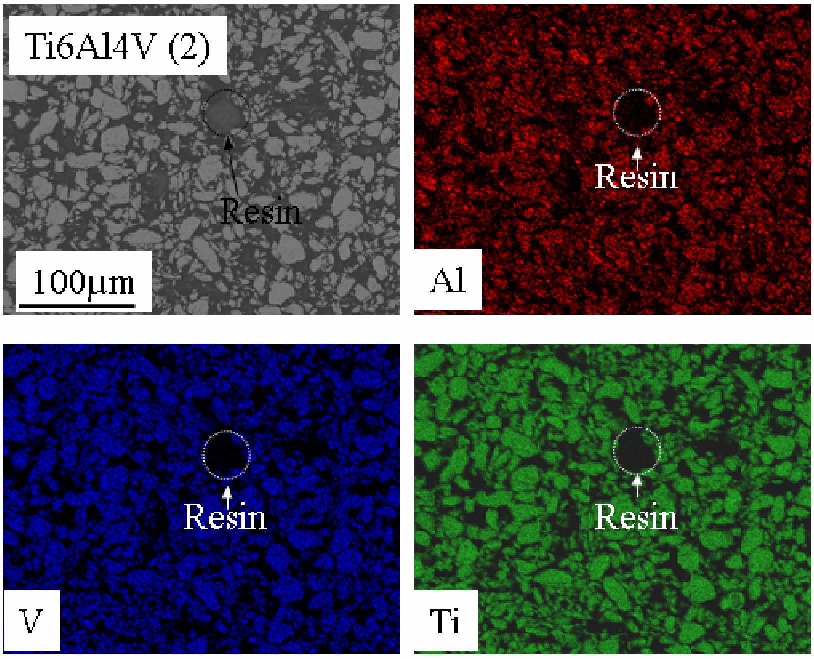

Figure 3-11. EDX-analyse of the starting powder Ti6Al4V(2). Upper left is the SEM image; Mapping of Aluminium (red colour image), Vanadium (blue); Titanium (green).

3.2 Reinforcement materials

In conformity with the extended bibliography about the different reinforcements for the manufacturing of TiMMCs given in Table 1-8, titanium diboride (TiB_2) and nano boron (nB) particles, carbon nano fibres (CNFs) and nano diamonds (NDs) were employed in this work.

By using of some nano-materials as reinforcement for titanium metal matrix composites, superior mechanical and physical properties were expected.

This significant influence on the properties achieved through the use of nano-reinforcements is due to their higher surface area compared to conventional reinforcement materials. For that reason micro and nano reinforcements were used, and the impact of their addition to the titanium and Ti-6Al-4V matrices was studied.

In this section, all of the reinforcing materials are characterised in detail; it involves the same methods as employed for the titanium based powders. In the next sub-sections all the necessary information about them are reported. Considering their basic composition they were classified in two categories, boron based and carbonaceous reinforcement materials.

3.2.1 Boron based materials: TiB_2 and Nano/Micro Boron particles.

On one hand, the particles of TiB_2 were required with low oxygen content and a particle size median of 10µm. After a search of a good supplier, finally the TiB_2 powder was ordered from an Asiatic manufacturer (Minmetal).

On the other hand, it was difficult to realise the idea to introduce nano boron (nB) particles due to a lack of powder suppliers. Finally one supplier was found.

The nano boron (nB) particles were manufactured by a DC-Plasma process. This process uses powder with conventional size which is blown into a DC Plasma.

The powder is then vaporized in a DC plasma, and subsequent cooling leads to condensation of the atoms. By adjusting the process conditions (cooling conditions) the size of the particle can be adjusted.

The requirement for the powder properties with respect to the size were 50 – 100 nm, low oxygen content and protecting coating (Low dangerous powder for health and explosion). However, after a long shipment time the received powder was quite different compared to the requirements.

The main problems were the agglomeration of nano-particles, the particle size distribution and high oxygen content. The nano-Boron particles present a bimodal particle size distribution such as observed in Figure 3-12.

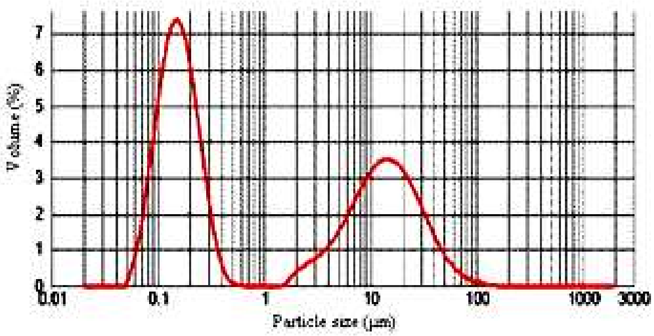

Figure 3-12. Particle size distribution of boron particles determined by Mastersizer2000.

Chemical analysis of the TiB_2 and boron particles, i.e. oxygen and nitrogen contents, were realized by LECO TC500. Moreover, the particle size distribution was measured by Mastersizer2000. The results are listed in the following Table 3-8.

Table 3-8. Chemical analysis and particle size distribution of TiB_2 and boron particles. * Oxygen analysis carried out one and half year after its use as reinforcement.

Type of reinforcement particles	Impurity content		Particle size distribution (μm)		
	O mass%	N mass%	d_{10} (μm)	d_{50} (μm)	d_{90} (μm)
TiB_2*	2.30	0.14	5.14	16.69	81.34
Boron	10.60	0.53	0.10	0.28	24.64

Furthermore, the theoretical density of the reinforcements was measured by the pycnometer “AccuPy 1330V3.3” as listed in Table 3-9. Additionally, impurities of Mg and Al were detected in the nB particles. The size and quality were not as expected (see Figure 3-14). The powder was not within the specifications; nevertheless, due to lack of other options the powder was introduced into metallic matrices.

Table 3-9. Theoretical density values obtained by the pycnometer and compared to the literature values of the TiB_2 and boron particles.

Powder material	Density by pycnometer (g/cm^3)	Density in the literature (g/cm^3)
TiB_2	4.13	4.50-4.62
Boron	2.64	2.34

Concluding the characterisation of these reinforcements, SEM images of the TiB_2 (see Figure 3-13) and boron particles (Figure 3-14) were taken by the Zeiss HRSEM equipped with EDAX and EDS/EBSD Detectors.

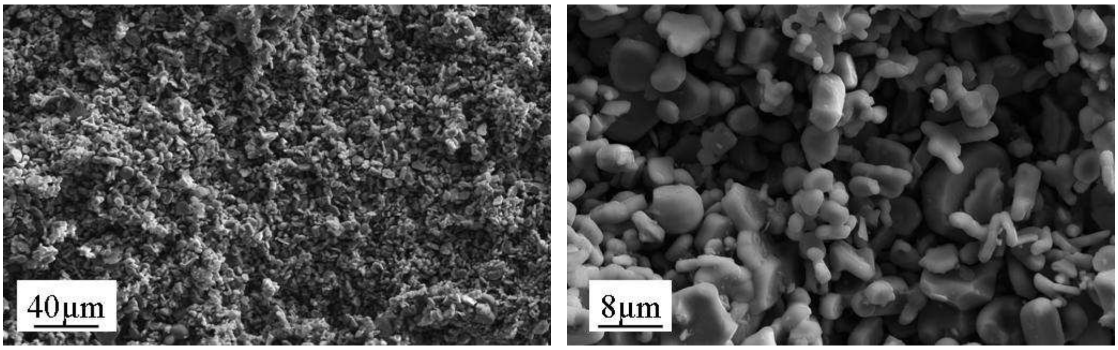

Figure 3-13. SEM images of TiB_2 particles.

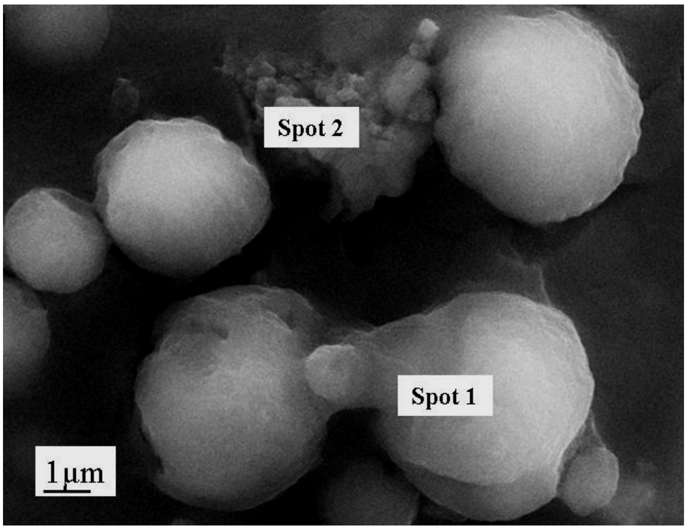

Figure 3-14. SEM images of boron particles.

Additional EDAX analysis shows considerable impurities of magnesium (Mg) in the boron particles. The measured points were on the agglomerates observed around the larger particle and in the boron particle. These results are listed in the following

Table 3-10. EDAX analysis of the nano-boron particles

Element	**In the boron particle (spot 1)**	**In the agglomerates (spot 2)**
Concentrion	(mass%)	(mass%)
B	99.3	96.3
O	0.5	0.5
Mg	0.3	0.4
Al	0.1	2.8

3.2.2 Carbonaceous materials

3.2.2.1 Nano Carbon Fibres (CNFs)

The family of carbon nano-fibres (CNFs) offers a wide range of applications for the aerospace, industrial and automotive industry in the field of mechanical reinforcement, thermal management and electrostatic dissipation. In the case of reinforced titanium matrices, the use of carbon nano-fibres was studied as solution to improve their mechanical properties [78, 79]. The characterisation of the CNFs was carried out in a similar way as that for the other reinforcement materials. The results obtained are reported in Table 3-11.The geometrical descriptions, also the mechanical and chemical properties, were taken from the supplier data sheet (Table 3-12).

Table 3-11. Characteristics of the CNFs: Density by pycnometer, oxygen and nitrogen contents by LECO TC 500 and particle size distribution by Mastersizer 2000. *Dimensions of CNFs according to the manufacturer.

Type of reinforcement	Impurities		Dimensions		Density comparison	
	Oxygen (mass%)	Nitrogen (mass%)	A_s (m^2/g)*	D. (nm)*	Py. density (g/cm^3)	Th. density (g/cm^3)
(CNFs)	0.11	0.05	20-100	80-150	1.95	1.8-2.1*

CNFs: Carbon nano-fibres; A_s: Specific area
Py. density: density: pycnometer density; D.: diameter;

Additionally, some sketches of the structure of the fibres and an SEM picture of the CNFs are shown in Figure 3-15 and Figure 3-16 (according to the manufacturer).

Table 3-12. Carbon nano-fibre properties (according to the manufacturer (Electrovac))

Properties of the CNFs	
Young's Modulus	500 GPa
Tensile Strength	7 GPa.
Temperature Stability (air)	550 - 750°C
Specific Weight	1.8 – 2.1 g/cm^3
Max. Current Density: up to	1013 A/cm^2
Thermal Conductivity: up to	2000 W/mK

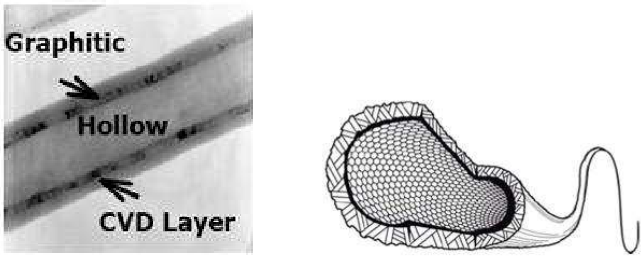

Figure 3-15. Description of the CNFs used (according to the manufacturer information).

The geometry of the CNFs contributes to the formation of fibre agglomerates, as shown in Figure 3-16. Therefore it was difficult to obtain images of isolated nano-fibres.

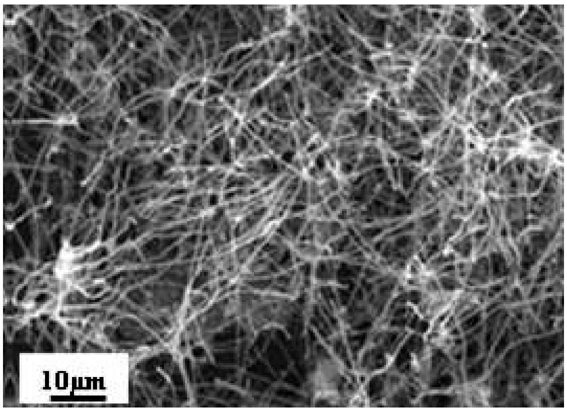

Figure 3-16. SEM picture of Carbon nano-fibres according to the manufacturer.

3.2.2.2 Nano Diamonds

The nano-diamonds (NDs) were purchased from two suppliers. Firstly, one type of nano diamond powder was employed (ND(1)). After the results of the chemical analysis, a high content of oxygen was detected (see Table 3-13). For that reason, a second type of nanodiamond powder was purchased (NDs(2)).

The specifications of this second NDs(2) powder are also reported in the next table. All of the data are according to the manufacturer. The fabrication process of the NDs(2) was based on a detonation process.

As observed in the next Table 3-13, the particle size of NDs(2) is lower than the size of NDs(1). Nevertheless the NDs(1) presents higher oxygen content. The next SEM images show the morphology of each type of nanodiamond powder NDs(1) and NDs(2). At the same magnification, the particles of NDs(2) cannot be recognised (see in Figure 3-17).

The NDs(1) showed a spherical morphology. Some particle diameters are marked and measured in the next Figure 3-18. For the NDs(2) it was not easy to measure the diameter from the SEM image. The agglomerates of the nano particles of NDs(2) are shown in Figure 3-19.

Table 3-13. Properties of the NDs powders.*According to the manufacturer.

Type of NDs and supplier	Oxygen (mass%)	Nitrogen (mass%)	D (nm)	Purity	Density (g/m^3)	Specific surface area (m^2/g)
NDs(1) **(Bulgarian institute)**	9.33	2.67	60-100*	-	-	-
NDs(2) **(NaBond Technologies)**	7.1	-	4-6*	98-99%	3.05-3.3	282.83

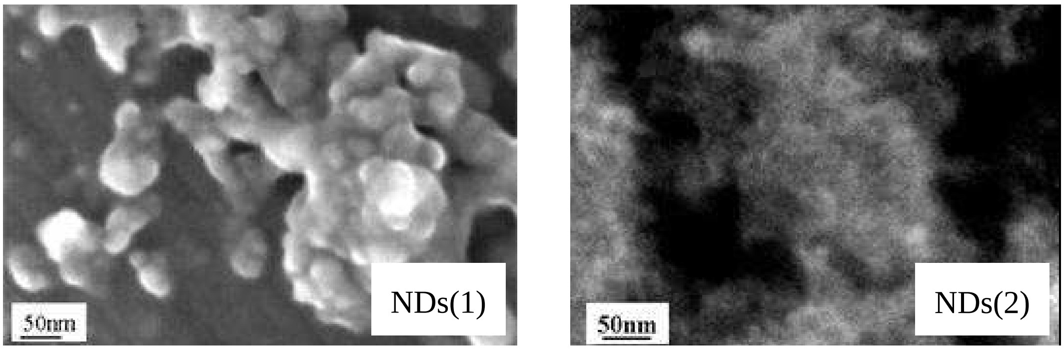

Figure 3-17. SEM images of NDs(1) and NDs(2)

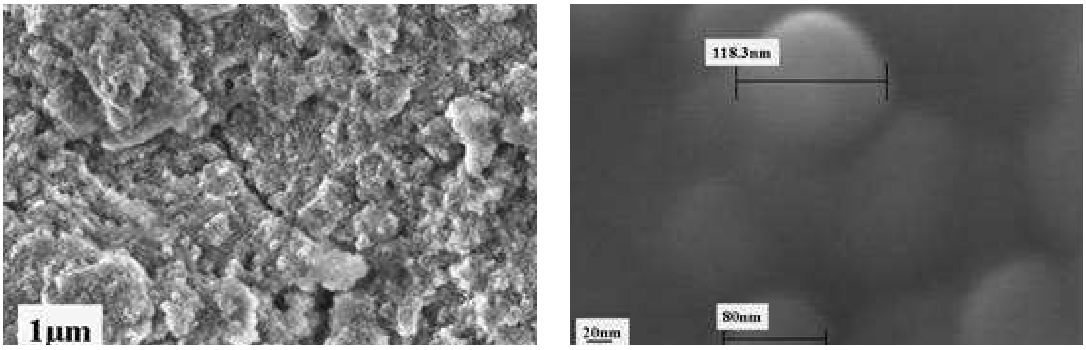

Figure 3-18. SEM images of NDs (1) powder.

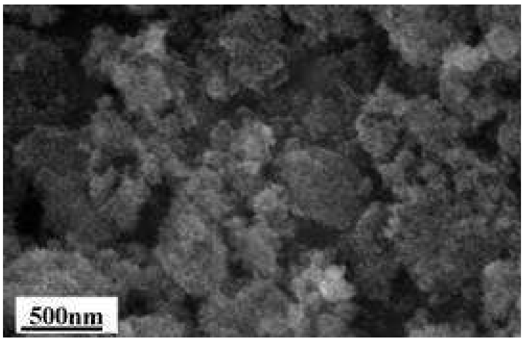

Figure 3-19. SEM image of NDs (2) powder.

4 Experimental work

4.1 Introduction

In this chapter the experimental work is described including the starting materials and the manufacturing processes used. In addition, the characterisation technique for each type of composite is reported.

The manufacturing of different types of composite materials took place via different powder metallurgical processes. Consequently, the chapter was divided into three important parts in order to achieve systematically the principal objectives and to provide a major understanding of the aim of the work.

Firstly the selection of the most promising titanium based matrix materials was carried out. Thereby, the testing of the starting titanium based powders (CPTi, TiH_2 and Ti6Al4V) was realized.

This selection is based on the results of the characterisation of the titanium compacts.

The powders were processed by conventional Cold Pressing (CP) testing at several mechanical pressures and in different handling atmospheres (air and Argon). Thereafter, a sintering study was performed at different temperatures and experimental setups.

In the second and third part, the fabrication of the titanium composites took place. The most suitable titanium based powders and the two types of Ti-6Al-4V powders were employed for that purpose.

The manufacturing of the composites was carried out through powder metallurgical methods: Conventional Cold Pressing-Sintering (CP-S). Conventional Hot Pressing (HP) and Inductive Hot Pressing (iHP), depending on the type of composite material to be produced. This second and third part was defined according to the type of the reinforced matrix (titanium or its alloy). The parts are respectively subdivided according to the reinforcement material used (TiB_2, nano/micro boron particles, carbon nano fibres and nano diamond particles).

Within the classification of the composites considering their reinforcement materials, the whole manufacturing process of each type of composite was explained. To simplify this, diagrams show the starting materials used and the powder metallurgical processes employed.

Finally, the characterisation techniques used for studying the properties of the composite produced are reported.

Concluding, the results specimen characterisation are represented, listed and discussed at the end of each experimental part.

4.2 Pure Titanium Matrices

In this part, titanium specimens without reinforcement were produced from the six types of titanium based powders . To carry out this first experimental part, a bibliographic search about the processing parameters for the consolidation of titanium was done. The characterisation of all the titanium compacts was realised.

The results of this characterisation were evaluated and compared with regard to the starting powder used for the production of the compacts. Thereafter, the two most suitable starting powders were selected.

4.2.1 Raw Materials

The purity of the raw materials was always a selection criterion at the beginning of the experiments. That is because a high impurity content possibly results in low mechanical properties of the compacts, e.g. causing embrittlement [87, 88].

The well known affinity of titanium for oxygen, nitrogen, carbon and hydrogen, Ti also being able to dissolve these interstitials in the lattice, and the tendency to contamination is more pronounced with decreasing particle size of the powder. That is why working with titanium requires special protection from the atmosphere, and this determines the sintering conditions [89].

The oxygen affinity of titanium is a fact that cannot be eliminated. However, at least any increase of this oxygen content during the sintering stage can be prevented by proper processing conditions.

In this first experimental part, the six titanium based powders (CPTi(1), CPTi (2) and TiH_2 (3) TiH_2 (4) TiH_2(5) and TiH_2 (6)) were employed. Their properties (particle size, oxygen content and density) were listed in the previous Table 3-2 and Table 3-3.

4.2.2 Conventional manufacturing process (CP+S)

The cold pressing and the sintering conditions were fixed on the basis of an intensive bibliographic search of the process parameters for the fabrication of titanium based specimens (titanium and Ti6Al4V) via cold pressing and sintering. For results see the next table.

Table 4-1. Compaction and sintering parameters for the fabrication of sintered compacts from Ti6Al4V and CPTi powders as given in the literature.

Forming		**Sintering**			
Powder / Size	Pressure (MPa)	T (°C)	Time	Other conditions	
CPTi and Ti6Al4V starting powder					
Ti “sponge” + Al/V (BE) 149 µm [90]	CP.	1260°	4h	Vacuum at $1.33x10^{-3}$ mbar	
ir.Ti+Al/V (BE) <150 µm [91]	CP. 400MPa	1260°	4h	Vacuum	
ir.Ti + Al/V (BE) <44 µm [92]	CP. 415-690MPa	1100°-1260° 1200°-1300°	2-4h	Vacuum at $1.33x10^{-5}$ to 10^{-4} mbar	
ir.Ti + Al/V (BE) 177µm [93]	CP. 415MPa	1260°	4h	Vacuum	
80%Ti+20%HA 100 µm + 10 µm [94]	1st. U. CP. 10MPa 2nd. CIP 290MPa	1150°	1.5h	$1.33x10^{-4}$ mbar	
Ti6Al4V/HA 116 µm [74]	PIM	1050° 1100° 1150°	30min 45min 60min	Heating rate 5/7.5/10 K/min	Cooling rate 5/20/40 K/min
TiC-VC-10%Co <18%Ti/72%VC [66]	U.P. 350MPa	1250º-1350º 1350º/1400º/1450º	1h		
Ti6Al4V 74-250 µm [95]	CP. 400MPa	1200º	2h	Ar Atmosphere	
Electrolytic Ti HDH-Ti; TiH_2 [96]	250-1000MPa	950°-1350°	4h	Vacuum	
Ti powder [97]	278MPa	1040º-1100°	2h	Vacuum	

BE: Blended elemental powder production;	U: Uni-axial
P.: Pressing;	CP.: Cold Pressing;
CIP.: Cold Isostatic Pressing;	PIM.: Powder Injection Moulding
HA: Hydroxide Apatite	ir. Ti :irregular Ti powder

The sintering in high vacuum is regarded as a suitable sintering condition for the production of titanium compacts.

The sintering time was optimised from 1h used at the beginning to 2h after evaluation of the results of specimen characterisation.

The other important sintering parameter is the temperature. Two sintering temperatures were tested, 1200° and 1300°C.

To support the description of the manufacturing process of the titanium compacts (without reinforcements), the next Figure 4-1 and Figure 4-2 shows the Flow sheet of the process.

Firstly the starting powder with the highest oxygen content (TiH_2(6)) was employed for the preliminary experiment searching the optimal sintering setup. The reduction of the oxygen content after sintering of the green compacts was the goal of the first experimental part.

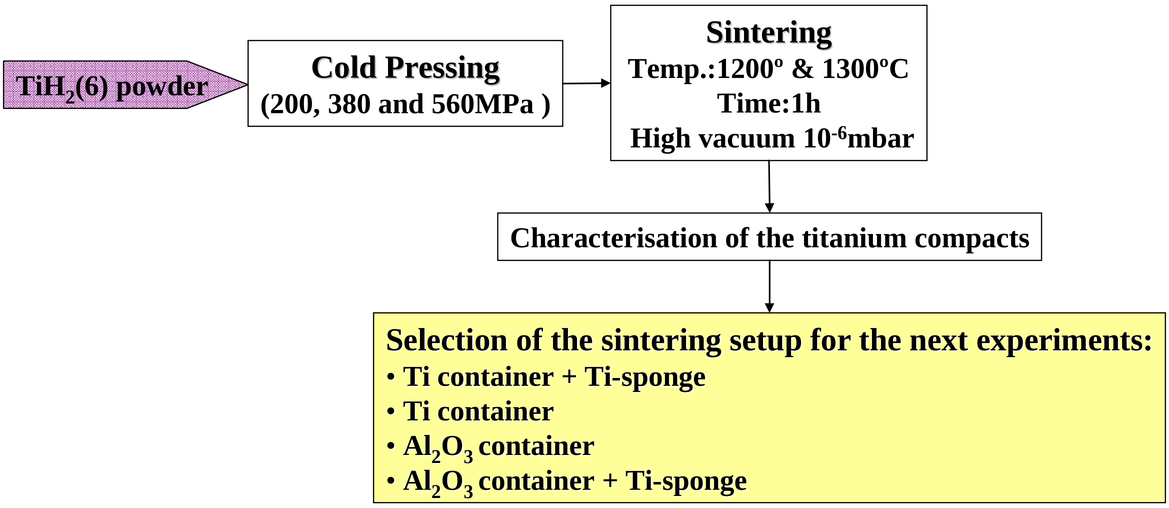

Figure 4-1. Flow sheet of the first experiments using the finest powder (TiH_2 (6)).

Due to its highest oxygen content, the finest powder (TiH_2 (6)) was selected for this part. It was compacted and then sintered using different sintering setups.

After that, the other five titanium starting powders (TiH_2 and CPTi) were consolidated using the most suitable setup previously selected.

The following Figure 4-2 describes the procedure for the investigations done with the five Ti powders.

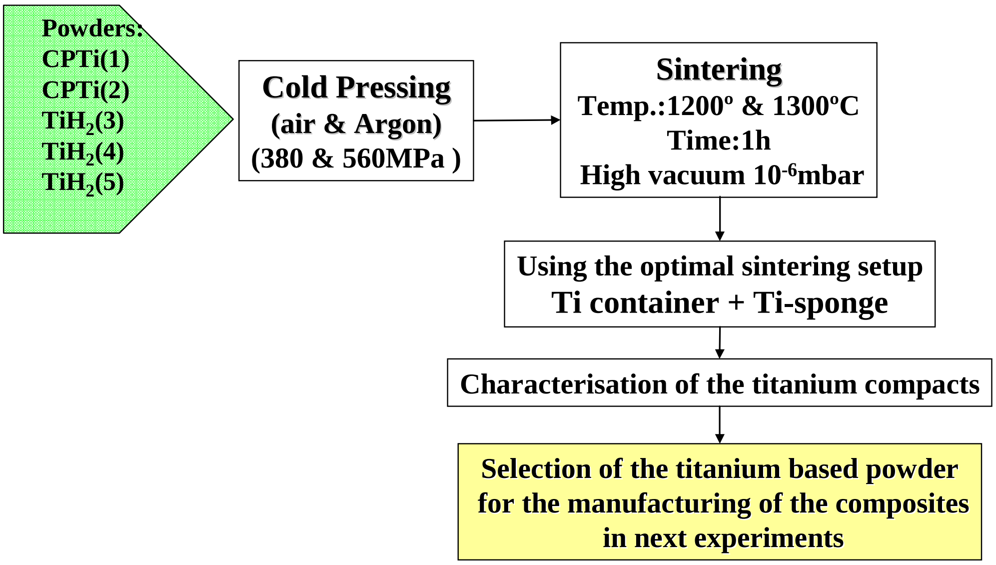

Figure 4-2. Flow sheet of the manufacturing process for titanium compacts, using the five titanium based powders and the most suitable sintering setup.

4.2.2.1 Cold Pressing (CP)

Screening of the cold pressing pressure for the finest powder (TiH_2 (6))

The highest oxygen content and finest titanium hydride powder (TiH_2 (6)) was placed in a cylindrical die (see in Figure 2-3 and Figure 2-4.). This titanium hydride powder was pressed at room temperature handled in air at pressures of 200 MPa, 380 MPa and 560 MPa in the way shown in chapter 3rd.

Cold pressing of the other five titanium based powders

The same procedure for cold pressing was employed for the compaction of the other titanium based compacts (see Figure 2-3).

The values of pressure used were 380 MPa and 560 MPa. The lowest pressure (200MPa) was not used due to the low densification observed after the characterisation of the sintered specimens compacted at this pressure.

These five powders were handled in air and in Ar. In this way, it may have a significant effect on the final oxygen content of the sintered specimens. However, all the cold compactions were performed in air.

4.2.2.2 Sintering

Screening of sintering conditions for the TiH_2 (6) starting powder:

The importance of the sintering setup was based on a strategy to limit and, if possible, reduce the content of oxygen and of the other interstitial impurities during sintering of the titanium based compacts. Hence, firstly a suitable sintering setup was worked out.

Therefore several assemblies were investigated and tested. All the setups were designed to reduce the contamination of the green compacts during the sintering stage. Two types of container, Ti and alumina, were used both with and without getter filling. Titanium sponge was used as getter (see Figure 4-3).

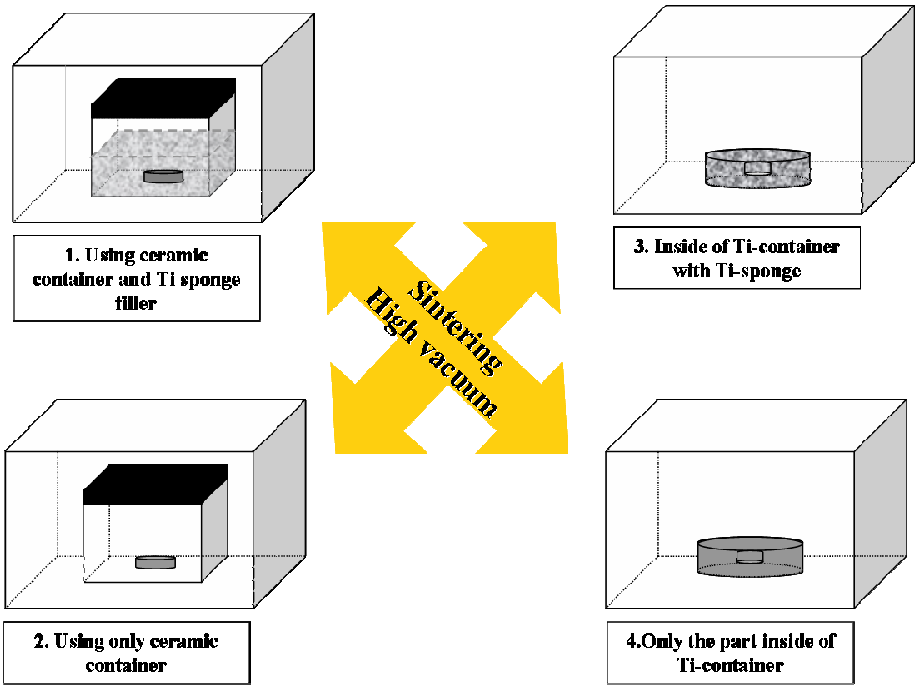

Figure 4-3. Different sintering setups for the manufacturing of titanium compacts from the TiH_2 (6) starting powder.

The filling acted as a getter for oxygen and other possible impurities coming from the furnace atmosphere.

The entire sintering process was carried out in high vacuum ($3x10^{-5}$ mbar indicated), using a Thermal Technology Inc. furnace model “Astro”.

Sintering temperatures ranged between 1200° and 1300°C. After reaching the nominal temperature, the samples were held at the chosen temperature for 1 h and then furnace cooled to room temperature.

The assembly of the different containers with and without Ti-sponge is described in the next Figure 4-4.

The four variants were sintered in one single run, in this way the operational parameters (Temperature, time and vacuum) were the same for all the sintered specimens.

However there was some risk of setup interaction, i.e. the getter in setups 2 and 4 positively affecting the results from setups 1 and 3 (danger of cross-effects).

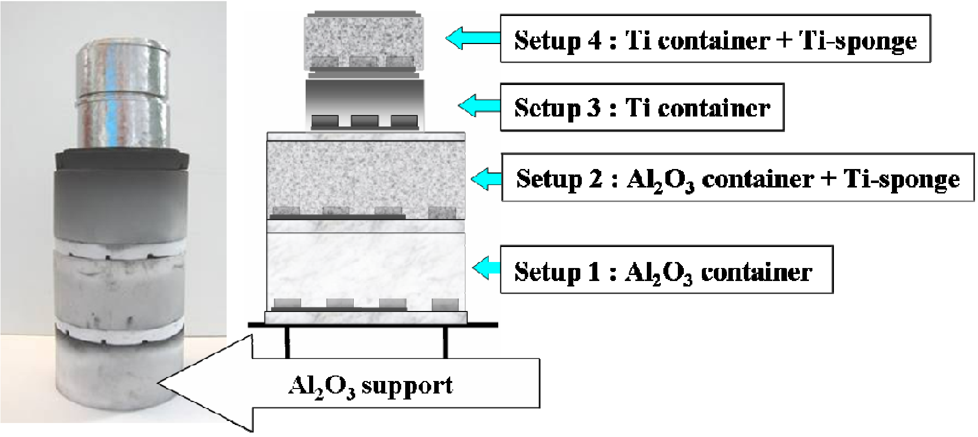

Figure 4-4. Photo and sketch after sintering of the four different sintering setups.

After sintering at 1200º and 1300ºC, the formation of titanium oxides on the two Al_2O_3 containers was observed (see in the Figure 4-4). Consequently, the Al_2O_3 container filled with Ti-sponge presented darker grey colour since it was more in contact with the titanium container and getter.

This darker grey colour could be due to titanium oxide or rather vapour deposited Ti that had been superficially oxidized during cooling. It was not clear; however it was evident that setups 2 and 4 are preferable.

Secondly, the sintering behaviour of different titanium powders (powder 1-5) was studied in addition to the optimisation of the fabrication parameters of compacts (two different cold compacting pressures).

In this second experimental part the selected setup 4 for the sintering stage was employed (see Figure 4-5).

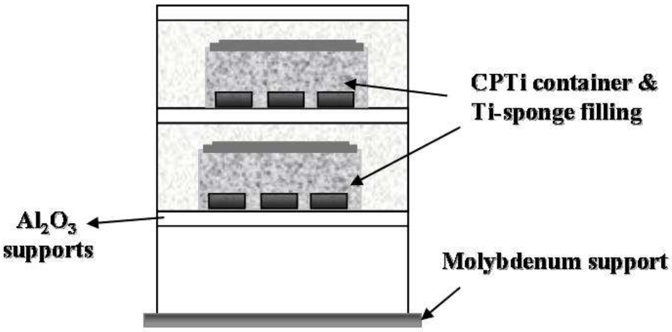

Figure 4-5. Assembly selected for the sintering of the titanium based compacts.

The results of this first experimental part (see below) have been used in the next parts of this research work.

4.2.3 Hot consolidation processes

The technique employed for the first hot consolidation of the compacts was inductive hot consolidation (iHP).

One important reason for the development of this method was the evaluation of the metal matrix microstructure.

Additionally, the possible reaction at high temperatures (950º/1000ºC) between the graphite die and the pure titanium based matrices was another reason to carry out this study. This test involved the use of graphite plates that were in direct contact with the Ti powders, without the protecting coating of boron nitride. In this way, the reaction between the carbon and titanium was easily possible.

The next Table 4-2 shows the processing parameters employed for the study of the titanium based matrices without reinforcements.

The temperature varied from 800º to 1050ºC. The influence of the heating rate at the lower temperature (800ºC) was also studied. For this study the powder grades CPTi(2) and TiH_2(4) were used due to their lowest oxygen content (see Table 3-2).

Table 4-2. Inductive hot pressing parameters used for the study of the titanium based matrices without reinforcements.

Hot pressing technique	**Processing parameters**					
	Temp. (ºC)	Die (mm)	Heating rate (K/min)	Holding time (min)	Pressure (MPa)	Vacuum (mbar)
Inductive HP	800	10 Ø	10	15	50	10^{-5}
	800	10 Ø	50	15	50	10^{-5}
	850	10 Ø	50	15	50	10^{-5}
	900	10 Ø	50	15	50	10^{-5}
	950	10 Ø	50	15	50	10^{-5}
	1000	10 Ø	50	15	50	10^{-5}
	1050	10 Ø	50	15	50	10^{-5}

4.2.4 Results of the characterisation techniques

For characterization of the final samples, the density was measured at room temperature using the Archimedes's method in water with or without paraffin impregnation depending on the relative density observed (below 95% of relative density always with paraffin).

Hardness (HV10) and the oxygen content of several samples were tested. Finally, the microstructural study of several specimens (compacted at 560 MPa) was carried out.

4.2.4.1 Titanium specimens from TiH_2 (6) starting powder.

In this part, the results obtained by the characterisation of the specimens from TiH_2 (6) are reported. As previously mentioned, the titanium compacts were cold pressed and sintered.

This technique employed (CP+S) was described in the previous chapter 2^{nd}. Thereby, just the results are shown.

Finally in a table the most representative values of density, hardness, oxygen content and the used processing parameters are summarised. Furthermore the microstructure of several specimens is also shown.

Density of the specimens:

The geometrical density of the green compacts in addition to the geometrical and Archimedes density of the sintered specimens are summarised in the next tables.

The manufacturing parameters used for the fabrication of the specimens are also reported.

Firstly, the results before and after sintering at 1200°C are shown in the following Table 4-3. Additionally, in Table 4-5 the results before and after sintering at 1300°C are listed.

Table 4-3. Density (geometrical and Archimedes) of the titanium compacts from TiH_2 (6) before and after sintering for 1h at 1200°C.

Cold pressure (MPa)	$T_{sintering}$ (°C)	Geometrical density of green compact (g/cm^3)	Geometrical density of sintered compact (g/cm^3)	Archimedes density of sintered compact (g/cm^3)
200	1200°	2.68±0.01	4.38±0.06	4.55±0.03
380	1200°	2.91±0.03	4.30±0.12	4.54±0.02
560	1200°	3.08±0.02	4.35±0.03	4.51±0.11

Table 4-4. Density (geometrical and Archimedes) of the titanium compacts from TiH_2 (6) before and after sintering for 1h at 1300°C.

Cold pressure (MPa)	**$T_{sintering}$ (°C)**	**Geometrical density of green compact (g/cm^3)**	**Geometrical density of sintered compact (g/cm^3)**	**Archimedes density of sintered compact (g/cm^3)**
200	1300°	2.67±0.02	4.41±0.16	4.54±0.01
380	1300°	2.91±0.03	4.38±0.09	4.46±0.11
560	1300°	3.07±0.02	4.41±0.02	4.53±0.02

Considering as reference the density of commercial pure titanium 4.54 g/cm^3, the values of the relative density of the specimens are calculated and reported in the next Table 4-5.

Table 4-5. Values of the relative density of the titanium specimes from TiH_2 (6) at three different pressure compacted and sintering for 1h at 1200° and 1300°C.

Cold pressure (MPa)	**Green specimens**	**T.$_{sintering}$ (°C)**	**Sintered specimens**
	Geometrical density (%)		Archimedes density (%)
200	59.4±0.1	1200°	100.2±0.6
380	64.6±0.7		99.9±0.5
560	68.4±0.3		99.3±2.4
200	59.2±0.4	1300°	100.1±0.2
380	64.6±0.6		98.1±2.5
560	68.2±0.5		99.8±0.4

On one hand, the cold compacting pressure has an effect on the density values of the green compacts, increasing the relative green density from 59% (at 200 MPa) up to 68% (in samples consolidated at 560 MPa). However, the pressure values do not influence the final values of the relative density (geometrical and Archimedes density) of the sintered specimens.

Hardness and oxygen analysis of several specimens:

The results of the hardness and oxygen analysis for the different sintering conditions are given in the Table 4-6. The influence on the oxygen content, when using Ti-sponge as getter in the different containers, is also observed and evaluated in the next Table 4-6.

Table 4-6. Results (oxygen content and hardness) of the specimens from the TiH_2 (6) powder (the starting oxygen content of the powder was 1.47 mass%).

Cold pressure (MPa)	$T_{sintering}$ (°C)	Container material	Getter	Oxygen (mass%)	Hardness (HV10)	Arch. Density (g/cm^3)
380	1200	Alumina	-	1.87	457	4.54
380	1300	Ti	-	1.69	479	4.54
560	1300	Ti	-	1.64	482	4.53
560	1300	Ti	Ti sponge getter	1.24	477	4.50
380	1300	Alumina	Ti sponge getter	1.45	480	4.54

In general, the hardness of the sintered specimens is higher than the theoretical hardness (HV10) for pure commercial titanium (CPTi) grade 4 (260 HV10). It is due to the high oxygen content of the sintered specimens. The oxygen content of CPTi grade 4 is stipulated and standardised to 0.4mass% [2]; however all the sintered samples from the TiH_2(6) present values of the oxygen content up to 1.20 mass% The compacting pressure (380 MPa and 560 MPa) does not significantly affect the oxygen content (1.69 mass%. and 1.64 mass%. respectively) of the sintered specimens at the same sintering conditions (1300°C using a titanium container). But there is definitely an effect if Ti getter is used. At the same compacting pressure (380 MPa), the specimens sintered in the alumina container without getter (Ti-sponge getter) present higher oxygen content (1.87 mass%) than the samples sintered in the same container with getter (1.45 mass%). Also the use of the titanium container without getter reduces the oxygen content of the sintered specimens (1.69 mass%). The lowest oxygen content is observed for the specimen sintered into a titanium container with the Ti-sponge getter (1.24 mass%); here the oxygen content drops to a level even lower than that of the starting powder. I.e. setup 4 is most suitable

Microstructural study:

The microstructural study of the sintered specimens is carried out considering the manufacturing conditions used for their production. The influence of cold compacting pressure on the final properties of the titanium specimens is not significant in comparison to the use of getter during the sintering process. For that reason, the next microstructural comparison is carried out according to the sintering setup employed and the sintering temperature. All of the specimens were cold pressed at the maximum pressure value (560 MPa). The images of the different microstructures of the sintered specimens are shown in the next **Fehler! Verweisquelle konnte nicht gefunden**

werden..

Comparison of TiH2 powder compacted at 560MPa in different sintering conditions		
Sintering conditions	Ti-sponge getter	No getter
1200°C **Al_2O_3** **Container**	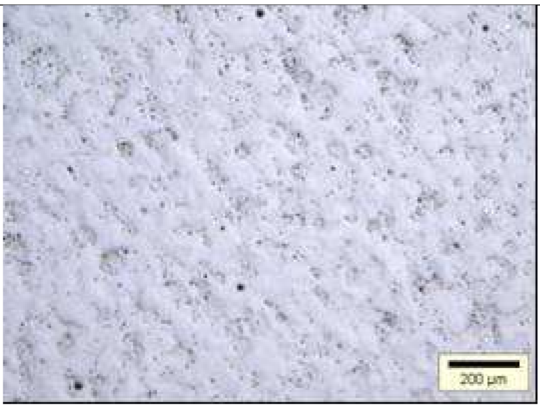	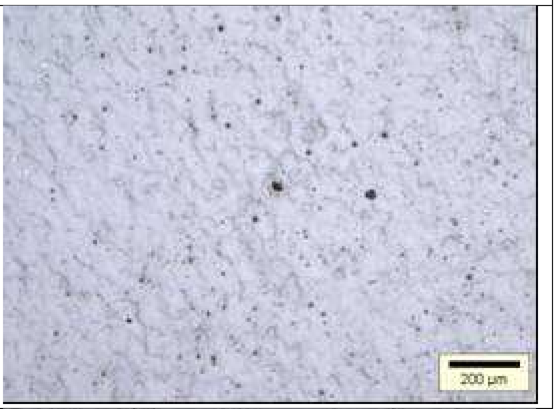
1300°C **Al_2O_3** **Container**	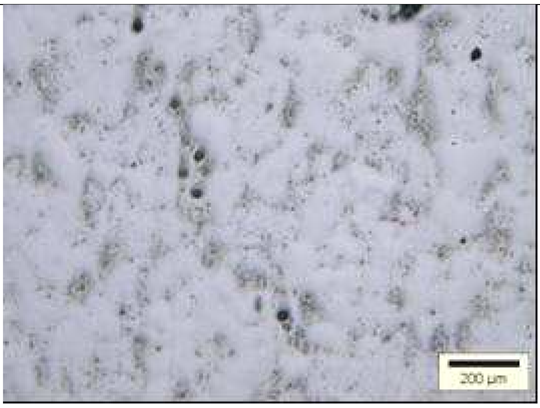	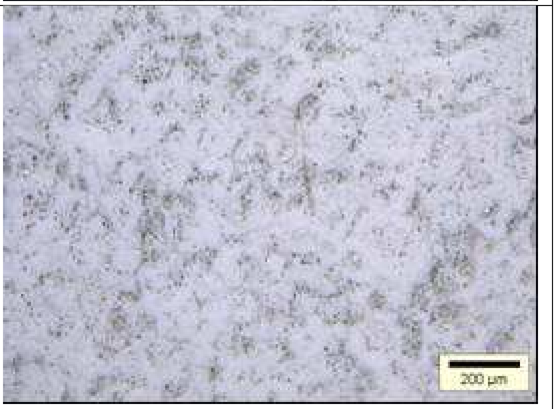
1300°C **Titanium** **Container**	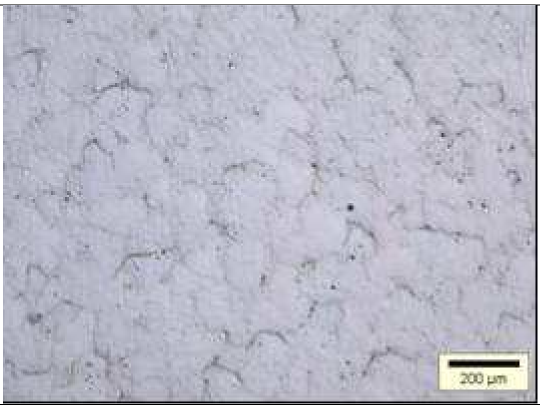	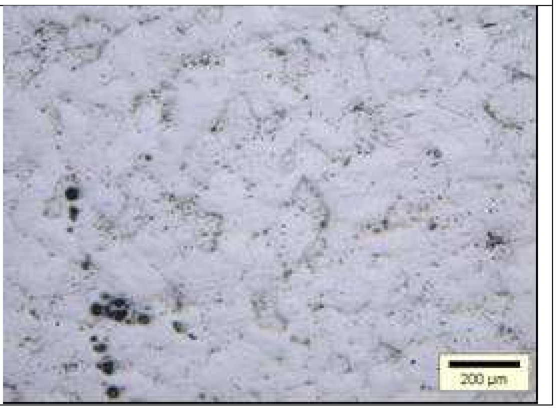

Figure 4-6. Microstructure of the sintered titanium specimens from TiH_2(6) cold consolidated at 560 MPa and sintered at different sintering conditions (sintering temperature, sintering container material and getter) .

The previous table shows the difference between the samples sintered at 1200° and 1300°C using different sintering assemblies. The sintering temperature has a significant influence on the porosity of the specimens. Furthermore the use of titanium getter causes a reduction of the oxygen content on the final samples and also a visible decrease of porosity at 1300°C when using a titanium container. This apparent difference in the porosity between the sintered specimens at 1200º and 1300ºC, was not in agreement with the values of relative Archimedes density showed in the previous Table 4-6. In particular, the specimens sintered at 1200º presented porosity that was not corresponding to the high Archimedes density showed.

Additional microstructure study was carried out in order to find some explanation for the high values of hardness and density observed previously.

Finally, powder impurities of Fe were detected (by EDAX analysis). Such impurities can increase the hardness and density of the samples. In this way, some correlation between the microstructure of the specimens from TiH_2 (6) and the results of their Archimedes density was justified.

At the beginning of these tests, the Fe content of this powder was considered according to the manufacturer (maximum Fe 0.05%mass.) These Fe impurities could be due to powder fabrication process (milled powder).

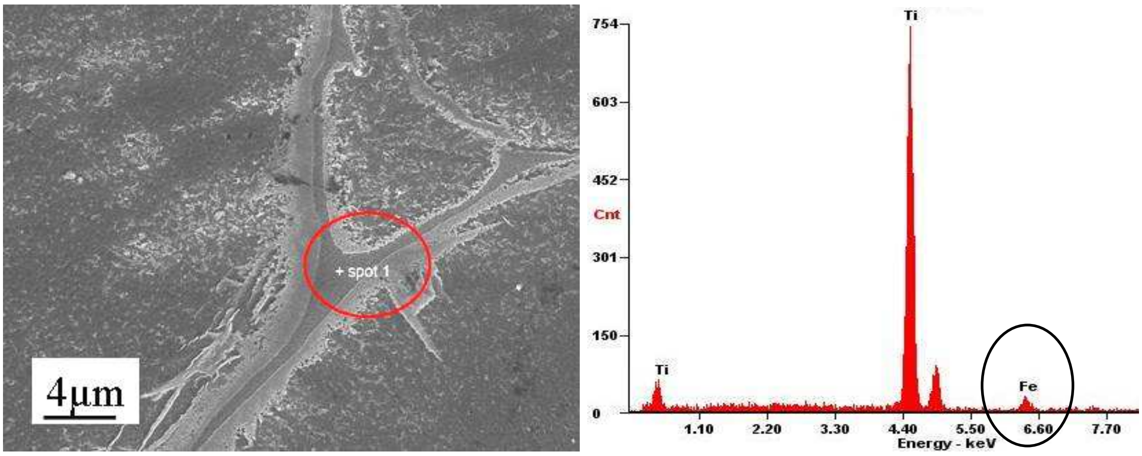

Figure 4-7. (left) SEM image of a titanium specimen from TiH_2 (6) powder. Compacted at 560MPa in air and sintered at 1300°C for 1h, into a titanium container without getter). Result of the EDAX analysis carried out in the titanium specimen (right).

Intermediate Conclusions

- High oxygen content and Fe impurities due to powder fabrication process (fine powder 2.7μm and milled powder) → high hardness material
- Influence of sintering arrangement (container material and/or Ti-sponge getter) → Oxygen content (mass%) reduction due to the titanium getter and titanium container
- Significant densification after sintering at 1200ºC and 1300ºC higher densification (around 99% was achieved)
- Slight influence of the compacting pressure oin the densification properties.

4.2.4.2 Titanium specimens from the titanium powders CPTi(1), CPTi(2), TiH_2(3) TiH_2 (4) and TiH_2 (5).

The titanium specimens described in this section were made from the five titanium based powder in which the oxygen content is below 0.80 mass%.

The results obtained were also compared to those obtained from the specimens produced from the TiH_2 (6) starting powder (it was handled in air).

The aim of this part is the study of their sintering behaviour and the evaluation of the properties of the sintered specimens. The results of the characterisation of the samples are shown.

Density values

The Archimedes density data of specimens from the five titanium based powders (CP(1), CPTi(2), TiH_2 (3), TiH_2 (4) and TiH_2 (5)) and the TiH_2(6) are described in the Figure 4-8 and Figure 4-9.

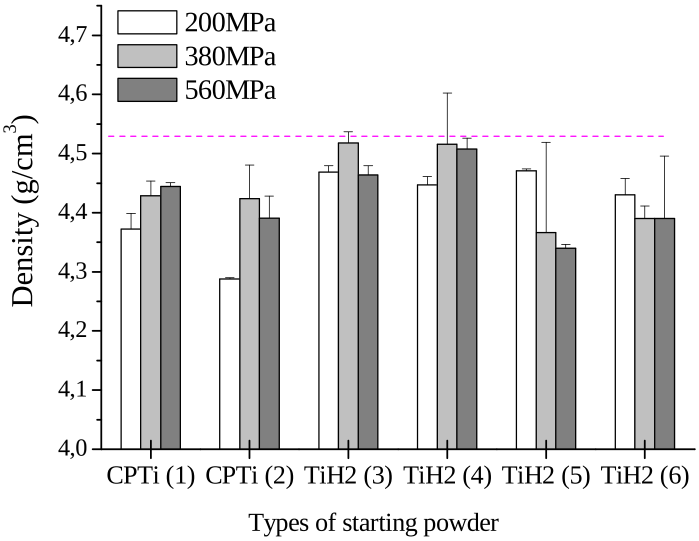

Figure 4-8. Density comparison of sintered specimens from different titanium powders, compacted at three different pressures sintered for 1h at 1200°C with Ti-getter (TiH2 (6) handled in air and the other five titanium powders compacted under Argon atmosphere).

The density measurements were carried out by Archimedes method in water using paraffin coating (although this was not really necessary since high levels of density were observed).

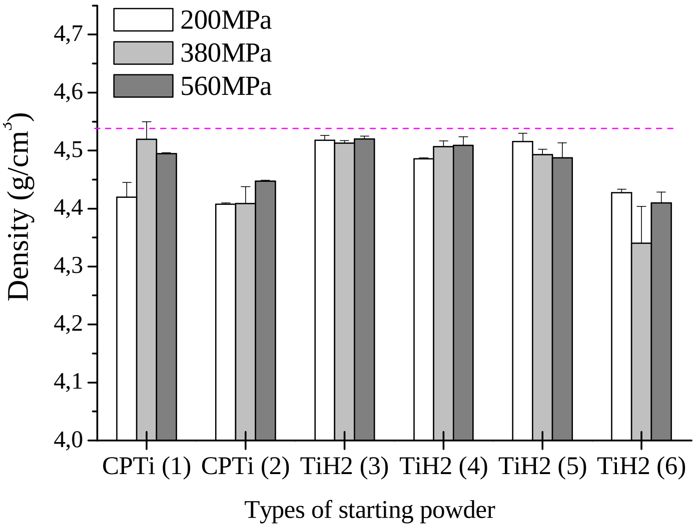

Figure 4-9. Density comparison of sintered specimens from different titanium powders, compacted at three different pressures sintered for 1h at 1300°C with Ti-getter (TiH2 (6) handled in air and the other five titanium powders compacted under Argon atmosphere).

The density values are shown in Table 4-7 as a function of the pressure used for the consolidation of the green specimens.

The reference density for commercial pure titanium is 4.54 g/cm^3 as reported in the previous Figure 4-8 and Figure 4-9. Considering the cold compaction pressure 200 MPa, 380 MPa and 560 MPa, the density values obtained are listed in the next tables. First the density table of specimens sintered at 1200°C is shown following the density table of compacts sintered at 1300°C.

Table 4-7. Archimedes density of the specimens compacted at three pressure and sintered at 1200ºC with Ti-getter (TiH2 (6) handled in air and the other five titanium powders compacted under Argon atmosphere).

Type of starting powder (sintered at 1200ºC)	**Archimedes density (g/cm^3)**		
	Compaction pressure used		
	200 MPa	380 MPa	560 MPa
CPTi (1)	4.37±0.03	4.43±0.02	4.44±0.01
CPTi (2)	4.29±0.00	4.42±0.06	4.39±0.04
TiH_2 (3)	4.47±0.01	4.52±0.02	4.46±0.02
TiH_2 (4)	4.45±0.01	4.52±0.09	4.51±0.02
TiH_2 (5)	4.47±0.00	4.37±0.15	4.34±0.01
TiH_2 (6)	4.55±0.03	4.54±0.02	4.53±0.11

As observed previously, the cold compaction pressure does not exert a significant effect on the Archimedes density of the sintered specimens. However the influence of the sintering temperature on such density values is evident (see Figure 4-10).

Table 4-8. Archimedes density of the specimens compacted at three pressure and sintered at 1300ºC with Ti-getter (TiH_2 (6) handled in air and the other five titanium powders compacted under Argon atmosphere).

Type of starting powder (sintered at 1300ºC)	**Archimedes density (g/cm^3)**		
	Compaction pressure used		
	200 MPa	380 MPa	560 MPa
CPTi (1)	4.42±0.03	4.52±0.03	4.49±0.00
CPTi (2)	4.41±0.00	4.41±0.03	4.45±0.00
TiH_2 (3)	4.52±0.01	4.51±0.00	4.52±0.00
TiH_2 (4)	4.49±0.00	4.51±0.01	4.51±0.02
TiH_2 (5)	4.52±0.01	4.49±0.01	4.49±0.03
TiH_2 (6)	4.54±0.01	4.46±0.11	4.53±0.02

In the next Figure 4-10 the Archimedes density values at the two different sintering temperatures are compared. The green samples were compacted at the same mechanical pressure of 560 MPa. Surprising values of density were observed for the specimens from TiH_2 (6), even after short sintering time (1h).

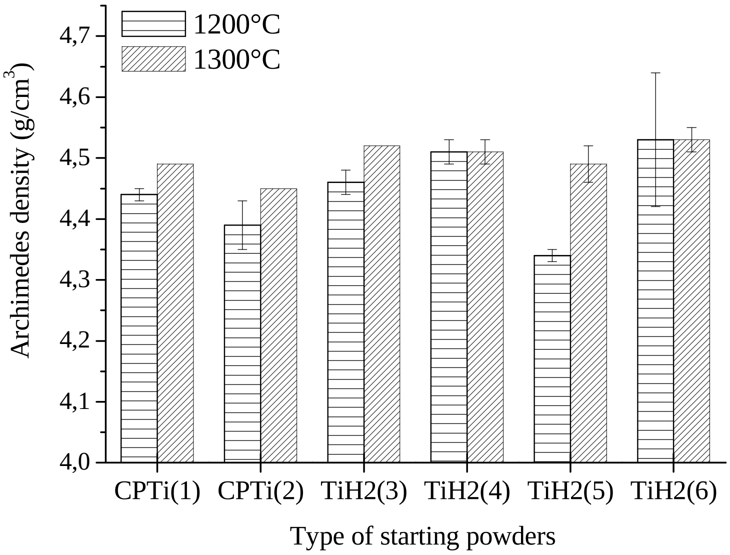

Figure 4-10. Archimedes density of the sintered specimens from the different types of starting powders at 1200° and 1300°. All of them were compacted at 560 MPa in air. The specimens from CPTi(1) to TiH_2(5) were handled in Ar. The specimens from TiH_2(6) were handled in air.

Hardness (HV10) measurement

The specimens sintered at 1200ºC presented lower density values than the specimens sintered at 1300ºC (see in previous Figure 4-10). It means that higher densification was achieved at 1300°C.

This information from the density measurement defined the optimal sintering temperature. In particular, the specimens sintered at 1300°C were more characterised in detail in comparison to the other ones sintered at 1200°C. Therefore the hardness measurements were carried out just for the sintered specimens at 1300ºC.

The hardness (HV10) of the sintered specimens from the six titanium based powders, cold compacted at 380 MPa and 560 MPa, are compared in the Figure 4-11. The theoretical hardness of pure titanium commercial grade 4 is 260 HV10 [11]. This hardness level is also given in the following Figure 4-11.

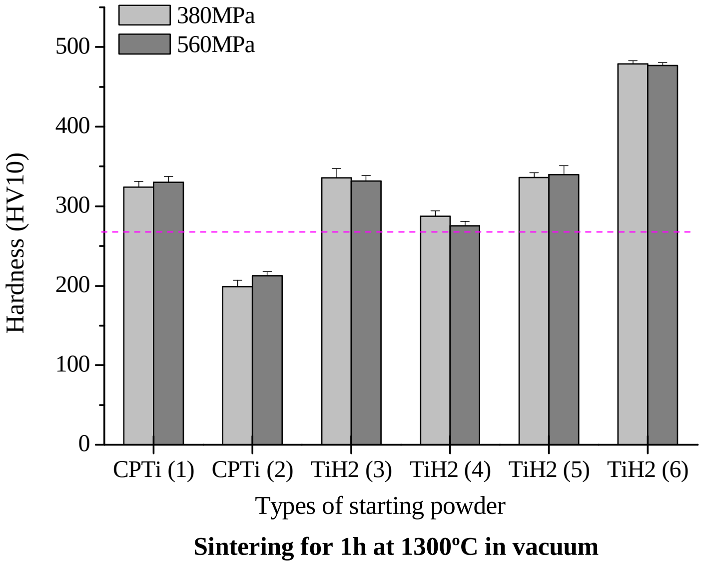

Figure 4-11. Hardness of samples cold compacted at two different pressures and sintered for 1h at 1300°C Ti-getter. (TiH_2 (6) handled in air and the other five titanium powders compacted under Argon atmosphere)

In addition to the hardness (HV10) of the specimens cold compacted (at 380 MPa and 560 MPa) and sintered (at 1300ºC for 1h), the values of the relative Archimedes density are summarised in the next table.

Table 4-9. Relative density (Archimedes) and hardness of samples cold compacted at two different pressures and sintered for 1h at 1300°C with Ti-getter. (TiH_2 (6) handled in air and the other five titanium powders compacted under Argon atmosphere)

Type of starting powder (sintered at 1300°C)	**Hardness (HV10)**		**Relative density (%)**	
	Cold compaction pressure used			
	380 MPa	560 MPa	380 MPa	560 MPa
CPTi (1)	324±7	330±7	99.5	99
CPTi (2)	199±8	212±5	97.1	98
TiH_2 (3)	335±12	331±7	99.4	99.6
TiH_2 (4)	287±7	275±6	99.3	99.3
TiH_2 (5)	336±6	340±11	99	98.8
TiH_2 (6)	479±4	477±4	95.6	97.1

An additional plot of the hardness values vs. density and oxygen content are shown in Figure 4-12.

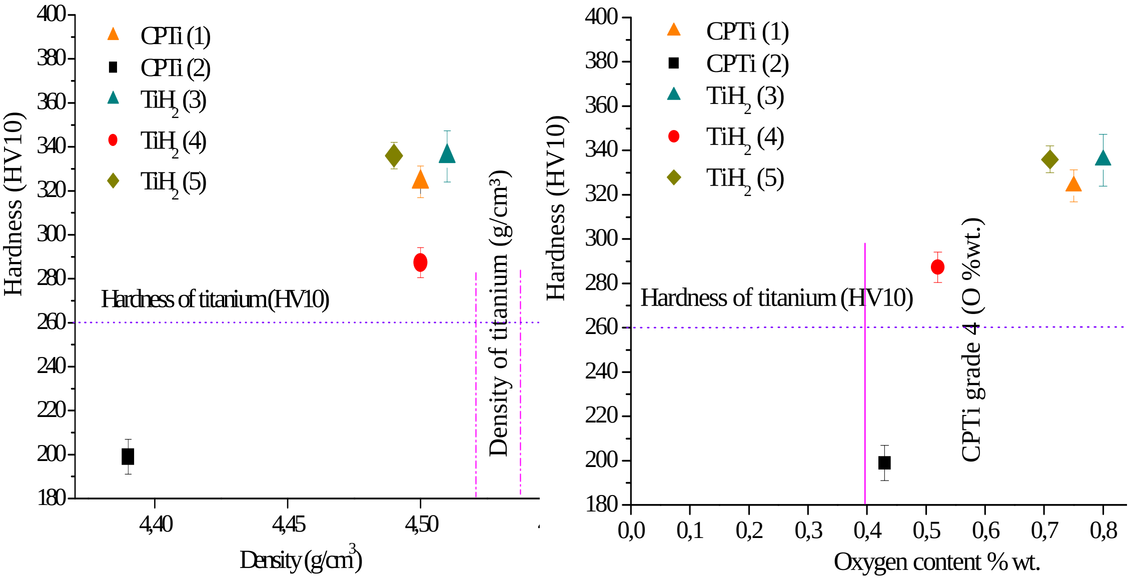

Figure 4-12. Hardness (HV10) vs. Arch. density and oxygen content, respectively, of the five titanium specimens compacted at 380 MPa and sintered for 1h at 1300°C in high vacuum. Hardness (HV10) and density (g/cm³) values for CPTi are taken from [3]

Chemical analysis

The characterization of the final samples showed that there is no significant difference of the oxygen content between the specimens handled in air and Ar, respectively (see Table 4-10. However, in all cases the surprising and so far inexplicable fact is observed that the green compacts contained in part dramatically more oxygen than both the starting powders and the sintered specimens, respectively. This effect was particularly pronounced with the specimens prepared from TiH_2 powders.

Table 4-10. Comparison of oxygen content in the starting powder, green specimens (in Argon and air compacted at 380 MPa) and sintered specimens (cold compacted in Argon at 380 MPa).

Type of powder	**Oxygen content (mass%)**			
	Starting powder	Green specimens handled		Sintered specimens, (after handling in Ar)
		in Argon	in air	
CPTi (1)	0.59	0.84	0.84	0.75
CPTi (2)	0.45	0.41	0.44	0.43
TiH_2 (3)	0.77	1.60	1.90	0.80
TiH_2 (4)	0.67	1.20	1.30	0.52
TiH_2 (5)	0.62	1.40	1.50	0.71

Additionally, chemical analysis was carried out to test if there was some relationship between oxygen and nitrogen content (mass %) of the green specimens, vs. the use of lubricant (paraffin) and the mechanical pressure of the compaction (200MPa and 560Pa). The next Figure 4-13 shows approx. the quantity of lubricant applied to the die wall. It was approx. 50%vol. less than the used for previous compaction (see Table 4-9).

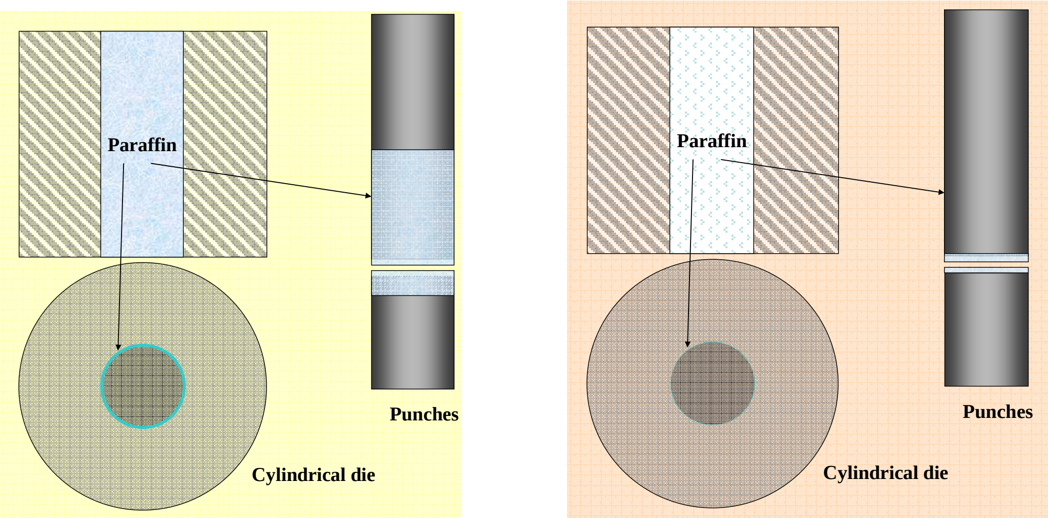

Figure 4-13. Paraffin applied on the die walls before the compaction: left figure represents the paraffin previously applied (at the beginning of the experimental part). The figure on the right represents the paraffin used in this last serial of experiments. It shows approx. 50%vol. less of paraffin.

In those previous compactions, the paraffin applied was previously dissolved in gasoline. Here, for the compaction, the paraffin was carefully applied directly on the die walls (no use of gasoline as solvent). The die was the same for all the compaction of the starting powder (see cylindrical die in Figure 2-3). Two starting powder were selected for this test. One of each CPTi and TiH_2 powder, with low oxygen content (CPTi(2) 0.45 mass% and TiH_2(4) 0.67 mass, see Table 4-9). Thus, the oxygen and nitrogen content (mass%) of green compact from CPTi(2) and TiH_2 were analysed.

Table 4-11. Comparison of oxygen content (mass %) in the starting powder and green specimens (in air compacted at 200 MPa and 560MPa).

Type of powder	**Oxygen content (mass%)**				
	Starting powder	200MPa		560MPa	
		No Lubricant	Lubricant	No Lubricant	Lubricant
CPTi (2)	0.48±0.08	0.49±0.08	0.52±0.11	0.60±0.01	0.59±0.05
TiH_2 (4)	0.69±0.07	0.85±0.20	0.85±0.25	0.86±0.05	0.88±0.08

Higher levels of oxygen are always presented in the green specimens from TiH_2 (4). The use of lubricant increases the oxygen content (mass%). This increase occurs in all the green specimens (from both starting powder) (see Table 4-11). Also, it is more pronounced at highest pressure (560 MPa) for specimens from TiH_2 (4) powder. In general, the mechanical pressure doesn’t affect significantly on the oxygen content. The analysis of nitrogen showed elevated content for all the green specimens from TiH_2 (4) (> 0.100 mass%) (see Table 4-12). The use of lubricant affect slightly the nitrogen content (mass%) independently of the starting powder and mechanical pressure used (200 MPa or 560 MPa).

Table 4-12. Comparison of nitrogen content (mass %) in the starting powder and green specimens (in air compacted at 200 MPa and 560MPa).

Type of Powder	**Nitrogen content (mass%)**				
	Starting powder	200MPa		560MPa	
		No lubricant	Lubricant	No lubricant	Lubricant
CPTi (2)	0.002±0.001	0.003±0.001	0.006±0.003	0.005±0.001	0.006±0.001
TiH_2 (4)	0.157±0.057	0.156±±0.001	0.167±0.001	0.181±0.006	0.171±0.041

Ending this study, after one and half year the oxygen content (mass%) of starting powders CPTi(2) and TiH_2 (4) are increased from 0.45 to 0.49 mass% for the CPTi(2) (aprox. increase of 9%), and from 0.67 to 0.69 mass %. (approx. increase of 3%).

As conclusion, the use of lubricant can influence the oxygen and nitrogen content of the green compact. Using 50 vol % less of lubricant, the oxygen of green compacts from TiH_2 (4) was reduced from 1.20 mass % to 0.86 mass % (approx decrease of 28%).

In particular for TiH_2(4) specimens, there was also a variation of oxygen content from the starting powder (0.69 mass%) to the green compacts (0.85 mass% at 200 MPa and 0.86 mass % at 560 MPa). Although in previous test with 50 vol % more of lubricant, such increase of oxygen (from the raw powder to the green compacts) was more marked.

Insignificant variation of nitrogen content (mass %) between the starting powder and the green specimens compacted at 200MPa and 560MPa was observed, independently of the starting powder.(i.e, nitrogen max. 0.214 mass% measured in starting powder TiH_2 (4) and max. 0.212 mass % measured in green compact at 560MPa using lubricant). The mechanical pressure used for the compaction of the green compacts doesn’t affect significantly the oxygen and nitrogen content (mass%).

Microstructural study of the specimens:

Firstly, the microstructural study of the specimens sintered at 1200°C showed the lower densification obtained at this temperature. In Figure 4-14, images of titanium compacts are shown (specimens from CPTi(1) starting powder compacted at 200 MPa and 560 MPa).

The influence of the mechanical pressure can be slightly observed. Visually, sample compacted at lowest pressure (200MPa) presented bigger porous size.

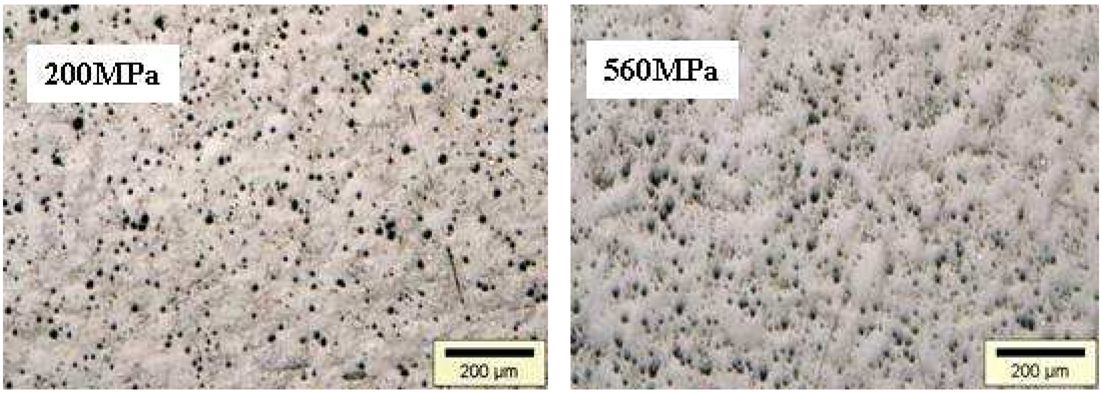

Figure 4-14. Images of the microstructure of titanium specimens from CPTi(1) consolidated at 200MPa (left) and 560MPa (right) and sintered at 1200°C for 1h in vacuum.

For the other four starting powder similar effect in the microstructure was also found. The lowest densification was confirmed by the microstructure study, for that reason the hardness measurement of these specimens (sintered at 1200ºC) were not necessary to determine the optimal sintering temperature for further tests.

By the use of SEM, the microstructures of the sintered specimens at 1300ºC from the five titanium based powders are shown in the next Figure 4-15 to Figure 4-17.

Very similar porosity is observed for both specimens from the commercial pure titanium powders.

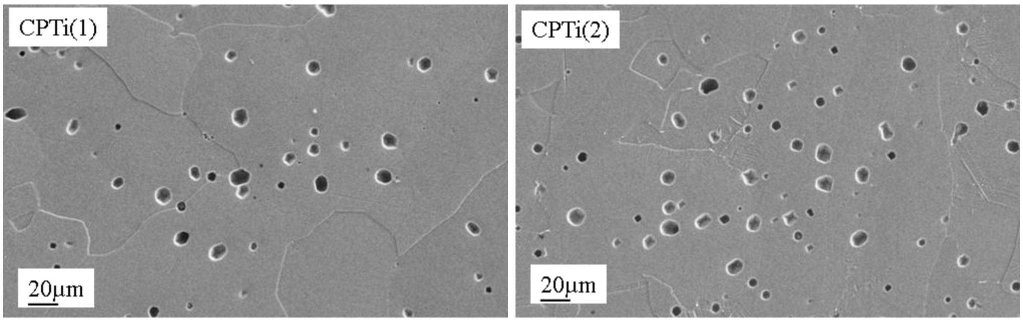

Figure 4-15. Sections (SEM (SE2) images) of the specimens from CPTi(1) (left) and CPTi(2) (right) consolidated at 560 MPa and sintered at 1300°C for 1h in vacuum.

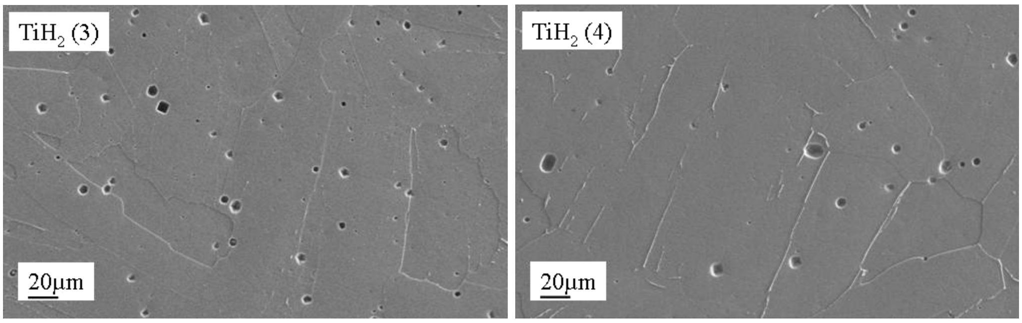

Figure 4-16. Sections of the specimens from TiH_2 (3) (left) and TiH_2 (4) (right) consolidated at 560 MPa and sintered at 1300°C for 1h in vacuum.

In contrast, finer porosity is found in the specimens from TiH_2 powders. In the case of the sample from TiH_2(5) the porosity is minimal (see Figure 4-17).

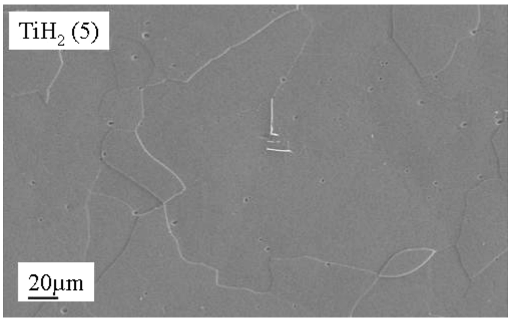

Figure 4-17. Section of TiH_2 (5) consolidated at 560 MPa and sintered at 1300°C for 1h in vacuum.

Intermediate Conclusions

- Surprising oxygen affinity of some starting powders (all the TiH_2 powders and CPTi(1)) after their cold compaction.
- Important influence of the impurities of the starting powders on the final properties of the titanium specimens (i.e., high hardness of sintered samples). Marked effect of the lubricant used for the cold compaction on the oxygen content of the green compacts.
- Low densification at lowest temperature (1200ºC). Sintered Ti with density > 99% was achieved at 1300ºC (e.g, specimens from TiH_2(4))
- Insignificant influence of the mechanical pressure (380 MPa and 560 MPa) on the oxygen content of the green samples, also on densification and hardness properties of the sintered specimens.
- Two most promising powders were selected for further investigations: the selection was carried out considering the low oxygen content in each type of powder material (CPTi and TiH_2). In this way, CPTi(2) and TiH_2(4).

4.2.4.2.1 Hot pressed Titanium based specimens.

The previous study of the starting powders showed the two powders, CPTi(2) and TiH_2(4), as most advisable titanium based powder to the manufacturing of TiMMCs because of their acceptable oxygen content (lower oxygen content mass% compared to the other starting powder of each type CPTi and TiH_2).

Additionally, after preliminary cold compaction and sintering experiments, hot consolidation tests (iHP) were carried out. Different processing conditions (consolidation temperature and heating rate, time was always 15 min for these tests) were tested in order to evaluate the behaviour of titanium specimens from these two titanium based powder.

Thus, all the results obtained can be used as reference for the further fabrication of the TiMMCs.

Then the consolidated titanium samples were considered as non-reinforced titanium matrices. In each of the following experimental test series, these titanium matrices (from CPTi(2) and TiH_2(4) powders) were fabricated simultaneously (i.e. the graphite die was filled with a determined quantity of each starting powder, CPTi(2) and TiH_2(4)).

Hence, their values of density, hardness (HV10) and oxygen content (mass%) can be always compared to the reinforced composites produced at the same processing conditions, e.g. temperature.

These hot pressing tests were done at different temperatures (Table 4-2). Thereafter these titanium compacts were characterized. The density and hardness values of these titanium compacts are shown in Figure 4-18 and Figure 4-19, and summarised in Table 4-13.

Moreover, several measurements of hydrogen and oxygen content were also done. Due to the size limitation in the inductive hot press (titanium specimens could be prepared with Ø10mm only) their mechanical properties could not be tested.

Concluding the characterisation of these titanium matrices, a study of the microstructure of the specimens was carried out. Finally, Intermediate Conclusions were briefly listed.

Archimedes density

A comparison of the Archimedes density of the specimens from CPTi(2) and TiH_2(4) powders hot consolidated at different inductive hot pressing temperatures is represented in the next Figure 4-18. The influence of the temperature was more significant for the specimens from TiH_2(4) powder.

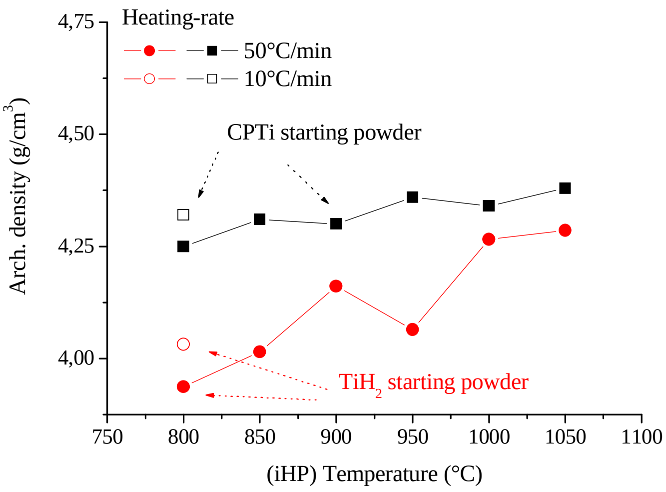

Figure 4-18. Arch. Density of the titanium specimens (from CPTi (2) and TiH_2 (4)) made by iHP at different processing condition (holding time=15 min, high vacuum and 50 MPa).

After the consolidation at 800ºC, the value of Archimedes density was down to 4 g/cm^3; however at 1000ºC it increased to 4.25 g/cm^3 (aprox.).

Contrary, the decrease of the heating rate involved considerable increase of the Archimedes density at the temperature tested (800ºC).

Hardness measurement

The hardness was studied as function of the temperature during inductive hot pressing.

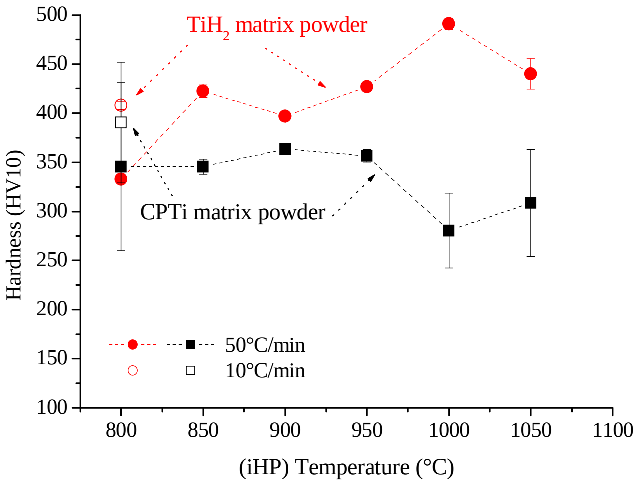

Figure 4-19. Hardness of the titanium specimens (from CPTi(2) and TiH_2(4)) fabricated via iHP at different processing conditions (holding time=15 min, high vacuum and 50 MPa).

In the following Table 4-13, Archimedes density and hardness of the different specimens are summarised. The different heating rates are also listed. At low heating rate (10 K/min) only a run at 800°C was done.

Table 4-13. Arch. density and hardness of the titanium specimens (from CPTi(2) and TiH_2(4)) made by iHP at different processing condition (temperature and heating rate).

Inductive HP Temp. (ºC)	Type of starting powder			
	CPTi (2)		TiH_2 (4)	
	Arch. density (g/cm^3)	Hardness (HV10)	Arch. density (g/cm^3)	Hardness (HV10)
Heating rate 10K/min				
800	4.03	255±3	4.32	393±12
Heating rate 50K/min				
800	3.94	264±1	4.25	338±40
850	4.02	248±13	4.31	353±10
900	4.16	251±4	4.30	341±13
950	4.07	240±3	4.36	334±10
1000	4.27	248±5	4.34	354±1
1050	4.29	249±5	4.38	361±11

The temperature increased the density of the specimens from this starting powder while the hardness presented approximately constant values.

At the same heating rate (50 K/min), the effect of the consolidation temperature for the specimens from the other starting powder (TiH_2(4)) was more marked for the hardness than for the density values. However, the decrease (10 K/min) of the heating rate involved a significant increase in both properties; it means

Study of the microstructure and micro-hardness (HV0.01)

By inspection of the titanium samples with the light microscope, several changes in the microstructure were found (see in Figure 4-20 to Figure 4-22).

Observing the specimens hot consolidated at 800°C with a heating rate of 10 K/min, on one side the specimen from TiH_2(4) starting powder does not exhibit any information about its microstructure in comparison to the specimen from CPTi(2) (see Figure 4-20). This titanium specimen (from CPTi(2)) shows two different, light (1) and dark (2) grey, phases, which were detected in the light microscope. Theses two phases are also observed at higher iHP temperatures (1000° and 1050°C with heating rate of 50 K/min). Moreover, the size of the light phase is increasing with the temperature.

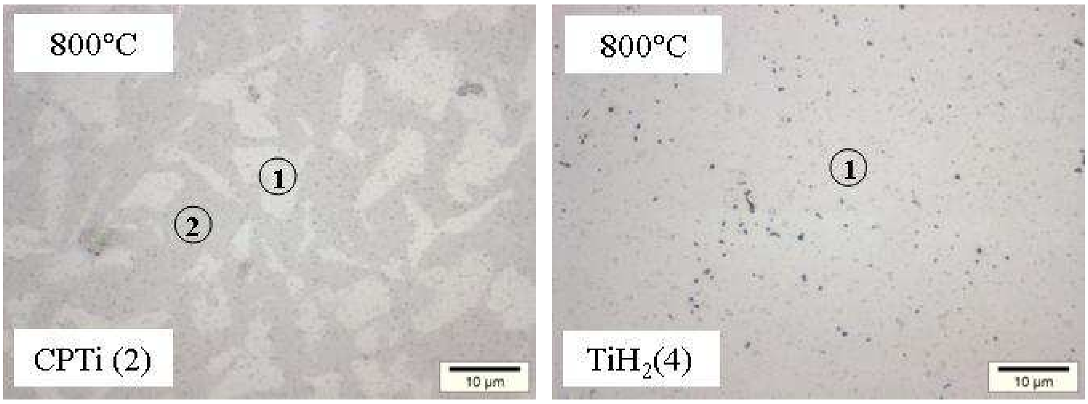

Figure 4-20. Microstructures of specimens from the starting powders CPTi(2) (left) and TiH_2(4) (right), produced by inductive hot pressing at 800°C for 15 min and a heating rate of 10 K/min.

The specimens from TiH_2(4) compacted at 1000° and 1050°C show a martensitic (light needles) microstructure which is not detected by the light microscope for the sample hot consolidated at 800°C (10K/min heating rate) (see in Figure 4-21 and Figure 4-22).

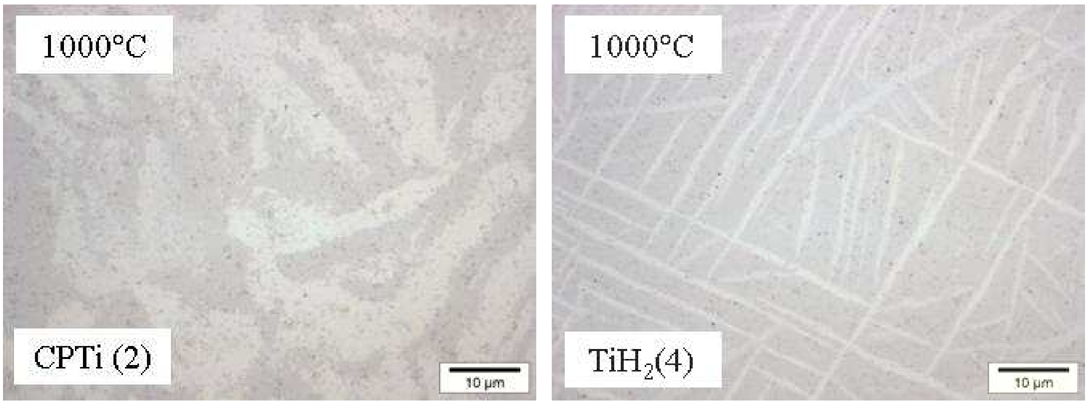

Figure 4-21. Microstructures of titanium specimens from the starting powders CPTi(2) (left) and TiH_2(4) (right), produced by inductive hot pressing at 1000°C for 15 min and a heating rate of 50 K/min.

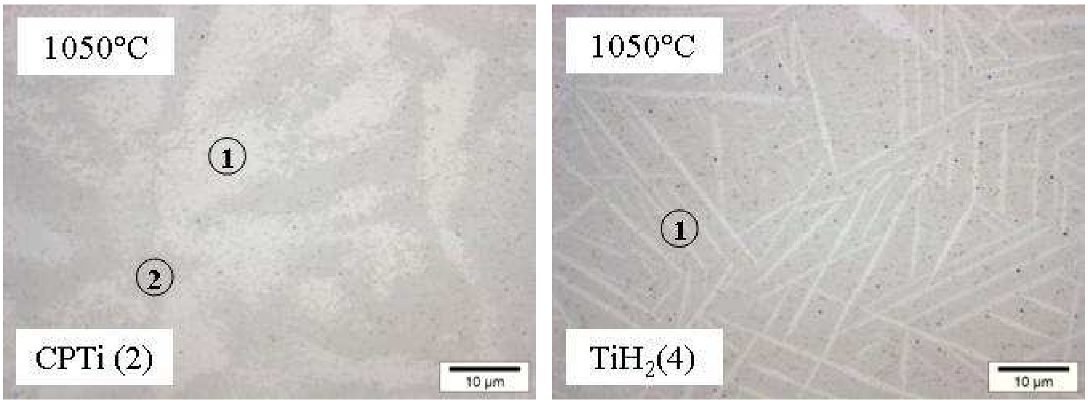

Figure 4-22. Microstructures of titanium specimens from the starting powders CPTi(2) (left) and TiH_2(4) (right), produced by inductive hot pressing at 1050°C for 15min and a heating rate of 50 K/min.

The microhardness measurements are performed in the points marked 1 and 2, two indentations were made per phase. Point 1) being the light phase and 2) the dark one for the compacts from CPTi(2) powder, the microhardness measurement is done in these two points. In the compacts from TiH_2(4) powder, the microhardness test was performed only in one point because only one phase was observed. These results are shown in the next Table 4-14.

Table 4-14. Micro-hardness of the titanium specimens in the different phase observed (see Figure 4-20 to Figure 4-22). Titanium specimens from CPTi(2) and TiH_2(4)) fabricated via iHP at different processing conditions (holding time=15 min, high vacuum and 50 MPa).

iHP: Temperature & Heating rate	**CPTi (2)**		**TiH_2 (4)**
	MicroH. (HV0.01)		MicroH. (HV0.01)
	1	2	1
800°C & 10 K/min	347±7	388±21	408±4
800°C & 50 K/min	406 ±49	285±4	333±3
1050°C & 50 K/min	270±3	246±2	440±16

SEM images give a little more information about these light and dark phase for the compact from CPTi(2), but it does not clarify the presence of two phase for compacts from pure titanium phase. Using the SEM, significant microstructure changes are presented on the microstructure of the specimens. The iHP temperature range investigated is from 800° to 950°C (with the same heating rate, 50 K/min). SEM images are taken using the BSE detector. The comparison of the microstructure of the specimens is shown from Figure 4-23 to Figure 4-25.

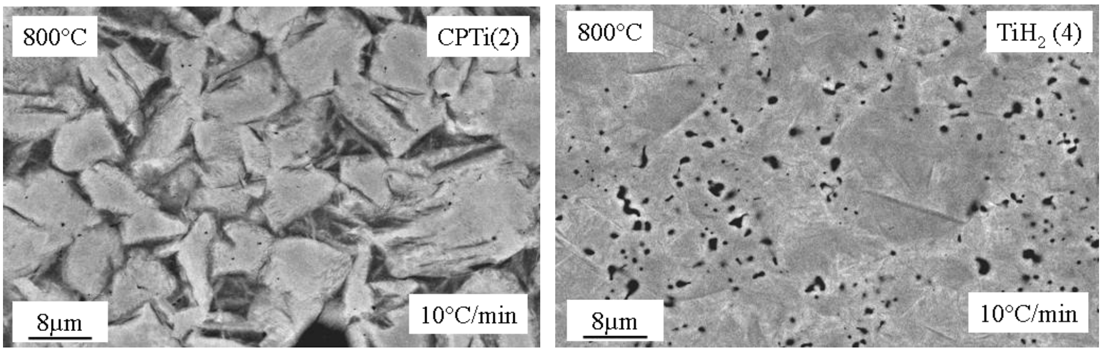

Figure 4-23. Microstructure of specimens from the starting powders CPTi(2) (left) and TiH_2(4) (right), produced by inductive hot pressing at 800°C for 15min and a heating rate of 10 K/min.

Some round pores (black) of very small (0.5μm) size are observed in the specimens hot consolidated at 800°C with a heating rate of 10 K/min from the TiH_2(4) powder. In the case of the sample from CPTi(2) powder, the grain size is easily recognised. The next microstructural comparison is shown according to the increase of the inductive hot pressing temperature in intervals of 50 K from 800°C to 1050°C and considering the same heating rate for the manufacturing of all the specimens (50 K/min).

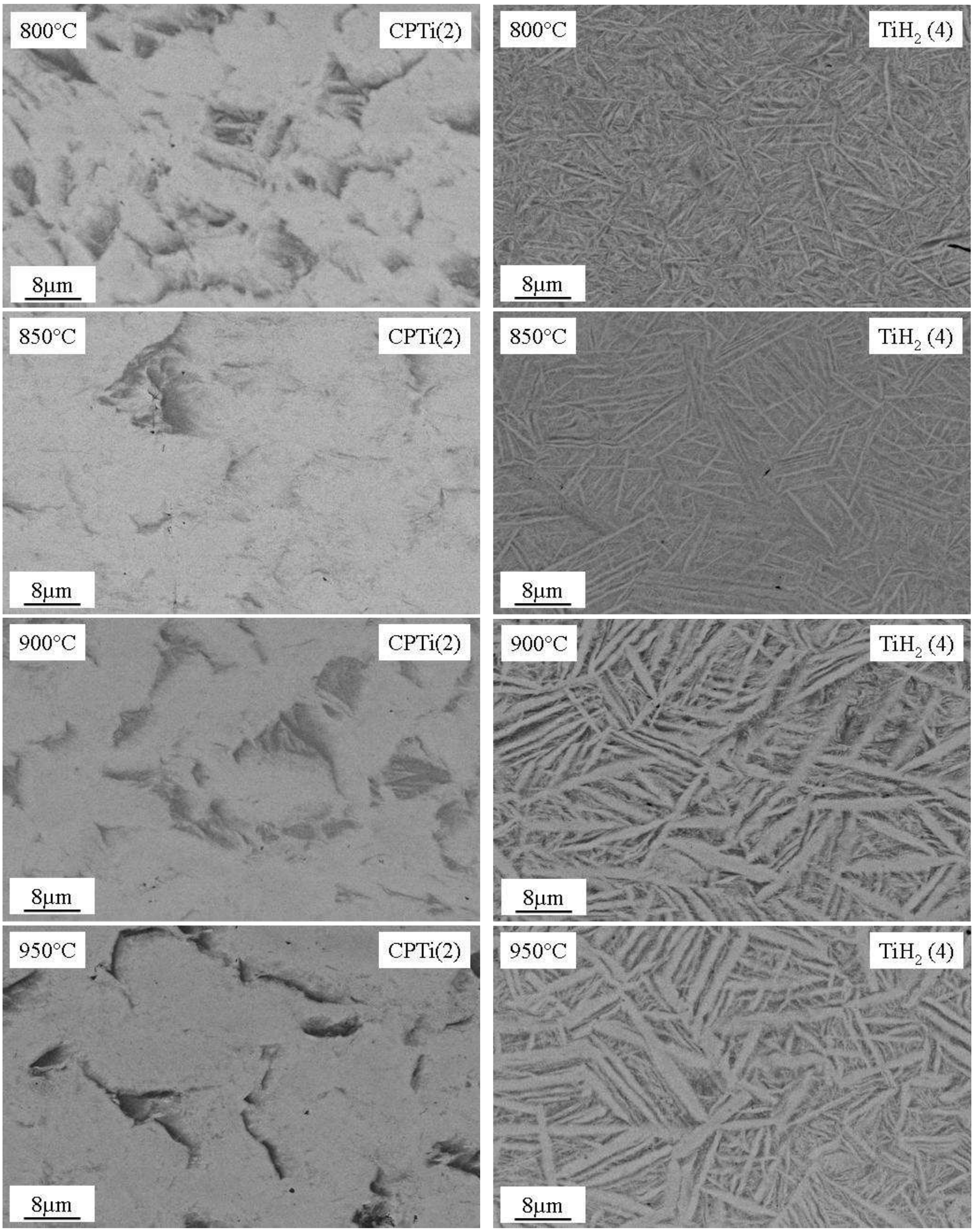

Figure 4-24. Microstructure of titanium specimens from the starting powders CPTi(2) and TiH_2(4) produced by inductive hot pressing from 800 to 950°C for 15 min and a heating rate of 50 K/min.

There is a slight microstructural change with temperature for specimens from the

TiH_2(4) starting powder (right). The width of the needles grows a little. From the temperature of 850°C to 900°C the martensitic (light grey) structure becomes larger. Also the grain size of the microstructure of samples from CPTi(2) slightly increases with the temperature.

There is no porosity in the samples produced at the higher temperatures (1000°C and 1050°C). This confirms the increase of the density of the specimens with higher temperature.

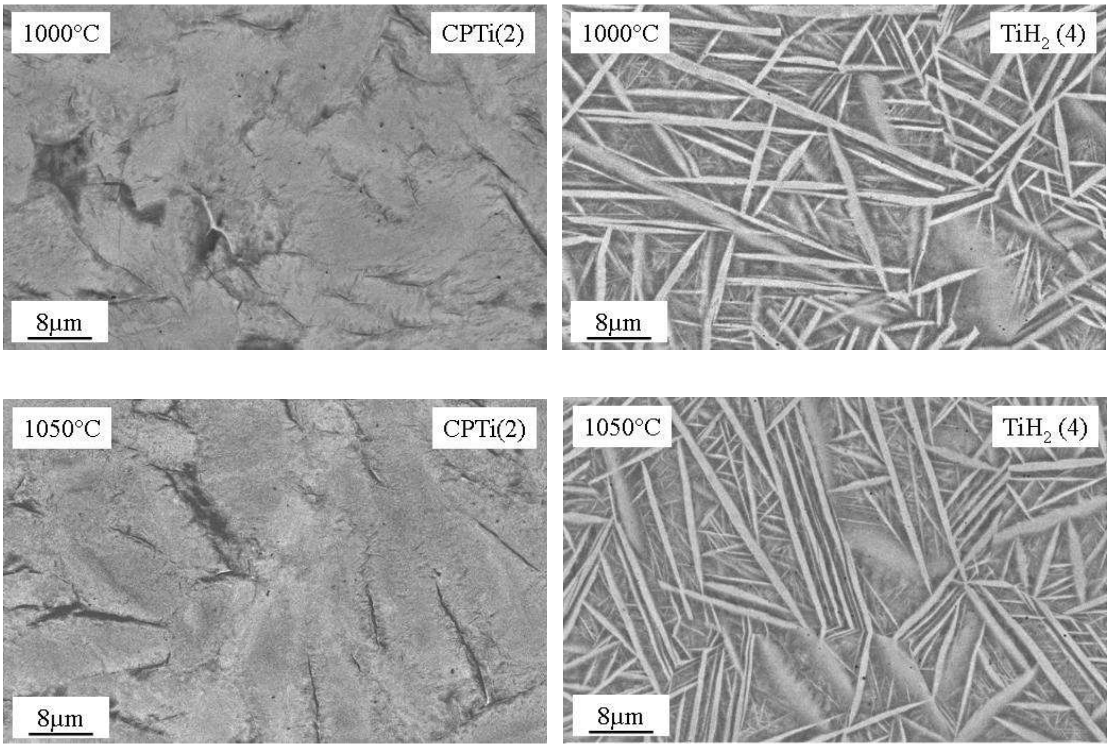

Figure 4-25. Microstructures of titanium specimens from the starting powders CPTi(2) (left) and TiH_2(4) (right), produced by inductive hot pressing at 1000°C and 1050°C for 15 min and a heating rate of 50 K/min.

Previous investigation about the influence of the interstitial elements such as nitrogen and hydrogen in solid solution in titanium showed the similar martensitc microstructures for specimens with considerable nitrogen and hydrogen contents [16, 98]. Based on these previous works, the effect of nitrogen on the microstructure is to promote the formation of these needles of alpha titanium. This is a most interesting observation, because this needle-like Widmanstätten structure is characteristic of titanium alloys that have been annealed above the alpha-beta transformation temperature. By the use of polarised light microscope, the same martensitic structures are detected (see Figure 4-26). The growing of this needle microstructure is increased by the iHP temperature. Additionally some particles from the metallographic preparation are also seen on the microstructural sections of the specimens.

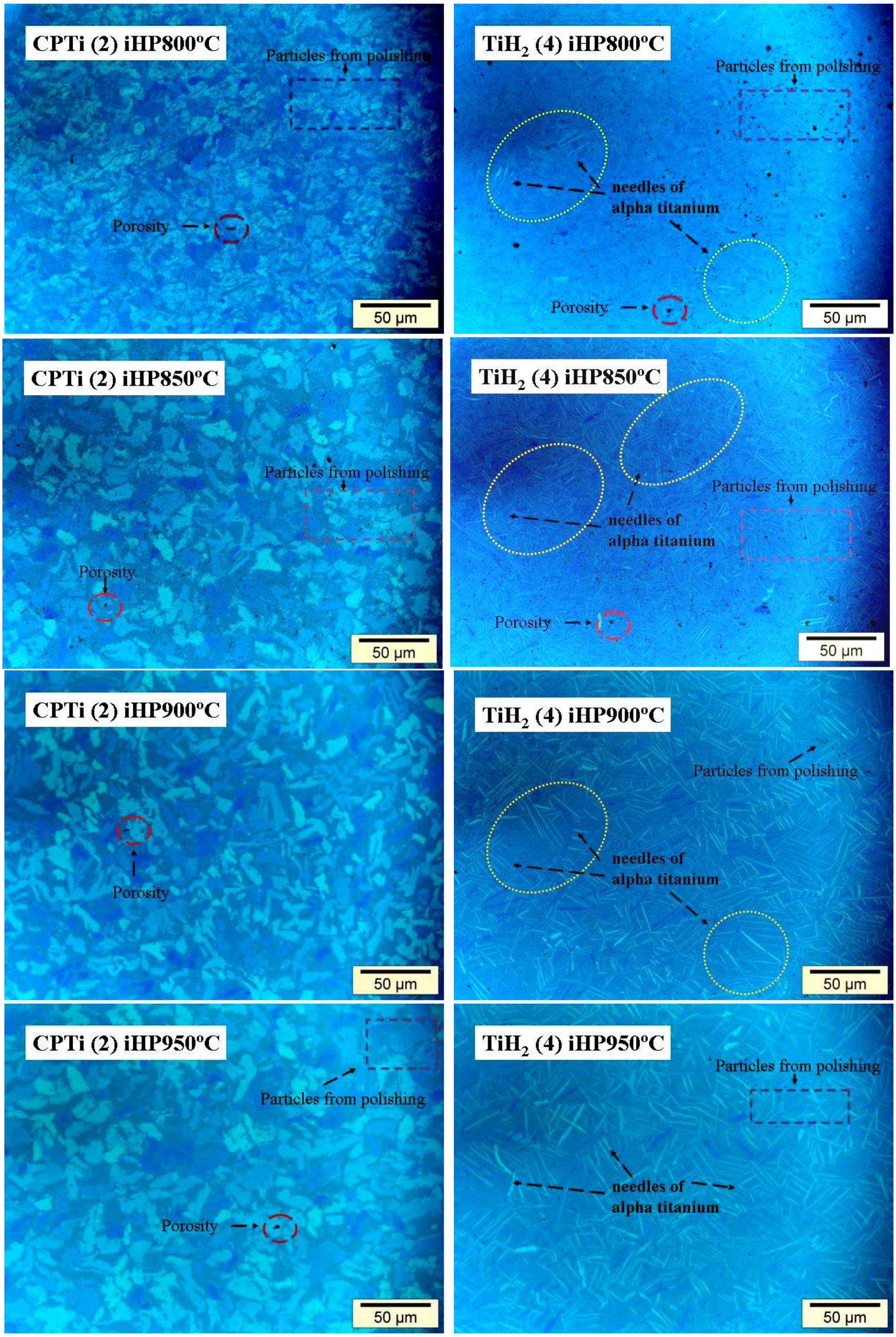

Figure 4-26. Images (by polarized light microscope) from microstructures of titanium specimens from the starting powders CPTi(2) (left) and TiH$_2$(4) (right), produced by inductive hot pressing from 800°C to 950°C for 15 min and a heating rate of 50 K/min.

As remarked, the conclusion is that nitrogen in solid solution in titanium causes this needle formation. For that reason, in specimens from starting powder CPTi(2) such characteristic needle microstructure was not visible due to the lower nitrogen concentration (max 0.006 mass%). The influence of the high level of nitrogen and oxygen content (masss%) is also evident in the hardness of the specimens.

Chemical analysis

The oxygen and hydrogen contents were analysed in the titanium specimens fabricated at the lowest and highest temperature, respectively (see in the next Table 4-15). The specified processing conditions and the starting powder used for the manufacturing of the samples are also listed. The nitrogen content of these titanium specimens could not be analysed. Unfortunately, the specimen mass was to low to enable further analytical runs.

Table 4-15. Chemical analysis of the titanium specimens (from CPTi(2) and TiH_2(4) powders) at the lowest and highest processing temperature (iHP for 15 min and 10 K/min or 50 K/min).

iHP: Temperature & Heating rate	**CPTi (2)**		**TiH_2 (4)**	
	Chemical analysis (mass%)		Chemical analysis (mass%)	
	Oxygen	Hydrogen	Oxygen	Hydrogen
800°C & 10 K/min	0.49	0.17	1	0.95
800°C & 50 K/min	0.49	0.19	0.89	0.74
1050°C & 50 K/min	0.44	0.07	0.81	0.50

Intermediate Conclusion

- The impurities of the starting powder such as oxygen and nitrogen affected the microstructure and hardness of the final specimens considerably.
- Increase of the iHP temperature promoted the growth of these needle-like Widmanstätten structures for the specimens from TiH_2(4). Al lowest iHP (800ºC) temperature, this structure was detected insignificantly. Additionally, the densification was in general better at high iHP temperatures.
- At the same iHP temperature (800ºC), the decrease of heating rate from 50 K/min to 10 K/min contributed to better densification.
- Higher oxygen content are observed at lowest iHPT (800ºC) and heating rate (10 K/min).

4.3 Titanium Metal Matrix Composites (TiMMCs)

Following the structure of the research work, four sequential divisions of this section, “Reinforced Titanium Matrices”, were defined. They were fixed according to the type of reinforcement materials used (TiB_2, nano/micro Boron, carbon nano fibres or nano diamond particles).

Moreover, additional subdivisions into the reinforcement material part were considered on the basis of the PM technique employed for the manufacturing of the composites.

4.3.1 TiMMCs reinforced by TiB_2 particles

TiMMCs reinforced by TiB_2 particles was the first composite material produced in this work.

The stable Ti + TiB_2 system is widely known and has been studied in previous works. For that reason this composite material is only produced here by the conventional cold pressing and sintering process. In this way, the training in the production of composite material via powder metallurgy technique was carried out. Because of the moderate cost of this reinforcement material, it was use for the training in manufacturing of TiMMCs.

4.3.1.1 Manufacturing processes

Beginning with the description of the composites from CPTi and TiH_2 matrix powders, a process flow sheet is presented in the following Figure 4-27. It represents the manufacturing process of the titanium MMCs reinforced with particles of titanium diboride (TiB_2).

The previous determination of an optimum sintering setup and the evaluation of the processability of all the titanium powders as matrix material contributed to finding the most suitable procedure for the fabrication of titanium matrix composites via cold pressing and sintering. Because of flexibility and simplicity, conventional cold-pressing and sintering processing was used.

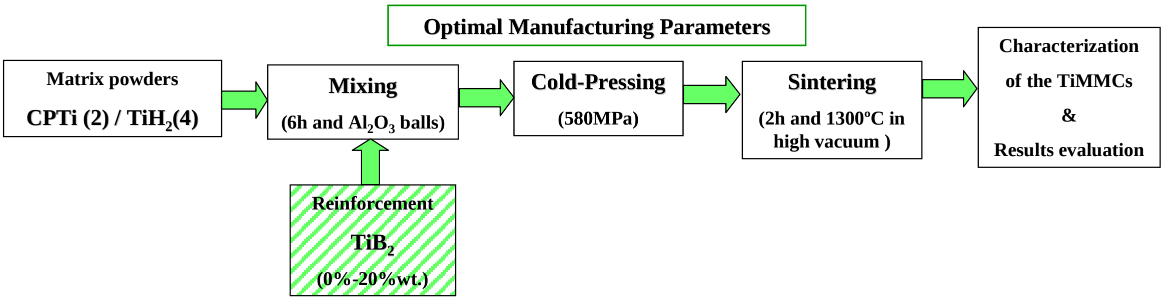

Figure 4-27. Manufacturing flow sheet for Ti MMCs reinforced using particles of titanium diboride (TiB_2).

Powder Preparation

The manufacturing process commenced with the powder preparation. At the first stage, mixing of the powder took place.

As shown in the flow sheet (see Figure 4-27), the two most promising titanium powders (CPTi(2) and TiH_2(4)) were mixed with the respective amounts of titanium diboride (TiB_2) (see in Table 4-16). The calculation of the boride contents was done considering as theoretical density for CPTi 4.54g/cm³ and for TiB_2 4.62g/cm³ [58, 99]

Table 4-16. Contents of the TiB_2 used for the TiMMCs

TiB_2 content into the matrix							
(%vol.)	0	0.49	0.98	4.92	9.80	14.78	19.72
(mass%)	0	0.50	1	5	10	15	20

The mixing took place during 6h in a tubular Sintris mixer using cyclohexane as liquid, to avoid powder agglomerations, and ceramic balls (Al_2O_3) with 5 mm diameter. The wet mixed powders were completely dried during 16 hours. The dried powder was the dry blended for 30 minutes without the ceramic balls. After that the powders were ready to be compacted.

Compaction and sintering of the TiMMCs

The consolidation was done as previously described. Cold pressing was done at 580 MPa, handling the powder in air. The die used was cylindrical (Ø12 mm). The final geometry of the green compacts was a cylinder (see Figure 2-11), diameter 12 mm and 3 mm high (approx.). At the beginning, there was only the cylindrical die available to produce the compacts. For that reason, only cylindrical samples were produced.

The sintering parameters were selected as a result of the previous experiments, in which the six titanium based powders have been tested. Therefore, the optimum assembly and the high sintering temperature (1300ºC) were chosen for manufacturing of the composites. However, the sintering time was extended to 2 h in order to further reduce the porosity in the final samples.

4.3.1.2 Results of the characterisation and discussions

Finally, the compacted and sintered samples were characterized.

Geometrical density measurements before and after sintering were carried out as well as Archimedes’s, in addition to analysis of the oxygen content and hardness (HV10) measurements of several specimens. The microstructure of some compacts was also studied, as were the correlations between density, hardness (HV10), and oxygen content.

Density and hardness of the titanium composites:

The calculation of the theoretical density of the composites was done considering the values of the density described in the bibliography. The Archimedes density of the specimens was measured in water with paraffin impregnation.

The next Figure 4-28 shows the comparison of density (the relative density) and the hardness vs. the content of TiB_2 (mass%). These titanium composites were compacted at 560 MPa and sintered in high vacuum at 1300° for 2 h. For the titanium compacts without reinforcement the sintering time was just 1 h.

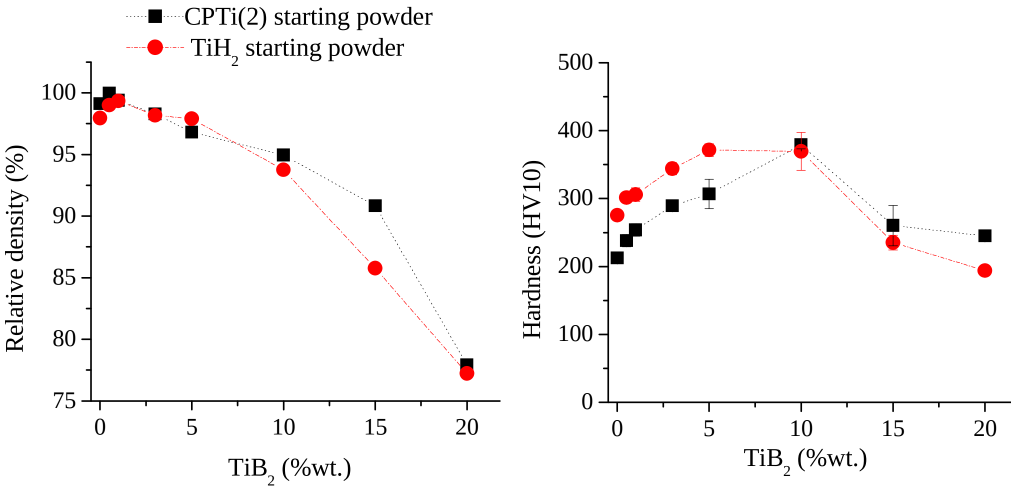

Figure 4-28. Density and hardness vs. content of TiB_2 of the titanium composites from CPTi(2) and TiH_2 (4) starting powder. They were compacted at 560 MPa and sintered for 2 h at 1300°C. The titanium matrices without reinforcement were compacted at 560 MPa and sintered for 1 h at 1300°C

As the previous graphic shows, the density and hardness values for both matrices increase markedly up to 1 mass% of TiB_2. From 3% to 10 mass% of the reinforcement content the hardness increases while the density goes slightly down.

At 10 mass% of TiB_2, the hardness of the compacts attains up to 380 HV10 for the composite from CPTi(2) and 370 HV10 for that from the TiH_2(4) powder, and the relative density levels are around 95 rel%.

Above 10 mass% reinforcement, the hardness decreases as a result of lower density (75 to 90 rel%) (See in Figure 4-28).

Additionally, all the previous values of the density (geometrical green density, geometrical and Archimedes sintered density) and the hardness of the compacts from CPTi(2) and TiH_2(4) with the different TiB_2 concentrations are also summarised in the next Table 4-17.

Table 4-17. Density (green density, geometrical and Archimedes sintered density) and hardness of the titanium specimens from CPTi(2) powder reinforced with different contents of TiB_2. The titanium matrix without reinforcement was compacted at 560 MPa and sintered for 1 h at 1300°C. The composites were compacted at 560 MPa and sintered for 2 h at 1300°C.

CPTi + TiB_2(mass%)	**Th.density**	**Green density (g/cm³)**	**Geom. After sintering (g/cm³)**	**Arch. density (g/cm³)**	**Hardness (HV10)**
0 (1h 1300ºC)	4.540	3.67	4.37	4.45	213
0.5	4.541	3.82	4.34	4.54	238
1	4.542	3.89	4.37	4.51	254
3	4.542	3.74	4.49	4.46	289
5	4.544	3.70	4.29	4.40	307
10	4.548	3.71	4.30	4.32	379
15	4.552	3.63	3.68	4.15	260
20	4.556	3.57	3.52	4.14	245

In spite of the lower density (78% relative density), the hardness of the composite with 20 mass% of TiB_2 is superior to the hardness of the matrix without reinforcement.

Table 4-18. Density (green density, geometrical and Archimedes sintered density) and hardness of the titanium specimens from TiH_2(4) powder reinforced with the different contents of TiB_2. The titanium matrix without reinforcement was compacted at 560 MPa and sintered for 1h at 1300°C. The composites were compacted at 560 MPa and sintered for 2h at 1300°C.

TiH_2 + TiB_2(mass%)	**Th.density**	**Green density (g/cm³)**	**Geom. After sintering (g/cm³)**	**Arch. density (g/cm³)**	**Hardness (HV10)**
0 (1h 1300ºC)	4.540	3.157	4.513	3.55	275
0.5	4.541	3.721	4.376	4.46	301
1	4.542	3.659	4.422	4.45	306
3	4.542	3.228	4.500	4.46	344
5	4.544	3.299	4.500	4.45	371
10	4.548	3.280	4.190	4.26	369
15	4.552	3.305	3.710	3.90	235
20	4.556	3.349	3.402	3.91	194

In the Table 4-17 a significant reduction of the geometrical density of the sintered composite with 15 mass% and also at 20 mass % of reinforcement is shown. This fact is due to irregular geometry of the sample after sintering.

Smaller irregularities in the dimensions of the samples involve significant variation of their geometrical density because of the limited dimensions (12 mm diameter and 3 mm high).

By increasing the TiB_2 content in the titanium matrix, the specimens from TiH_2 become more fragile in comparison to the specimen without reinforcement. This was observed during the handling of the samples (green and sintered), and also the hardness decreased (at 20 mass% of TiB_2 194 HV10).

Oxygen content

Oxygen analysis was done on four of the composites with lowest and highest reinforcement content. In the next table, these results are listed in addition to the mean values of hardness (HV10) and Archimedes density for each type of composite.

Table 4-19. Comparison of the composites with lowest and highest reinforcement content.

Starting matrix powder	**TiB_2(mass%)**	**O (mass%)**	**Arch. density (g/cm^3)**	**Hardness (HV10)**
CPTi	0.5	0.44	4.54	238
	20	1.35	4.14	245
TiH_2	0.5	0.61	4.46	302
	20	1.44	3.91	194

High levels of oxygen content were, surprisingly and so far inexplicably, observed at the highest TiB_2 content for both starting matrix powder. In the case of the compacts from the TiH_2(4) powder the oxygen content was always higher than in the compacts from the CPTi(2) powder. This high oxygen content in the composites with 20 mass% can come from the reinforcement materials (2.30 mass%).

Microstructural study

In the images of the composite with 10 mass% and 15 mass% of reinforcement is observed how the porosity in the samples increases above 10 mass% of TiB_2. Larger pores are observed on the specimens from CPTi(2) with 15 mass% of reinforcement, it confirms low densification at his reinforcement concentration.

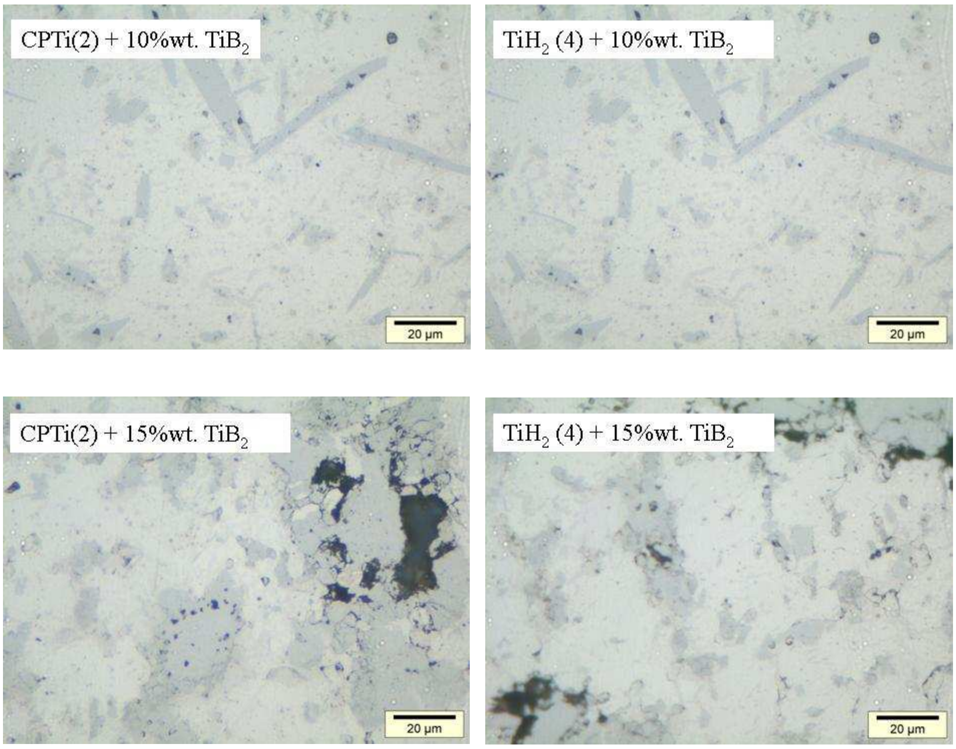

Figure 4-29. Microstructure of specimens from CPTi(2) (left) and TiH_2(4) (right) matrix powders with 10 mass% and 15 mass% of TiB_2. (cold pressed at 560 MPa and sintered at 1300°C for 2h in vacuum).

Finally, SEM images were taken in the SE mode. They show the microstructure of the most representative specimens. In the following Figure 4-30, titanium composites with 5 mass% of TiB_2 particles are shown. For both composites, the distribution of the TiB_2 is homogeneous.

Additionally, the anisotropy of the TiB_2 (needles) is also found in the titanium matrices. Moreover, the porosity in both titanium matrices is similar.

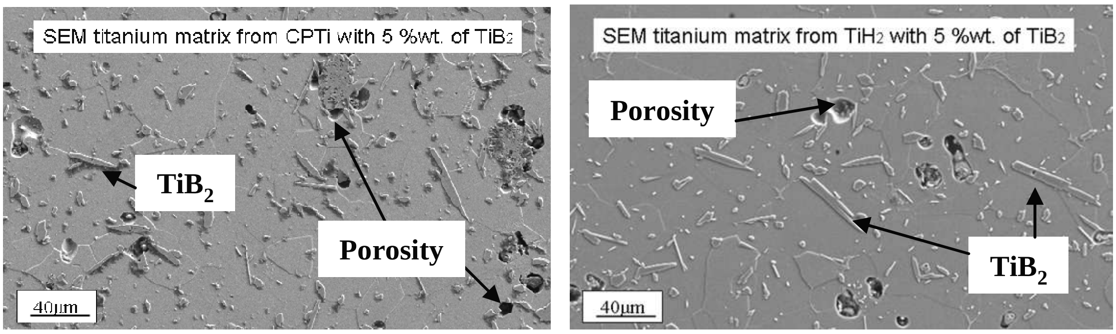

Figure 4-30. SEM (SE2) of microstructures of sintered Ti-TiB_2 composites. Compacted from CPTi(2) and TiH_2(4) starting powders with 5mass% of TiB_2 respectively and sintered for 2h at 1300°C in vacuum.

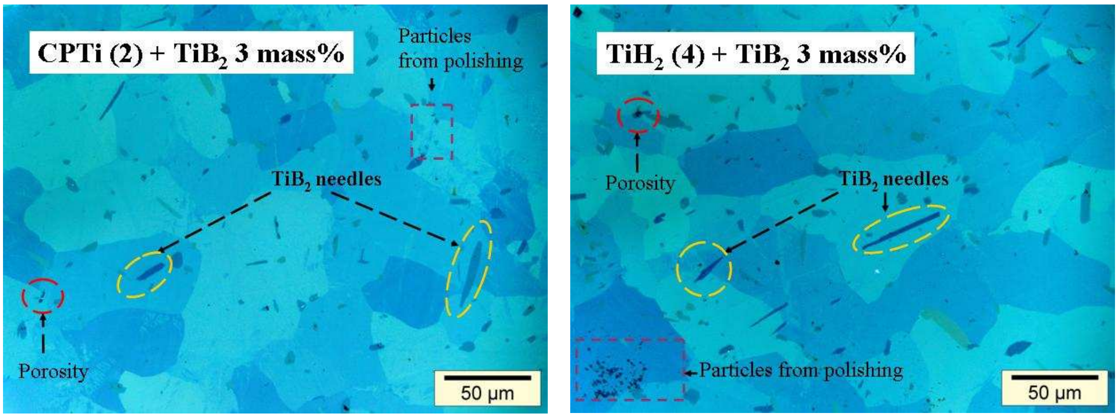

Figure 4-31. Images of microstructures of sintered Ti-TiB$_2$ composites. Compacted from CPTi(2) and TiH$_2$(4) starting powders with 3 mass% of TiB$_2$ respectively and sintered for 2h at 1300°C in vacuum.

Intermediate Conclusions

- Due to the small size of the samples, mechanical properties could not be measured and compared to the theoretical ones.
- Up to 10 mass% of TiB$_2$ content, relative density > 93% was achieved.
- At 10%wt. of TiB$_2$, a possible optimisation of time/temperature could increase relative density.
- High oxygen content was measured in the TiMMCs, consequently high hardness values are obtained. This influence of oxygen on the hardness was previously documented [18].
- The addition of TiB$_2$ increases the oxygen content of the final composite, affecting its properties. (Theoretically, there is 0.46 g of oxygen in 20g of TiB$_2$)
- Anisotropy of the TiB$_2$.particles is observed after sintering.

4.3.2 TiMMCs reinforced with Nano/Micro Boron particles

4.3.2.1 Manufacturing processes

Hot consolidation processes were used for the fabrication of TiMMCs reinforced with nano-boron particles. The influence of the processing parameter and condition on the properties and microstructure of the TiMMCs was one of the objectives of these experiments and also how the properties of TiMMCs with different nano-boron contents were influenced by the different processes and their parameters (e.g., iHP temperature).
Comparisons between conventional hot pressing and inductive hot pressing techniques were carried out considering the results obtained after the sample characterisation.
The cold pressing and sintering process was not used for the manufacturing of these TiMMCs because the main objective of this experimental part was the optimisation of the hot consolidation techniques for this kind of reinforcement material. The description of the fabrication procedures for the titanium matrices reinforced with nano/ micro Boron particles are represented in the Figure 4-32 and Figure 4-33.

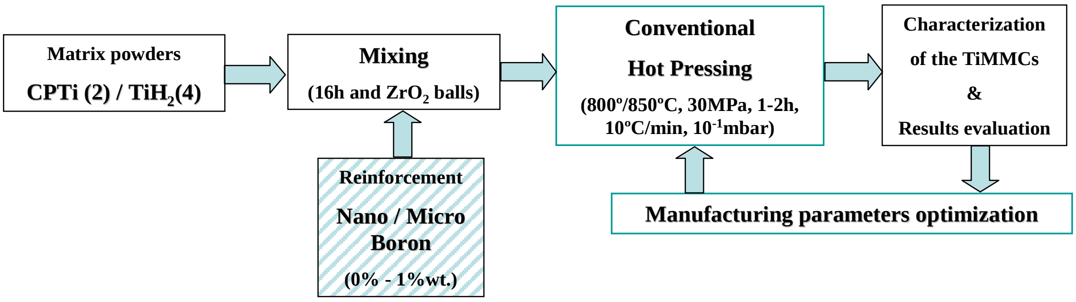

Figure 4-32. Manufacturing flow sheet of the titanium matrices reinforced with nano/micro particles of boron (B) via conventional hot pressing (HP).

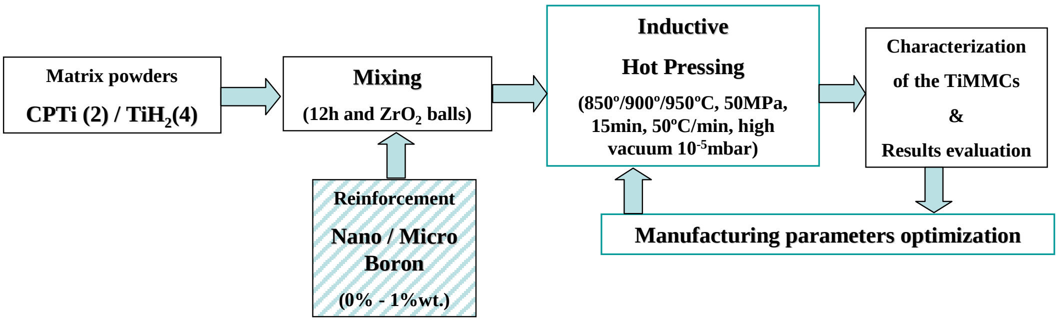

Figure 4-33. Manufacturing flow sheet of the titanium matrices reinforced with nano/micro particles of boron (B) via inductive hot pressing (iHP).

The same starting powders were used for the manufacturing of compacts via inductive hot pressing, with the main difference of a shorter cycle time and higher heating rate. Also for conventional hot pressing all the powder were compacted in the same runs at the same temperature; inductive hot pressing die presented the geometrical limitation that in one runs just two or three type of mixing powder could be hot consolidated.

Powder Preparation

The blending of all the powders was performed in the same way in which the titanium based matrices were reinforced with TiB_2 particles.

The two titanium powders (CPTi(2) and TiH_2(4)) were mixed with the respective amounts of nano/micro boron particles (B) (see Table 4-20). The content of boron in the titanium matrix was selected according to the final application of the material (which necessitates warm deformation, different from the previous composites (Ti-TiB_2)). This composite should be deformed via forging. For that reason the boron content is not more than 1 mass% For the calculation of the reinforcement contents, the density of boron particles was taken as 2.46g/cm³ and 4.54g/cm³ for the pure titanium matrix [99]

Table 4-20. Contents of nano/micro boron particles used as reinforcement for the fabrication of TiMMCs

Boron content in the matrix					
% vol.	0.00	0.19	0.56	0.92	1.83
% wt.	0.00	0.10	0.30	0.50	1.00

Due to the size of the reinforcement material, the nano/micro boron particles, there was higher risk of powder agglomerations. Therefore, smaller ceramic balls (ZrO_2) with 3 mm diameter were employed.

During 12 h the wet mixing of the powders took place. Following, the drying of the mixing during 16 hours took place. Next, the powder was again (dry) blended for 1 h without the ceramic balls. Finally, the powders were ready to be consolidated via conventional and inductive hot pressing, respectively.

Hot Compaction Processes

In this part of the work, conventional hot pressing and inductive hot pressing methods were used for the development of the titanium composites reinforced with nano/micro boron particles. Several processing parameters were varied and optimised simultaneously. However, as described in the manufacturing chapter, many parameters were constant in both hot pressing tests.

The next Table 4-21 shows the processing parameters and conditions used in both hot consolidation processes (HP and iHP).

Table 4-21. Processing parameters of the conventional and inductive Hot Pressing technique.

HP technique	Processing parameters					
	Temp. (ºC)	Die dimensions	Heating rate (K/min)	Holding time (min)	Pressure (MPa)	Vacuum (mbar)
Conventional HP	850°	100mm Ø	10	120	30	10^{-1}
	850°	13.5x13.5mm²	10	60	30	10^{-1}
	800°					
Inductive HP	950°	10mm Ø	50	15	50	10^{-5}
	900°					
	850°					

The first test was carried out via conventional hot pressing. By the use of the graphite die with the 12 squares (13.5x13.5mm²) (see in Figure 2-6), the total load is distributed among the samples.

The graphite die with the 12 squares (13.5x13.5mm²) was used (in the same run), each cavity was loaded with powders with different reinforcement content. In this way, all the material compositions were hot consolidated at the same time.

However, the pressure acting on the specimens during the hot consolidation is not totally homogeneous. This factor can affect the properties of the different samples consolidated at the same temperature but in different cavities of the graphite die.

4.3.2.2 Results of the characterisation of the samples and discussions

As mentioned in the chapter of the characterisation techniques, after the hot consolidation, the samples were removed from the die and prepared to be characterised. Density, hardness, chemical analysis and microstructural studies were carried out for all the samples.

The mechanical properties, flexural and tensile strength were measured in specimens with the specified geometrical dimension.

The results of the characterisation of the titanium based composites were reported and the different manufacturing processes were compared.

Concluding, several comparisons between the manufacturing techniques employed were done, e.g. runs done at the same temperature and using the same starting powders.

4.3.2.2.1 Conventional hot pressing technique (HP)

The processing parameters were varied and also the geometry of the graphite dies. Firstly, the smaller samples were produced. Density, hardness and oxygen content were measured. The use of larger graphite dies made it possible to fabricate plates with Ø 100 mm from which reasonably large test specimens could be prepared. This means, the mechanical properties (flexural and tensile properties) could be measured.

As previously mentioned, the properties of specimens consolidated at the same temperature (850°C) can show variation of the mechanical properties by using different graphite dies, on one side the die with the 12 square cavities and on another side the larger die (100mm Ø).

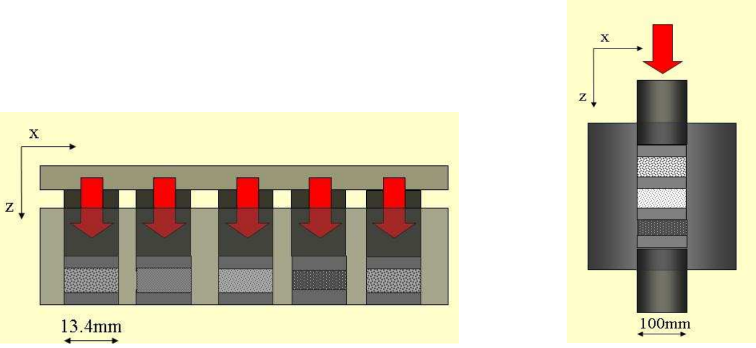

Figure 4-34. Hot Pressing test with the different dies used: left it is the die with the twelve cavities (13.4x13.4mm^2); right the cylinder die with 100 mm diameter.

The powder consolidated in the smaller square suffers more contact with the walls of the die. Although these smaller graphite cavities are always lined with a thin graphite foil coated with boron nitride (BN), the ratio of contact area/volume (A_c/V_T) of these smaller titanium composites is larger in comparison to the composites consolidated into the larger graphite die.

There was additional effect because of scatter in the former case (between the cavities, see Figure 4-35).

Due to different load distributed and the inhomogeneous load received on the graphite punches, the composites consolidated at the same temperature and from the same starting powder and boron concentration, just for changing the high of the filling, can present different final properties (see in Table 4-38). Therefore, the composites from different starting matrix powder,(CPTi(2) and TiH_2(4)), and also different boron concentration presented different additional load distribution because of the difference between the filling heights before the hot pressing process.

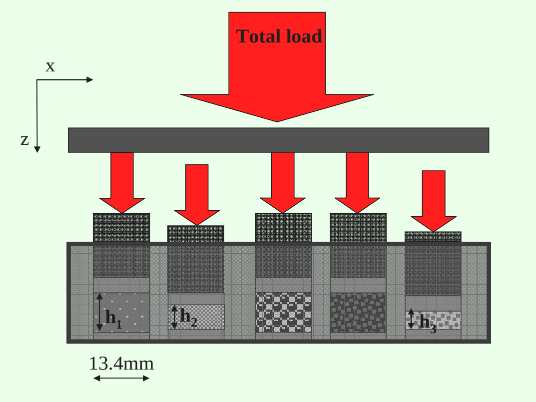

Figure 4-35. Load distribution for 12-cavities graphite die by hot pressing technique (exaggerated).

TiMMCs hot consolidated at 800ºC and 850ºC for 1h

After the hot consolidation of the titanium powder with the different contents of nano-boron, 12 samples were produced (13.5 x 13.5 x 4mm^3). The next Figure 4-36 shows the final geometry of the compacts produced from titanium based matrices reinforced with the different boron content (mass%). The "z" axis is the direction of the pressure.

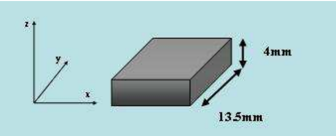

Figure 4-36. Geometry (13.5x13.5x4mm^3) of the composites after HP at 800º and 850ºC for 1h using the special multi-cavity graphite die (see Figure 2-6)

- *Density, hardness and oxygen content measurement*

In Figure 4-37, the relative density (Archimedes density with paraffin) and hardness values vs. the boron content (mass%) of the different TiMMCs, are shown. In this first HP test, four different boron contents (see in Table 4-20) were employed. As listed in the previous Table 4-21, the value of the pressure was 30 MPa, and the vacuum was 10^{-1} mbar.

In the Table 4-22 the properties of the composites produced at 800°C are shown, and next in the Table 4-23 those of the composites fabricated at 850ºC. The Archimedes density, the theoretical and relative density and hardness are listed.

The addition of nano-boron particles contributed to the increase of the hardness. It can be related to the high oxygen content of this reinforcement material. Because of the high impurity level (nitrogen mass% and oxygen mass%) of the starting powder TiH_2 (4), the hardness of the specimens from this titanium based powder was always higher than that of specimens from CPTi(2).

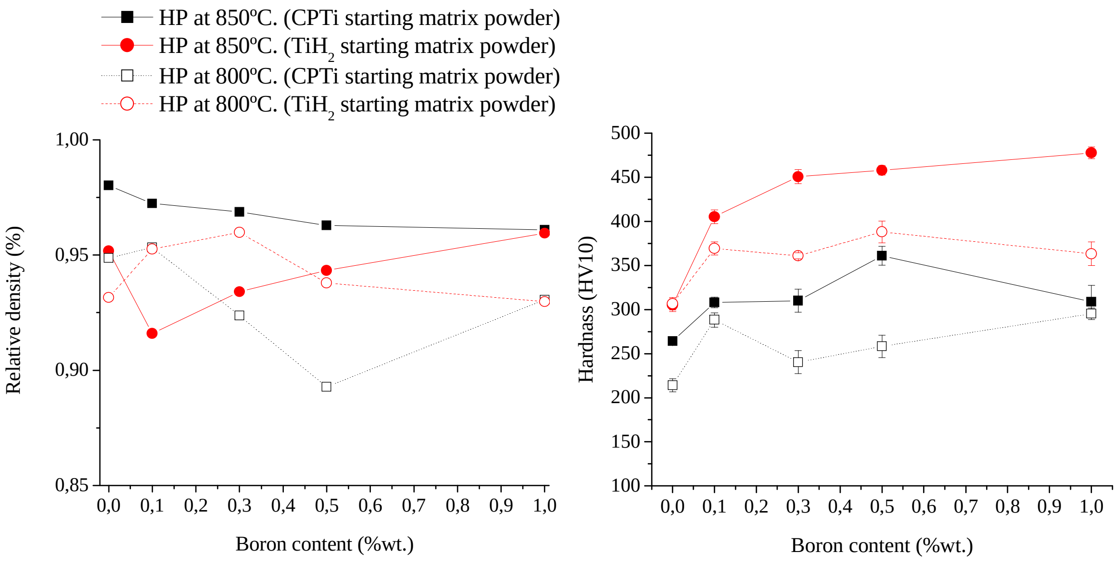

Figure 4-37. Relative density and hardness of the composites vs. the boron content (mass%). The specimens were hot consolidated via HP at two temperatures.

Table 4-22. Archimedes and relative density, and the hardness of the composites with varying boron content (mass%). The specimens were hot consolidated via HP at 800°C for 1h.

HP at 800°C for 1h	**Arch. density (g/cm3)**	**Th. Density (g/cm3)**	**Rel. density (%)**	**Hardness (HV10)**
Matrix +Boron (mass%)				
CPTi(2)				
0	4.31	4.54	94.87	214
0.1	4.32	4.54	95.33	288
0.3	4.17	4.53	92.17	240
0.5	4.20	4.52	92.85	258
1	4.19	4.50	93.06	295
TiH_2 (4)				
0	4.23	4.54	93.16	307
0.1	4.32	4.54	95.26	369
0.3	4.35	4.53	95.99	361
0.5	4.24	4.52	93.79	388
1	4.19	4.50	92.98	363

In general, for specimens consolidated at 800ºC and 850ºC the composites from TiH_2(4) present higher hardness values than those from CPTi(2) in spite of their lower relative density (see in Table 4-22 and Table 4-23).

Table 4-23. Archimedes and relative density, and the hardness of the composites with varying boron content (mass%). The specimens were hot consolidated via HP at 850°C for 1h.

HP at 850°C for 1h	**Arch. density (g/cm3)**	**Th. Density (g/cm3)**	**Rel. density (%)**	**Hardness (HV10)**	**Oxygen (mass%)**
Matrix +Boron (mass%)					
CPTi (2)					
0	4.47	4.54	98.36	307	0.58
0.1	4.41	4.54	97.24	369	-
0.3	4.39	4.53	96.87	361	-
0.5	4.35	4.52	96.29	388	-
1	4.33	4.50	96.09	363	-
TiH_2 (4)					
0	4.25	4.54	93.65	305	0.76
0.1	4.33	4.54	95.42	405	-
0.3	4.41	4.53	97.30	451	-
0.5	4.44	4.52	98.25	458	-
1	4.50	4.50	99.92	478	-

- *Microstructural study*

The next Figure 4-38 shows the microstructure of the composites from CPTi(2) and TiH_2(4) starting powder with 1 mass% of boron particles. The larger size of the boron particles can be observed as well as several pores in both composites.

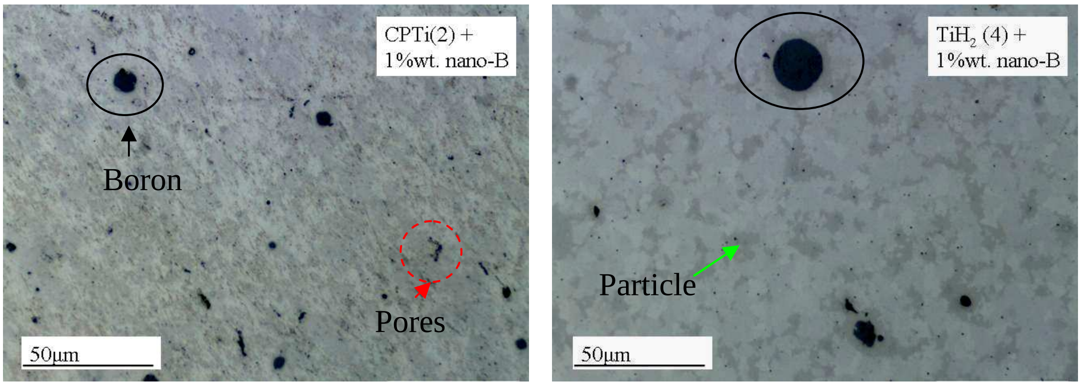

Figure 4-38. Microstructures of the composites from CPTi (2) (left) and TiH_2(4) (right), with 1 mass% of boron particles, HP at 850ºC for 1h. (Black=Boron particle, red=porosity; green=dark particles from the metallurgical preparation). (Images by light microscope)

Impurities (SiC from sandpaper and Al_2O_3 from polishing) from the metallographic preparation (smaller dark particles) are present on the surface of the composites (see in Figure 4-38). Additionally, the polarised light microscopy (LEICA DMI5000M) was used for the observation of the hexagonal close-packed structure of α-titanium. In this way, the microstructural study of the specimens reveals significant differences between the titanium composite matrices. For the matrices from CPTi(2) and TiH$_2$ (4) powders, the size of particle observed is different. On one side, for the composite from CPTi(2) the hexagonal grains of the α phase could be perfectly recognised. However for the composite from TiH$_2$(4) this microstructure is not as clear to detect. At 0.5 mass% of boron, the size of the particle grains is reduced because of the boron addition (see Figure 4-39). Even when increasing the temperature of the conventional hot pressing process, the same effect of B addition on the microstructure is observed. Also the pure titanium based matrices present a similar microstructure after the HP at 800ºC and 850ºC.

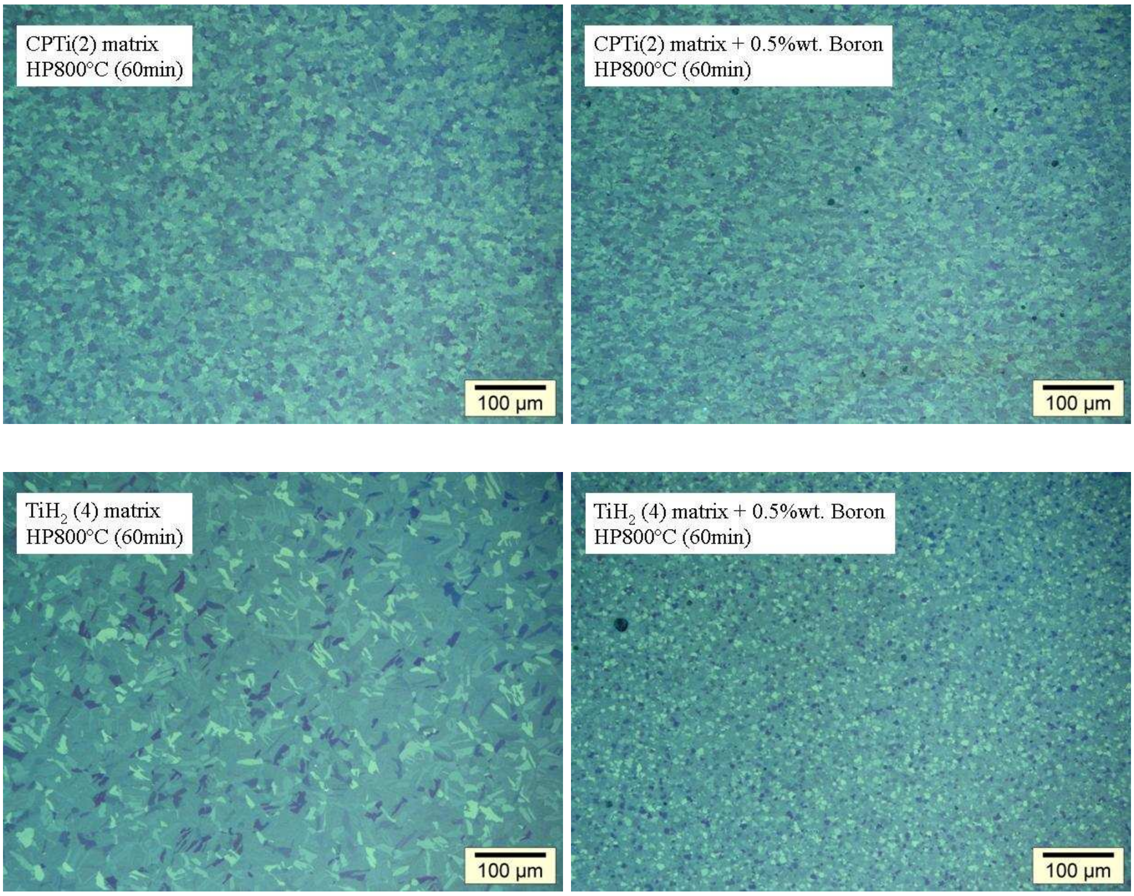

Figure 4-39. Microstructure of the pure titanium matrix from CPTi(2) andTiH$_2$(4) powders (left) and reinforced with 0.5 mass% of boron particles (right). HP at 800ºC during 1h. (Use of the die with 12-cavities).

In the next figures the microstructures of the titanium matrix, pure and reinforced with 0.5 mass% of boron particles after the HP process carried out at 850ºC are shown.

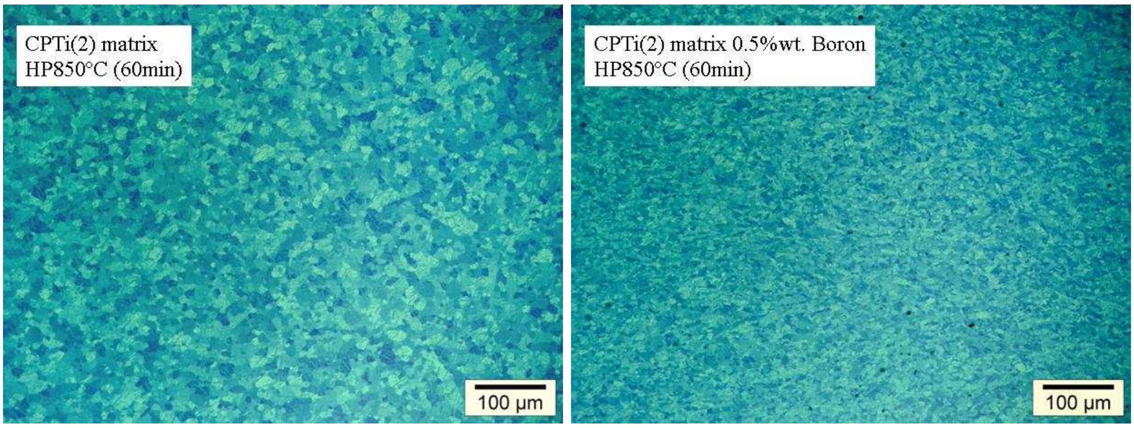

Figure 4-40. Microstructure of the pure titanium matrix from CPTi(2) powder (left) and reinforced with 0.5 mass% of boron particles (right). HP at 850ºC during 1h. (Use of the die with 12-cavities).

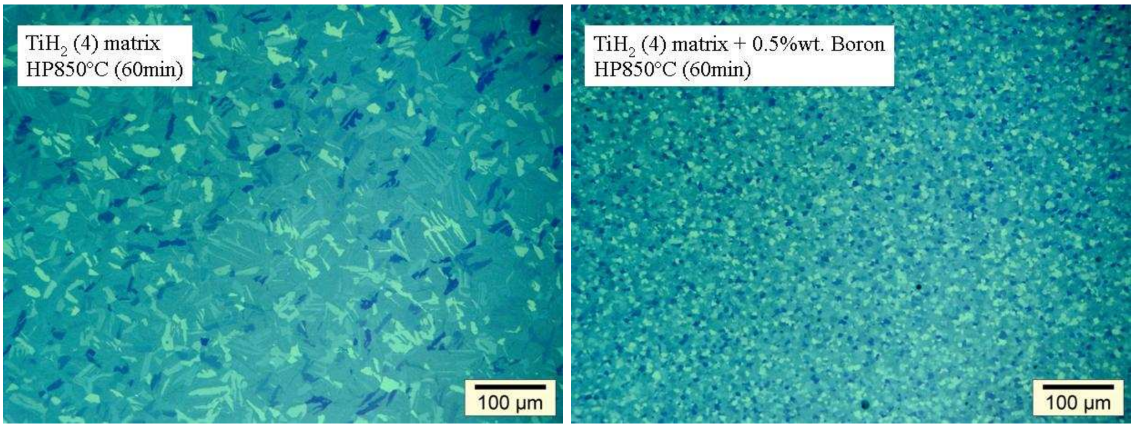

Figure 4-41. Microstructure of the pure titanium matrix from TiH_2(4) powder (left) and reinforced with 0.5 mass% of boron particles (right). HP at 850ºC during 1h. (Use of the die with 12-cavities).

Furthermore, SEM images (BSE signal) show the distribution of the boron particles in the titanium matrix (see in Figure 4-42).

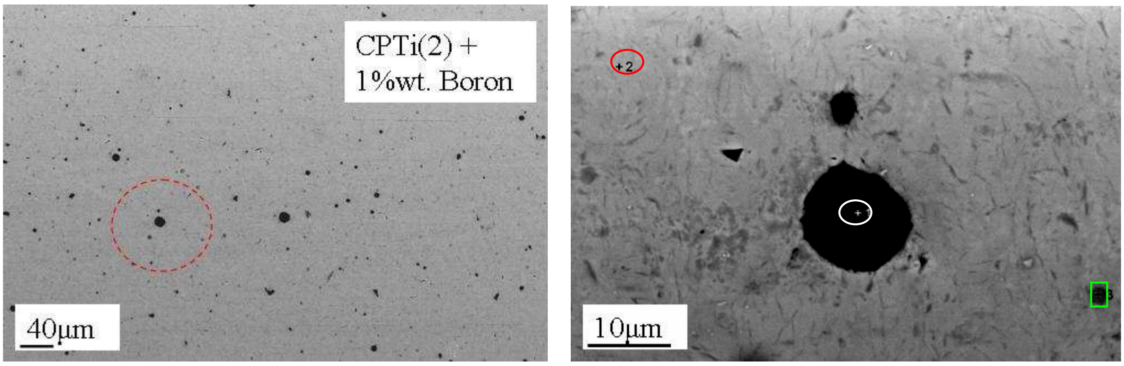

Figure 4-42. Boron particle in a CPTi (2) matrix. TiMMCs (with 1mass% of nano/micro-boron particles) hot consolidated at 850ºC for 1h. The SEM images are taken by the BSE detector.

Moreover, the porosity around the reinforcement particles is seen (Figure 4-43). In this way, it confirms the slight decrease of the density of the titanium composites with the increase of the reinforcement concentrations.

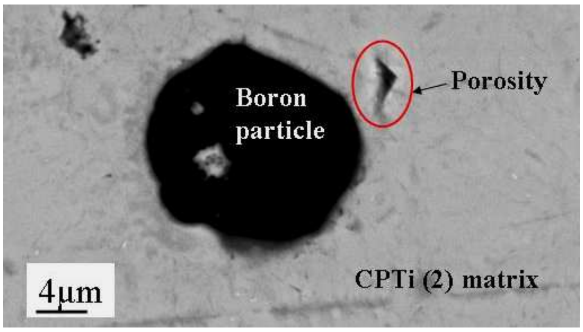

Figure 4-43. Boron particle in a titanium matrix (CPTi(2)). TiMMCs with 1mass% of nano/micro-boron particles (hot consolidated at 850ºC for 1h). The SEM images are taken by the BSE detector.

The element analysis on a section of the composite was done by EDAX. Since the EDAX-analysis of light element is not precise, this quantitative technique has to be considered as qualitative analysis here. The areas analysed are numbered (see in Figure 4-42 (right). The results are listed in the next Table 4-24. The signal of the BSE detector shows the dark region as elements with lower atomic mass, thus the boron particles are observed as the black and round features. Impurities on the boron particles from the powder, such as Mg, are detected. The next table shows the concentration of each element in three measurement points. The Mg came from the impurities of the nano-boron particles (see Table 3-10).

Table 4-24. EDAX analysis on the section of TiMMCs from CPTi(2) matrix powder reinforced with 1 mass% of boron particles. (HP at 850º for 1h).

TiMMCs from CPTi(2) (EDAX analysis)		
Spot 1 (white)		
Element	mass %	at %
B	97.99	99.18
Mg	1.63	0.73
Ti	0.38	0.09
Spot 2 (red)		
Ti	100	100
Spot 3 (green)		
B	36.32	71.65
Ti	63.68	28.35

TiMMCs hot consolidated at 850ºC for 2h

After the evaluation of the results from the TiMMCs, larger samples with defined boron concentration were produced. 0.1 and 0.5 mass% of boron were mixed into a Ti matrix (from the CPTi(2) starting powder). The characterisation of these larger plates involved the measurement of density, hardness and chemical analysis. Additionally, mechanical properties of these composites were measured. The results are shown in the next tables and figures. Finally a microstructural study of the composites was done.

- *Characterisation of the TiMMCs at room temperature (RT)*

First, the measurement of the density, hardness and chemical analysis was done. The results are reported in the next table. The nitrogen content could not be measured for the specimens from CPTi(2) with 0.5 mass% and 1 mass% of nano-boron particles due to the same technical problem with the LECO TC 500. For that reason these values are not given in the next Table 4-25.

Table 4-25. Results of the characterisation of the TiMMCs with different content (mass%) of boron. Hot pressed at 850ºC.

Matrix powder boron content (mass%)	Rel. density (%)	Hardness (HV10)	Oxygen (mass%)	Nitrogen (mass%)
CPTi (2)				
0	98	281±7	0.60	0.013
0.1	95	287±14	0.82	n.d.
0.5	87	266±70	0.80	n.d.
TiH_2(4)				
0	89	300±6	0.76	0.275
0.1	89	296±6	0.94	0.306
0.5	91	310±29	0.95	0.200

As is observed in the previous table, high impurity levels (oxygen and nitrogen mass%) are observed for the matrix and composites from TiH_2(4) starting powder. In general, with increasing boron content the oxygen content increases; this holds for both types of titanium matrix composites. Lower densification was observed for the specimens from CPTi(2) than from TiH_2(4) starting powder. One reason for that can be the difference between their sintering behaviour (studied previously, see chapter 3).

The addition of boron particles to the titanium based matrix results in slightly lower relative density (%) of the composites from CPTi(2). It is confirmed by the SEM images where the porosity appears around and on the surface of the boron particles (see the microstructural study). Although the oxygen content is high (approx. 0.8 mass%) for the composite with 0.5 mass% of boron the hardness is not so high, due to the low density of this composite. In the case of composites from TiH_2 (4), the oxygen levels go up to 0.95 mass%

This content of oxygen influences the hardness for these composites in spite of their low relative density (%). In addition to the density, hardness and oxygen analysis, mechanical properties, flexural and tensile strength, were measured at room temperature (RT) (see in Table 4-26). Three parallel measurements were made for each bending and tensile test. The tested specimens from the pure titanium matrix were not totally broken due to problems with the tensile testing machine.

Table 4-26. Properties of the TiMMCs with different boron content (mass%) at room temperature.

Matrix Powder	**Flexural tests**			**Tensile tests**		
Boron (mass%)	Flexural strength (MPa)	E-modulus (GPa)	ε (%)	Tensile strength (MPa)	E-modulus (GPa)	ε (%)
CPTi (2)						
0	1681±87	100±1	4.4	n.d.	n.d.	n.d.
0.1	1047±294	93±5	1.4	437±82	121±3	0.5
0.5	538±31	70±5	1	210±68	102±8	0.3
TiH_2 (4)						
0	398±34	80±3	0.7	95±24	95±8	0.1
0.1	409±30	78±5	0.6	91±54	84±40	0.2
0.5	638±14	85±9	0.9	189±97	131±21	0.4

The TiMMCs from TiH_2(4) matrix powder exhibited lower mechanical properties such as their elongation (%) because of the higher nitrogen levels (>0.15 mass%) measured. Also the high oxygen content (> 0.8 mass%) contributed to reduce the mechanical properties of these TiMMCs.

- *Fractographic study*

In the next Figure 4-44, the fracture surfaces of the composites are given. These SEM images were taken by the secondary electron detector. Because the samples from the pure titanium matrix from CPTi(2) were not broken, the fracture area of the pure matrix could not be evaluated (only for the tensile test)

However, the fracture modes observed for the composite (CPTi(2) matrix with 0.1 and 0.5mass% of boron) are shown in the next SEM images.

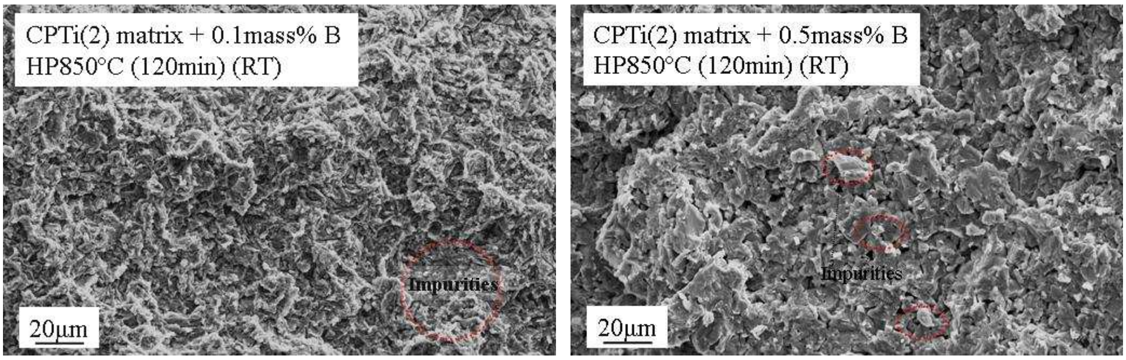

Figure 4-44. Study of the fracture surfaces of the TiMMCs from CPTi(2) matrix powder with 0.1 and 0.5 mass% after the measurement of tensile strength at room temperature. The specimens were consolidated via HP at 850°C during 120 min.

Additionally, impurity particles were seen on the fracture area of these specimens. Many impurities were also detected in the fracture area for composites from TiH_2(4) matrix powder.

In general, they do not present any ductile failure. It confirms the low values of elongation obtained after the tensile test at room temperature.

- *Characterisation of the TiMMCs at higher temperature*

Additionally, tensile tests were performed at higher temperatures (250° and 450°C). It was done only for composites made from CPTi(2) matrix powder. Two parallel measurements were made for each type of material (CPTi pure matrix and with 0.1 and 0.5mass% of boron). The specimens tested came from the larger hot pressed plates. These plates were cut according to the standard dimension for the tensile test (see in previous chapter 2). Additional horizontal cutting was carried out, too. In case of samples without reinforcement, a thin layer from both surfaces was removed to eliminate areas potentially contaminated with O, N or C (see Figure 4-45). These samples without the oxide layer were tested at 250° and 450°C.

Figure 4-45. Surface layer of the samples from CPTi(2) powder without reinforcement (from the tensile pieces 4 and 5) This layer could be oxide or simply dirty Ti.

Then, two specimens of the same composition were tested at 250ºC and 450ºC. In the next table, the mean of the ultimate tensile strength and the elongation of each composite are summarised.

The lower values of the mechanical properties of these composites are observed at the high boron concentration (0.5 mass%) in Table 4-27. Furthermore, the matrix without reinforcement at 250ºC presented marked elongation. Also it is observed for the titanium matrix with 0.1 mass% of nano-boron particle. Their elongation is still very high.

Table 4-27. Tensile properties of the TiMMCs from CPTi(2) matrix powder with different boron content (mass%) at three temperatures.

Tensile test at three temperature (°C)						
CPTi(2) matrix	Tensile strength (MPa)			Elongation (%)		
Boron (mass%)	20°	250°	450°	20°	250°	450°
0	n.d.	306±1	213±4	n.d.	40	13
0.1	437±82	331±17	133±4	0.5	21	15
0.5	210±68	485±41	176±2	0.2	4	30

Additionally after the tensile tests, hardness measurements (HV30) of specimens tested at 250º and 450º were carried out on both faces of the tensile test bars, to check if interstitials had been introduced from the punch faces during hot pressing. Moreover, the hardness, of one sample of pure titanium matrix (CPTi(2)) tested at room temperature, was also measured.

The values of hardness are listed in the next Table 4-28.

It is observed that the hardness (HV30) of the specimens increases slightly with the addition of boron. However, there are no differences between both faces in all specimens, i.e. selective pickup of C or N during hot pressing is not probable; at best integral contamination may have occurred

Table 4-28. Hardness meassurement (HV30) of the specimens from CPTi(2) starting powders reinforced with 0.1 and 0.5 mass% of boron after the tensile test.

Sample	**Hardness (HV30)**		
CPTi 0 mass% of B	**Part 1**	**Part 2**	**Part 3**
RT	291±5	286±2	274±2
250ºC	291±6	294±6	
450ºC	283±5	280±6	

Sample	**Hardness (HV30)**	
CPTi 0.1 mass% of B	**Part 1**	**Part 2**
250ºC	300±13	304±13
450ºC	302±5	298±6
CPTi 0.5 mass% of B	**Part 1**	**Part 2**
250ºC	317±39	313±36
450ºC	320±35	323±46

Therefore, chemical analyses for the samples from the pure titanium matrix (CPTi(2)) were carried out. In addition to the oxygen content, nitrogen and carbon concentration were analysed. The objective of these analyses is to determine if there are some important differences between the carbon, nitrogen and oxygen content in the samples after the tensile test that might explain the outstanding mechanical properties of the specimens tested at 250º. During machining of the sample to standard test bar dimensions, thin surface layers from some specimens – the faces to the punch surfaces - were removed. These latter specimens were used for the tensile test at 250º and 450ºC. Because of that, also the chemical analysis of one of these thin layers was carried out.

The oxygen, nitrogen and carbon contents of specimens tested at 250º and 450º were represented in the next Table 4-29.

Table 4-29. Oxygen and nitrogen content of the titanium pure specimens after the tesile test at different temperatures.

Sample	**Oxygen mass%**	**Nitrogen mass%**	**Carbon mass%**
Ti 450°C	0.47 ± 0.01	0.013	0.058±0.008
Ti-250°C	0.45 ±0.01	0.014±0.001	0.053±0.006
Ti-RT	0.45 ±0.01	0.014±0.001	0.077±0.010
layer	0.85 ±0.00	0.090±0.012	n.d.

As the previous table shows, there are not any significant differences between the oxygen content of samples tested at room temperature and 250ºC. However, the nitrogen content is slightly higher for the thin layer removed from the specimens. This nitrogen could come from the BN (coating necessary for HP processing).

Thus, by removing a thin layer from the surface of titanium specimens, some nitrogen could be taken out. The outstanding elongation was observed for samples with low oxygen and carbon content.

However, the differences between the impurity contents are not as significant as to consider them an influence factor in the elongation.

Finally, the next images confirm the outstanding elongation for the titanium matrix without reinforcement. In Figure 4-46, there is a comparison between the visual elongation of the specimens tested at 250ºC (left with 0 mass%).

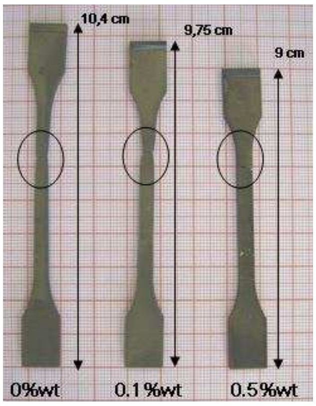

Figure 4-46. Length after tensile testing of the TiMMCs from CPTi(2) starting matrix powder reinforced with different boron contents (0%, 0.1% and 0.5%) after tensile test at 250ºC

Moreover, an additional comparison between the samples from the same material, pure titanium matrix from CPTi(2), tested at different temperature is showed in the next Figure 4-47. The numbers 1 to 5 are indicating the previous location in the larger sample (Ø100mm). The samples measured at RT could not be broken and also presented another thickness (samples 1, 2 and 3). The samples 4 and 5 were tensile tested at 250º and 450ºC respectively.

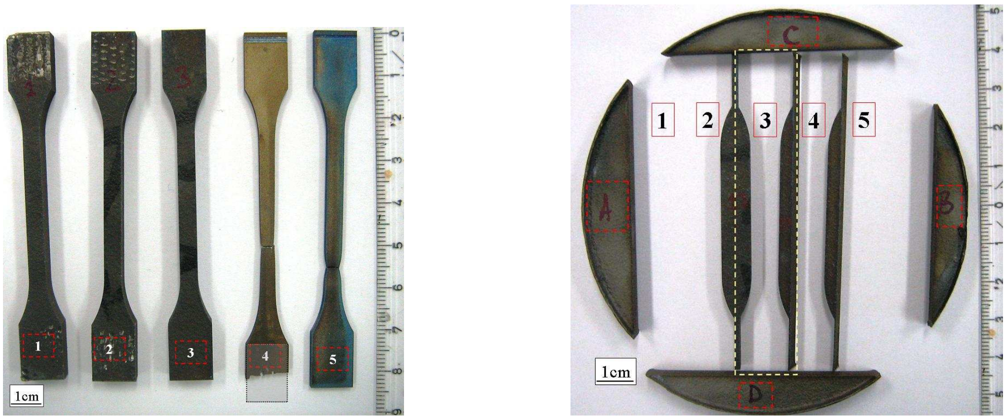

Figure 4-47. (left) Samples of CPTi (2) pure matrix, after tensile tests at different temperature (from RT to 450º). (right) Rests of the larger plate after cutting of the samples for tensile test.

- *Fractographic study*

After the tensile strength tests at elevated temperatures, the fracture area of the composites was evaluated. SEM images (see in Figure 4-48) of these surfaces were taken in order to study the type of fracture.

On microscopical scale, the fracture mode observed for the composite is principally ductile. The dimples shown in the next SEM images confirmed this. With increasing boron content, the ductile character of the fracture mode decreased (see SEM image for TiMMCs with 0.5 mass % of boron particles) while it tended to increase at higher testing temperature.

On macroscopical scale, for the composite with higher boron content the mode of fracture was brittle because there was no visible reduction of the fracture area.

The porosity in addition to the increase of the reinforcement particle content results in lower ductility of the composite.

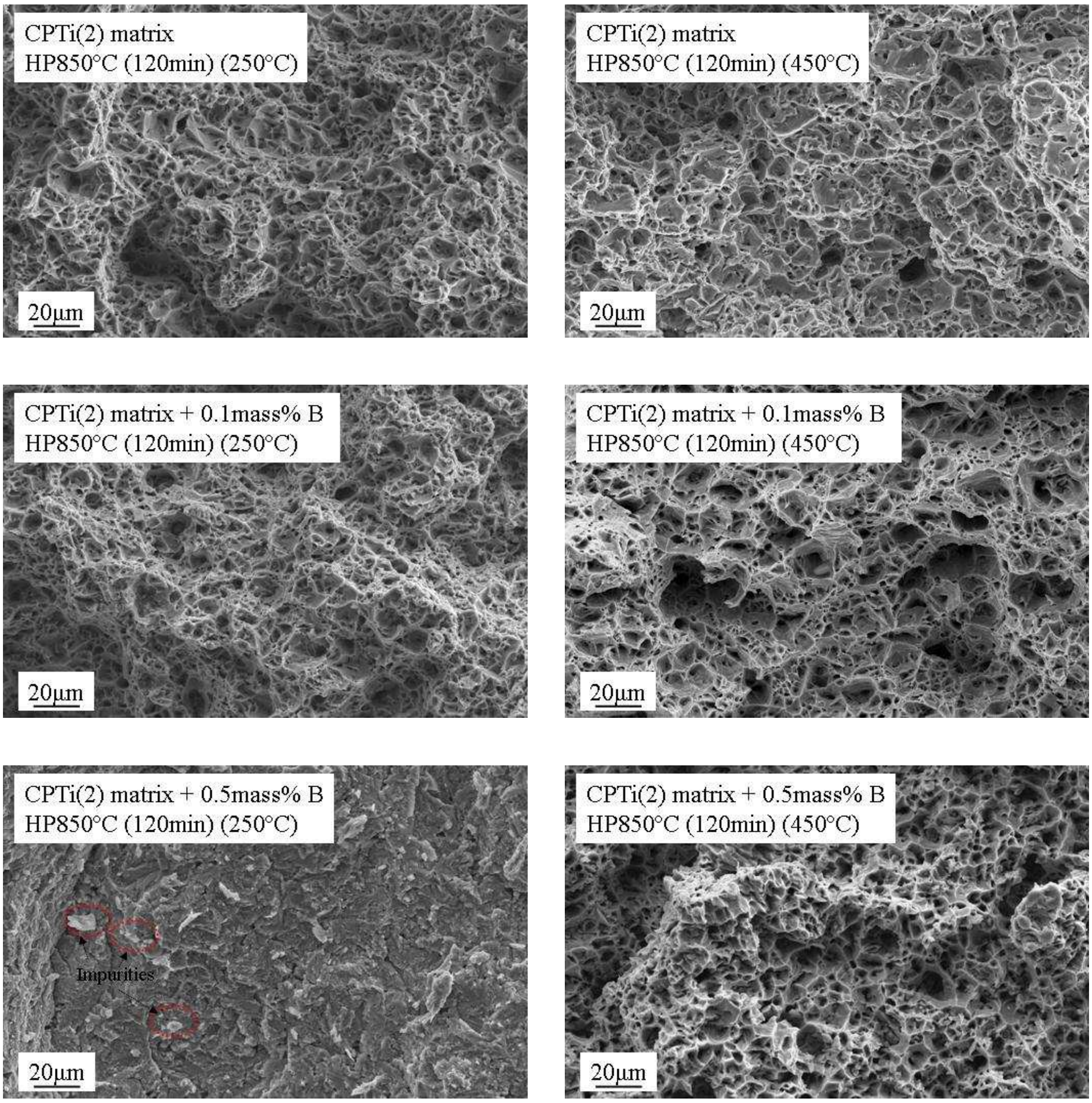

Figure 4-48. Study of the fracture surfaces of the TiMMCs after the measurement of tensile strength at 250º and 450ºC. The specimens were consolidated via HP at 850ºC during 120 min.

Comparison of relative density and hardness of TiMMCs produced at the same temperature and mechanical pressure in different graphite dies

The use of different graphite matrices for the hot pressing tests involves the manufacturing of specimens with different geometries, on one side square and with smaller section (13.5 x 13.5 x 4mm^3) and on another side larger flat-disc-shaped specimens (Ø100mmx5mm). Several of these specimens have the same boron content, 0.1 mass% and 0.5 mass% However, the use of different graphite dies and variation of the hot pressing time (1h or 2h) influences the final properties of the composites. Although the compaction temperature, mechanical pressure and the starting powders are the same for the production of the composites, their final properties change slightly. An important reason is the distribution of mechanical pressure between the twelve punches for the samples hot consolidated in the square cavities. In Table 4-30 and Table 4-31 the properties of the specimens with different shapes but consolidated at the same temperature of 850°C are compared.

Table 4-30. Comparison of the results of the specimens from CPTi(2) with different boron content (mass%) after HP at 850°C during 1h for the smaller square specimens and 2h for the larger specimens.

Matrix powder	**Type of section of HP die**			
CPTi (2)	13.4 x 13.4 mm²		100mm Ø	
Boron content (mass%)	Rel. density (%)	Hardness (HV10)	Rel. density (%)	Hardness (HV10)
0	98	307±3	98	281±7
0.1	97	369±6	95	287±14
0.5	96	388±11	87	266±70

Table 4-31. Comparison of small and large specimens from TiH_2(4) with different boron content (mass%) after HP at 850°C during 1h for the smaller square specimens and 2h for the larger specimens.

Matrix powder	**Type of section of HP die**			
TiH_2 (4)	13.4x13.4 mm²		100mm Ø	
Boron content (mass%)	Rel. density (%)	Hardness (HV10)	Rel. density (%)	Hardness (HV10)
0	94	305±7	89	300±6
0.1	95	405±8	89	296±6
0.5	98	458±6	91	310±29

The values of relative density and hardness were measured from one sample of each type of material.

The smaller specimens (13.4x13.4 mm²) were hot compacted for 1h. This time was increased up to 2h for the larger specimens (Ø 100mmx5mm). Even when increasing the holding time for the HP test, the density of the larger samples is lower. For the larger samples the amount of powder used was around 180 g vs. 3.5 g employed for the smaller samples.

The BN coating can affect more the smaller specimens because of the larger contact area in comparison to the larger samples.

The total contact area for the smaller specimens is 526.5mm^2 (A_c) and the specimen volume is 546.75mm^3.(V_T). For the larger samples the total area is 16014 mm^2 (A_c) and the volume is 39250mm^3(V_T). It means the smaller samples present higher ratio A_c/V_T. Because of that, the nitrogen contamination is more probable for these smaller specimens. This fact can be the reason of their higher hardness observed in the previous Table 4-31.

An inadequate hot compaction could cause the variation of the relative density of the TiMMCs (larger specimens with 0.5 mass% of boron particles).

Because of that the oxygen and impurities of the starting powder and the reinforcement increase the hardness of the material in general.

4.3.2.2.2 Inductive hot pressing technique (iHP)

Due to the limitation of the specimen geometry in iHP, the characterisation of the samples was restricted to measurement of the hardness, density and oxygen content. Furthermore, a microstructural study completed the characterisation.

In one inductive hot pressing cycle, two specimens are always produced at the same time, one from the CPTi(2) and the other one from TiH_2(4) matrix powder with the different boron particles contents. It is important to observe the powder compacts were prepared in line here (stacked along the axis of loading) and not parallel, as in conventional HP with 12-cavities die. This means that the pressure is the same for both compacts.

TiMMCs were prepared by inductive hot pressing at 850° and 900°C for 15 min.

At the beginning of this experimental series, two temperatures were tested, 850° and 900°C. The four boron contents used for via HP was also used for the iHP tests (listed in Table 4-21). In the following Figure 4-49 the comparison between the composites from the two titanium matrices with varying boron contents are presented, as is the temperature used for the hot consolidation of the composites (850°C and 900°C).

In the next Table 4-32, Archimedes, theoretical and relative density in addition to hardness (HV10) are listed for all the material compositions compacted at 900° and 950°C via iHP.

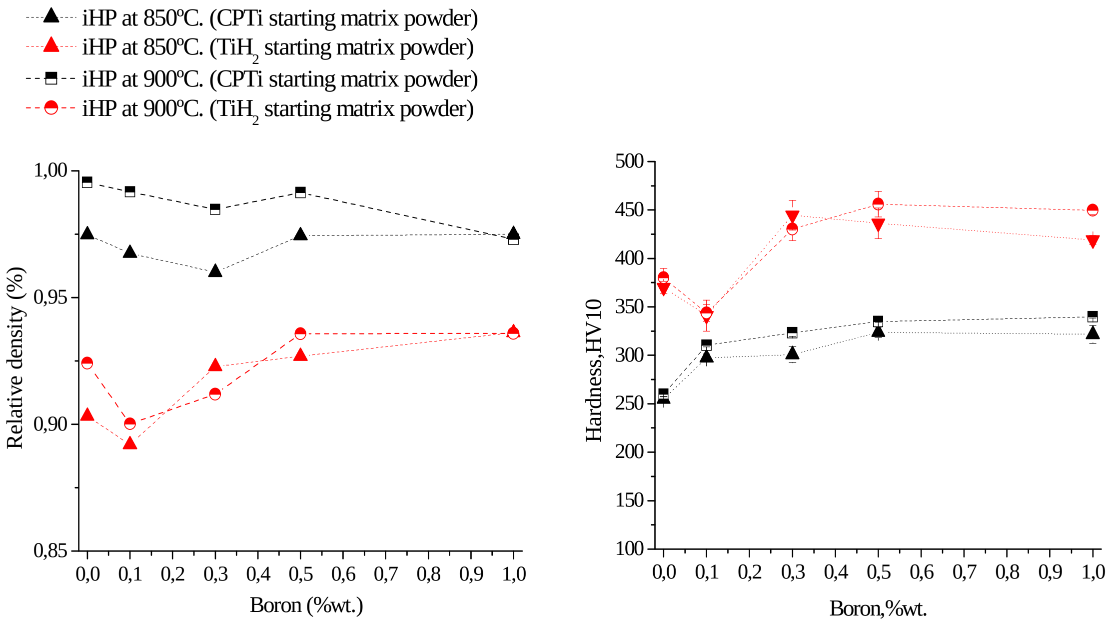

Figure 4-49. Relative density and hardness of the composites vs. the boron content (mass%). The specimens were hot consolidated via iHP at two temperatures.

Additionally, oxygen and nitrogen analysis was carried out for the composites with 1 mass% of nano-boron particles. These values were also compared to the titanium matrix values. Higher nitrogen content present in the specimen from TiH_2(4) with 1 mass% of nano-boron contributed to increasing up to 450HV10 the hardness of the composite. (Th. Hardness for CPTi grade 4 is 260HV10).

Besides, by increasing the temperature the densification of these samples increased up to 99.5 % (pure CPTi matrix).

Table 4-32. Archimedes and Relative density (measurement using paraffin) and the hardness of the composites with different boron content (mass%). The specimens were inductive hot pressed consolidated at 850°C and 900°C for 15 min.

Matrix (iHP Temp.)	Boron content (mass%)	Arch. density (g/cm3)	Th. Density (g/cm3)	Rel. density (%)	Hardness (HV10)	Oxygen (mass%)	Nitrogen (mass%)
CPTi(2) (850°C)	0	4.43	4.54	98	255	0.56	0.005
	0.1	4.39	4.54	97	297	n.d.	n.d.
	0.3	4.35	4.53	96	301	n.d.	n.d.
	0.5	4.41	4.52	97	324	n.d.	n.d.
	1	4.39	4.50	97	322	1.07	0.007
TiH_2(4) (850°C)	0	4.10	4.54	90	370	1.26	0.190
	0.1	4.05	4.54	89	341	n.d.	n.d.
	0.3	4.18	4.53	92	445	n.d.	n.d.
	0.5	4.19	4.52	93	436	n.d.	n.d.
	1	4.22	4.50	94	419	2.09	0.160
CPTi(2) (900°C)	0	4.52	4.54	100	260	0.57	0.005
	0.1	4.50	4.54	99	310	n.d.	n.d.
	0.3	4.46	4.53	99	323	n.d.	n.d.
	0.5	4.48	4.52	99	335	n.d.	n.d.
	1	4.38	4.50	97	340	0.57	0.003
TiH_2(4) (900°C)	0	4.20	4.54	92	380	0.88	0.158
	0.1	4.08	4.54	90	344	n.d.	n.d.
	0.3	4.13	4.53	91	430	n.d.	n.d.
	0.5	4.23	4.52	94	456	n.d.	n.d.
	1	4.21	4.50	94	450	1.93	0.201

Comparison of TiMMCs prepared by inductive hot pressing at 850º ,900ºC and 950ºC for 15 min

Comparing the results of density and hardness measurements, the increase of the temperature involves in general an increase in the density of the composites. Thereby, the temperature of 950ºC was additionally tested.

The composites produced at 950ºC via iHP had 0.1% and 0.5mass% boron (see Figure 4-50). In one iHP cycle two samples are produced, each one from different titanium based matrix (CPTi(2) and TiH_2(4).

The Figure 4-50 shows the values of relative density and hardness of the TiMMCs. In general, the hardness of the composites is slightly increasing with the temperature. Strange density values at 900°C were detected, in particular for 0.5 mass% of boron. It could be due to an error occurred during the Archimedes density measurement.

Slight increase on the hardness values with the addition of the boron particles is also seen (see in Table 4-33).

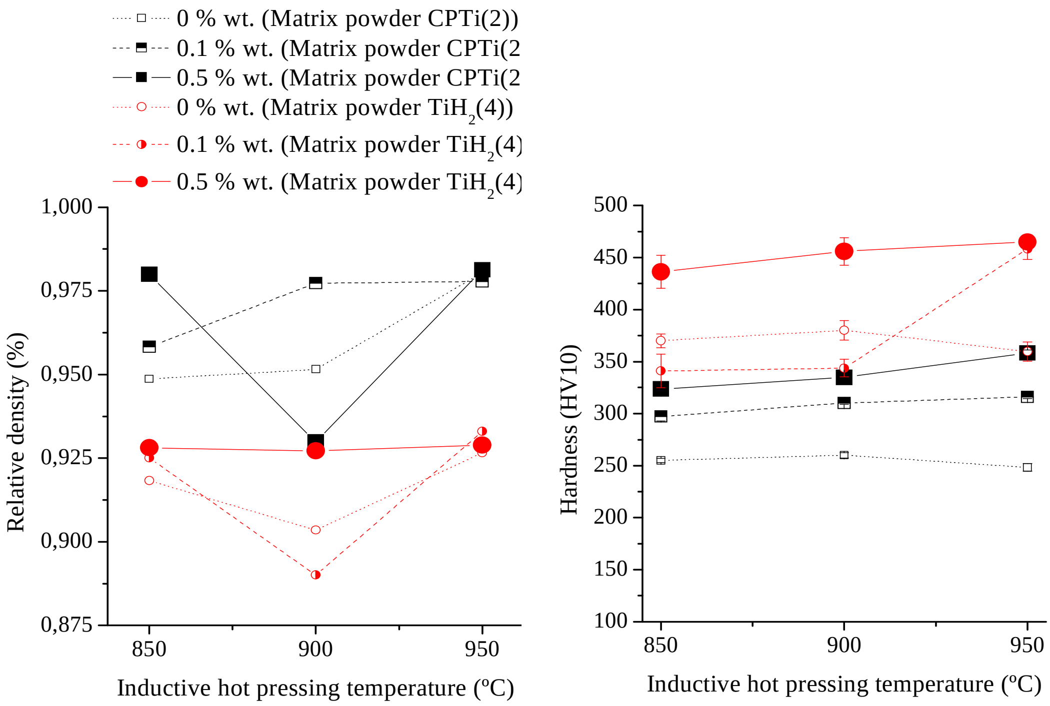

Figure 4-50. Comparison of the relative density and hardness values vs. the inductive hot pressing temperature used for the manufacturing of TiMMCs from the CPTi(2) and TiH_2(4) matrix powders with two boron concentration (0.1% and 0.5mass%). 50K/min of heating rate and 15min of holding time.

In the case of the composites from TiH_2(4), they achieve high hardness for the boron content of 0.5 mass%

Table 4-33. Archimedes density and hardness of the titanium composites from CPTi(2) iHP produced at different temperature. (for all of them 50 K/min heating rate and 15 min holding time)

CPTi(2) Matrix	**Pure metal matrix**		**0.1mass% of boron**		**0.5mass% of boron**	
Temp. (ºC)	Arch. Density (g/cm^3)	Hardness (HV10)	Arch. density (g/cm^3)	Hardness (HV10)	Arch. density (g/cm^3)	Hardness (HV10)
850	4.31	255	4.35	297	4.40	324
900	4.32	260	4.43	310	4.28	335
950	4.45	248	4.44	316	4.44	358

Concluding, the specimens from TiH_2(4) present higher hardness for all the boron levels in spite of their low relative density (see in Table 4-34).

This can be due to the high oxygen and nitrogen content measured, even for the titanium base without the reinforcement (see in Table 4-32).

Table 4-34. Archimedes density and hardness of the titanium composite from TiH_2(4) iHP produced at different temperature. (for all of them 50K/min heating rate and 15min holding time)

TiH_2(4) Matrix	**Pure metal matrix**		**0.1mass% of boron**		**0.5mass% of boron**	
Temp. (ºC)	Arch. Density (g/cm^3)	Hardness (HV10)	Arch. density (g/cm^3)	Hardness (HV10)	Arch. density (g/cm^3)	Hardness (HV10)
850	4.12	370	4.05	341	4.20	436
900	4.10	380	4.04	344	4.19	456
950	4.21	360	4.23	458	4.20	465

Microstructural study

Finally, the microstructure of several TiMMCs has been studied. The most representative images of these TiMMCs are shown in the next figure.

Polarised light microscopy was also used for the observation of the hcp α-Ti. Comparing the matrices from CPTi(2) and TiH_2 (4) powders, the grain size for the composite from CPTi(2) could be observed and their orientation studied, on the contrary, the microstructures of the other matrix (TiH_2(4)) does not manifest any specific orientation.

Similar particles from the metallographic preparation were also detected (sand and polishing media)

High concentrations of hydrogen could cause the stabilization of ß-phase at room temperature in spite of significant content of oxygen and nitrogen as alpha stabilizing elements [15, 16].

In particularly for composites from TiH_2 matrix powder, the hydrogen concentration can be more significant. The presence of ß phase (body-centred cubic structure) is more evident for the composites from TiH_2 (4) powder (see previous results of iHP in Table 4-15).

In previous study of hot consolidation via iHP of the two type titanium based powder, the concentrations of hydrogen in specimens from TiH_2 (4) were considerable (range from 0.5 at iHP temperature 1100° to 0.9 mass% at 800°C) compared to of specimens from CPTi(2) (<0.2mass% at iHP temperature 800°C).

The alpha phase (hcp) and beta phase (bcc) can be distinguished. In this way, by the use of polarised light the orientation of alpha phase can be seen; in contrast the beta phase can not be detected visually.

On base of that, the specimen from CPTi(2) that presented lower hydrogen content, showed a differentiable alpha phase (by the use of polarised light).

For that reason the hardness, of the composites from TiH_2(4) starting powder, is higher than in the composites from CPTi(2) matrix powders. The nitrogen and hydrogen contents increase the hardness of the composites.

Additionally, the same distribution of the boron particles in the titanium based matrix observed for the TiMMCs produced via conventional HP is also seen in the previous images of the composites produced through iHP.

Furthermore, the addition of boron particles and increasing their content in the matrix resulted qualitative in lower grain size, which is favourable for the mechanical properties. However at higher boron concentration (1 mass%), the oxygen content increases (1.93 mass% of oxygen for the composite from TiH_2(4) matrix hot consolidated at 900°C for 15 min) and also some porosity is observed around the boron particles. This can be also observed for the composites produced through inductive hot pressing (see Figure 4-51). As examples in the next Figure 4-51, some pores around and at the surface of the boron particles are observed. It means, the increase of the boron content can reduce the density of the composite, even if this composite is fabricated at higher temperature as e.g. 950°C. The EDAX analysis gives some approximate chemical information about the boron particle in the titanium matrix.(see Figure 4-52. Qualitative line profiles of Ti, B and Mg detected by EDAX analysis on a boron particle in the titanium matrix (produced from CPTi(2)) iHP at 850°C (15min holding time)). Definitely, boron reinforcement is not “nano-reinforcement” since” micro-particles are observed. This also shows and confirms that some boron particles have a certain amount of impurities (Mg). Such impurity came from the nano-boron particles (it was observed previously in Figure 3-14).

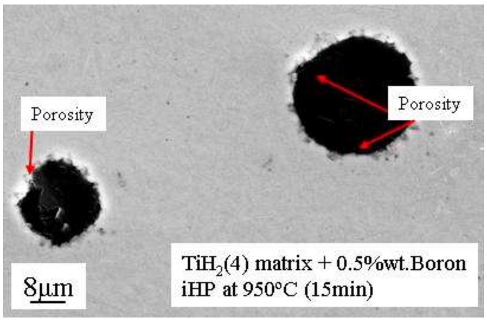

Figure 4-51. SEM image (BSE) of boron particles in a titanium based matrix (from TiH_2(4) powder) produced through inductive hot pressing at 950°C during 15min.

Visually, there was no reaction between the titanium matrix and the boron reinforcement (this EDAX analysis was used as qualitative method for chemical information about the boron particle in the titanium matrix.).

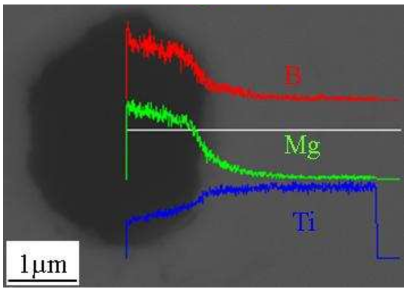

Figure 4-52. Qualitative line profiles of Ti, B and Mg detected by EDAX analysis on a boron particle in the titanium matrix (produced from CPTi(2)) iHP at 850°C (15min holding time)

Finally, a comparison between the microstructure of the different specimens from CPTi(2) and TiH_2(4) stating powder consolidated at different iHP conditions are illustrated in the next Figure 4-53. Moreover, the influence of the nano-boron addition on the microstructure of the specimens can be appreciated. There are important differences between the microstructures. Samples from CPTi(2) matrix powder showed a defined grain (alpha phase). However, for specimens from TiH_2(4) matrix powder, the grain cannot be seen.

The light polarised microscope can be used to identify visually the type of titanium based matrix used for the manufacturing of the TiMMCs.

Moreover, the decrease of the densification is also observed at 1 mass% of nano-boron particle.

In general for all the composites, the larger size of the boron particles can found.

The impurities from metallographic preparation were always present as SiC particles. After an intense cleaning of the cross section, the impurities were still present. The efforts to eliminate such impurities did not give any appreciable result.

Figure 4-53. Microstructure of titanium and titanium matrix composites reinforced with 1 mass% boron produced by inductive hot pressing (iHP) at different temperatures (15 min holding time and 50 K/min heating rate).

iHP Temp. (°C)	**Titanium based matrix**	**Titanium based matrix + 1 mass% of boron particles**
850	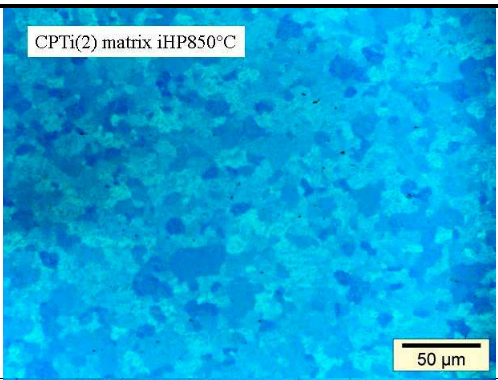	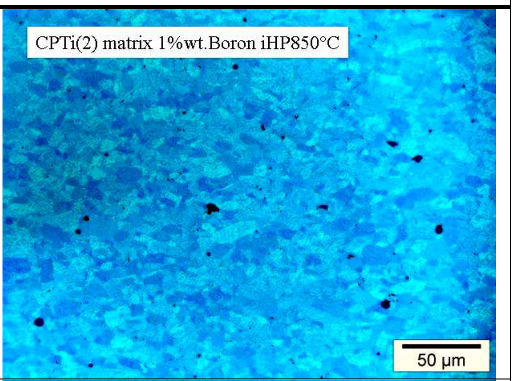
850	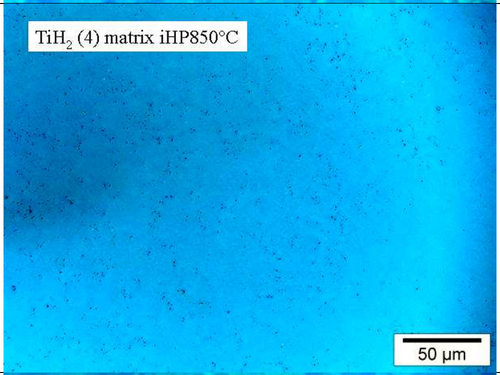	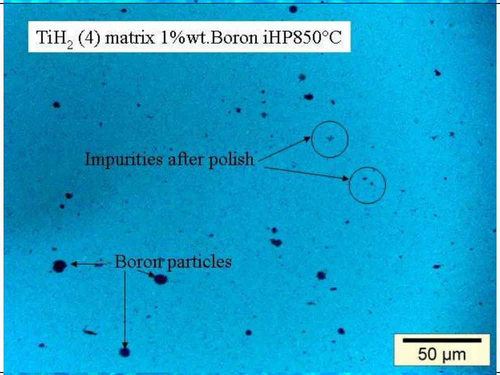
900	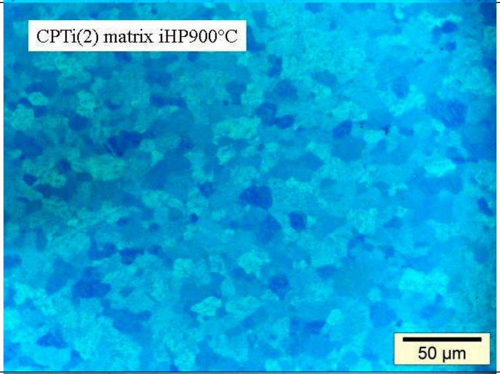	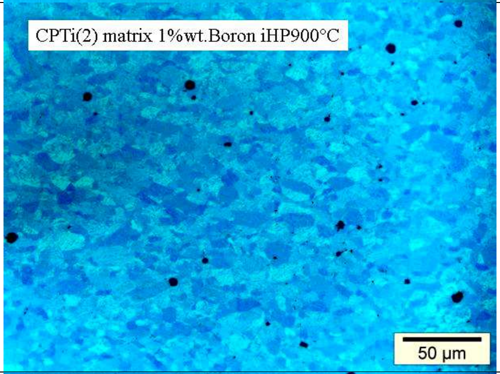
900	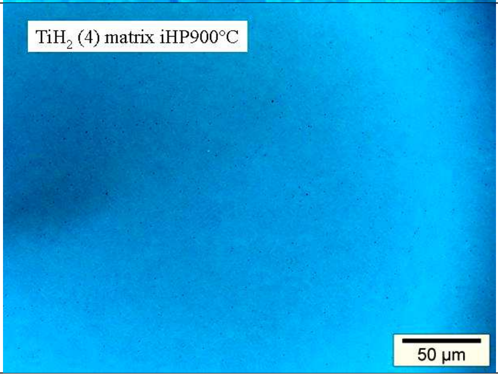	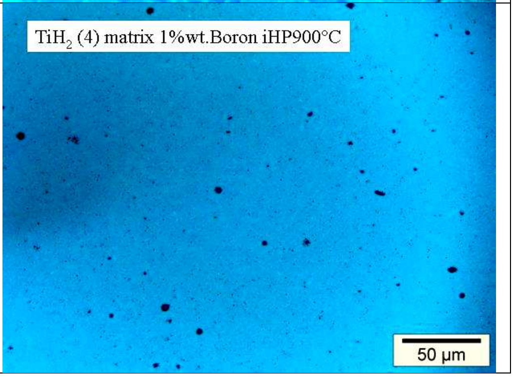

4.3.2.2.3 Comparison of conventional and inductive hot pressing results and discussion

First a comparison of the values of density and hardness takes place as well as of the oxygen and nitrogen content of few TiMMCs. Concluding, a microstructural study of several specimens is carried out.

A comparison of the relative density and hardness from the samples prepared at the same hot pressing temperature

Considering the previous values of density and hardness of the TiMMCs, several comparisons of them were made. The reference parameter was the temperature of the hot consolidation process.

In both hot pressing processes, the temperature could be properly varied. In contrast, the compaction pressure and vacuum conditions were imposed by the hot pressing equipment (see Table 4-21). The processing time was set for each manufacturing technique in accordance with previous experiments. In the next Figure 4-54 and Table 4-35, the relative density (%) and hardness (HV10) values of TiMMCs produced using the two hot consolidation processes at 850°C are shown and listed. The different boron contents used were reported in the previous Table 4-20. The holding time, heating rate and vacuum levels have been specified previously for each process (see in Table 4 19).

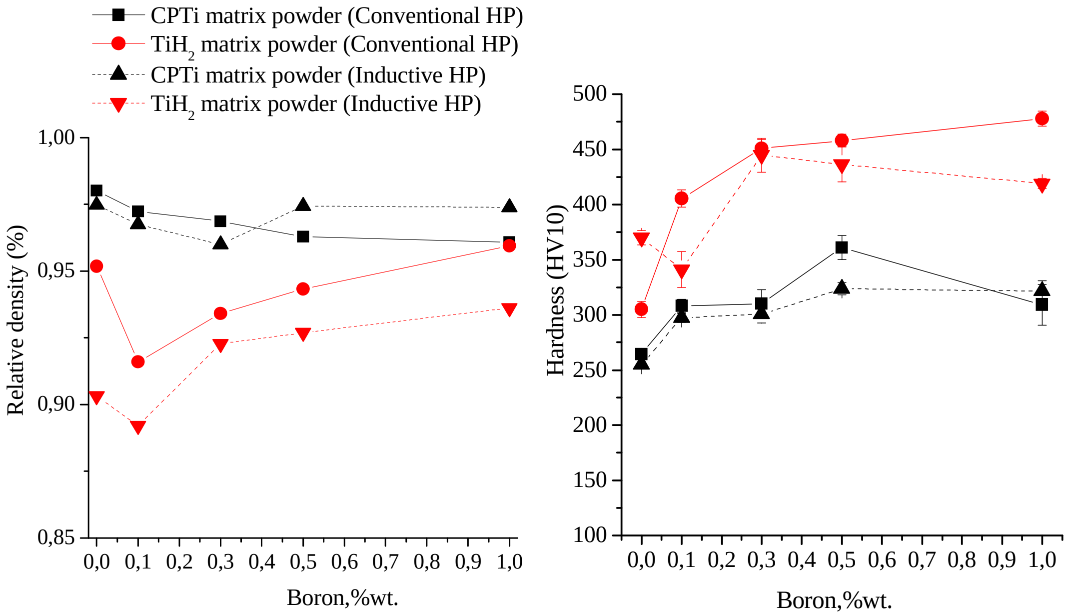

Figure 4-54. Relative density and hardness of the specimens after the consolidation by HP (time=60min) and iHP (time=15min) at 850°C.

The previous values of relative density (%) and hardness (HV10) are also listed in the next Table 4-35.

Table 4-35. Relative density (%) and hardness (HV10) of the TiMMCs reinforced with the different boron contents, hot consolidated through conventional HP and inductive HP, respectively, at the same temperature (850°C).

Matrix +boron (mass%)	HP850°C (60min) (10 K/min)		iHP850°C (15min) (50K/min)	
	Rel.density (%)	Hardness (HV10)	Rel.density (%)	Hardness (HV10)
CPTi(2)+ boron (mass%)				
0	98.02	264	97.48	255
0.1	97.24	308	96.75	297
0.3	96.87	310	96.00	301
0.5	96.29	361	97.44	324
1	96.09	309	97.39	322
TiH_2(4)+ boron (mass%)				
0	95.18	305	90.32	370
0.1	91.60	405	89.20	341
0.3	93.41	451	92.28	445
0.5	94.33	458	92.69	436
1	95.95	478	93.62	419

Chemical analysis:

Oxygen and nitrogen content were analyzed for several specimens, titanium based matrices without reinforcement materials and composites with higher boron content.

The results of the chemical analysis of the titanium based matrices are listed in Table 4-36.

The high nitrogen content observed was for specimens from TiH_2 (4) matrix powder. This high nitrogen content was detected previously for this type of starting powder.

Also the BN from the iHP die coating can contribute to such increased nitrogen content, although the main contribution came from the starting matrix powder (min. 0.1 mass%). For that reason, the specimens from CPTi(2) matrix powder did not manifest high levels of nitrogen since there was not appreciable nitrogen in the matrix powder (max 0.003 mass%) and after the iHP consolidation the concentration of nitrogen was constant (0.005 mass% at 850º and 900º) and insignificant compared to the specimens from TiH_2.

Table 4-36. Oxygen and Nitrogen content of the two titanium matrices (CPTi(2) and TiH_2(4) consolidated using HP and iHP processes at different conditions.

Matrix powder	HP800ºC (60min)		HP850ºC (60min)		iHP850ºC (15min)		iHP900ºC (15min)	
	Oxygen (mass%)	Nitrogen (mass%)	Oxygen (mass%)	Nitrogen (mass%)	Oxygen (mass%)	Nitrogen (mass%)	Oxygen (mass%)	Nitrogen (mass%)
CPTi (2)	0.66	0.032	0.52	n.d.	0.56	0.005	0.571	0.005
TiH_2 (4)	0.81	0.076	0.77	n.d.	n.d.	0.191	0.878	0.158

Secondly, the oxygen content of the TiMMCs fabricated at 850ºC via HP during 60 min was analysed. The results of the chemical analysis are compared in the next Table 4-37. The boron content (mass%) was 0.1 mass% and 0.5 mass%

Table 4-37. Oxygen content of the TiMMCs with 0.1 mass% and 0.5 mass% of boron. These TiMMCs were fabricated via HP at 850ºC (time=60min; pressure=30MPa; vacuum=10^{-1}mbar).

Starting powder	Pure Matrix	Boron content (mass%)	
		0.1mass%	0.5mass%
	Oxygen (mass%)		
CPTi(2)	0.515	0.82	0.63
TiH_2 (4)	0.768	1.46	1.62

Microstructures

Finally a representative comparison of microstructures was done for the titanium composite reinforced with the boron particles (0.1 mass%) and consolidated by hot pressing, conventional (HP) or inductive (iHP).

Some impurities (SiC particles) from the metallographic preparation (after polishing) are seen in general on the surface of all the titanium specimens.

The microstructure of the composites from CPTi(2) produced by different process and conditions presents similar grain sizes (approx.). However for the composites from the other matrix powder (TiH_2(4)) significant differences between the microstructures of composites produced via HP and iHP were shown. These different microstructures can be caused by different concentrations of interstitials in the titanium matrix. Considerable hydrogen, in addition to high nitrogen and oxygen content from the starting powder, marked important difference between the samples from each grade of starting powder.

In particular, residual hydrogen had more significant influence on the microstructure of the specimens from (TiH_2(4)) matrix powder.

Because nitrogen was always present in the samples from this powder (TiH_2(4)), nitrogen would affect in the same way all the samples (from the same powder since it came from the starting powder). For that reason the nitrogen was not mainly responsible for the different microstructures of samples from the same starting powder (TiH_2(4)).

However there was a marked difference between both hot consolidation processes (HP and iHP); it was the process time

The hydrogen from the starting powder (TiH_2(4))did not have enough time to react and leave the titanium matrix during the short time of iHP process (max.15min). the time of the conventional hot pressing cycle, in contrast, was sufficiently long to reduce the hydrogen content from the titanium matrix. This phenomenon was also observed for the study of the titanium matrices iHP compacted at different iHP temperatures (nextFigure 4-55).

Figure 4-55. Microstructures of TiMMCs reinforced with 0.1mass% of boron particles and hot pressed via conventional hot pressing (HP) and inductive hot pressing (iHP) at different temperatures (°C).

Process and Temp.(°C)	**CPTi (2) + 0.1mass% Boron**	**TiH_2(4) + 0.1mass%Boron**
HP 800° (60min)	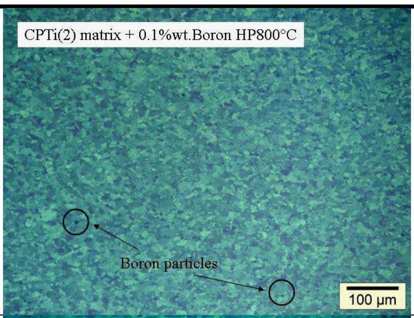	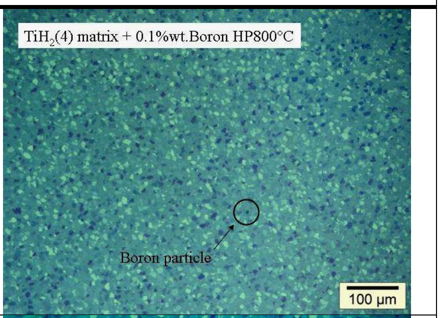
HP 850° (60min)	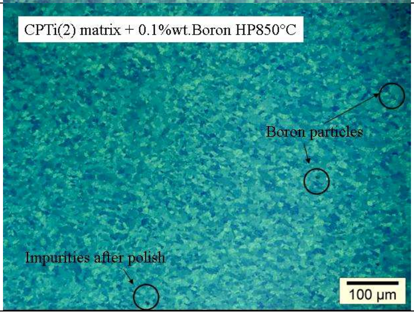	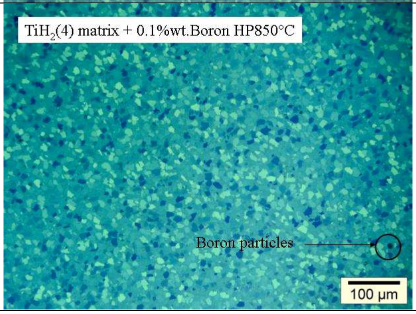

iHP 850° (15min)	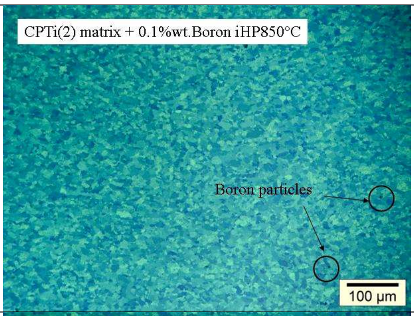	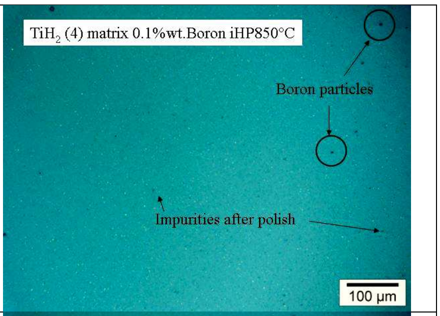
iHP 900° (15min)	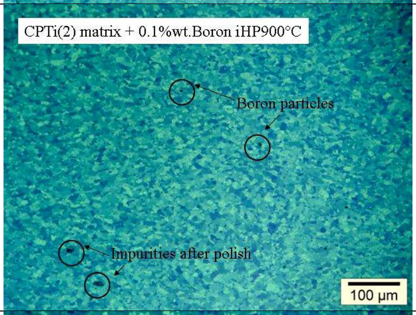	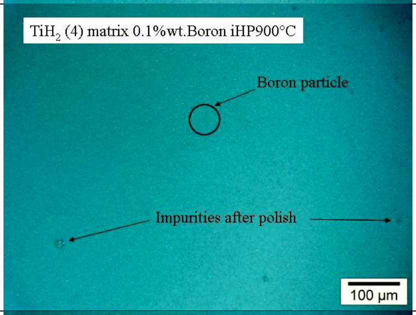
iHP 950° (15min)	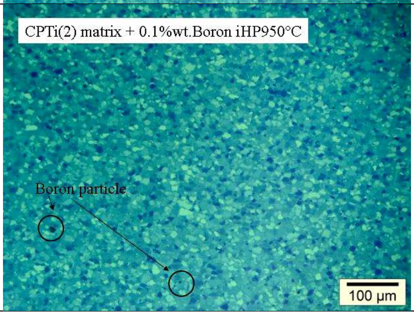	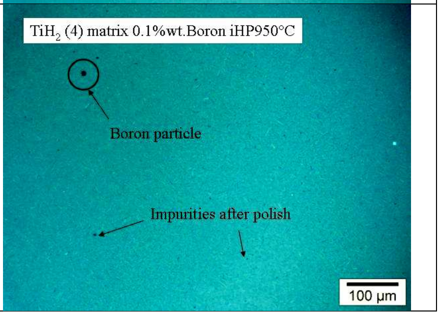

Intermediate Conclusion

- High nitrogen and oxygen content from the starting powder (TiH_2(4)) decreases the mechanical properties of the composite materials.
- Impurities from the reinforcement material (nano-boron particles) are detected in the final composites.
- The addition of boron particle decreases the densification and increases the oxygen in the TiMMCs, not improving their mechanical properties.
- Outstanding properties of the CPTi matrix at elevated temperature are observed; the reason for this large difference to room temperature is however not clear.
- The use of different graphite dies at the same processing parameters influences the final properties of the composites.

4.3.3 TiMMCs reinforced with Carbon nano fibres (CNFs)

4.3.3.1 Manufacturing processes

Due to their geometry, the CNFs as nano-reinforcement present problems regarding uniform dispersion in the matrix. In previous work, it was observed that there was an agglomeration of the reinforcement. From the beginning of the use of this type of reinforcement, the CNFs are heavy agglomerated and can not easily be deagglomerated.

In spite of these agglomeration problems, CNFs are shown as outstanding reinforcement material, for that reason it was also tested in this present work.

The homogeneous distribution of the CNFs in the metal matrix is a very important factor to achieve the desired level of mechanical properties in the composite. For that reason, the optimisation of the mixing process was mandatory at the beginning of the experimental work with CNFs. For that, the preparation and evaluation of four mixing procedures using different processing conditions was done at the beginning of this section.

Manufacturing of the titanium composites reinforced by CNFs is described in the next Figure 4-56 and Figure 4-57. Firstly, the Figure 4-56 shows the optimisation of the mixing stage.

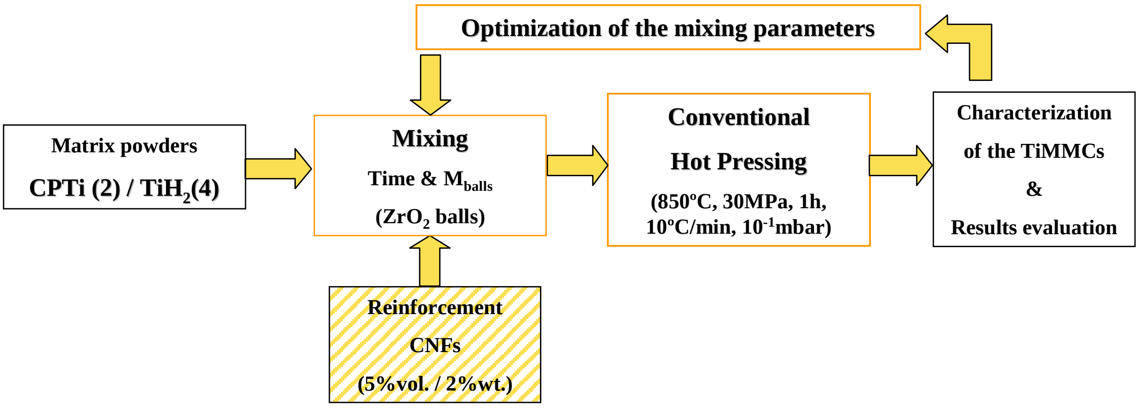

Figure 4-56. Manufacturing flow sheet of the titanium matrices reinforced with carbon nano-fibers (CNFs) via conventional hot pressing (HP). The mixing process was optimised.

Figure 4-57 shows the manufacturing of the TiMMCs reinforced with CNFs and fabricated by iHP.The optimised parameter; mixing time and amount of the ceramic balls (M_{balls}) were also reported.

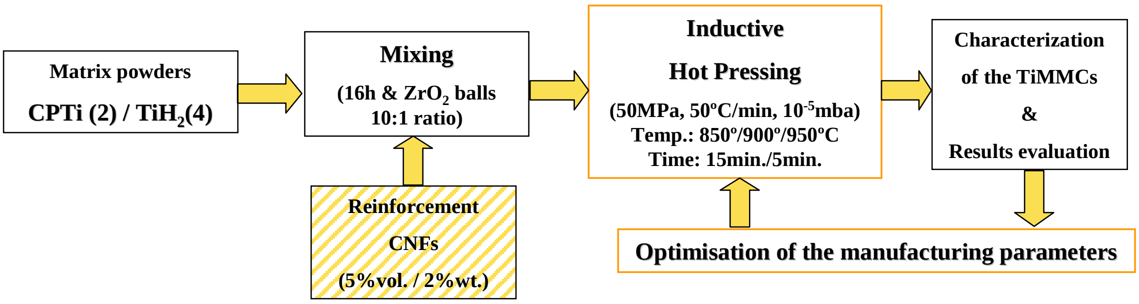

Figure 4-57. Manufacturing flow sheet of the titanium matrices reinforced by carbon nano-fibers (CNFs) consolidated via inductive hot pressing (iHP). The inductive hot pressing parameters were optimised (Ball:Powder ratio is 10:1)

Powder Preparation

In the first manufacturing stage, mixing of the powder took place. The amount of 2 mass% (5 vol.%) of CNFs was added to each titanium based matrix powder as reinforcement.

By varying the time and the mass ratio balls-starting powder (M_{balls}/M_{powder})(see in Table 4-38), the first optimisation of mixing was performed. The mixing balls were the same type as employed for the Ti-nanoboron mixing. Also the solvent (cyclohexane) was necessary. Furthermore, this stage was done in the same “Sintris mixer”. The slurry (titanium based powders and CNFs in solvent) was dried for 12 hours. Next, the mixtures were again blended for 30 min without the ceramic balls. This second blending of the powders was carried out in order to eliminate the small cluster of dried powders observed principally for the TiH_2(4). Finally, the powders were ready to be consolidated; firstly this was done via conventional HP. After hot consolidation, the specimens were characterised. The results of this characterisation were decisive to select the most appropriate mixing procedure. The best dispersion of the CNFs in the titanium matrix was related to high density values. In case of agglomerated nano fibres, porosity due to the clusters was observed.

Table 4-38. Different combinations of mixing time and amount of ceramic balls.

Weight ratio	**Mixing time (h)**
10:1	16
5:1	16
5:1	8
5:1	32

Thereafter, the optimised mixing procedure was used for the manufacturing via inductive hot pressing of this type of TiMMCs.

The parameters employed to produce the composite powder mixture were:

- The optimal mixing time was **16h**
- The weight ratio of the ceramic balls was **10:1** (ball/powder ratio). It means that for 10 g of powders mixture, 100 g of ceramic balls are necessary.

Hot Consolidation

For the fabrication of the titanium composites reinforced with Carbon nano-fibres (CNFs) both conventional and inductive hot pressing techniques were employed.

- *Conventional Hot Pressing:*

This technique was first used to fabricate composites from the four different mixtures. The graphite die used and its preparation for the HP test was previously described in the chapter 2nd and was also used for the fabrication of the titanium matrices reinforced with nano/micro boron particles (see Figure 4-35).

There was the similar problem of load distribution. In this case the two starting powders were reinforced with the same content of CNF (2%vol.).

To reduce this phenomenon the die preparation was carried out by filling in the way described in the next Figure 4-58, the filling height for consolidation of TiMMCs from TiH$_2$(4) matrix powder being (h$_1$) and from CPTi(2) (h$_2$). After the hot pressing, 12 samples were produced (approx. dimensions 13.5x13.5x4mm^3).

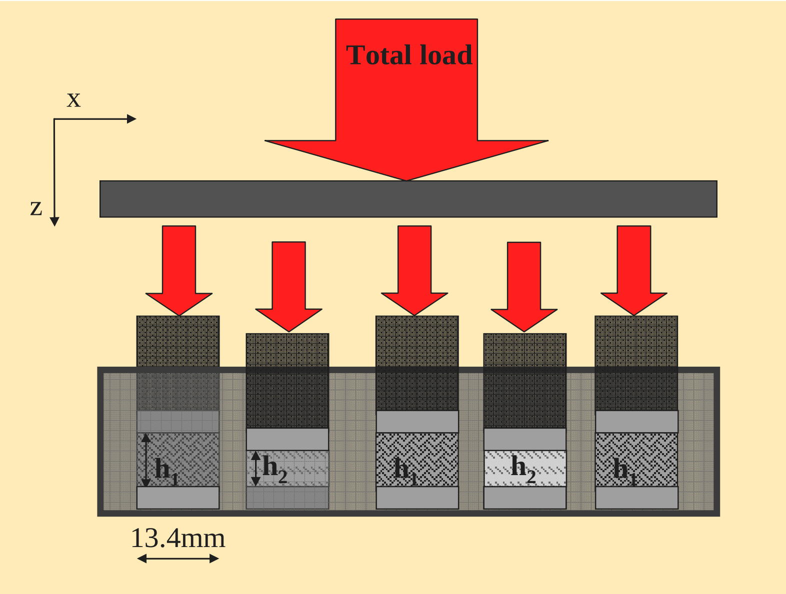

Figure 4-58. Load distribution for 12-cavities graphite die by hot pressing technique for the manufacturing of TiMMCs reinforced with 2%vol.

- *Inductive Hot Pressing:*

The composites were fabricated by iHP from the optimal mixing. The temperature and the holding time of the inductive hot pressing process were varied. Their effects on the final properties and microstructures of the specimens were evaluated and studied.

The next Table 4-39 shows the processing parameters employed during each manufacturing process.

The values of hot compaction pressure and vacuum were fixed for the whole tests in both methods. The holding time was set according to the technique employed (60 min for HP and 15 min for iHP).

Table 4-39. Conventional and Inductive Hot Pressing parameters. for the manufacturing of titanium based composites with CNFs.

Hot Pressing Process	**Temperature (°C)**	**Holding time (min)**		**Heating rate (K/min)**	**Pressure (MPa)**	**Vacuum (mbar)**
Conventional HP	850	60		10	30	10^{-1}
Inductive HP	850	15		50	50	10^{-5}
	900	15		50	50	10^{-5}
	950	15	5	50	50	10^{-5}

4.3.3.2 Characterisation of the samples and discussions

After both consolidation processes, the samples were removed from the die. Following, they were characterized.

Moreover, possible reactions between the CNFs and the titanium based matrix were evaluated by XRD analysis. Finally, the microstructural study of the TiMMCs was done.

4.3.3.2.1 Hot pressing technique (HP)

- *Density and hardness*

The results of the density measurement (Archimedes density using the spray “water-stop”) and hardness (HV10) were compared in Figure 4-59 and listed in Table 4-40.

The density of the specimens from TiH_2(4) is slightly higher than the density for TiMMCs from CPTi(2). The reason of that could be the different load during the HP processing. The punches to compact the TiMMCs from TiH_2(4) received a little more load, thus the densification of these specimens is slightly better.

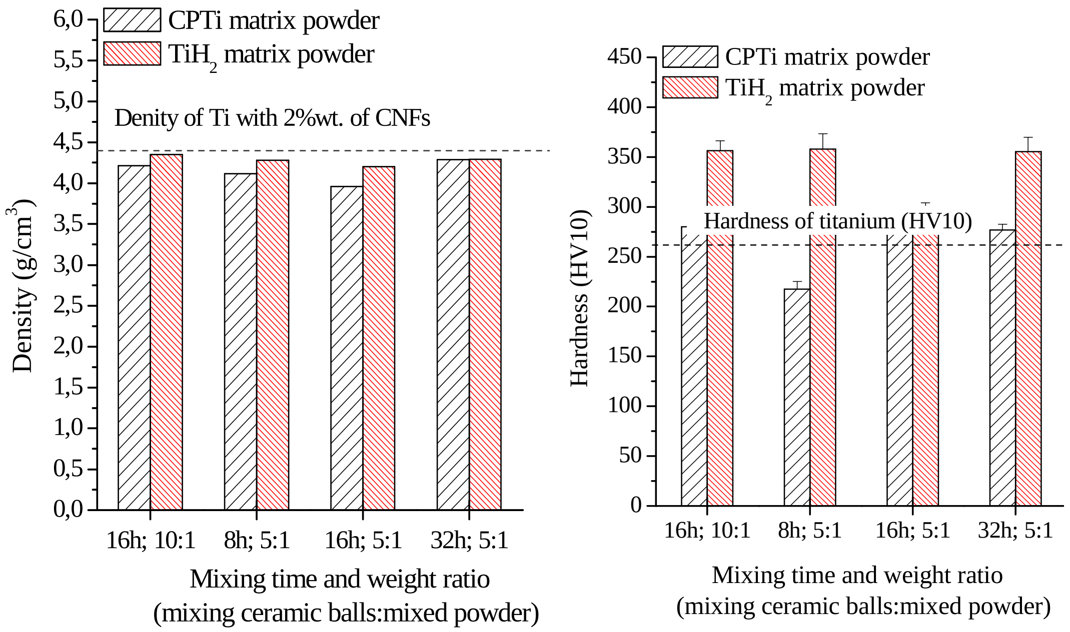

Figure 4-59. Arch. Density and hardness (HV10) of the TiMMCs produced after HP (850ºC, 1h at 30MPa) vs. the different mixing procedures

The oxygen content of the specimens from the first mixing procedure (16h and 10:1) is also reported in the next Table 4-40.

In general, the higher hardness value of the composite from TiH$_2$(4) matrix is closely related to the high oxygen and nitrogen content.

Table 4-40. Density and hardness (HV10) of composites with 2 mass% of CNFs prepared by different mixing procedures and produced via HP (the theoretical density used for the calculation of the relative density is 4.51g/cm³).

Mixing Conditions	**CPTi(2) matrix + 2 mass% CNFs**			**TiH$_2$(4) matrix + 2 mass% CNFs**		
time; M_{balls}/ M_{powder}	Rel. density (%)	Hardness (HV10)	Oxygen (mass%)	Arch. density (g/cm³)	Hardness (HV10)	Oxygen (mass%)
16h; 10:1	95.57	280	0.75	98.62	356	1.14
8h; 5:1	93.31	218	n.d.	97.09	358	n.d.
16h; 5:1	89.76	278	n.d.	95.25	299	n.d.
32h; 5:1	97.26	277	n.d.	97.30	355	n.d.

- *Microstructural study*

This representative study of the microstructure in addition to the previous results of density and hardness contributed to the selection of an optimal mixing procedure to prepare further mixture of the powders.

Thus, these mixtures are going to be used for the manufacturing of the TiMMCs via inductive hot pressing.

The next figure shows the different microstructures of the TiMMCs reinforced with 2 mass% of CNFs. The suitable dispersion of the CNFs into both titanium matrices is observed for the specimens from the mixture carried out during 16h and using 100g of ceramics balls for 10g of powder.

Also the dispersion of the CNFs after 32h of mixing time is acceptable; however it is not economical since the results of density and hardness are more or less similar to the values obtained after the mixing during 16h with 100g. (More mixing time is more cost for the production of materials with similar agglomeration and properties). Thus having similar results, the short time is always favourable. For that reason 16h is an optimal time for the mixture preparation.

In the next figure different sections of specimens compacted via HP at 850ºC for 1h in vacuum are illustrated. These specimens come from different mixing routes but the composition of CNFs was the same in all of them.

Observing the next figure, the image of the specimen from the powder mixed during 32h (5:1) presented the better distribution of CNFs.

Only the section image showed better properties of this specimens because the density and hardness measured were very similar to the specimens mixed for 16h and with double ball weight (10:1).Then, considering the density as a selection factor, the further mixing runs were carried out during 16h and using 10:1 as weight ratio (M_{balls}:M_{powder}).

Figure 4-60. Representative microstructure study (qualitatively) of the TiMMCs reinforced with the content of CNFs (2 mass%) which powder mixing is carried out during different time (h) and weight of ceramic balls (g).

Mixing time and ball weight for 5g of power mixture	CPTi (2) + 2mass%CNFs	TiH$_2$ (4) + 2mass%CNFs
1) 16h 100g balls	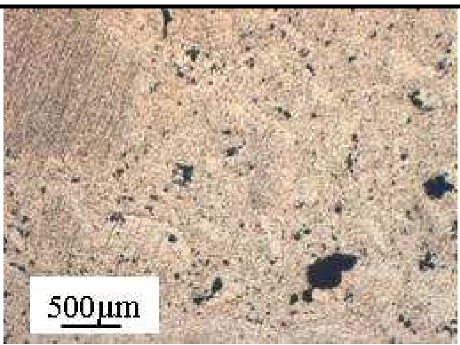	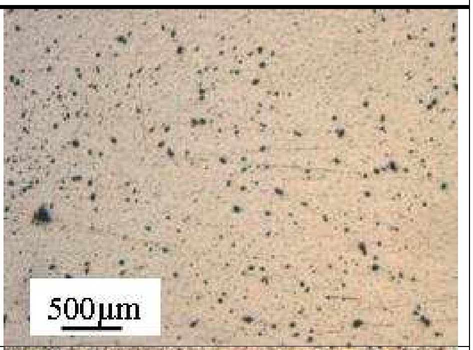
2) 8h 50g balls	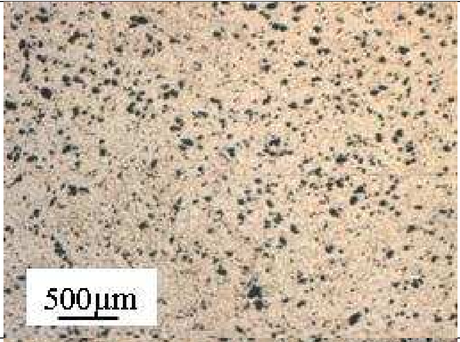	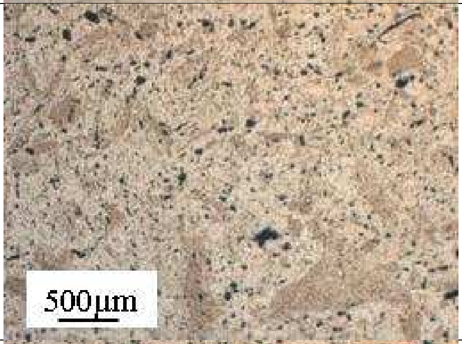
3) 16h 50g balls	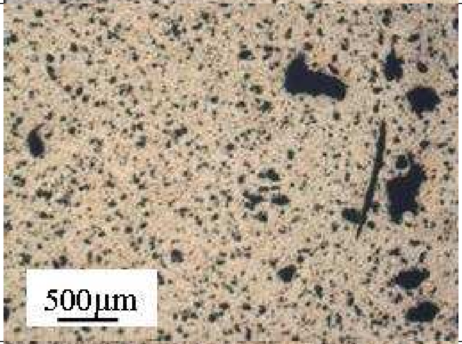	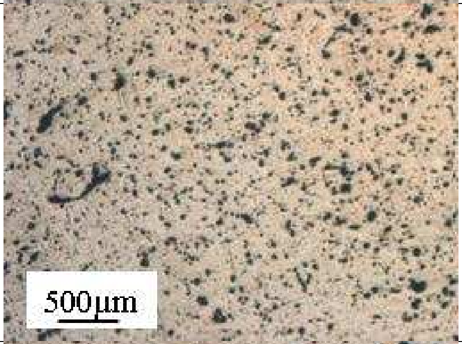
4) 32h 50g balls	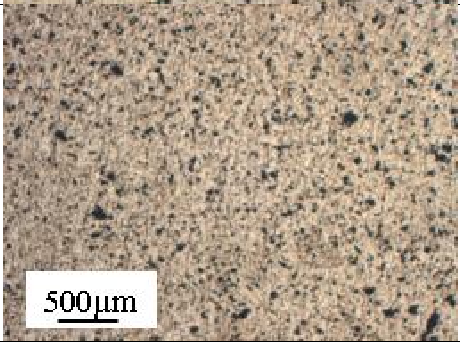	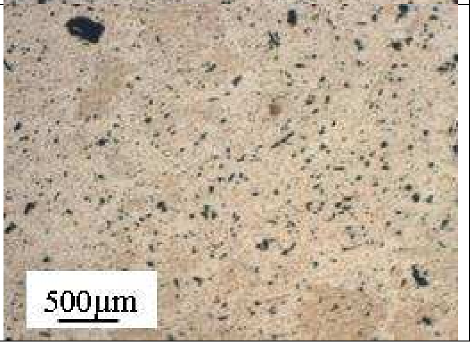

Additionally, the next Figure 4-61 confirms the existence of pores in the place where the CNFs are agglomerated.

A interesting question could be if the pores observed are really pores or parts of the CNF clusters that had been removed during polishing. The density was calculated before the metallographic preparation, for that reason this porosity would not affect the values of density previously reported.

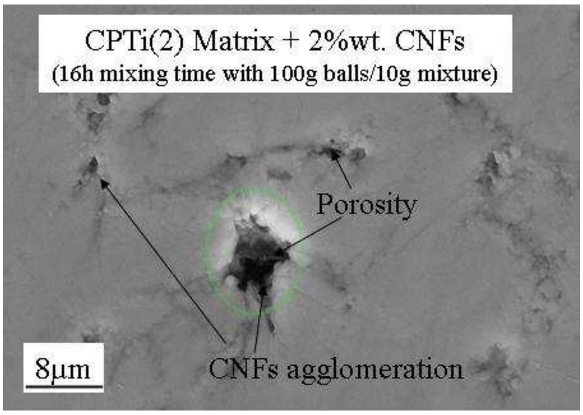

Figure 4-61. SEM image of the topography (SE2) of the TiMMCs from CPTi(2) matrix powder reinforced with 2 mass% of CNFs. The powder preparation was 16h mixing time and using 100g of ceramics balls/ 10g of powders mixture; hot consolidated via HP at 850°C for 1h.

Additionally in the next Figure 4-62, a CNF agglomeration is seen. These CNFs lay in a crater observed previously on the section of the TiMMCs from CPTi(2) matrix reinforced with 2 mass% of CNFs.

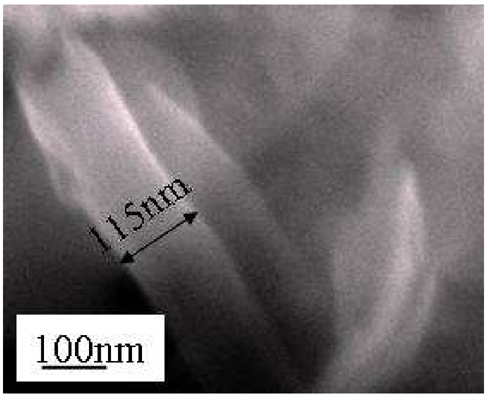

Figure 4-62. CNFs agglomeration in a titanium matrix after hot pressing (HP at 850°C).

4.3.3.2.2 Inductive hot pressing technique (iHP)

- *Density, hardness and oxygen content*

The density (Archimedes density using the spray “water-stop”) and hardness (HV10) are reported in the Figure 4-63.

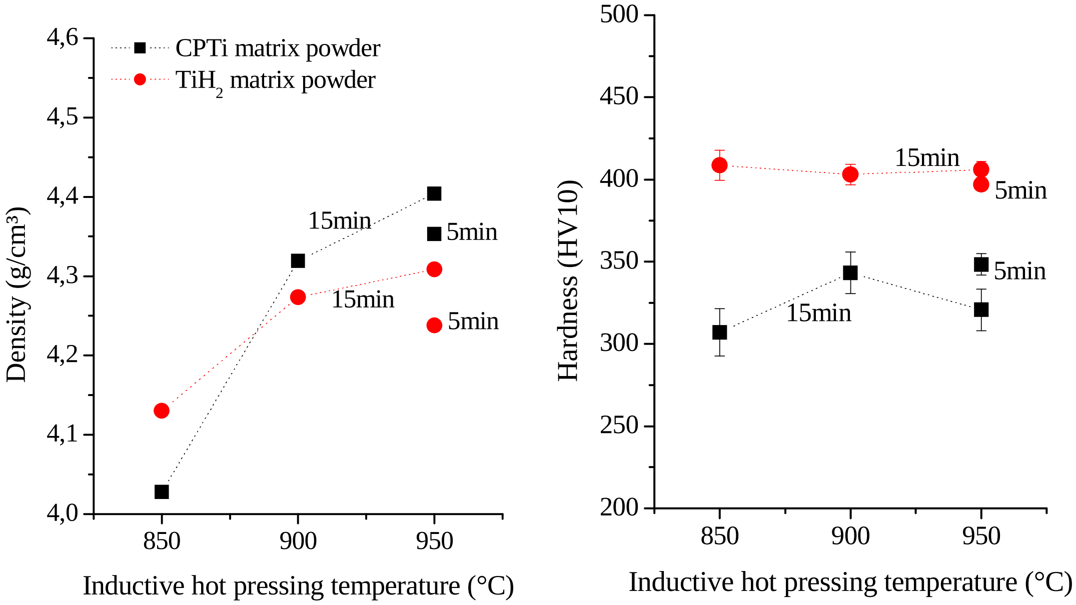

Figure 4-63. Arch. Density and hardness (HV10) of the TiMMCs produced by iHP (in high vacuum 10^{-5}mbar at 50 MPa) vs. the different processing parameters.

Next, oxygen content, density and hardness of the composites manufactured at 950°C are shown in Figure 4-64.

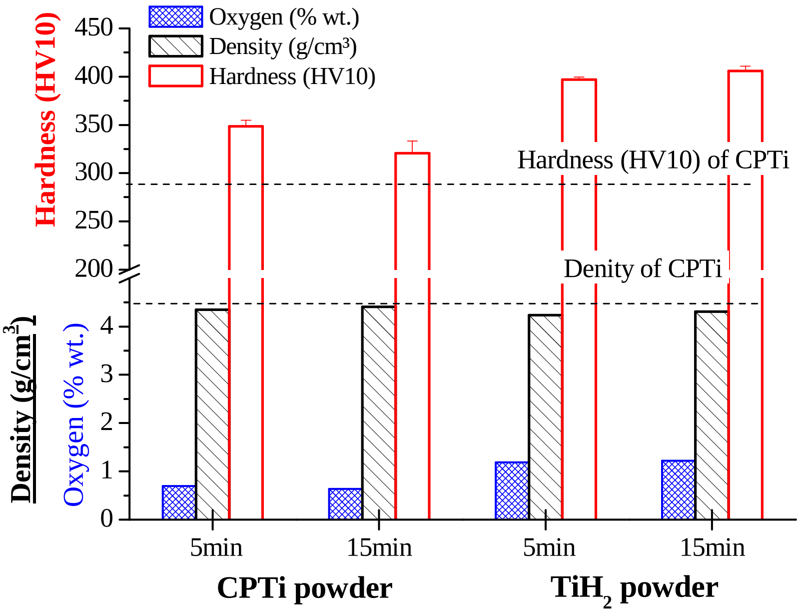

Figure 4-64. Oxygen content, hardness and density of the TiMMCs produced via inductive hot pressing (iHP) at different manufacturing conditions (at heating rate 50 K/min, temperature 950°C and high vacuum).

To summarise the previous comparison, in the next Table 4-41 the values of the density, hardness and oxygen content of the TiMMCs are listed.

Table 4-41. Density and hardness (HV10) for the composites with 2 mass% of CNFs produced via iHP. (the theoretical density taken as 4.51g/cm³).

Mixture	iHP Temp. (°C)	iHP time (min)	Rel. density (%)	Hardness (HV10)	Oxygen (mass%)
CPTi(2) +2mass%CNF	850°	15	89	307	0.57
	900°	15	96	343	n.d.
	950°	15	98	321	0.63
	950°	5	97	348	0.70
TiH_2(4) +2mass%CNF	850°	15	92	403	1.54
	900°	15	95	406	n.d.
	950°	15	96	409	1.22
	950°	5	94	397	1.20

The composites from TiH_2(4) matrix powder always present the higher oxygen content that involves higher hardness values for these composites in spite of their lower relative density.

Increasing temperature lowers this high oxygen content for this type of composites. Although the short time of iHP cycle doesn’t affect the oxygen content for the composites from TiH_2(4), in the case of the other specimens from CPTi(2) the influence of the time is slightly noticeable. These differences were not significant.

- *Microstructure study*

In the microstructures of the composites, differences between the composite from each matrix powder were detected.

However, the appearance of clusters of CNFs was observed for both titanium matrices (see in **Fehler! Verweisquelle konnte nicht gefunden werden.**), which is a consequence of the mixing problems well known from CNFs. Even after the improving of this mixing procedure these agglomerates are seen.

Another phenomenon, which all the titanium composites showed, was the existence of dark regions. It was more significant on the border of the CNFs agglomerates (Figure 4-66). Also, the influence of the holding time affected the formation of these dark regions.

In the next figure, the section microstructures of the different specimens are illustrated and compared.

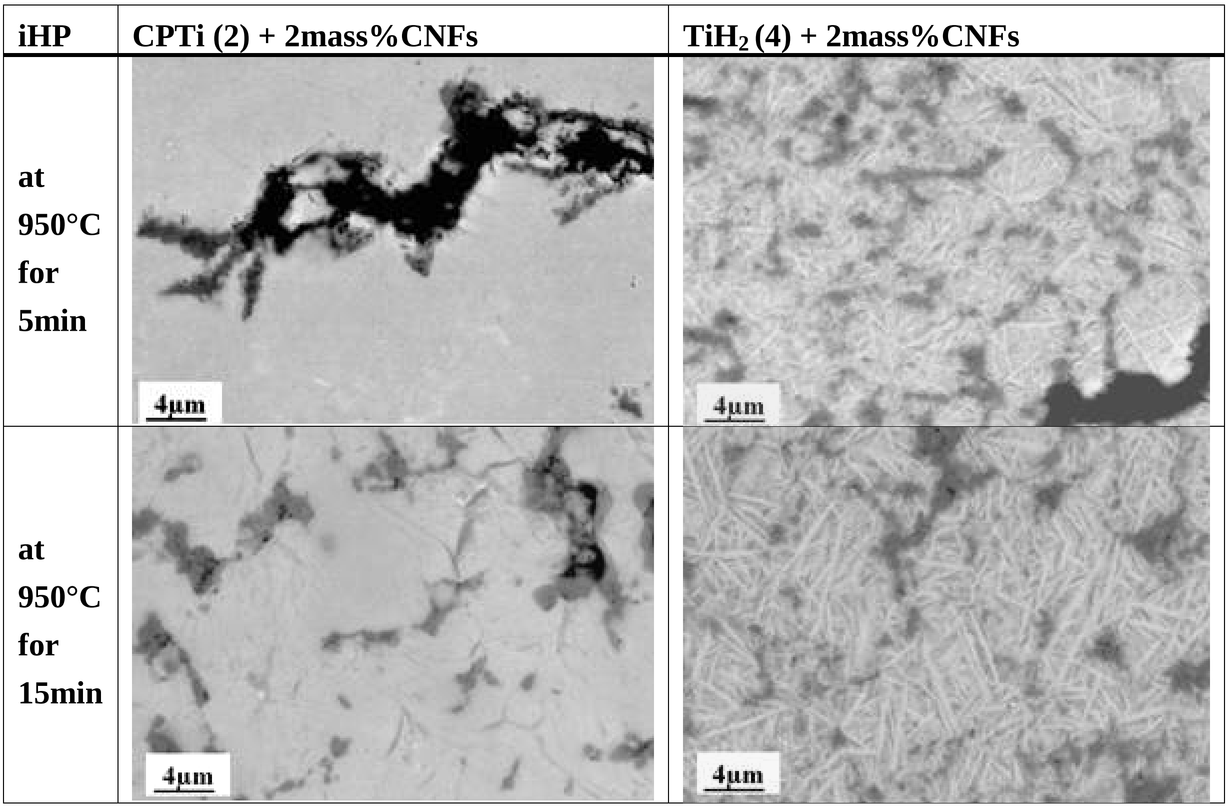

Figure 4-65. Microstructures of the TiMMCs from the CPTi(2) and TiH_2(4) matrix with 2 mass% of CNFs, produced via iHP at 950°C varying the holding time 5min and 15min. (SEM images by BSE detector)

In the next Figure 4-66 a cluster of CNFs located in a titanium matrix (CPTi(2)) is shown.

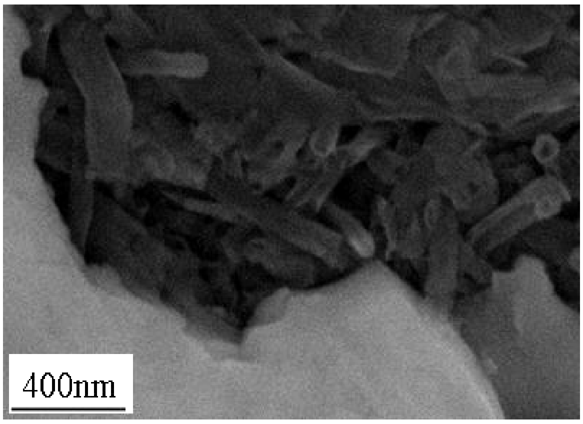

Figure 4-66. SEM image of a cluster of CNFs in the titanium composite from CPTi(2) matrix with 2 mass% of CNFs (hot pressing at 950°C and 50MPa for 5min in high vacuum).

- *XRD analysis*

Observing the previous microstructure images (see **Fehler! Verweisquelle konnte nicht gefunden werden.**), the dark regions could be the result of reactions between the matrix and the carbon based reinforcement. In order to check the existence of titanium carbides [59], XRD analysis of several composites was done (see Figure 4-67).

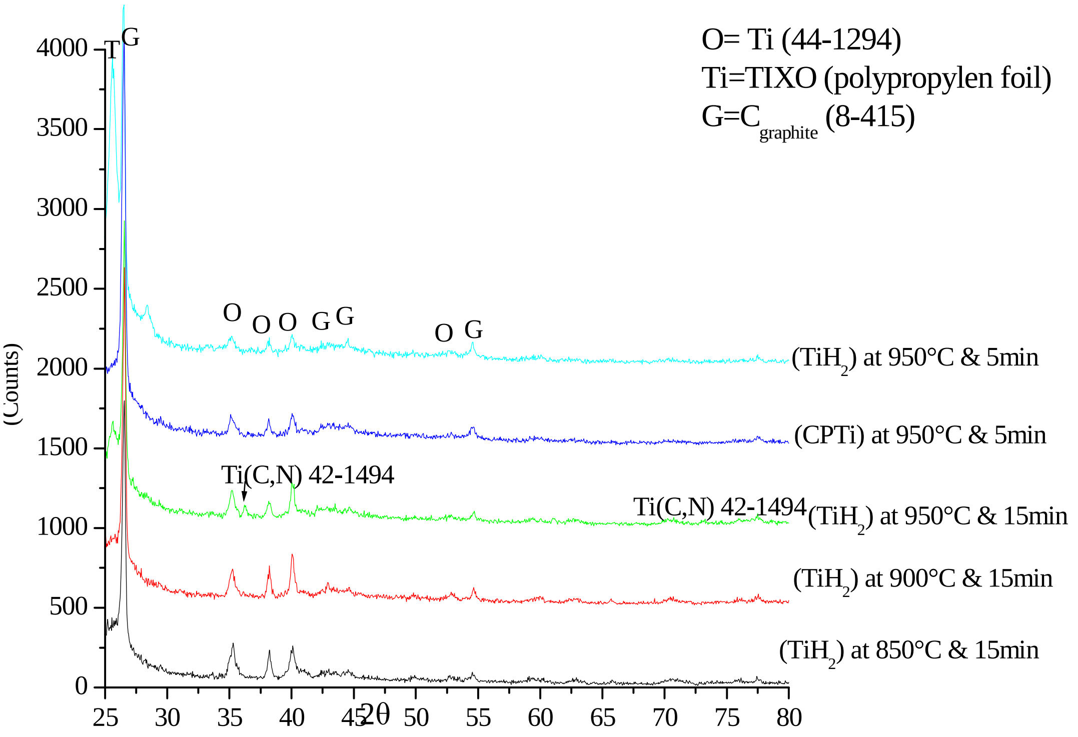

Figure 4-67. XR diffraction patterns of all the composites from TiH_2 and one composite from CPTi matrix compacted by iHP at maximum temperature for 5min. (2θ)

Thus it was found that in case of composites from TiH_2 hot pressed at 950°C for 15min, some TiC or TiN has been formed [100]. Here, the presence of nitrogen from the starting powder TiH_2(4) was evident. There was some reaction between the titanium matrix and the nitrogen at high temperature (950°C) during 15min. Also it could be due to the reaction between the Ti matrix and boron nitride coatings. However, the investigations were carried out on the section; in that case the influence of the BN coating was not appreciable. At the same temperature but for 5min of holding time, in contrast, there was no signal of such reactions.

4.3.3.2.3 Comparison of conventional and inductive hot pressing

- *Hardness values and chemical analyses*

In the next Table 4-42 the values of hardness and oxygen and nitrogen content are listed for the TiMMCs produced via HP and iHP at different processing conditions. For all of these titanium composites, the mixing parameters employed were 16 h and 10:1 ratio.

Table 4-42. Comparison of the properties of the TiMMCs manufactured at different processing conditions.

Matrix	Process	Parameters (Temp.; time)	Oxygen (mass%)	Nitrogen (mass%)	Hardness (HV10. ±10)
CPTi (2)	HP	850°C; 60min.	0.75	0.02	278
CPTi (2)	iHP	850°C;15min	0.57	0.01	307
CPTi (2)	iHP	950°C; 15min.	0.63	0.02	321
CPTi (2)	iHP	950°C; 5min.	0.70	0.02	348
TiH_2 (4)	HP	850°C; 60min.	1.14	0.13	299
TiH_2 (4)	iHP	850°C; 15min.	1.54	0.17	409
TiH_2 (4)	iHP	950°C; 15min.	1.22	0.15	406
TiH_2 (4)	iHP	950°C; 5min.	1.20	0.15	397

The specimens from CPTi(2) presented lower values of oxygen content. Also the nitrogen concentration are lower than the concentration (nitrogen mass%) for specimens from TiH_2 (4). It is normal considering the elevated levels of nitrogen measured for this starting powder.

An interesting increase of the nitrogen concentration is observed for the specimens from CPTi(2) in comparison to the lower contents detected in the starting powder (CPTi(2) max. 0.002 mass%).

This increase can be due to the hot consolidation processes since powders are directly in contact with the BN coating. However, there was no appreciable reaction between CPTi and BN in a similar range as that between TiH_2 and BN. Also, the high N level comes from the starting powder.

- *Microstructure study*

In the next figure a representative microstructure comparison of titanium matrices from both starting powders (CPTi(2) and TiH_2(4)) reinforced with 2 mass% of CNFs is shown. Additionally, the processing parameters are also reported.

The same clusters are seen for both types of composites consolidated through HP and iHP. It means an optimal dispersion allows a reduction of the porosity. However it is very difficult to achieve such optimal dispersion.

T,°C	Starting matrix powder with 2%vol of CNFs	
	CPTi	TiH2
850 HP 60min	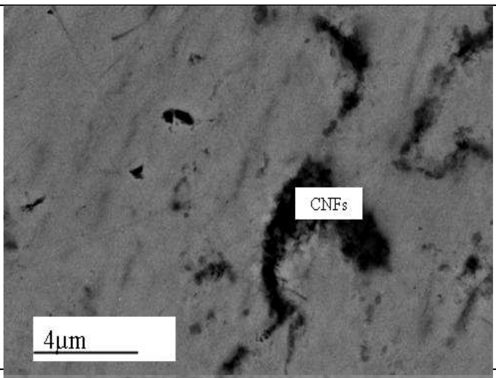	n.d.
850 iHP 15min	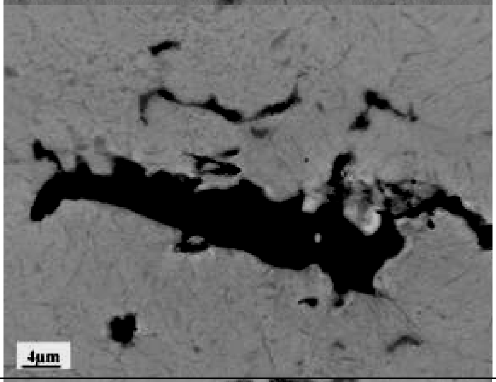	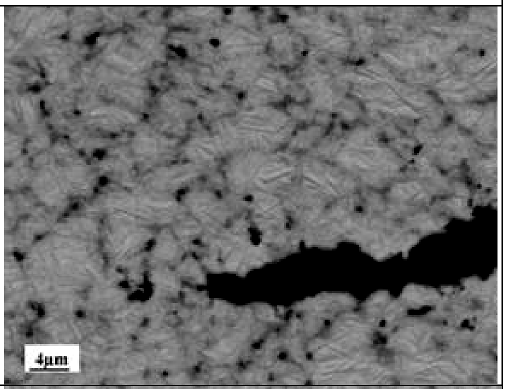
900 iHP 15min	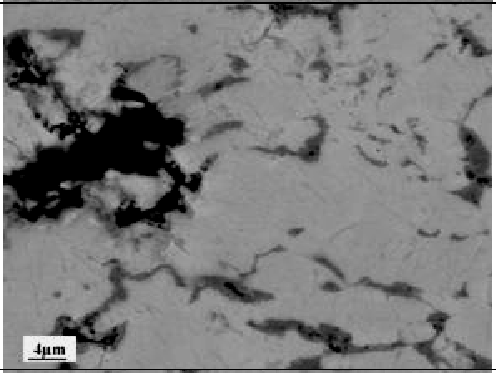	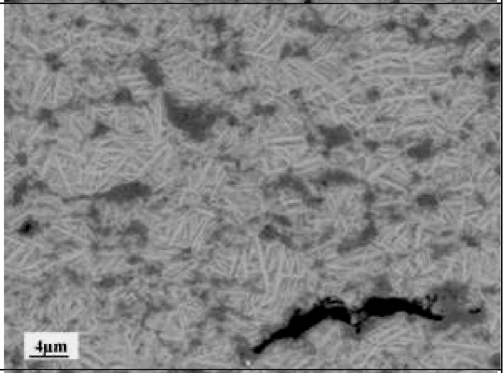
950 iHP 5min	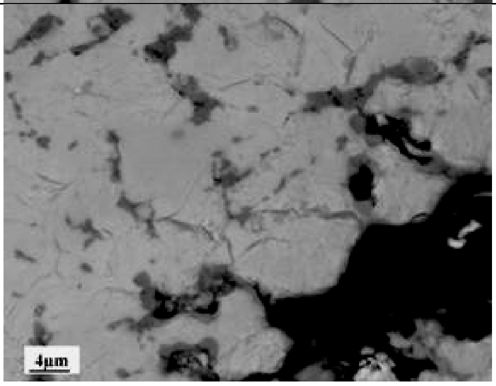	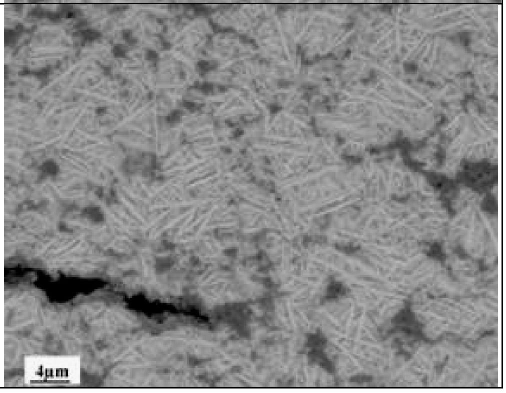

Figure 4-68. Representative microstructures of the TiMMCs from the CPTi(2) and TiH_2(4) matrix with 2 mass% of CNFs, produced via HP and iHP varying the temperature and holding time 5min and 15min. (SEM images by BSE detector)

Intermediate Conclusions

- In general, the main problem is the agglomeration of the reinforcement material (CNFs). Clusters of CNFs are observed on all the section of specimens produced
- Further improvement in the dispersion of CNFs into a titanium based matrix can improve the mechanical properties of the composites, e.g. better densification
- Reaction of CNFs with the titanium from the matrix is observed at higher temperatures (up to 900ºC)
- There is an additional effect on the densification of the TiMMCs because of the use of 12-cavities.

4.3.4 TiMMCs reinforced with Nanodiamond particles (NDs)

4.3.4.1 Manufacturing processes

In the manufacturing process of titanium based matrices reinforced with nanodiamond particles, all the three fabrication techniques were employed. As starting titanium based powder CPTi (2) was always used. Because of the high oxygen and nitrogen in addition to possible residual hydrogen, the TiH_2(4) powder was not used for all these three processes. Only for the first manufacturing process (iHP), this TiH_2(4) was employed as matrix powder. The reason was the chronology of the test. The first fabrication technique used was iHP. The decision to use only CPTi(2) was taken after several evaluations of characterisation results.

These three manufacturing techniques are represented in the next diagrams (see from Figure 4-69 to Figure 4-71). Firstly, the production of the TiMMCs via inductive hot pressing was done (see Figure 4-69).

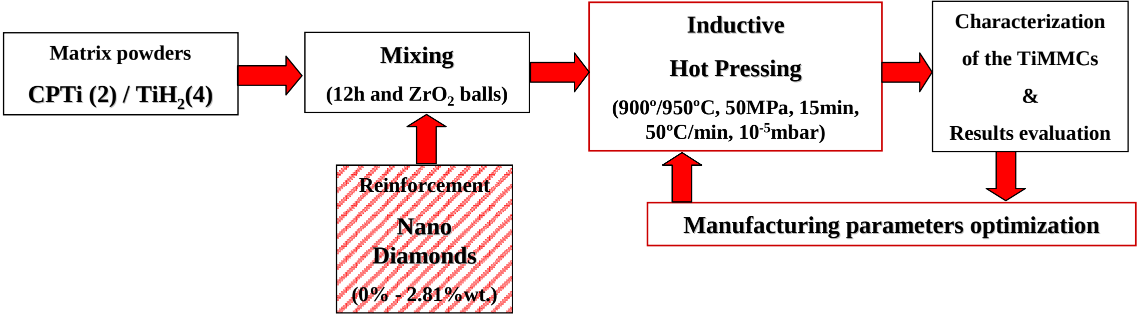

Figure 4-69. Manufacturing flow sheet of the titanium matrices reinforced by nano-diamond particles (NDs(1)) via inductive hot pressing.

The mixing time was increased to 12h in order to improve the dispersion of the nanodiamonds in the titanium matrix. In the second and third tests, only the titanium matrix powder CPTi(2) was employed, and the content of nano diamond particles was fixed to 1.8 vol% (1.43 mass%) (see Figure 4-70 and Figure 4-71).

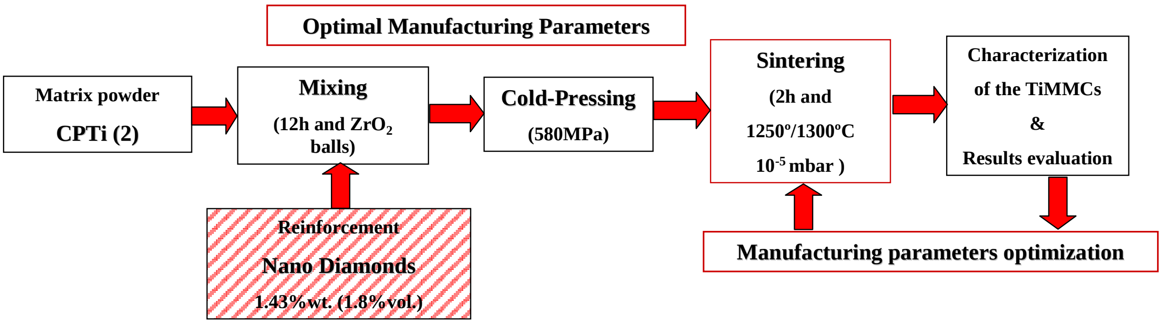

Figure 4-70. Manufacturing flow sheet for conventional cold-pressing and sintering of the TiMMCs (CPTi(2)) reinforced by nano-diamond particles (NDs(2)).

In the conventional hot pressing all the processing parameters used were already optimised.

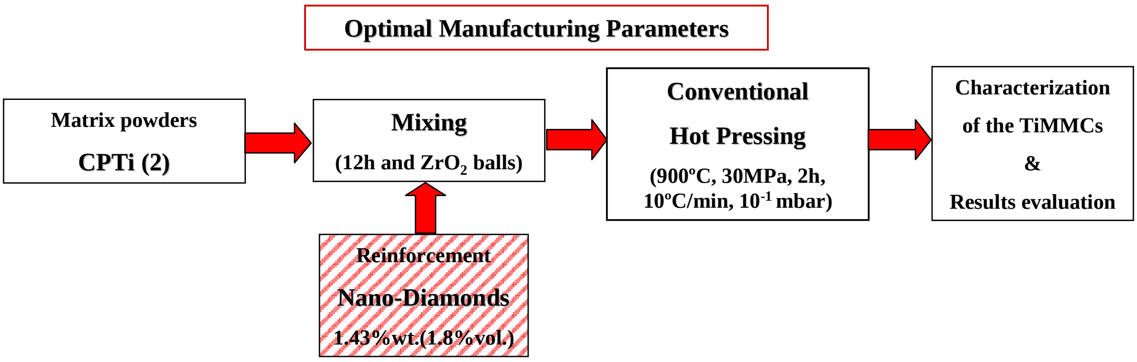

Figure 4-71. Manufacturing flow sheet for conventional hot pressing of TiMMCs (CPTi(2)) reinforced by nano-diamond particles (NDs(2)) via.

Powder preparation

This stage can be divided into two subparts according to the chronology of the tests and also considering the starting materials used for the manufacturing of the TiMMCs.

Firstly two starting titanium based powders were tested (CPTi(2) and TiH_2(4)) in addition to the first nano-diamond powder (NDs(1)) ordered. The results of the characterisation were decisive to carry out the other two manufacturing processes. Only one titanium starting powder (CPTi(2)) was used as matrix powder and new nano-diamond (NDs(2)) powder had to be ordered due to the poor quality of the first one.

- *Reinforced matrices from CPTi(2) and TiH_2(4) powders with NDs(1):*

First, different NDs contents were added to each matrix powder (see in Table 4-43).

Table 4-43. Contents of nano diamond particles (NDs) used as reinforcement for the fabrication of TiMMCs

Reinforcement content into the matrix					
mass%	0.00	0.14	0.70	1.40	2.81
%vol.	0.00	0.18	0.90	1.80	3.60

The nanodiamond particles used at the beginning were NDs from the supplier (1) (NDs(1)). The addition of this reinforcement and the powder preparation of the different mixtures were carried out in the same way as described in the previous chapter. These different mixtures were prepared to fabricate the TiMMCs by way of inductive hot pressing.

After the chemical analysis of this NDs(1), its high oxygen content was revealed. Thereafter, just in these first test series this NDs(1) was used. A new supplier of nano diamond particles with lower oxygen and impurity content was searched for.

In the second and third experimental series, the use of one titanium matrix powder was employed.

The decision to use CPTi (2) and not the TiH_2(4) was due to the higher oxygen and nitrogen content in composites from TiH_2(4) observed in previous composites from this powder.

In this second and third part, the main objective was the evaluation of the mechanical properties of the TiMMCs reinforced using the nano diamond particles.

Hence, the favourable composites were from the titanium matrix with lower oxygen content. Also, this was applicable to the reinforcement materials NDs(2).

- *Reinforced matrix from CPTi(2) powder with NDs(2)*

As mentioned before, the second type of nanodiamond particles NDs(2) was added to the titanium matrix powder CPTi(2).

The reinforcement content was 1.8 vol%. It was already fixed after the evaluation of the properties of the first TiMMCs series, in which the different contents of NDs were tested.

The same mixing of CPTi (2) with 1.8 vol% of NDs(2) was employed to produce the TiMMCs through the techniques of conventional hot pressing and cold-pressing and sintering, respectively.

Powder consolidation

- *Inductive hot pressing (iHP)*

The different mixtures of both titanium based powders with the different nanodiamond particle contents were hot consolidated using inductive hot pressing.

The processing parameters are listed in the next Table 4-44.

- *Conventional hot pressing (HP) and cold-pressing (CP) and sintering processes*

Afterwards, the specimens from CPTi (2) with the 1.8 vol% of NDs(2) were manufactured by the conventional hot pressing or cold-pressing and sintering processes.

For the HP, the diameter of the pressing die used was 65 mm. For the cold pressing process, a die with rectangular section (6.4 x 55mm^2) was utilised. That means, larger samples could be produced through HP and CP-sintering processes in order to measure mechanical properties, e.g. flexural properties.

The next table shows the processing parameters employed for the fabrication of titanium composites with nanodiamond particles as reinforcement material.

Table 4-44 Processing parameters for inductive hot pressing, conventional hot pressing and cold-pressing and sintering techniques.

Hot Pressing Process	Temperature (°C)	Holding time (min)	Heating rate (K/min)	Pressure (MPa)	Vacuum (mbar)
Inductive HP	900	15	50	50 (iHP)	10^{-5}
	950	15	50	50 (iHP)	10^{-5}
Conventional HP	900	120	10	30 (HP)	10^{-1}
Cold Pressing and sintering	1250	120	10	580 (CP)	10^{-5}
	1300	120	10	580 (CP)	10^{-5}

iHP: inductive hot pressed. HP: conventional hot pressed. CP: cold pressed.

Heat Treatment (HT) [11]

Heat treatment is common for Ti alloys; for plain Ti it is not effective. However, heat treatment was applied here also for plain Ti matrix material as a reference. The reason of that was to evaluate if there was any difference in the mechanical properties after HT. This heat treatment was simultaneously carried out with the heat treatment for Ti6Al4V-MMCs (they will be described in detail further on). After the sintering of the titanium compacts at 1300°C, titanium samples without reinforcement were selected for a heat treatment (see in Figure 4-72).

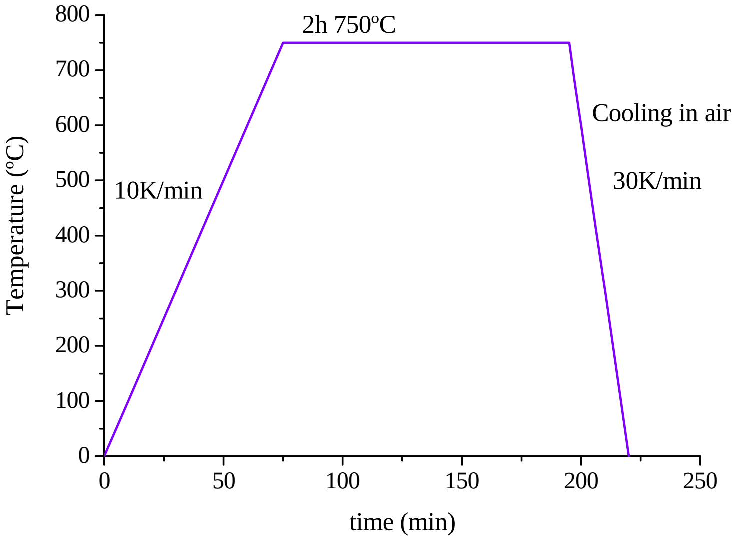

Figure 4-72. Heat treatment (HT) employed for the titanium compacts without reinforcement.

It was planned to obtain a possible improvement of the mechanical properties (especially elongation) of the titanium specimens. Reference values of heating rate and cooling condition were taken from the bibliography. The previous Figure 4-72 showed how the heat treatment was carried out.

The cooling rate was calculated to be approx. (30 K/min). Thereafter, the specimens were characterised in parallel with the other specimens prepared without heat treatment.

4.3.4.2 Characterisation of the specimens - results

4.3.4.2.1 Inductive hot pressing technique (iHP)

- *Density, hardness and oxygen content*

The Archimedes density was measured in water using the water-stop spray. The results are represented in the following Figure 4-73.

For the determination of the relative density, the theoretical density considered for the nano-diamond particles was 3.52g/cm^3.

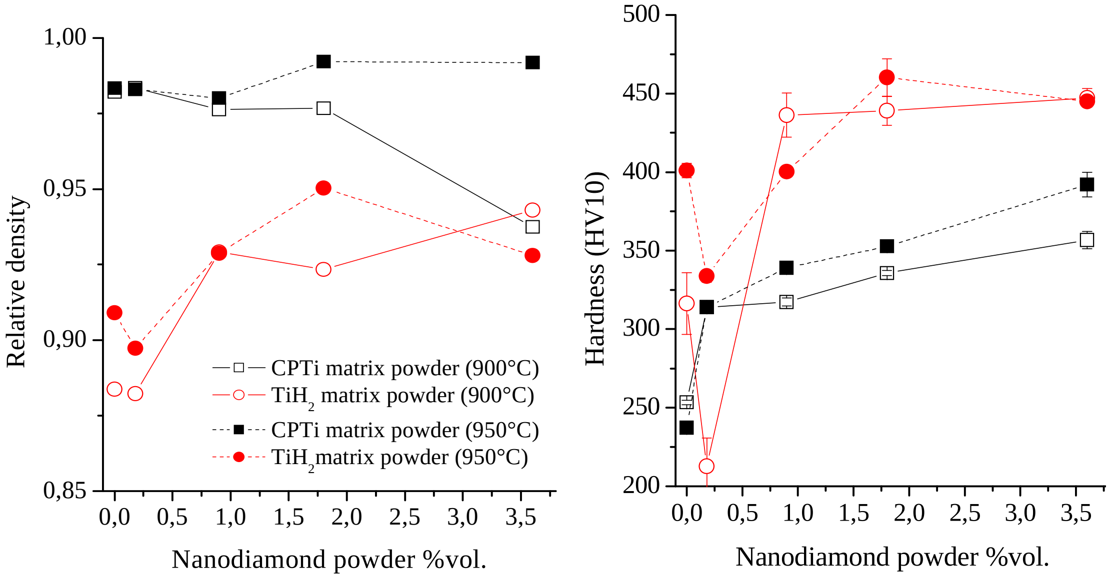

Figure 4-73. Relative density and hardness (HV10) of the TiMMCs produced after iHP (in high vacuum 10^{-5}mbar at 50MPa) vs. the different nanodiamond contents.

The oxygen content of both titanium based matrices (from CPTi(2) and TiH$_2$(4) powders) compacted at 900° and 950°C was analysed.

Furthermore, the oxygen content of the TiMMCs with 3.6 vol%. of NDs fabricated at the same temperature was measured. These results are presented in Table 4-45.

The addition of the reinforcement has a significant influence on the oxygen content of the composites. Due to the nano-size of the diamond particles, the oxygen content is high. Thus, the incorporation of the nanodiamonds to the titanium matrix considerably increases the oxygen content of the titanium specimens. This is observed for the different types of TiMMCs (from both matrices).

The increase of the processing temperature reduces the oxygen content of the composites.

The hardness is closely related to the oxygen content of the sample. It is clearly observed on the composite from CPTi(2) matrix.

Because of the low oxygen content of the pure titanium matrix without nanodiamond particles, its hardness is approximately the theoretical hardness for titanium grade 4 (see in Table 4-45).

Table 4-45. Arch. density, hardness (HV10) and oxygen content after inductive hot pressing at 950ºC for 15min. (Theoretical density for nano-diamond particles 3.52g/cm^3)

iHP.Temp. 950ºC	**NDs (vol%)**	**Arch.density (g/cm^3)**	**Th.density (g/cm^3)**	**Rel. density (%)**	**Hardness (HV10)**	**Oxygen (mass%)**
Matrix						
CPTi(2)	0.00	4.46	4.54	98	237	0.41
	0.18	4.46	4.54	98	314	n.d.
	0.90	4.44	4.53	98	339	n.d.
	1.80	4.49	4.52	99	353	n.d.
	3.60	4.47	4.50	99	392	0.63
TiH_2(4)	0.00	4.13	4.54	91	401	0.42
	0.18	4.07	4.54	90	334	n.d.
	0.90	4.21	4.53	93	400	n.d.
	1.80	4.30	4.52	95	460	n.d.
	3.60	4.18	4.50	93	445	1.04

- *Microstructural study*

The microstructures of the most representative specimens are shown in the next Figure 4-74.

The specimens were fabricated through inductive hot pressing at the same process temperature and holding time. The content of nano-diamond particles was varied.

In general, after the metallographic preparation some particles are on the surface, even after intensive cleaning.

These impurities are observed and can cause problems to detect the NDs location in the metal matrix.

	iHP at 900ºC (15min)	
Matrix	CPTi (2)	$TiH_2(4)$
	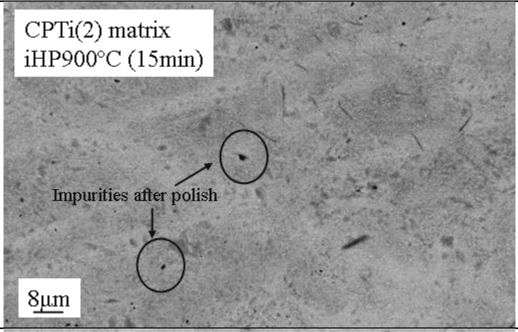	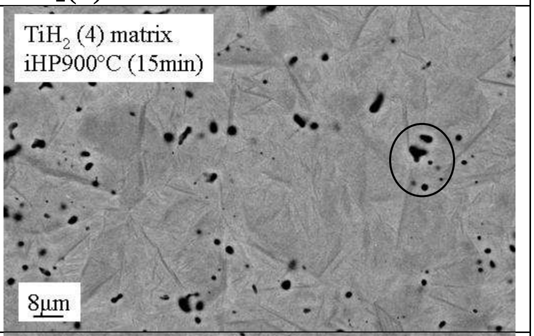
+ NDs 0.18 vol%	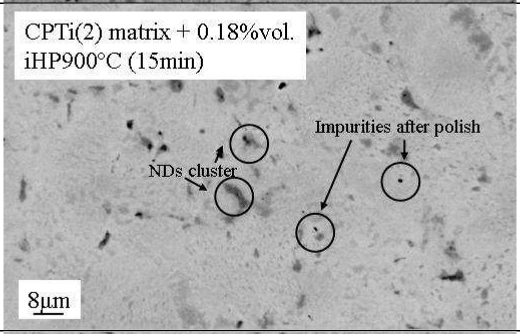	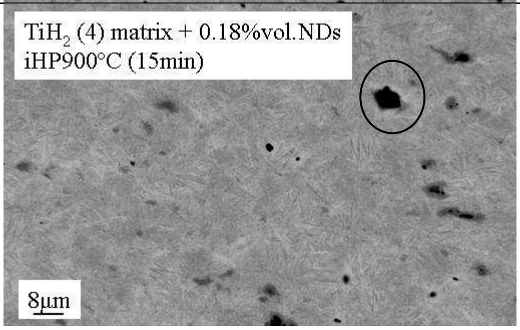
+ NDs 1.8 vol%	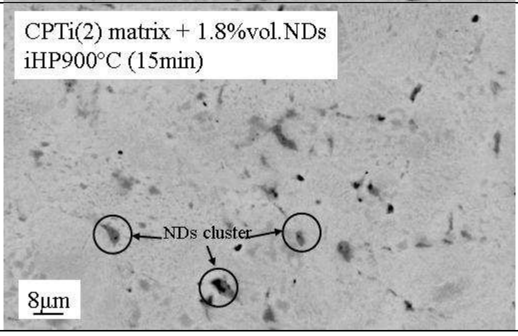	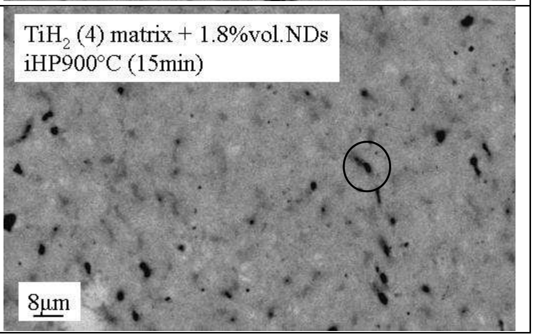

Figure 4-74. SEM images of the microstructure of TiMMCs from CPTi(2) and $TiH_2(4)$ matrices with different NDs contents, produced by iHP at 900ºC during 15 min.

Many pores are found in the samples from $TiH_2(4)$ matrix (in black circle). Moreover, several clusters of nanodiamond particles are seen in both titanium matrices. Differences between the matrices are also evident. Slight needle structures are observed characteristic for composites from $TiH_2(4)$ matrix powder. The short processing time (iH-time) was not enough to eliminate all the hydrogen from composite matrix. For that reason, some residual hydrogen in addition to the nitrogen from the starting powder ($TiH_2(4)$) contributes to growth of these needles. The matrix from CPTi(2) does not show any grain structure. However, in the microstructure of the matrix from $TiH_2(4)$ is a martensitic microstructure [13, 98] is slightly visible, thus it justifies the high values of hardness as well. The same structure was observed previously after the iHP consolidation of titanium matrices (without reinforcement) due to the higher hydrogen and nitrogen content measured.

4.3.4.2.2 *Cold pressing and sintering at 1250° and 1300°C*

After the consolidation and sintering of TiMMCs reinforced with 1.8%vol. of NDs, their characterisation took place. Additionally, three specimens of CPTi pure matrix produced via CP+S (sintered at 1300ºC for 2h) were heat treated. The objective of this heat treatment was to find some difference between the specimens. These specimens are CPTi matrix without HT, CPTi matrix after HT and TiMMCs reinforced with 1.8%vol. All of them were sintered at 1300º.
Moreover, properties of all the samples sintered at 1250ºC and 1300º are compared.

- *Density and hardness measurements*

The average values of density and hardness of the titanium specimens cold compacted at 560 MPa and sintered at two temperatures (1250° and 1300°C) are represented in the Figure 4-75. The Archimedes density was measured using the water-stop spray.

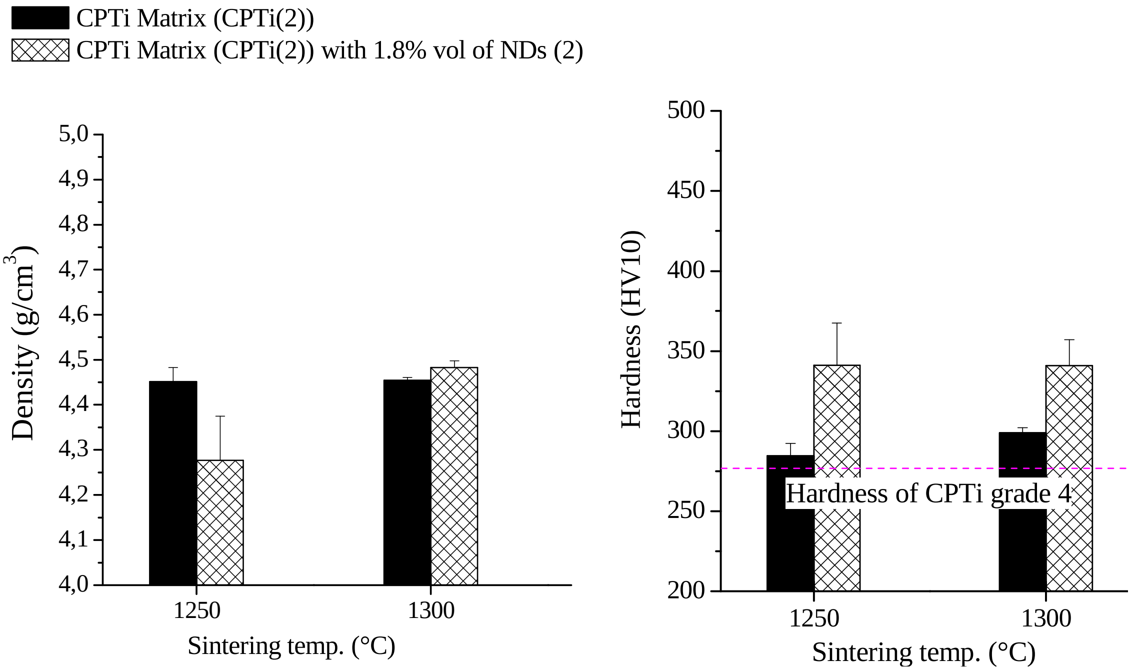

Figure 4-75. Average values of Arch. density and hardness of the TiMMCs cold compacted at 560 MPa and sintered at two temperatures.

By increasing the sintering temperature, the density of the TiMMCs reinforced with 1.8 vol% of nanodiamond particles increases while the hardness is approximately the same for both sintering temperatures (1250ºC and 1300ºC). The hardness differences between titanium matrix reinforced and the pure titanium matrix (CPTi(2)) are significant. An increase (approx.) of 30% for both reinforced titanium matrices is observed, considering 260 HV10 as theoretical value for the titanium (commercial purity titanium grade 4). However, the density of these specimens decreases significantly.

- *Chemical analysis and mechanical properties*

By the use of a die with the specified dimensions, the geometry of the samples was sufficient for flexural tests without any machining operation. The average values of the properties of the composite with 1.8 vol% (NDs) and the titanium matrix (without reinforcement) are presented in the next table. Furthermore, oxygen analysis of several specimens was carried out. These results and their flexural properties are listed in the next table.

Table 4-46. Properties and oxygen content of titanium specimens and TiMMCs with 1.8 vol% of NDs(2) particles, compacted at 560 MPa and sintered at two temperatures.

Starting Powders	**T (°C)**	**Flexural strength (MPa)**	**E (%)**	**Arch. density (g/cm^3)**	**Th. density (g/cm^3)**	**Relat. density (%)**	**Hardness (HV10)**	**Oxygen (%wt).**
CPTi(2)	1250	538	1.7	4.43	4.51	98	287	0.57
CPTi(2) +NDs(2)	1250	457	0.6	4.25	4.49	95	337	0.86
CPTi(2)	1300	1228	2.9	4.46	4.51	99	297	0.59
CTi(2)+HT	1300	893	1.2	4.24	4.51	94	324	0.73
CPTi(2) +NDs(2)	1300	848	0.9	4.47	4.49	99	349	0.73

HT: Heat treatment

- *Microstructural study*

In Figure 4-76, the microstructure of the TiMMCs sintered at 1250° and 1300° is shown.

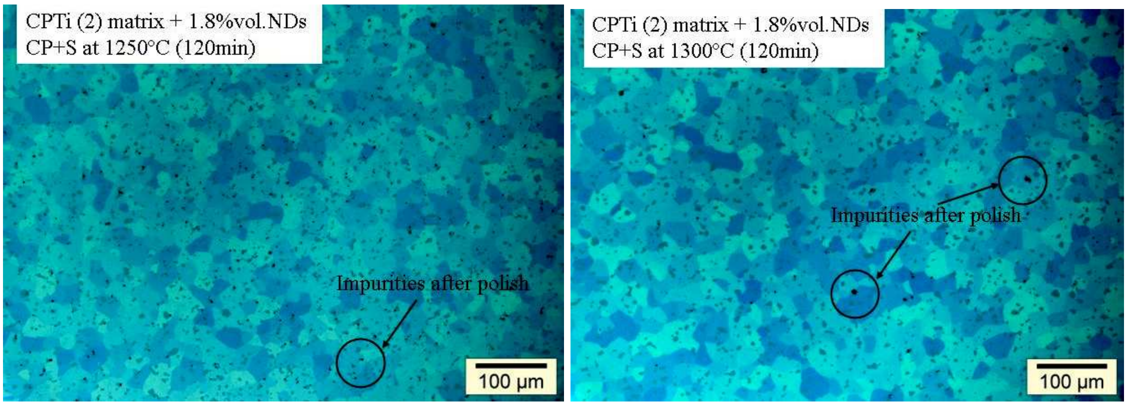

Figure 4-76. Microstructure of TiMMCs from CPTi(2) reinforced with NDs particles (1.8 vol%) and cold pressed (at 560 MPa) and sintered at different temperatures: left image of TiMMC at 1250° and right at 1300°C.

For these composites from CPTi(2) powder, it is possible to observe the alpha grains. Also several impurities are usually seen on the surface of the TiMMCs after polishing. In the next SEM images the reaction between the carbon and the titanium matrix can be observed.

The formation of TiC is detected after the sintering of the composites at 1250º and 1300ºC. Due to admixed nano-diamond particles clustering was observed in the section of these TiMMCs.

The carbonaceous reinforcement and titanium from the matrices resulted in the formation of TiC (at 1250º and 1300ºC).

The reduction of the porosity with the increase of the sintering temperature is seen in the next figure.

It confirms the results of the Archimedes density and hardness of the composites as well as the improvement of the mechanical properties. The relatively large TiC areas indicate that some agglomeration of nano-diamonds that reacted with the Ti of the matrix had occurred.

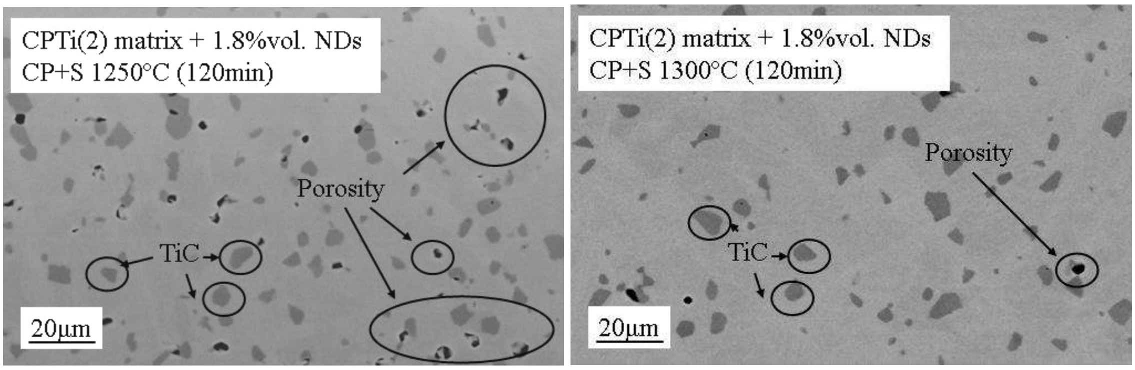

Figure 4-77. SEM images (BSE) of the microstructure of TiMMCs from CPTi(2) reinforced with NDs particles (1.8 vol%.) and cold pressed (at 560 MPa) and sintered at different temperatures: left image of TiMMC at 1250º and right at 1300ºC.

4.3.4.2.3 Hot pressing technique

TiMMCs produced by hot pressing at 900°C for 2h.

- *Density, hardness, chemical analysis and mechanical properties*

The values of relative density (%) and hardness (HV10) of the pure titanium matrix and the titanium matrix reinforced with 1.8 vol%. of NDs(2), fabricated via HP at 900°C for 2h, are shown in the following Table 4-47.

The results obtained after the bending tests (see chapter 4) in addition to the oxygen and nitrogen content of the specimens are also listed in Table 4-47.

Table 4-47. Properties of TiMMCs fabricated via HP at 900°C for 2h. The matrix powder was CPTi(2) and the reinforcement concentration was 1.8 vol%. of NDs (2).

Starting Powders	Relative density (%)	Hardness (HV10)	Flexural strength (MPa)	ε (%)	Oxygen (mass%)	Nitrogen (mass%)
CPTi(2)	99.7	313±3	996±13	1.8	0.51±0.18	0.022±0.012
CPTi(2)+NDs(2)	98.5	377±1	631±64	1.3	0.68±0.15	0.056±0.036

- *Microstructural study*

The nanodiamond particles are not easy to be detected by SEM; however there are some areas in the microstructure of the composite where they could be observed. In the next Figure 4-78 these areas can be seen. Additionally, little porosity is related to the place where NDs are detected.

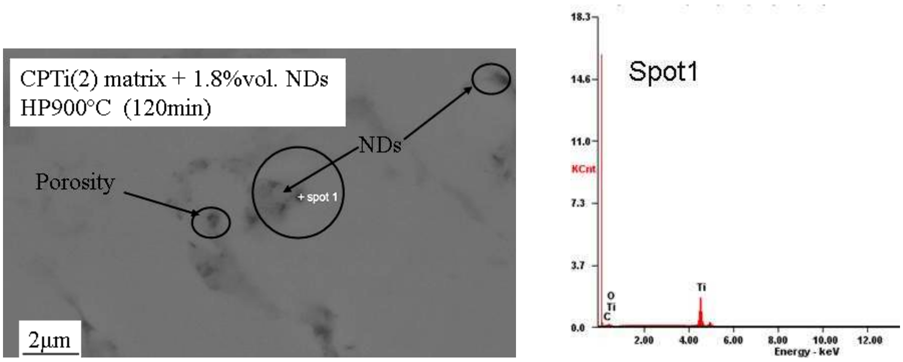

Figure 4-78. SEM image (BSE) of the microstructure of TiMMC from CPTi(2) reinforced with NDs particles (1.8 vol%.) and hot pressed at 900ºC for 2h.

Intermediate Conclusions

- High oxygen content of the nano-reinforcement contributes to increase the oxygen of the composite, i.e. decreasing the mechanical properties of composite material.
- Addition of nano-diamonds increases significantly the hardness of composite.
- The temperature of manufacturing of titanium matrices reinforced with NDs has to be 900ºC maximum to avoid reaction between Ti from the matrix and the carbonaceous reinforcement.
- CP+S is not recommendable to produce TiMMCs reinforced with nano-diamond particles. To achieve a good densification, the processing temperature has to be >1000ºC. At this temperature there is reaction between Ti from the matrix and the nano-diamonds (nano-diamond clusters).
- Heat treatment of CPTi matrix does not improve the mechanical properties of this material, as expected.

4.4 Ti-6Al-4V MMCs

As is well known, the titanium alloy Ti6Al4V presents attractive mechanical properties. In specific, e.g. aerospace, applications, because of high requirements for strength and fatigue resistance, the Ti6Al4V alloy is used instead of CP Titanium [2]. The use of this titanium alloy as matrix for the development of new titanium based composites offers an interesting area to be investigated. In this experimental section, the two starting Ti6Al4V powders described in the chapter 3 are employed for the manufacturing of TiMMCs. The reinforcement materials used were just two, the nano/micro boron and the nano-diamonds (ND(1) and NDs(2)). In general, the same fabrication techniques were used for the development of the Ti6Al4V MMCs. The experiments were performed in the same way and under similar parameters as the TiMMCs. Thereby the details of the tests are not extensively explained in this experimental part.

4.4.1 Ti-6Al-4V MMCs with nano/micro Boron

4.4.1.1 Manufacturing process

Similar to TiMMCs reinforced with nano-boron particles, Ti6Al4V-MMCs were also fabricated reinforcing the matrix with the same nano-boron particles. The manufacturing processes of the Ti6Al4V MMCs with nano/micron boron particles used are represented in the next Figure 4-79 and Figure 4-80. Chronologically, the first fabrication of Ti6Al4V-MMCs was carried out via iHP, using different boron contents.

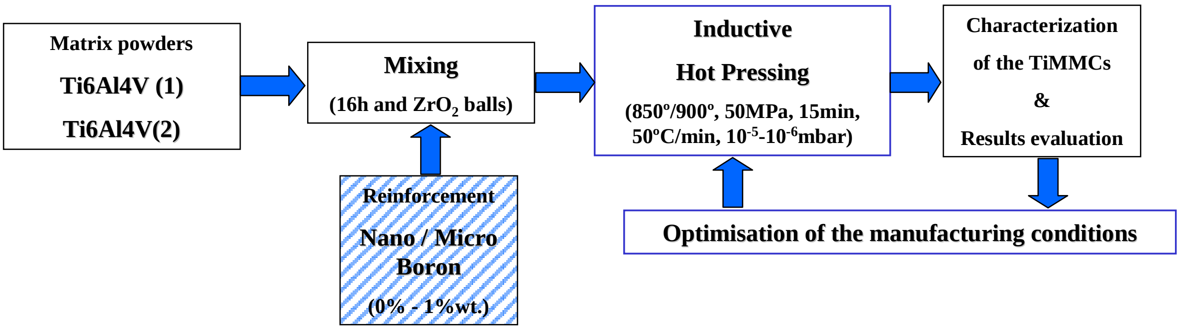

Figure 4-79. Manufacturing flow sheet of the Ti6Al4V matrices reinforced using nano/micro particles of boron (B) via conventional hot pressing (HP).

Afterwards, only hot pressing (HP) was used for the manufacturing process for the Ti6Al4V MMCs with nano/micron boron particles. The same processing conditions for the TiMMCs were used for the Ti6Al4V MMCs. The reason was to compare the influence of the same reinforcement material in different titanium matrices. Because of that, the same parameters and hot pressing conditions were used for the manufacturing of Ti6Al4V-MMCs. Since the starting powders were not fully homogeneous, iHP can be expected to result in less homogeneous materials than HP, esp. for powder (2). The best route from that viewpoint would be CP+S, but this is not recommendable if the boron reinforcement is to be retained as boron

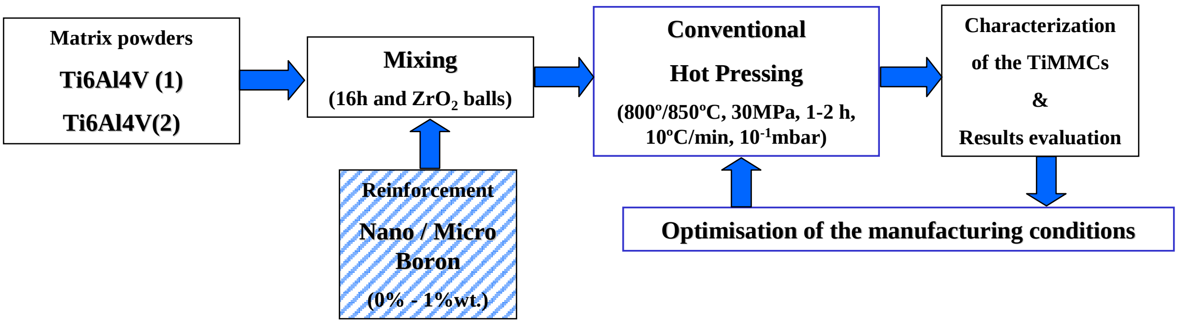

Figure 4-80. Manufacturing flow sheet of the Ti6Al4V matrices reinforced by nano/micro particles of boron (B) and consolidated via inductive hot pressing (iHP).

Powder Preparation

As mentioned before, boron particles were added in several concentrations to each Ti6Al4V matrix powder to fabricate the TiMMCs. These concentrations were shown in the previous Table 4-20. The mixing stage was carried out in the same way as described for the titanium based MMCs. The optimal time of mixing, solvent and ceramic balls employed were also the same.

Hot Compaction Processes

The consolidation of the composites was carried out using the two hot pressing techniques. The procedure was the same as described previously in the previous chapter 2. Moreover, the processing parameters and conditions reported in the next Table 4-48 are similar to the parameters used for the hot consolidation of the TiMMCs from titanium based starting matrix powders.

Table 4-48. Processing parameters of the conventional and inductive Hot Pressing techniques.

Hot pressing technique Ti6Al4V (1) and (2) starting powders	**Processing parameters**					
	Temp. (ºC)	Die size (mm)	Heating rate (K/min)	Holding time (min)	Pressure (MPa)	Vacuum (mbar)
Conventional hot pressing (HP)	850	100 Ø	10	120	30	10^{-1}
	850	13.5x13.5	10	60	30	10^{-1}
	800	13.5x13.5	10	60	30	10^{-1}
Inductive hot pressing (iHP)	900	10 Ø	50	15	50	10^{-5}
	850	10 Ø	50	15	50	10^{-5}

4.4.1.2 Results of the characterisation of the samples and discussions

Density, hardness, chemical analysis and microstructural study were carried out for all the samples. The mechanical properties, flexural and tensile strength were measured in specimens with the specified geometrical dimension (see chapter 2).

4.4.1.2.1 Conventional hot pressing technique (HP)

In the same way as the TiMMCs have been fabricated via HP, the processing parameters and conditions were varied for the Ti6Al4V-MMCs. Also, different geometries of the graphite dies were employed. Smaller samples were produced by the use of a graphite die with twelve square sections (see chapter 2). The density and hardness of all the compacts produced were measured. Furthermore, in several of them the oxygen content was analysed. Using larger graphite dies, additional samples were produced. This means, the mechanical properties, flexural and tensile properties of these Ti6Al4V MMCs could be tested.

Ti6Al4V MMCs hot consolidated at 800ºC and 850ºC for 1h:

- *Density and hardness measurement*

By the first hot consolidation, 12 samples (13.5x13.5x4mm^3) were produced. Figure 4-36 shows the final geometry of the fabricated Ti6Al4V MMCs with different boron contents (see Table 4-20). The processing conditions of the hot consolidation are listed in Table 4-21. The density and average hardness are represented in the following Figure 4-81 .The density of all the specimens was determined by the Archimedes method using paraffin for impregnation.

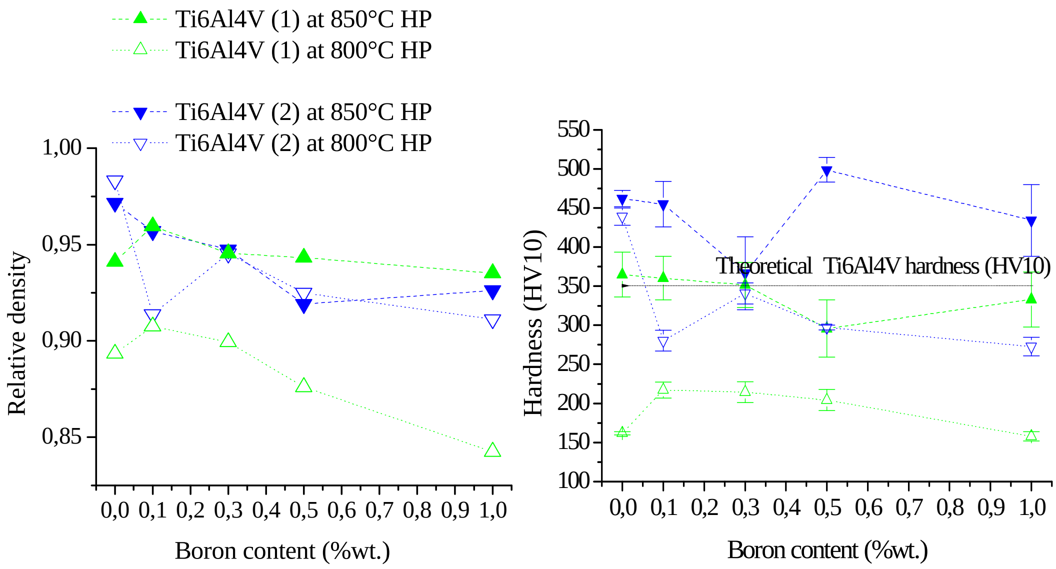

Figure 4-81. Density and hardness of the two types of Ti6Al4V matrices with different boron content (mass%) at two HP temperatures (800º and 850ºC).

As mentioned previously, the specimens consolidated at the same temperature (850°C) can show variation of the mechanical properties using different graphite dies. The powder consolidated in the smaller square suffers more contact with the walls of the die. This could affect the properties significantly. To evaluate it, an additional hardness study was realised, for the Ti6Al4V MMCs specimens produced via HP at 850ºC.

The hardness measurements were done at 17 points in one section of the specimen. Figure 4-82 shows the position of the indentation points on the section of the samples. 15 points were in the longitudinal line, and two more measurements were taken in the transversal direction (direction of the uniaxial pressure). The hardness values of 15 points are represented in the following Figure 4-83.

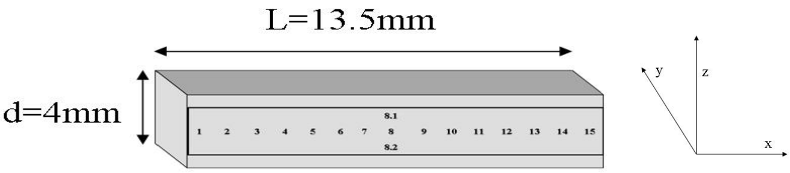

Figure 4-82. Local hardness measurements on the section of the specimens.

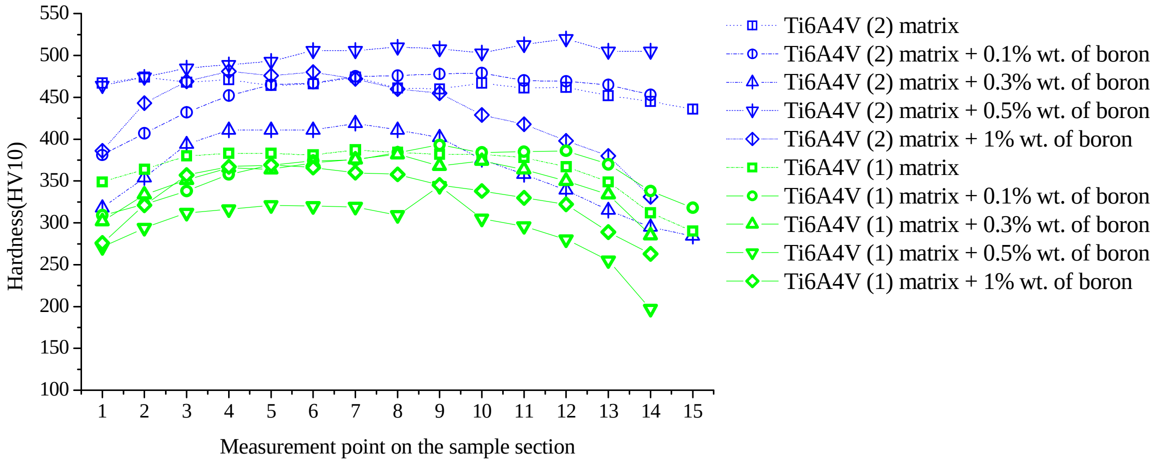

Figure 4-83. Local hardness measurement in the longitudinal direction of the Ti6Al4V MMCs.

The value of hardness on the other two points and the hardness measurement in the central point, for each specimen, are shown in the Figure 4-84.

As the figures show, the hardness of the composites from Ti6Al4V (2) is always higher than the hardness of the composites from Ti6Al4V (1).

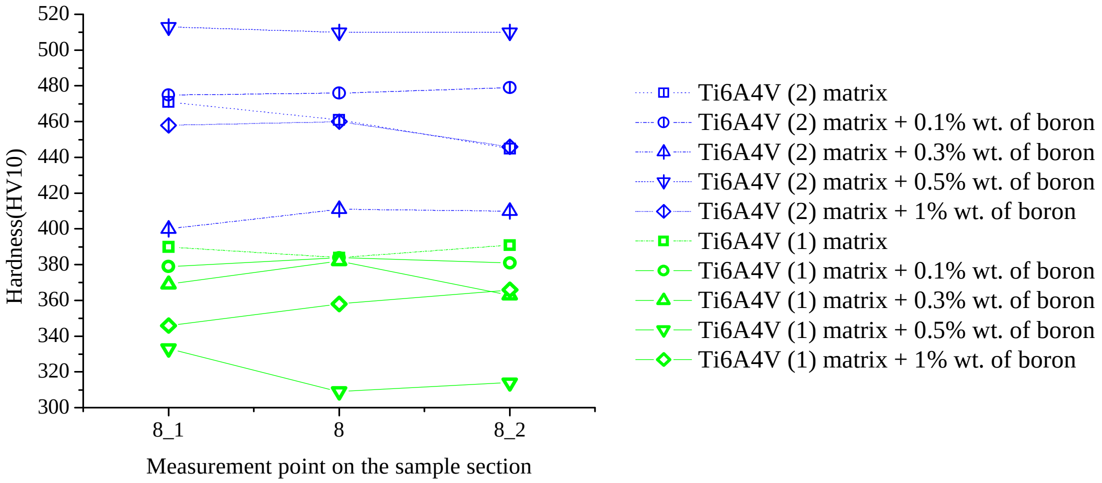

Figure 4-84. Local hardness measurement in the transversal direction (z-axis) for the Ti6Al4V MMCs.

- *Microstructural study*

The microstructures of the pure matrix and the composite with 1 mass% of boron particles is represented in the next Figure 4-85. The morphology of the boron particles is easily recognised. Additionally, some porosity is observed in the composites and matrices hot consolidated at 800ºC (see in Figure 4-85 and Figure 4-86).

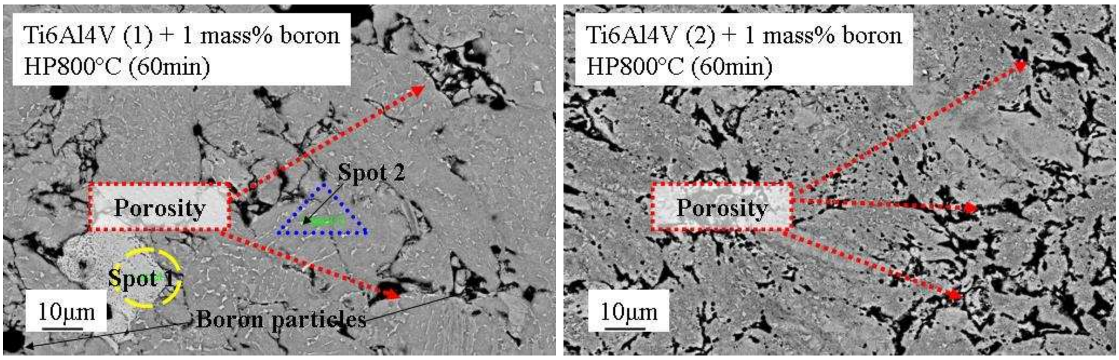

Figure 4-85. SEM images (BSE) of a Ti6Al4V composite from Ti6Al4V(1) (left) and Ti6Al4V(2) (right) powder with 1mass% of boron. HP at 800ºC and 1h.

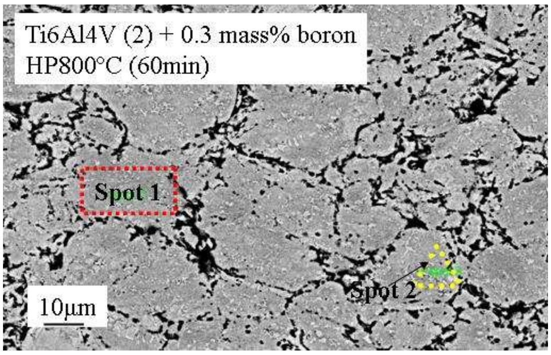

Figure 4-86. SEM image (BSE) of a Ti6Al4V composite from Ti6Al4V(2) powder with 0.3mass% of boron. HP at 800ºC and 1h.

EDAX analysis on the section of several specimens was carried out. Some impurities were observed on the section of specimen from Ti6Al4V(1) matrix powder. These impurities could come from the manufacturing process of the powder in addition to the powder preparation. The results of the EDAX analysis are shown in the next tables.

Table 4-49. EDAX-analysis in two spots on the section of the specimen from Ti6Al4V(1) powder with 1mass% of boron. HP at 800ºC and 1h

Element	**Spot1 (circle)**		**Spot 2 (triangle)**	
	mass%	At%	Mass%	at%
Al	3.69	6.57	6.84	11.57
Sn?	3.51	1.42		
Ca?	0.24	0.29		
Ti	75.48	75.67	87.47	83.34
V	14.51	13.67	5.69	5.10
Cr?	2.57	2.38		

Table 4-50. EDAX-analysis in two spots on the section of the specimen from Ti6Al4V(2) powder with 0.3mass% of boron. HP at 800ºC and 1h.

Element	**Spot1 (rectangular)**		**Spot 2(triangle)**	
	mass%	At%	mass%	at%
Al	11.13	18.22	4.17	7.21
Ti	84.80	78.24	86.96	84.67
V	4.07	3.53	8.87	8.12

This microstructural study verifies the values obtained for the hardness and density previously. The addition of boron particles increases the porosity. Moreover, the difference between both matrices is shown in the following table. The matrix from Ti6Al4V (1) shows the grain size more clearly in comparison to the matrix from Ti6Al4V (2). The temperature positively affects the density of the matrices. In case of the matrix from Ti6Al4V (1) this effect is more pronounced. At lower temperature, the porosity is markedly higher. Furthermore, the same impurities are commonly found for these specimens. The following figure shows a representative comparison of the microstructure of the section of Ti6Al4V-MMCs reinforced with 1 mass% of boron particles. Additionally, the pure Ti6Al4V matrix is compared to the reinforced matrix in order to determine some possible changes in the microstructure due to the boron addition.

HP Temp. (°C)	**Ti6Al4V based matrix**	**Ti6Al4V matrix + 1 mass% of boron particles**
800	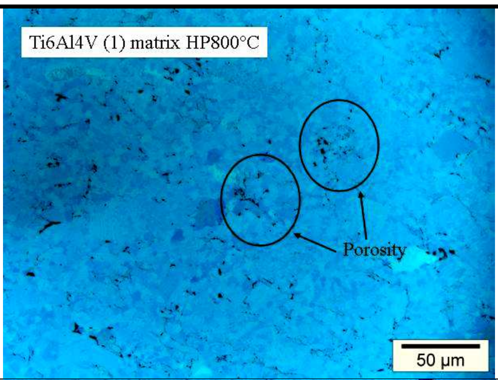	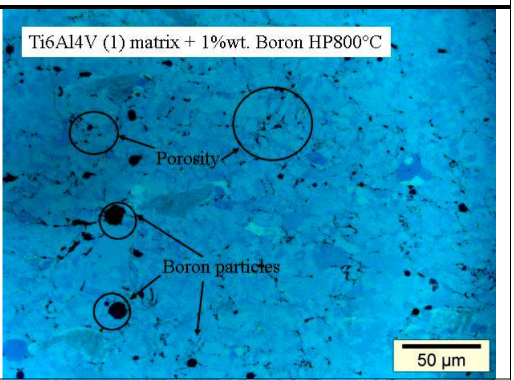
800	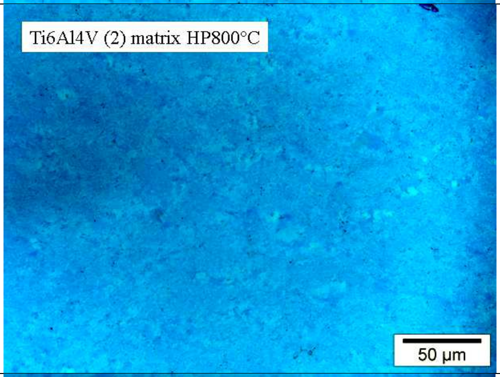	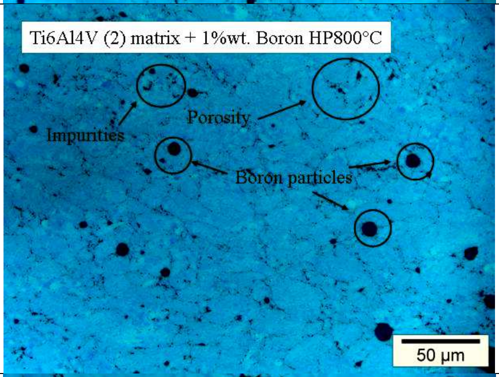
850	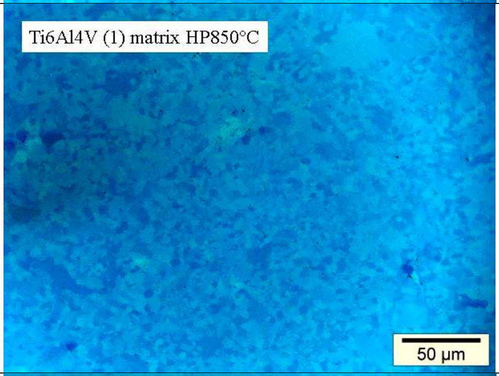	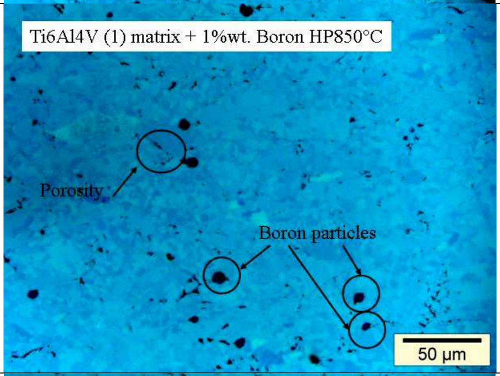
850	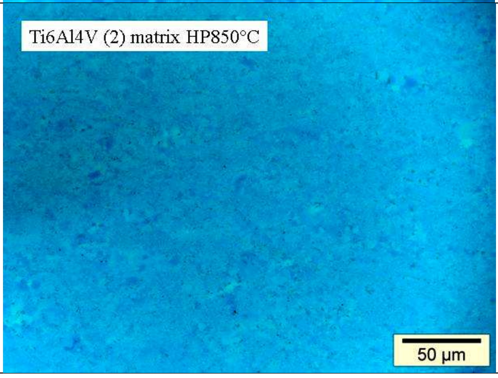	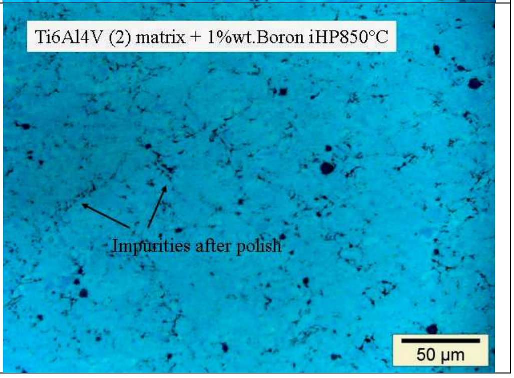

Figure 4-87. Comparison of microstructures of the Ti6Al4V matrices and composites reinforced with 1 mass% of boron produced by hot pressing (HP) at different temperatures (60min holding time and 10 K/min heating rate). . The polarised light microscope was used to take the images of the specimens.

Ti6Al4V MMCs hot consolidated at 850ºC for 2h

For the manufacturing of larger Ti6Al4V MMCs plates, 0.1% and 0.5%wt of boron content was used. The fabrication of these specimens was carried out in the same way than for TiMMCs plates. The same parameters were also tested in addition to the same graphite die (Ø100mm). Also the cutting and preparation of the samples for mechanical properties test were performed in parallel to the TiMMCs.

Concluding, a microstructural study of the composites and the matrices without reinforcement takes place.

- *Density, hardness measurement and chemical analysis*

Firstly the measurement of the density, hardness and the oxygen and nitrogen analysis of the specimens are carried out. The results are reported in the next Table 4-51.

Table 4-51. Density, hardness, oxygen and nitrogen content of the TiMMCs with different boron content (mass%).

Matrix powder boron content (mass%)	**Relative density (%)**	**Hardness (HV10)**	**Oxygen (mass%)**	**Nitrogen (mass%)**	**Carbon (mass%)**	**Sulfur (mass%)**
Ti6Al4V (1)						
0	99	400±3	0.33?	0.008	0.03	0.002
0.1	99	416±7	0.63	0.040		
0.5	98	416±9	0.72	0.063		
Ti6Al4V (2)						
0	99	472±8	0.94	0.016	0.93	0.001
0.1	99	486±12	0.74?	0.019		
0.5	98	501±8	1.01	0.012		

As is seen in the previous table, the highest hardness (501 HV10) value is found for the composite with the highest oxygen content (1.01 mass%). This composite was manufactured from the matrix Ti6Al4V(2) reinforced with 0.5 mass% of boron particles.

Concluding, it may be supposed that the oxygen content from the boron particles affects significantly the properties of the composites; but it is not really proven. There is not a good correlation between boron addition and final oxygen content. Therefore, it is not only the oxygen from boron that has to be considered. Additional oxygen analysis is necessary to evaluate this fact.

- *Mechanical properties measured at room temperature*

The mechanical properties, i.e. tensile and flexural properties, of the Ti6Al4V-MMCs from the starting matrix powder Ti6Al4V(1) and Ti6Al4V(2) were measured at room temperature. The results are listed in Table 4-52.

Table 4-52. Properties of the Ti6Al4V-MMCs with different boron content (mass%) at room temperature.

Matrix Powder	**Flexural tests**			**Tensile tests**		
Boron (mass%)	Flexural Strength (MPa)	E-modulus (GPa)	ε (%)	Tensile strength (MPa)	E-modulus (GPa)	ε (%)
Ti6Al4V (1)						
0	1397±34	106±5	1.6	1084±14	136±3	0.9
0.1	1244±60	106±3	1.5	632±123	111±20	0.6
0.5	1150±63	103±8	1.6	603±68	113±1	0.5
Ti6Al4V (2)						
0	817±80	107±4	1.1	411±43	128±4	0.3
0.1	659±76	107±7	0.8	329±41	132±3	0.2
0.5	610±72	109±3	0.7	291±37	137±5	0.1

- *Mechanical properties at higher temperatures*

The same tensile test equipment as used for the TiMMCs was employed for the Ti6Al4V-MMCs. The same temperatures (20°, 250°C and 450°C) as used for tensile testing of the Ti-MMCs were also used for the Ti6Al4V-MMCs. In order to evaluate the effect of the boron addition on the mechanical properties of the Ti6Al4V composites, the pure matrix material was also tested. Furthermore, before the tensile tests at higher temperature, several specimens of the pure matrix were heat treated. This treatment consisted in annealing the specimens for 2h at 750ºC and cooling in air. The same cooling rate as for titanium specimens was used for the Ti6Al4V samples This heat treatment was also described in the Figure 4-72. The objective of this heat treatment was to observe any variation on the mechanical properties and also microstructure of this titanium alloy samples. The results of the tensile tests performed at three temperatures are shown in the following Table 4-53.

Table 4-53. Tensile properties of the Ti6Al4V-MMCs from Ti6Al4V (1) matrix powder with different boron content (mass%) at three testing temperatures. How many parallel tests?

T. (°C)	**Ti6Al4V (1) after HT**			**Ti6Al4V (1) without HT**			**Ti6Al4V (1) with 0.1% wt. of boron, without HT**			**Ti6Al4V (1) with 0.5% wt. of boron, without HT**		
	UTS (MPa)	ε (%)	E (GPa)	UTS (MPa)	ε (%)	E (GPa)	UTS (MPa)	ε (%)	E (GPa)	UTS (MPa)	ε (%)	E (GPa)
20	952	0.8	133	1084	0.9	136	1084	0.8	111	632	0.6	113
250	n.d.	n.d.	n.d.	766	6.5	n.d.	811	6	n.d.	837	6.7	n.d.
450	532	7.7	n.d.	525	5.8	n.d.	586	7	n.d.	671	8.8	n.d.

HT: heat treatment. It was previously described: heating rate 10K/min; at 750ºC during. 2h and cool in air (approx. 30K/min)

UTS: ultimate tensile strength (MPa)

ε.: Elongation (%)

E.: E-modulus (GPa)

Compared to the elongation of TiMMCs from CPTi(2) matrix with the same boron content (see in Table 4-20) the specimens from the Ti6Al4V(1) do not exhibit any visible elongation after the tensile test at 250ºC (see in Figure 4-88). However, measurement at 450ºC shows that the deformation of the specimens increases considerably from 0.6% at room temperature to 8.8% at 450ºC.

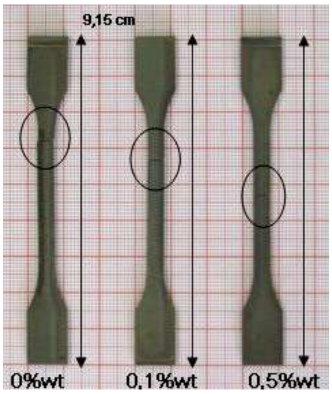

Figure 4-88. TiMMCs from Ti6Al4V powder with different boron content after tensile test at 250°C

A comparison of the deformation after the tensile test of the matrices from Ti6Al4V (1) without reinforcement, is shown in the next Figure 4-89. Also the heat treated matrices are shown after the tensile tests. The heat treatment (H.T.) that was previously mentioned implies 10 K/min up to 750°C, 2h holding time and cooling in air (30K/min).

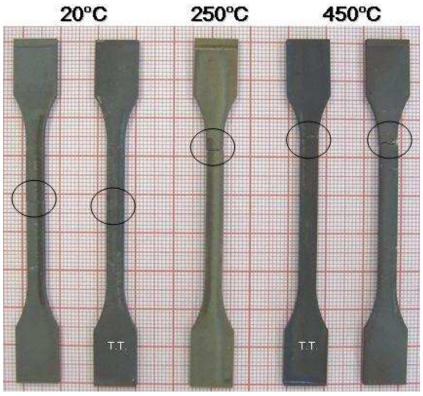

Figure 4-89. Deformation of the pure matrix from titanium alloy (Ti6Al4V (1)) after tensile tests at different temperatures (20º, 250º and 450ºC). TT: Matrix heat treated.

- *Fractographic study*

In Figure 4-90 a boron particle can be clearly seen in the metal matrix. It shows that there is no reaction between the boron particle and the metal matrix. Some porosity is also present around the boron particles.

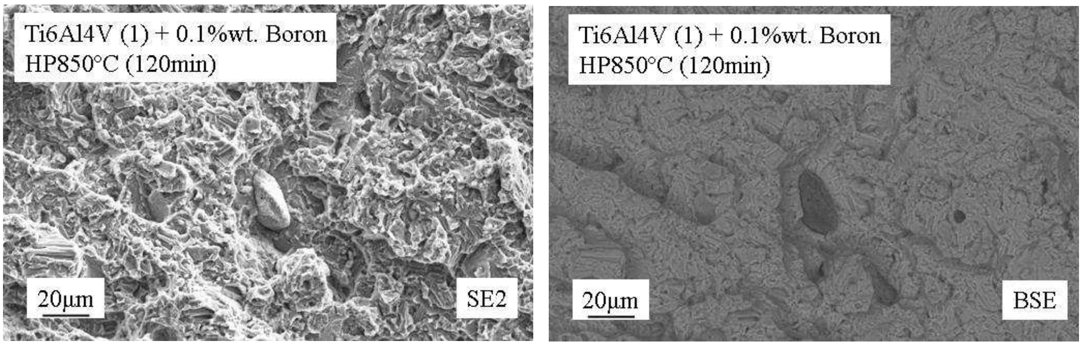

Figure 4-90. Fracture surface of the composite from Ti6Al4V (1) matrix with 0.1 mass% of boron particles. Difference between both images: left by SE and right by BSE detector.

4.4.1.2.2 Inductive hot pressing technique (iHP):

The characterisation of the samples involved the measurement of the density, the hardness and oxygen analysis. Moreover, the microstructural study of several Ti6Al4V-MMCs was carried out.

Ti6Al4V-MMCs inductive hot consolidated at 850ºC and 900º for 15min.

The same temperatures tested for TiMMCs, 850º and 900ºC, were used for the inductive hot consolidation of the Ti6Al4V-MMCs.

The four boron contents used for the reinforced titanium based matrices are listed in the Table 4-21.

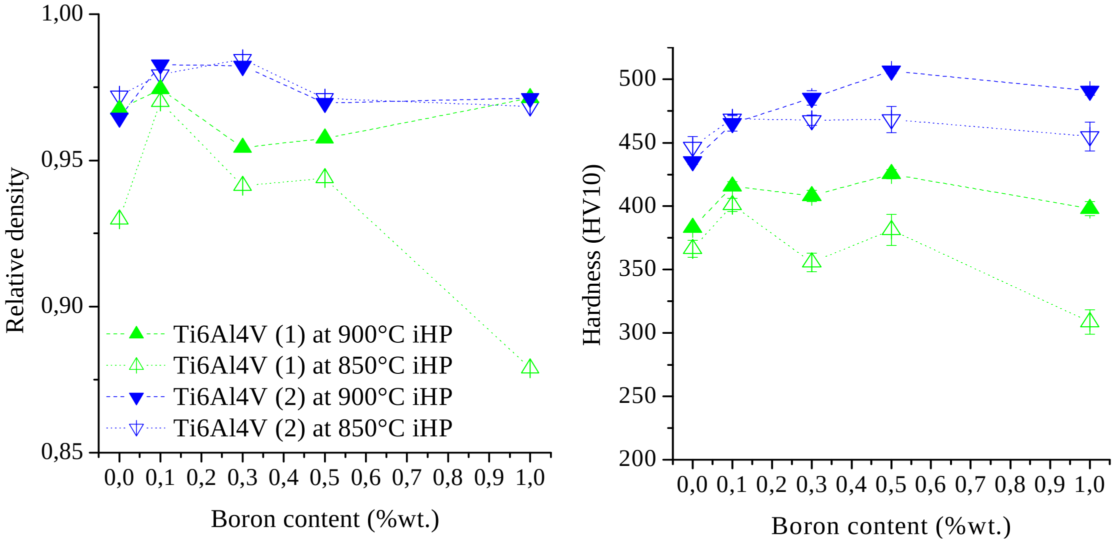

Figure 4-91. Relative density and hardness of the Ti6Al4V composites vs. the boron content (mass%). The specimens were hot consolidated via iHP at two temperatures.

Chemical analyses of several specimens were realised.

The increasing of the oxygen content with the addition of the nano/micro boron particles was evaluated. The nitrogen content was also analysed simultaneously. The results of these chemical analyses are presented in the following Table 4-54.

Table 4-54. Oxygen content of Ti6Al4V-MMCs produced via iHP at 850° and 900°C with different boron content.

Matrix powder	iHP Temp.(°C)	Boron (mass%)	O (mass%)	N (mass%)
Ti6Al4V (1)	850	0	0.3?	0.006
		1	0.79	0.024
Ti6Al4V (2)		0	0.66	0.016
		1	1.46	0.020
Ti6Al4V (1)	900	0	0.66	0.013
		0.1	0.84	0.014
		1	0.45?	0.005
Ti6Al4V (2)		0	1.19?	0.023
		0.1	1.850	0.039
		1	1.200	0.014

Microstructural study

The study of the microstructure of the composites from Ti6Al4V powders was carried out. In the next figure, SEM image (BSE) of a section of Ti6Al4V(1) matrix without reinforcement is showed. Additionally, the results of EDAX-analysis in different four spots are illustrated the next figure.

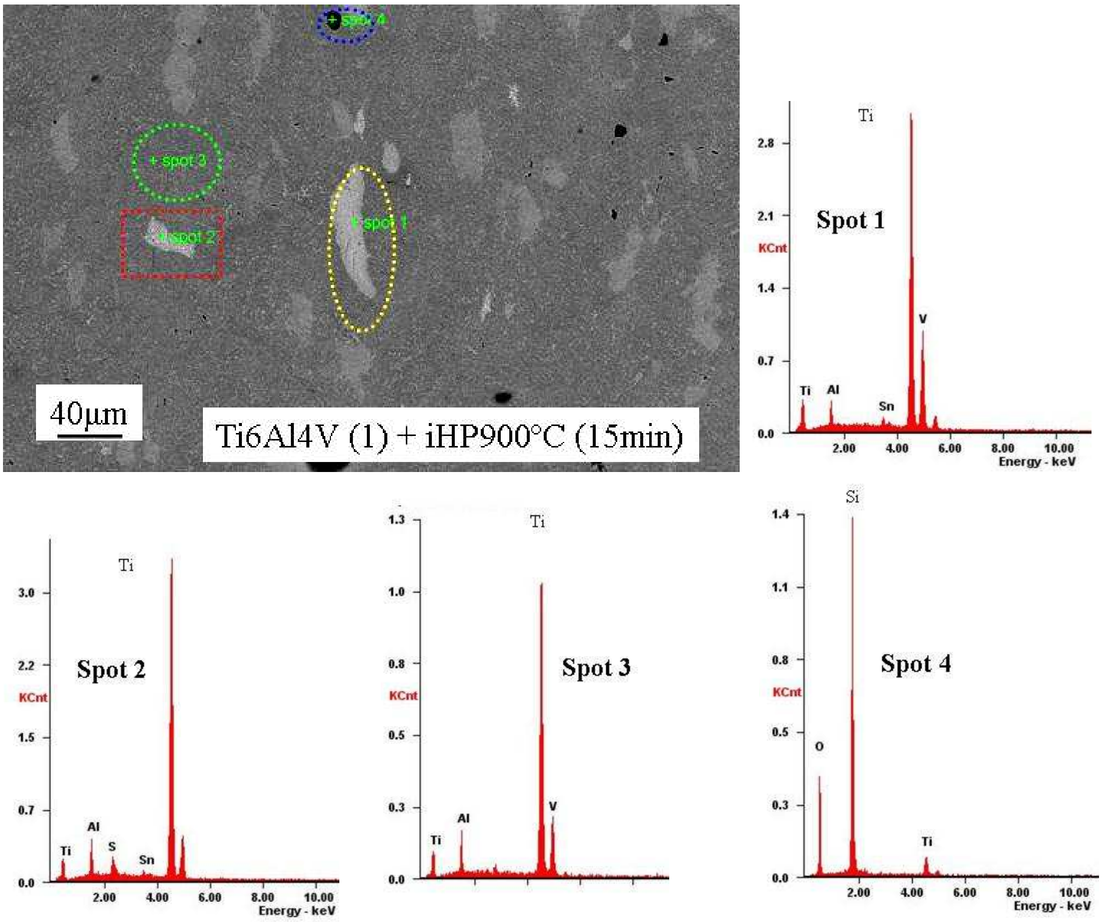

Figure 4-92. SEM-image (BSE) and EDAX-analysis in different spots marked in the previous of boron particles in a Ti6Al4V-matrix (from Ti6Al4V (1) powder) produced through inductive hot pressing at 950°C during 15min.

The spot 1 (yellow) and spot 2 (red) show several impurities from the starting powder. Also, in these two points there are Vanadium enriched areas.

There is some contamination of Sn. The impurity particle from the metallographic preparation is observed in the spot 4 (blue). The spot 3 shows main component of the Ti6Al4V alloy.

Moreover, an SEM image of a matrix from Ti6Al4V(1) reinforced with 1 mass% is illustrated in the next figure. The same impurities are observed in addition to the dispersion into the matrix of the boron particles. After iHP consolidation at 950ºC for 15min lower porosity. The black regions observed are the boron particles.

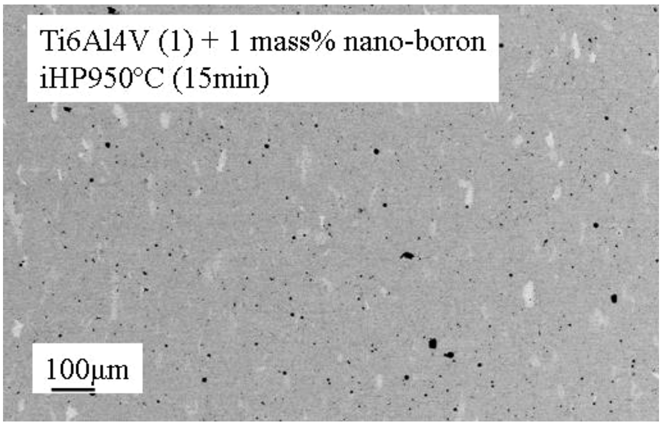

Figure 4-93. SEM image (BSE) of boron particles in a Ti6Al4V-matrix (from Ti6Al4V (1) powder) produced through inductive hot pressing at 950°C during 15min.

Intermediate Conclusion

- The compacts from Ti6Al4V(1) matrix powder present lower oxygen content, however some impurities are observed in the final composites.
- The boron reinforcement contributes to increase the oxygen in the composites. It is clearly observed from the mechanical tests.
- The adequate dispersion of the nano-diamond particles is achieved.
- There is decrease of the densification of the Ti6Al4V-MMCs at higher boron concentration.
- The addition of boron particles promotes inter-granular fractures, decreasing the ductility of the composite.

4.4.2 Nano diamond particles (NDs)

4.4.2.1 Manufacturing of the samples

At the beginning, the fabrication of the Ti6Al4V composites reinforced with nano diamond particles was carried out using two types of Ti6Al4V powder from different suppliers. The first manufacturing process used for the Ti6Al4V was inductive hot pressing.

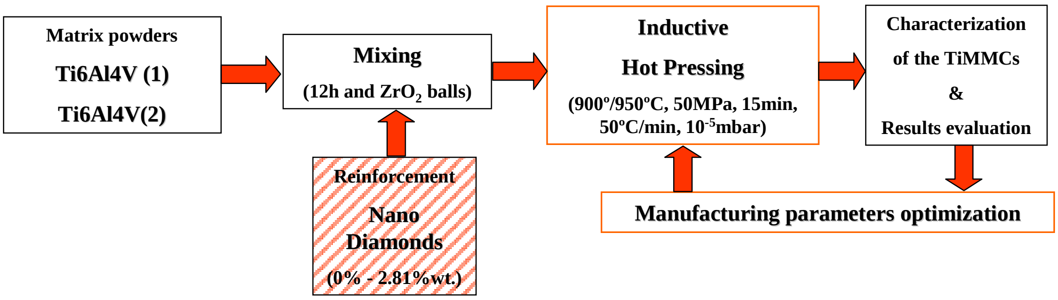

Figure 4-94. Manufacturing flow sheet for inductive hot pressing of the Ti6Al4V matrices reinforced using nano diamond particles (NDs(1)) (iHP).

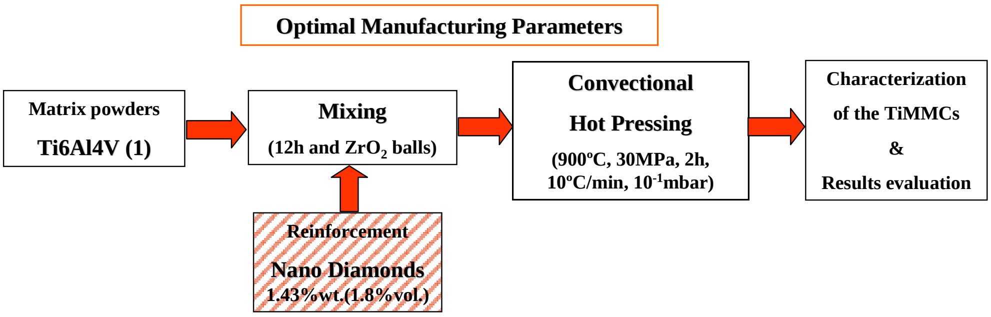

Figure 4-95. Manufacturing flow sheet for hot pressing (HP) of the Ti6Al4V matrices reinforced using nano diamond particles (NDs(2))

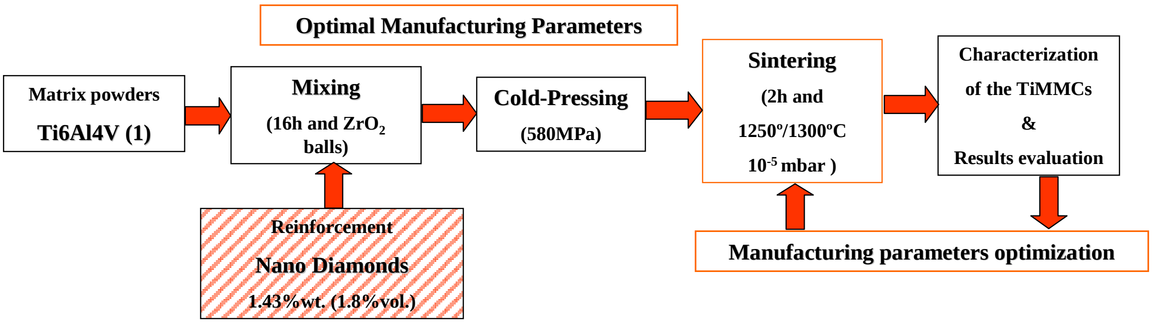

Figure 4-96. Manufacturing flow sheet for cold pressing and sintering of the Ti6Al4V matrices reinforced using nano diamond particles (NDs(2)).

4.4.2.2 Characterisation of the samples

4.4.2.2.1 Inductive hot pressing technique (HP)

- *Density, hardness and oxygen analysis*

Archimedes method was used to measure the density of the Ti6Al4V-MMCs in water using the water-stop spray. Hardness measurement and several oxygen analyses were done. The results of these measurements are represented in the following Figure 4-97 and Table 4-55.

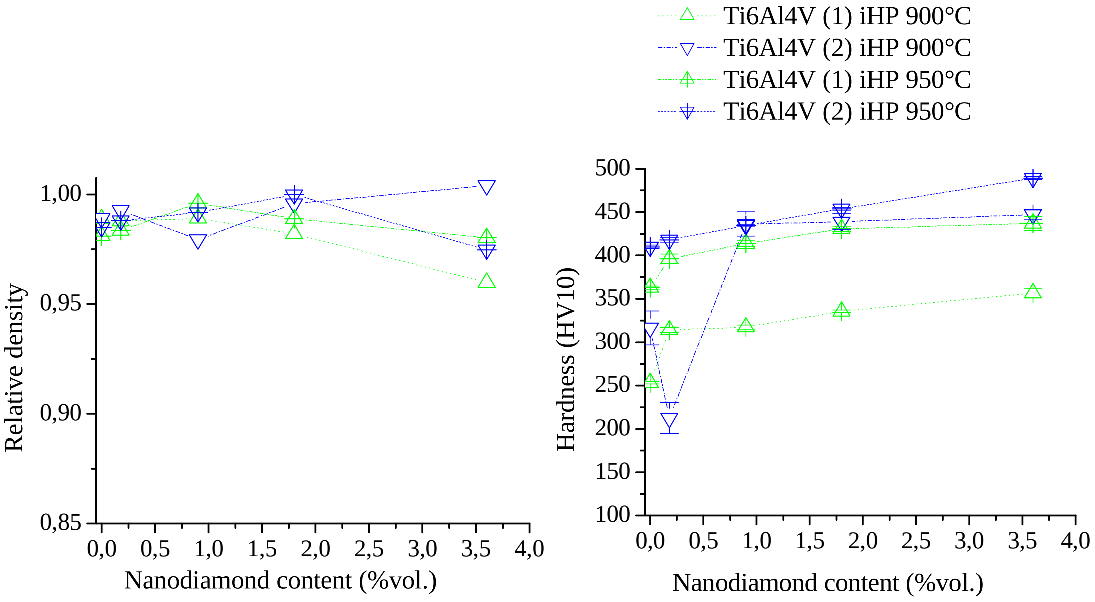

Figure 4-97. Relative density and hardness (HV10) of the Ti6Al4V-MMCs produced after iHP (in high vacuum 10^{-5}mbar at 50MPa) vs. nanodiamond content.

The oxygen contents of both titanium based matrices (from Ti6Al4V(1) and Ti6Al4V (2) powders) compacted at 900° and 950°C are listed in the Table 4-55. Moreover, the oxygen content of the Ti6Al4V-MMCs, produced with 3.6%vol. of NDs at the same temperatures, was measured and reported.

Table 4-55. Oxygen content of Ti6Al4V-MMCs produced via iHP at 900° and 950°C with a nano diamond particle content of 3.6% vol. Theoretical density of NDs 3.52g/cm^3.

Matrix powder	iHP Temp.(°C)	NDs (%vol.)	Arch. density (g/cm^3)	Hardness (HV10)	Oxygen (mass%)
Ti6Al4V(1)	900°	0	4.40	372	0.448
		3.6	4.24	384	0.791
Ti6Al4V(2)		0	4.40	417	0.718
		3.6	4.43	481	0.971

Ti6Al4V(1)	950°	0	4.37	367	0.505
		3.6	4.33	437	0.599
Ti6Al4V(2)		0	4.38	410	0.652
		3.6	4.31	489	0.906

- *Microstructural study*

The study of the matrices shows difference between the specimen from the Ti6Al4V (1) matrix and Ti6Al4V (2). Some impurities are observed on the surface of the specimens. In the matrix from Ti6Al4V (1) powder, by the use of the BSE detector, the different phases can be identified the light grey phase being the phase with the elements of high density (Vanadium).

In case of the composite from Ti6Al4V (2) powder this dark and light phases are not easy to recognize. In this powder (2), Al enriched areas would be expected, but there are not observed.

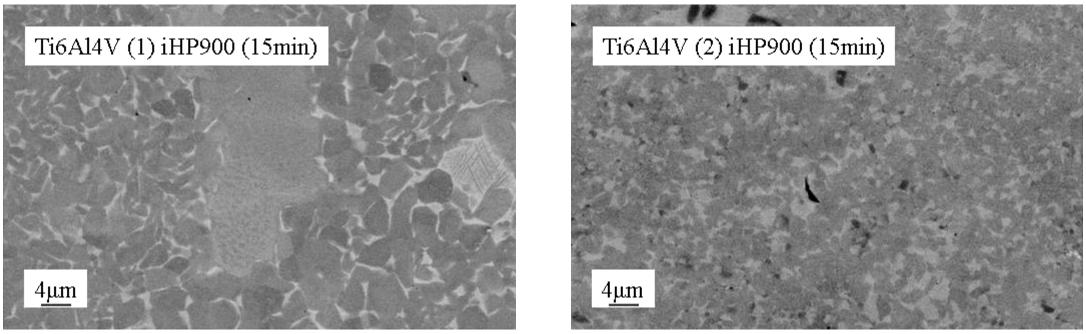

Figure 4-98. SEM images (BSE) of the microstructure of the different Ti6Al4V matrices without reinforcement, consolidated via iHP at 900°C during 15min.

Also the influence of the nano diamonds particles on the microstructure of the composite is evaluated (see in Figure 4-99)

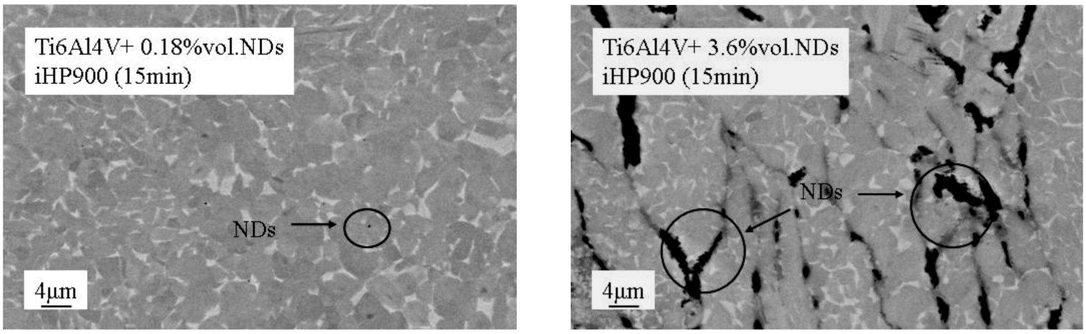

Figure 4-99. SEM images (BSE) of the microstructure of the different Ti6Al4V MMCs with the lowest and higher reinforcement concentrations (0.18%vol. and 3.6%vol.) consolidated via iHP at 900°C during 15min.

The addition to the nano diamond particles affects the density slightly. However the value of the hardness increases significantly.

One possible reason for that could be the formation of TiC, because of the reaction between the titanium from the matrix and the nano carbonaceous reinforcement.

The phenomenon of the particle boundary decoration is observed for 3.6 %vol. of NDs in the metal matrix.

This effect of the particle boundary decoration causes the decrease of the mechanical properties. For that reason the selection of finer starting matrix powder is very important, although this would result in higher oxygen levels.

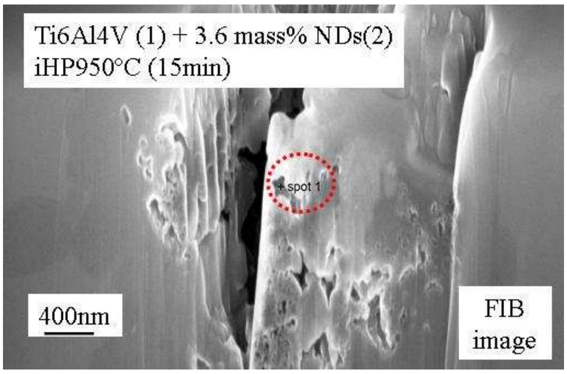

Element	mass %	at %
C	11.97	32.95
O	4.41	9.11
Ga?	2.78	1.32
Al	1.64	2.01
Ti	77.71	53.65
V	1.50	0.97

Figure 4-100. (left) SEM imagen from a FIB section of Ti6Al4V-MMCs reinforced with 3.6%vol. of nano-diamonds (iHP at 950º for 15min). (right) EDAX-analysis in the spot 1 on the section of the composite (Ti6Al4V(1) with3.6m%vol. of NDs(2)).

4.4.2.2.2 Cold pressing and sintering at 1250° and 1300°C

The dimension (approx.) of the samples after the sintering at 1250º and 1300º was cross section of 55 x 6.4 mm^2 (section of the rectangular die) and height 3.5mm (approx. the filling high of the rectangular die).

Firstly, the Archimedes density and hardness of the specimens was determined and compared at the two temperatures (1250º and 1300ºC). Afterwards, their mechanical properties (flexural tests) and oxygen content were measured.

- *Density and hardness measurement and mechanical properties*

The average values of density and hardness of the Ti6Al4V MMCs cold compacted at 560 MPa and sintered at two temperatures (1250° and 1300°C) are presented in Figure 4-101. The same die size as used for the cold pressing of titanium matrix reinforced with NDs (1.8vol%) was employed to produce the Ti6Al4V-MMCs at a NDs content of 1.8vol%). Therefore, the samples produced were suitable for flexural tests. The average values are presented in the next Table 4-56

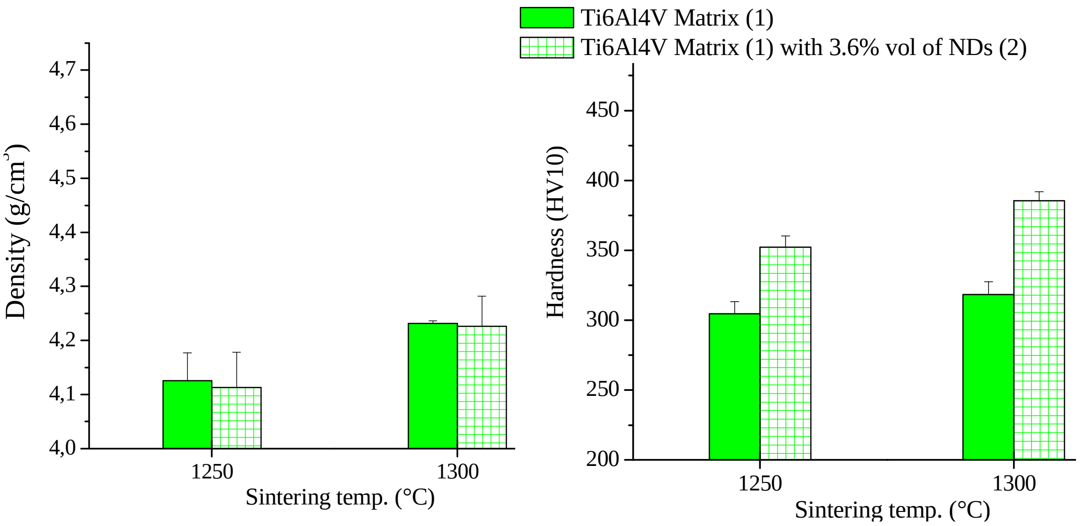

Figure 4-101. Average values of Arch. density and hardness of the Ti6Al4VMMCs cold compacted at 560MPa and sintered at two temperatures (1250º & 1300ºC).

Table 4-56. Flexural properties of the Ti6Al4V-MMCs with 1.8% vol. of NDs, cold compacted at 560MPa and sintered at two temperatures (1250° and 1300°) for 2h.

Starting Powders	T.(°C)	Flexural strength (MPa)	ε (%)	Arch. Density (g/cm^3)	Hardness (HV10)
Ti6Al4V	1250	392±147	0.9	4.13	305
Ti6Al4V+ND	1250	860±168	1.2	4.11	352
Ti6Al4V	1300	1383±153	2.3	4.23	318
Ti6Al4V+HT	1300	927±75	1.8	n.d.	n.d.
Ti6Al4V+ND	1300	856±194	0.80	4.23	386

HT: Heat treatment

Table 4-57. Properties and oxygen content of titanium specimens and Ti6Al4VMMCs with 1.8 vol% of NDs(2) particles, compacted at 560 MPa and sintered at two temperatures.

Starting Powders	T (°C)	Flexural strength (MPa)	ε (%)	Arch. density (g/cm^3)	Th. density (g/cm^3)	Relative density (%)	Hardness (HV10) ± std.	Oxygen (%wt)
Ti6Al4V	1250	341	0.6	4.14	4.45	93	296±12	0.71
Ti6Al4V+ND	1250	758	1.3	4.19	4.43	95	364±7	0.63
Ti6Al4V	1300	1585	1.9	4.23	4.45	95	318±20	0.56
Ti6Al4V+HT	1300	892	1.6	4.45	4.45	100	293±1	0.80
Ti6Al4V+ND	1300	631	1.1	4.21	4.43	95	387±3	0.60

- *Microstructural study*

In the Figure 4-102 the different microstructures of the matrices with and without reinforcement are shown.

At both temperatures (1250° and 1300ºC) some porosity is detected in the matrices without nano-diamonds.

However, this porosity is not observed for the composite sintered at 1300ºC

Moreover, the reaction between the titanium from the matrix and the reinforcement is evident after the sintering of the composites for both temperatures. It confirms the increase of the hardness with the addition of nano reinforcement.

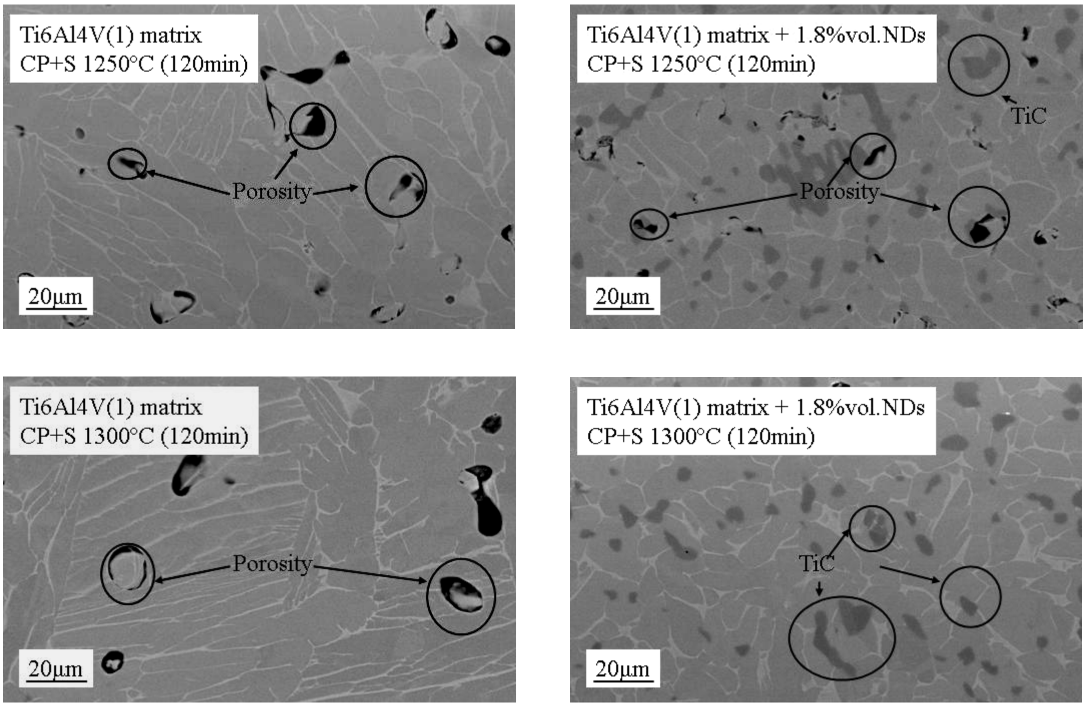

Figure 4-102. Microstructure (SEM images BSE) of the Ti6Al4V (1) pure matrices and MMC reinforced with 1.8 vol% of nanodiamond particles after sintering at two different temperatures, 1250° and 1300ºC. Similar microstructures are shown in the literature, e.g. Leyens-Peters p.15

4.4.2.2.3 Hot pressing technique (HP)

The larger plate of Ti6Al4V matrix with and without nanodiamond particles was hot pressed.

The NDs(2) content was 1.8 vol%. The relative density (%) and hardness (HV10) of the Ti6Al4V matrix and the Ti6Al4V matrix reinforced using 1.8vol% of NDs(2), fabricated via HP at 900°C for 2h, are shown in the following Table 4-47. The results of the flexural tests (see chapter 4.) in addition to the oxygen and nitrogen content of the specimens were also listed in this Table 4-58.

Table 4-58. Properties of a Ti6Al4V-MMCs fabricated via HP at 900°C for 2h. The matrix powder was Ti6Al4V (1) and the reinforcement concentration was 1.8 vol%. of NDs (2) particles.

Starting Powders	Archimedes density (g/cm^3)	Rel. density (%)	Hardness (HV10)	Flexural strength (MPa)	ε (%)	Oxygen (mass%)	Nitrogen (mass%)
Ti6Al4V (1)	4.42	99	394±4	1042±83	1.9±0.3	0.56±0.05	0.079±0.040
Ti6Al4V (1) +NDs(2)	4.43	100	451±1	717±77	1.9±1	0.51±0.01	0.042±0.028

- *Microstructural study*

In the following Figure 4-103 the microstructure of the composite produced after hot consolidation for 2h at 900ºC is shown. Some porosity is observed as well as impurities from the metallographic preparation. The distribution of the nanodiamond particles in the matrix could be slightly seen around the grain boundaries.

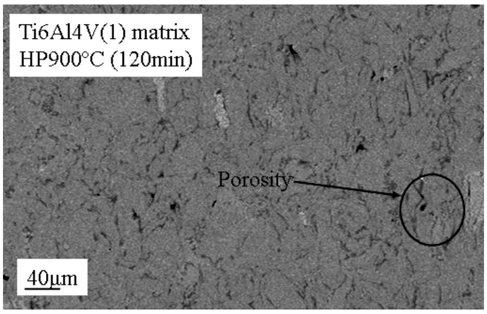

Figure 4-103. SEM image (BSE) of the composite from Ti6Al4V (1) with 1.8 vol% of NDs produced by conventional hot pressing for 2h at 900ºC.

Intermediate Conclusion

- Ti6Al4V(1) powder has lower oxygen content than Ti6Al4V(2) starting powder.
- Depending on the type of nano-diamonds, the oxygen content in the final composite can be increased or not. NDs(1) presents higher oxygen content of oxygen than NDs(2).
- Finer starting matrix powder can reduce the effect of the particle boundary decoration. This effect causes decrease of the mechanical properties.
- By increasing the sintering temperature, the densification of the composites is better.
- To produce Ti6Al4V-diamond composites, the CP+S process is not recommendable because of the reaction between Ti+C. For manufacturing of TiC reinforced composites, cheaper C sources than nano-diamonds are available.

5 Summary

In this chapter 5, the discussions of the results of this work are summarised. An overview of the most interesting results is also given and commented in this chapter. Additionally, open questions are summarised.

This chapter is describing the different factors that have impact on the properties of the composites. These factors are the starting material used (type of the matrix powder and type of reinforcement material) and the consolidation technique employed (type of manufacturing process, parameters tested and pressing dies used for the consolidation). As studied before, all of them present some influence on the specimens produced (on the microstructure and mechanical properties).

Ending this chapter 5, the main achievements of this work are summarised.

5.1 Influence of the starting materials

The starting material has an important influence on the final properties of the composites produced. The quality of the raw material (oxygen, nitrogen, impurity level, etc.) and also the reinforcement for the metal matrix play an important role. For that reason, sound characterisation of all the starting materials had to be performed.

The selection of the most suitable starting powder depends on the desired final properties of the composite material. This is related to the final application of the composite material.

5.1.1 Influence of the matrix powders

In order to obtain composite materials with low oxygen content and outstanding properties, the search and testing of different material powders (CPTi, TiH_2 and Ti6Al4V) as matrix powder are considered as important tasks at the beginning of this work.

CPTi and TiH_2 powders are used as starting powders to produce the plain titanium matrices. Previous studies show TiH_2 powder as an interesting alternative to produce titanium compacts [84, 85]. For that reason, four TiH_2 powders from different suppliers have been tested as matrix powders in addition to two CPTi powders.

Beginning the experimental work, the conventional cold pressing and sintering process is used for the manufacturing of pure titanium matrices from the six different titanium based powders. Changes of the mechanical pressure for the cold compaction and sintering parameters (temperature and time) allow the comparison and study of the behaviour of the powders. The development of this experimental part is performed in order to find the most suitable matrix powders (one of each type of material powder, CPTi and TiH_2) for the fabrication of the TiMMCs.

The TiH_2(6) is the starting powder with the highest oxygen content (1.47 mass%) and has also the lowest particle size (mean diameter 7 µm). This powder was used to determine an optimum sintering assembly that can prevent the increase (or possibly even lower) the oxygen content in the final titanium specimens. Because of its high oxygen content, this TiH_2(6) is used only for this first task.

By the use of matrix powders with lower particle size (such as TiH_2(5)), the densification observed in the microstructure (see in Figure 4-17) is better than for the coarser matrix powders. Nevertheless, the content of oxygen in the compacted specimens is higher, as a result of the larger specific surface area.

Considering the results of the characterisation of the starting powders and the sintered titanium specimens, the decision was to use CPTi(2) and TiH_2(4) as the two most promising powders for subsequent experiments.

The values of hardness (HV10) and oxygen content for these two powders are close to the theoretical ones (CPTi grade 4). In the next Figure 4-12, the lowest oxygen content is seen for the compacts made from powder CPTi(2). Comparing the specimens made from TiH_2 powder, the titanium compacts from TiH_2(4) presents a hardness and oxygen content close to the theoretical values for the CPTi grade 4. It was decided to use the CPTi(2) and TiH_2(4) powders as matrix powder for the manufacturing of the TiMMCs.

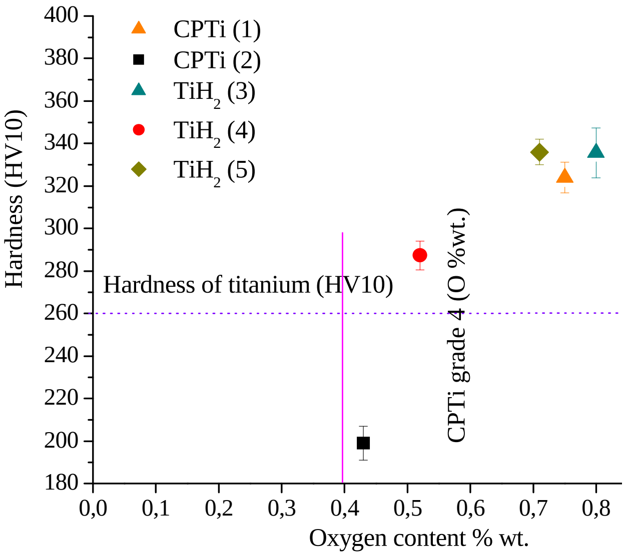

Figure 4-12. Hardness (HV10) vs. oxygen content of the five titanium specimens compacted at 380 MPa and sintered for 1h at 1300°C in high vacuum. Hardness (HV10) and density (g/cm³) values for CPTi are taken from the literature ([3]

One specific phenomenon observed for the TiH_2 starting powders, and the green and sintered compacts made from these powders, is the variation of oxygen content in the different states (powder, green compact, sintered sample). There is a significant increase from the starting powder to the green compact (from TiH_2(4) starting powder 0.67

mass% to 1.30 mass% of the green compacts). Then, a reduction of this high oxygen content is observed for the sintered specimens (for TiH_2(4) as starting powder from 1.30 mass% in the green compacts to 0.52 mass% in the sintered specimen). This phenomenon could be related to the handling of the powders.

The use of excessive paraffin as lubricant (die wall lubrication with paraffin has been applied) for the cold compaction increased the oxygen content of the green compacts, but apparently the paraffin residues are then removed during sintering.. There is an important “Open Question” how this effect occurs in detail, but it is not of practical relevance.

Higher content of nitrogen in the starting powder (i.e. 0.1mass% for TiH_2(4)) affects considerably the final properties, hardness, mechanical properties and microstructure of the titanium specimens.

The influence of this high nitrogen in addition to residual hydrogen in specimens from TiH_2(4) powder contributes to the formation of needle-like Widmanstätten microstructure. Therefore, manufacturing of titanium composites (TiMMCs) from TiH_2 involves the production of a TiMMC with higher hardness than the TiMMCs from CPTi powder.

In the study of the titanium based matrices (produced via iHP), the microstructure of the matrices from TiH_2 (4) is similar to a martensitic microstructure (iHP in the range from 800º to 1050ºC for 15min). That microstructure can possibly explain the higher hardness values of these composites.

The oxygen content for the Ti6Al4V powder types (Ti6Al4V(1) and Ti6Al4V(2)) is very similar (0.5 mass%). However, oxygen analysis shows the higher oxygen content for the composites from Ti6Al4V(2). Probably because of its smaller particle size, the Ti6Al4V(2) powder is more sensitive to oxygen during subsequent processing.

Consequently, the higher oxygen level affects directly the mechanical properties of the composites produced from this grade of matrix powder, i.e, lower mechanical performance.

In summary, it is important to carry out a good selection of the adequate raw material since the sintering behaviour and properties are affected by impurities (e.g. oxygen, nitrogen, and hydrogen, particle size). Concluding, in order to produce TiMMCs the CPTi(2) powder is the most appropriate grade, and also the Ti6Al4V(1) powder to fabricate Ti6Al4V-MMCs.

Recommendation: In further works with titanium and its alloy as powder materials, low levels of nitrogen and oxygen should be used. The employig of TiH_2 powder for the manufacturing of TiMMCs is not recommendable because some residual hydrogen causes worse mechanical properties; also the higher nitrogen levels are detrimental.

Additionally, the use of finer starting powder could avoid the effect of the particle boundary decoration (principally observed for nano-diamonds particles). This effect causes decrease of the mechanical properties since reinforcing phases that are not evenly distributed but concentrated at the former particle boundaries do not strengthen but in fact weaken the material.

5.1.2 Effects of TiB_2 and boron particles on the properties of the titanium based composites

TiB_2 reinforcement

Only the two most promising commercial titanium and TiH_2 powders are used here as matrices reinforced by the addition of TiB_2 particles.

These composites are fabricated via cold pressing at 560 MPa and sintered during 2h at 1300ºC. For the sintering, the optimal sintering assembly is employed.

By the addition of TiB_2 and boron particles, an improvement of the hardness is observed up to a determined concentration (10 mass%). Below this content the behaviour of the composite is better in that respect (high densification and hardness). For contents >10 mass% of the reinforcement the hardness of the composite decreases considerably, mainly as a result of a reduced densification.

The characterisation of this type of reinforcement shows that this powder presents high oxygen content (2.3 mass%).Thus at higher content of TiB_2 (20 mass%), the oxygen content of the composite is significant higher (1.35 mass% for the composite made from CPTi(2) and 1.40 mass% for the composite made from TiH_2). Thus, the addition of TiB_2 particles might be supposed to cause the incorporation of additional oxygen into the titanium based matrix and is also related to lower densification (this is observed on the microstructure of the composites). As a consequence of this low densification, the hardness of this type of composites is decreased.

Nano-Boron particle reinforcement

The manufacturing of the composite reinforced by nano-boron particles is done for the matrices from CPTi(2) and TiH_2, but also using the Ti6Al4V(1) and Ti6Al4V(2) starting matrix powder. The nano-boron particles are used as reinforcement material in order to improve the mechanical properties of the titanium based matrices. The quality of the nano-boron powder ordered here is not satisfactory to carried out the manufacturing of the TiMMCs and Ti6Al4V-MMCs. The larger particle size (in fact micro-powder in state of nano-powder) and higher oxygen content have a marked impact on the final properties of the composite materials. The final results show that the addition of this type of boron particle (micro-particles in state of nano-boron particle), even using lower concentration (0.1 and 0.5 mass%), does not improve the properties of the final specimens. It is far away from the objective of this work.

The main idea for this low content is to obtain a material with significantly improved mechanical properties, being able to be forged (hot deformed) at the same time.

In the TiMMCs from CPTi(2) powder, the optimal boron content is 0.1 mass% The hardness at this concentration increases for the composites produced via HP (at 800º and 850ºC) and via inductive hot pressing (850º, 900º and 950º). However this does not happen in the case of TiMMCs produced from TiH_2(4) powder via iHP (850º and 900º). At 0.1 mass%, these TiMMCs present an inexplicable decrease of the hardness. This behaviour is not clear until now. The behaviour of the composite from Ti6Al4V is in general similar to the TiMMCs from CPTi(2) matrix (the hardness increases with the boron particles addition).

On the other side, a similar increase of the hardness is qualitatively observed for all the TiMMCs produced by HP and iHP (at 950ºC) from TiH_2(4) powder and CPTi(2).

The oxygen content of this boron powder is quite high, probably because of the formation of boric oxides at the surfaces. Consequently, additional oxygen is added to the titanium base. The influence of this higher oxygen content is seen on the final mechanical properties of these composites.

In the smaller specimens produced (by HP at 800º and 850ºC and iHP at 850º and 900ºC), the higher hardness values even at low density can be a consequence of this higher oxygen content.

The larger dimension of the TiMMCs and Ti6Al4V-MMCs reinforced with 0.1% and 0.5 mass% of boron (fabricated via HP at 900ºC for 1h) allow the measurement of the mechanical properties (tensile and bending properties) of these specimens.

The mechanical tests carried out at different temperature show the behaviour of the composites at these temperatures (20º, 250º and 450ºC). At room temperature, the results show lower mechanical properties (tensile strength and ε of these composites.

In the next Figure 5-1 and Figure 5-2, the most representative mechanical properties (tensile strength) of these specimens are compared.

Depending on the testing temperature, the composite made from CPTi(2) and Ti6Al4V(1) powders show different mechanical properties. Also the influence of the boron concentration is observed on the tensile properties. Higher ultimate tensile strength is observed at room temperature for the pure matrices. When increasing the testing temperature up to 250ºC, the composites with 0.5 mass% of boron offer better properties than the pure matrices tested at the same temperature (250ºC). This happens for both types of composite matrices. Thus, depending on the testing condition/application condition the behaviour of the composite are better than the pure matrices. Comparing the elongation, the titanium matrix (without reinforcement) presents the better ε (%) when testing the specimen at 250ºC ($\varepsilon = 22.50\%$), in contrast the matrix from Ti6Al4V (1) does not present such elongation at the same testing temperature. Carrying out the tensile test at 450ºC, specimens from Ti6Al4V(1) exhibit better elongation properties than the pure matrix. The comparison of the composites from CPTi(2) matrix and Ti6Al4V(1) matrix, respectively, is represented in the next Figure 5-1 and Figure 5-2.

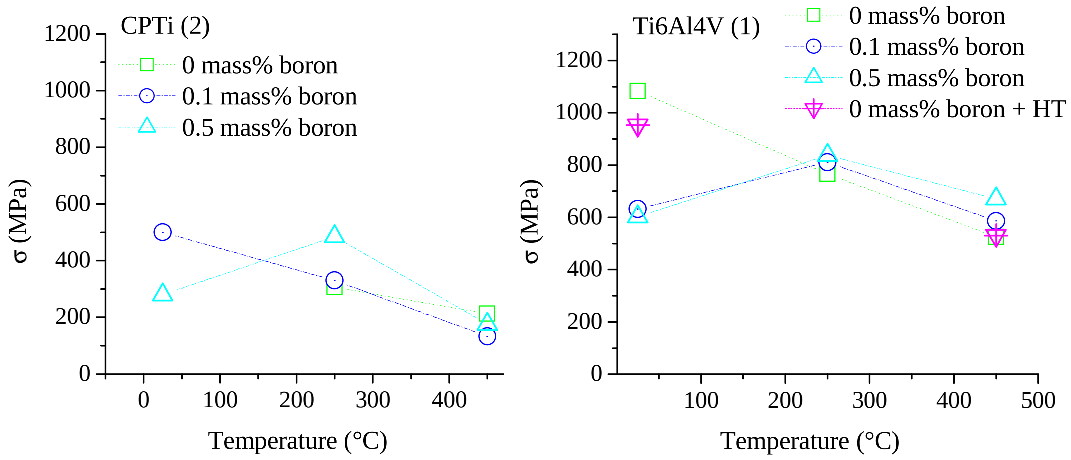

Figure 5-1. UTS vs. the testing temperature (20º, 250º and 450ºC) for different boron content sof the TiMMCs and Ti6Al4V-MMCs.

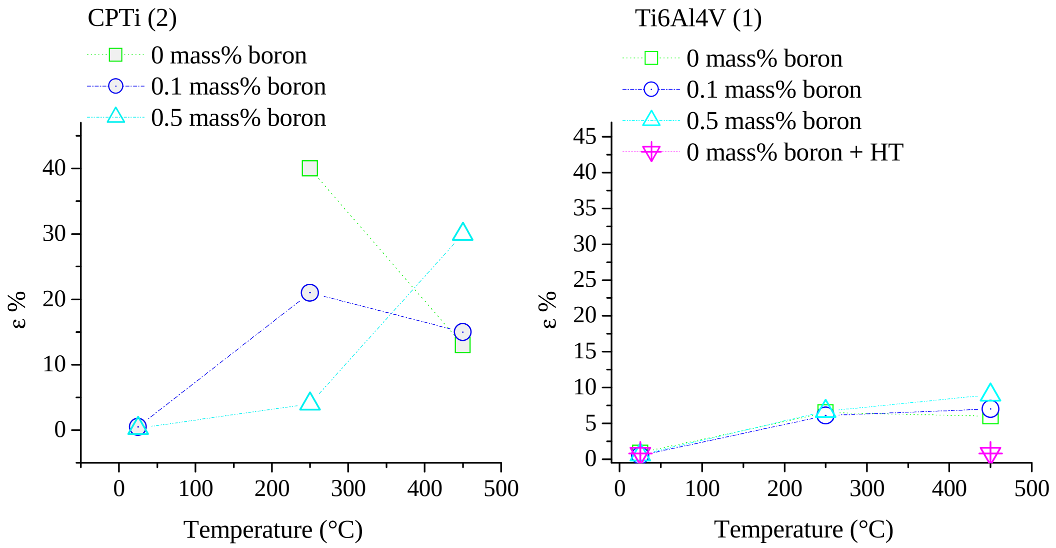

Figure 5-2. Elongation vs. the testing temperature (20º, 250º and 450ºC) for different boron content sof the TiMMCs and Ti6Al4V-MMCs.

The results, after the tensile test for the TiMMCs at 250ºC, show excellent elongation values for the pure CPTi matrix (>20%) and for the reinforced matrix with 0.1 mass% boron (>15%). At 450ºC, the elongation of these two materials, pure CPTi and reinforced matrix with boron 0.1mass%, decreases. The lowest elongation for the

TiMMCs is observed at room temperature. These results are similar as previous results reported by Zwicker [18]. They are shown in the next illustration.

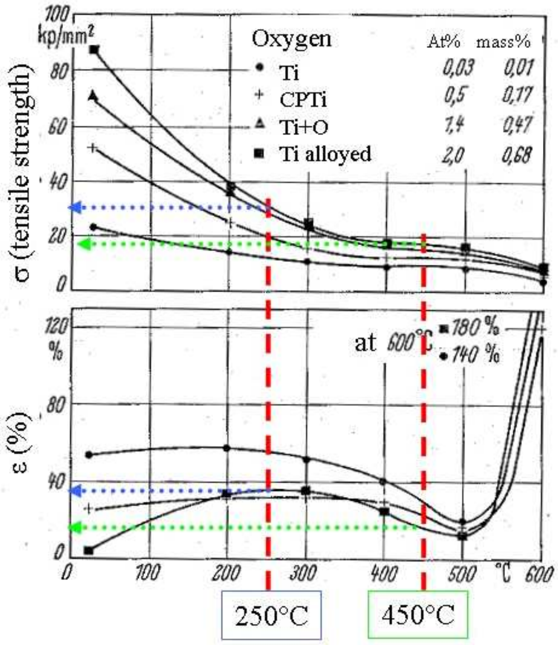

Figure 5-3. Influence of the oxygen content and the temperature on the tesile strengh and elongation of titanium [18].

Concluding, the microstructural study shows the differences between the matrices and the morphology of the reinforcement materials. The porosity related to the boron particles is always present in all the composites reinforced with these particles (see in Figure 5-4).

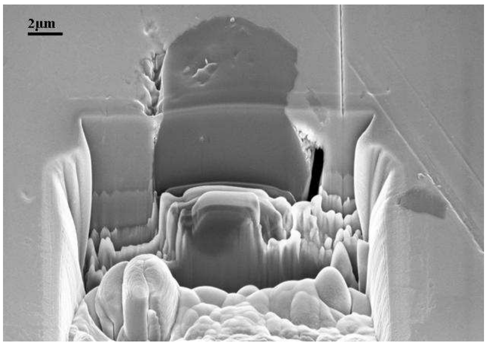

Figure 5-4. FIB image of a nano/micro boron particle in the Ti6Al4V matrix. (HP at 900°C for 2h

By EDAX analysis, impurities of magnesium (Mg) on the boron particles could be detected. Concluding, in general for all the TiMMCs and Ti6Al4V tested, the mechanical properties at higher temperature are better for the composites than for the pure matrix. The high oxygen content of the composites is related to the addition of the boron particles. The incorporation of boron particles implies the incorporation of Mg impurities to the final composite. Finally, good dispersion of boron particles in the metallic matrix is a positive result observed for the composites. This can be observed for example in the Figure 4-35.

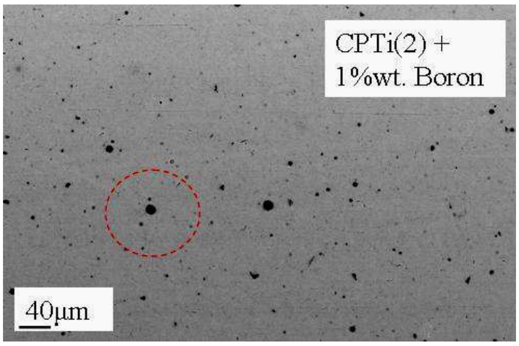

Figure 4-42. Boron particle in a CPTi (2) matrix. TiMMCs (with 1mass% of nano/micro-boron particles) hot consolidated at 850ºC for 1h. The SEM images are taken by the BSE detector.

Recommendation: in general boron addition, especially micro/nano boron, has a marked effect on the microstructure increasing the porosity. In further works, TiB_2 and B particles should present lower oxygen content. Another recommendation is the use of nano-boron of higher purity (not Mg impurity) for further investigations (if available).

5.1.3 Effect of the carbonaceous reinforcements

The motivation of using carbon nano-fibres and nano-diamonds is always to improve the properties of the matrix. The addition of nano-reinforcement material to a metal matrix is an interesting way to get better composite materials, not only mechanical improvement but also that of further properties such as wear resistance, etc.

The main difficulty of this kind of reinforcements, carbon nano fibres (CNFs) and nano-diamond (NDs) particles, is their tendency to agglomerate in a matrix. Therefore the dispersion plays an important role; even by using intensive dispersion processes clusters and agglomerates are observed in the composites.

Thus, around these clusters some porosity is formed, decreasing the density of the composite material. Therefore with increasing concentration (vol%) of these nano reinforcements (CNFs and NDs), the influence on the densification of the composite is worse. Many agglomerates can cause a higher porosity in the composite.

Comparing both types of reinforcements, the NDs are easier to disperse in comparison to the CNFs. However the nano-diamond particles have higher oxygen content.

Another problem is the reaction between the carbon and the titanium from the matrix during the sintering or the hot pressing processes. By the formation of TiC, the TiMMCs presents higher hardness; however the advantages that the nano-fibres in principle offer as reinforcement are lost (see in Figure 5-5).

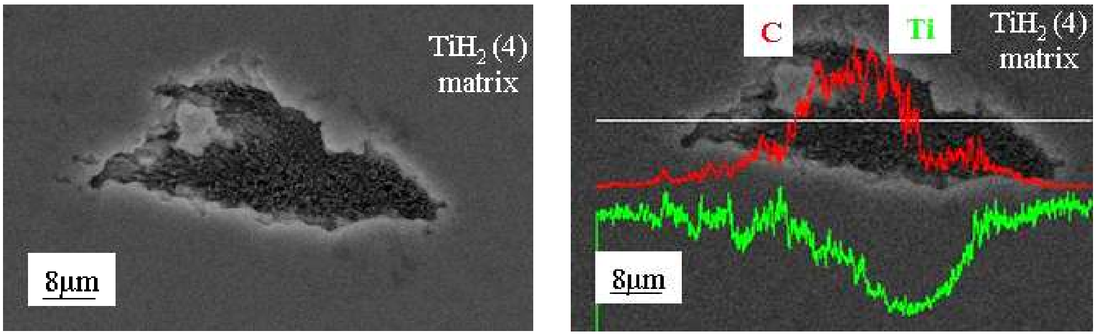

Figure 5-5 SEM image of a CNFs cluster into the TiH$_2$(4) produced via iHP during 5min at 950ºC.

Moreover, the addition of CNFs or NDs can increase the oxygen content of the final composites compared to the original content in the matrix powders, independently of the type of starting matrix powder. This effect is not as strong as for the boron particles. The mechanical properties show the effect of the nanodiamonds on the deformation (%) and flexural strength (MPa) of the specimens. The better properties are observed for the pure matrices. By increasing the sintering temperature, the behaviour of the composites and the matrices become better.

Table 5-1. Summary of the flexural properties of the pure matrix and TiMMCs and Ti6Al4V-MMCs reinforced with 1.8 vol% and sintered for 2h at different temperatures (1250º and 1300ºC).

Matrix	**Sintering at 1250º**		**Sintering at 1300º**	
	σ(MPa) TRS	ε %	σ(MPa)	ε %
CPTi	560	1.62	1228	2.88
CPTi+HT	n.d.	n.d.	866	1.51
Ti6Al4V	392	0.94	1383	2.32
Ti64+HT	n.d.	n.d.	927	1.78
CPTi+ND (1.8%vol.)	409	1.68	783	0.82
Ti6Al4V+ND (1.8%vol.)	860	1.21	856	127

Furthermore, the ND addition inhibited grain growth up to a certain concentration level (1.8 vol%); above this concentration the appearance of possible agglomerates around the grain boundaries lowers the densification in the composites. In this way, the microstructural evolution is affected significantly by this addition of NDs, in particular for the composites from CPTi powder (see in Figure 5-6). The same effect on the microstructure caused by the NDs addition is observed in the composite from Ti6Al4V (1) powder.

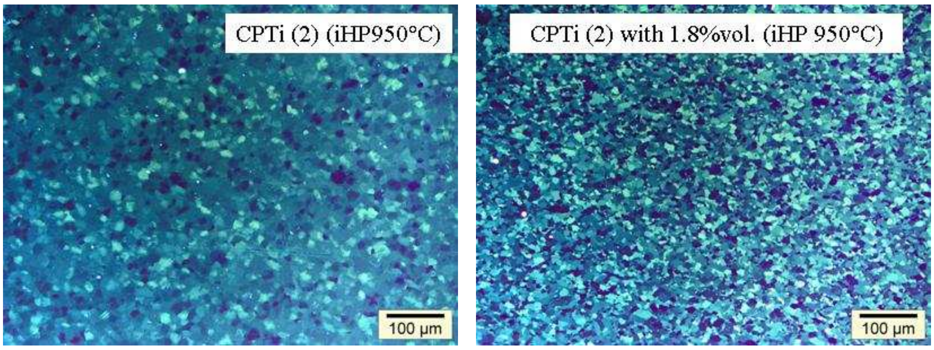

Figure 5-6. Microstructure of pure titanium matrix and TiMMC reinforced with 1.8 vol% of NDs. Both specimens produced simultaneously via iHP at 950ºC for 15min.

Recommendation: CNFs are presented in several publications as very good reinforcement material; however the problem of dispersion in the metal matrix limits their use for TiMMCs. The many agglomerations cause an adverse impact in the porosity of the composite materials (decreased densification). Before using CNFs as reinforcement material, their dispersion has to be improved.

On another side the nano-diamond particles are an interesting reinforcement material for TiMMCs. However, at higher concentration of nano-diamond particles, the effect of particle boundary decoration is more marked. This effect decreases the mechanical properties of the composite. During sintering at 1250º and 1300º the admixed nano-diamond particles reacted with the Ti from the matrix ($C+Ti\rightarrow TiC$). The phase TiC improves the strength of the matrix. However this is an expensive way to obtain a reinforced titanium matrix. The addition of other carbonaceous particle material (i.e, graphite) would be a cheaper and simply way to achieve the same reinforced titanium matrix. Nano-diamond particles are an expensive reinforcement material, for that reason it is recommendable to use consolidation temperatures below 900ºC. Then the optimal manufacturing processes will be hot pressing methods.

5.2 Influence of the manufacturing process

The manufacturing process employed for the production of a composite is directly related to its final properties. Three powder metallurgical techniques have been used here for the production of different composite materials. At the same time, each technique has to be optimised according to the type of composite and its final requirements. The variation and optimisation of the different processing conditions is an important task. Thus, the influence of the manufacturing processes on the final properties of the composites plays an essential role for producing composite materials with better behaviour.

5.2.1 Cold pressing and sintering technique

- *Compaction pressure*

The pressure for the cold compaction has an insignificant influence on the final properties such as the hardness and density of the final specimens.

At the beginning of the experimental work, six different titanium based powder were compacted at different mechanical pressures. In particular, the $TiH_2(6)$ was cold pressed at three compaction pressures and the other five titanium based powder were compacted at two. There was not any influence of the mechanical pressure on the density and hardness of the titanium specimens. Only the microstructure of the sintered samples shows slightly less porosity. For that reason in this work the higher values of the pressure (560 MPa) is used.

- *Handling of the powder*

The compacts made from powder which was handled in air or argon, respectively, did not show any difference after the sintering process e.g. in their oxygen content. Therefore the handling of the powder in this work was generally carried out in air.

- *Sintering setup*

The first experiments were carried out in order to optimise the sintering stage. The aim of this first work was to find an optimum sintering setup which allows the reduction of the oxygen content in the compacts. This setup consists of a titanium container filled with titanium sponge as getter. Then, using this suitable sintering set up, the oxygen content in the final compacts does not increase. This is a positive effect achieved on the final mechanical properties.

Even using that optimal sintering set up, if the starting powder presents high oxygen content ($TiH_2(6)$ has 1.47 mass% oxygen), the final content of oxygen in the specimens cannot be reduced totally. Because of that, in the rest of the work for the sintering process the most suitable sintering assembly was employed.

Furthermore, the powder with the highest oxygen content ($TiH_2(6)$ has 1.47 mass% oxygen) was not used further.

- *Sintering temperature*

The results of hardness and density after the sintering process at 1200ºC (used only for titanium compacts), 1250ºC (used only for composites reinforced with NDs particles) and 1300ºC are compared. The values of hardness and density are better for specimens sintered at 1300ºC. Therefore, to fabricate titanium compacts and titanium based composites the optimum sintering temperature is 1300ºC.

- *Sintering time*

The temperature and time are closely related to the hardness and density values. The same effect of the temperature on these properties of the compacts and composites is also observed for the sintering time.

The short sintering time tested was 1h and the longer one was 2h.

After the sintering for 1h at 1200ºC, the microstructural study of the compacts revealed high porosity. Even at 1300ºC several pores were detected, hence the time was increased to 2h.

Recommendation: There is some influence of the lubricant on the oxygen content of the final specimens. For that reason, excessive use of lubricant for the cold pressing process should be avoided.

Additionally, the suitable sintering temperature for titanium specimens is 1300ºC. However, for reinforced titanium matrix with carbonaceous materials as CNFs ans NDs should not be sintered at this temperature if the reaction between Ti and C is not desirable. In case where the TiC would be desired, it can be obtained just by mixing titanium based powder with some cheaper carbonaceous materials and sintered at this temperature (1300º). Time depends on the volume of the samples (shorter time ,approx. 1h, will be sufficient for smaller samples)

5.2.2 Conventional hot pressing technique

Many factors have to be considered in this process, the hot pressing parameters (temperature and time) applied as well as the graphite die used, are the most important. Other factors, such as the mechanical pressure, the heating rate and the atmosphere, i.e. high vacuum, were the same for all the experimental tests.

- *Hot pressing die*

After the production of specimens from the same matrix and mixture powder, by the use of two types of graphite dies (smaller die: 13.5x13.5mm^2; larger die: 100mmØ), different values of the properties (hardness (HV10) and relative density (%)) and oxygen content (mass%) are found.

Using the die with twelve cavities (dimension of one cavity is 13.5x13.5mm^2), the advantage that this die offers was the production of composites with different reinforcement concentration in one singly run and thus at the same nominal parameters.. However due to the smaller dimension of the cavity, the powder was more in contact to the walls of the cavity. It was always lined with a thin graphite foil coated with boron nitride (BN). The probability for contamination of smaller samples is higher. This problem could be solved using the larger dies (100mm and 65mm Ø).

Moreover, the use of a larger graphite die was necessary for the production of specimens to test their mechanical properties.

Also the mechanical pressure during hot pressing was not exactly the same for the samples produced in the larger dies and the smaller in the twelve cavities. This factor affects also the final properties of the specimens. Furthermore, if the filling of the 12 cavities was not exactly adjusted for the different powder mixes – which is extremely difficult -, different effective pressures could be expected, higher compacts taking a larger fraction of the total load (see also below).

- *Hot pressing temperature*

The increase of the hot pressing temperature involves usually an improvement of the density and hardness properties of the samples. There is also some exception for the hardness values.

Then, the main effect of the temperature is observed during the microstructural study and it affects the densification of the composites. The range of temperatures tested is from 800º to 900ºC. At 800ºC (only used for composites reinforced with boron particles), the porosity in the specimens produced at this temperature was quite pronounced. For the same starting materials, at 850ºC the densification of the final samples increased. In the case of the composites reinforced by carbonaceous reinforcements, the phase diagram for Ti-C presents at 920º the reaction temperature between titanium and carbon. The carbon comes from the reinforcement materials. Thus, to avoid the reaction between the titanium matrix and the C-reinforcements the hot pressing temperature has to be below this level of 920ºC.

- *Holding HP time*

Concluding the influence factor of the hot pressing process on the final properties of the specimens produced, the hot pressing time is reported. In the first production of composites via hot pressing, the graphite die with the twelve cavities was used. Due to the smaller size of the samples, the holding time required was just 1h. However, the results of the density values were not satisfactory. Consequently for the next production cycles, the holding time was increased. The optimal value of time is 2h.

In general, there is a close relationship between the size of the HP die and the holding time, such as longer holding time for larger die.

Recommendation: Larger graphite die is better to the smaller in order to characterise the samples (on larger samples, mechanical properties can be measured).

There is a problem for the twelve cavities die related to load distribution (see Figure 5-7. If the cavities are not filled with the same type of powder, each powder batch – and thus the according graphite punch - has different height. Hence, each powder receives different load because of the different punches height. This is represented in the next Figure 5-7. The main recommendation is to use the same powder and filling height for 12-cavities dies always.

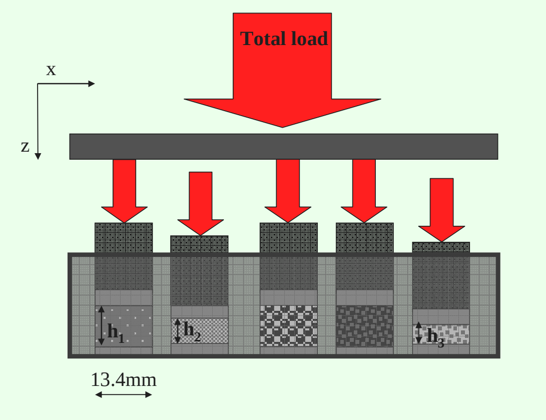

Figure 5-7. Load distribution for 12-cavities graphite die by hot pressing technique.

5.2.3 Inductive hot pressing technique

The inductive hot pressing process offers short cycle time and high heating rate as the advantage in comparison to the conventional hot pressing process. However this iHP technique has important restrictions of the geometry of the die used. The smaller dimensions of the heating chamber do not allow the use of larger dies.

However, the iHP temperature, the holding time and the heating rate play an important role on the final properties of the samples.

- *Inductive hot pressing temperature*

Possibly, the temperature of the iHP process is the most important parameter to vary. The effect of its changes can be clearly observed from the properties of the samples. The hardness and density values as well as the microstructure of the samples are affected by changes of the iHPT.

Additionally, variations of the iHP temperature involve variations of the impurity content (Oxygen, hydrogen and nitrogen). In general, when increasing the temperature the oxygen and hydrogen contents are lower.

Important differences are seen for the specimens from TiH_2 matrix powder. The increase of the iHP temperature implies noticeable changes of the microstructure, such as the formation of martensitic microstructure. Due to the high cooling rate, the formation of this structure can be originated.

Also, hydrogen as impurity (from the starting powder) can contribute to the formation of this martensitic microstructure as well as to the higher hardness values.

In general, for all the samples produced via iHP, the density and hardness are positively affected by the increase of the temperature.

However, the same problem as for HP, i.e. the temperature to produce composites with the carbonaceous reinforcements (CNFs and NDs), is also present in iHP process. The reaction between the titanium from the matrix and the different types of reinforcement has to be avoided. As advantage, due to the short cycle time, higher temperature than 920ºC (reaction temperature between Ti-C) can be tested.

- *Inductive hot pressing time*

The time used normally for the iHP tests was 15 min, although 5 min was also tested for a few samples. The oxygen content of the samples produced via iHP with a holding time of 5 min were at higher levels.

This reduction of the time to 5 min was insufficient to eliminate the hydrogen of the starting powder in the matrix. Thus, the hydrogen concentration in the samples from TiH_2 was higher. Also higher oxygen content was analysed for these specimens.

The advantage of this 5 min is considerable reduction of cycle time to produce a composite material; however the impurity content was too much to achieve good levels of mechanical properties. For that reason, the time used for iHP was 15min.

- *Inductive hot pressing heating rate / cooling rate*

Two heating rates, 10 K/min and 50 K/min were tested for the fabrication of titanium specimens.

Using a heating rate of 10 K/min to 800ºC, there is an improvement of the densification comparing to the values after the heating rate of 50 K/min (at 800ºC). Under these conditions, oxygen and hydrogen content for the samples produced using 10 K/min are higher than using 50 K/min.

Concluding, the main advantage of this iHP technique is the short cycle time and it is related to the use of high heating rates. Therefore for all the rest of the iHP tests, the heating rate was fixed to 50 K/min.

Recommendation: The manufacturing of TiMMCs from TiH_2 matrix powder is not advised because of the short processing time. Residual hydrogen is observed in the composites from this matrix powder (TiH_2(4)). Due to this and additional impurities such as oxygen and nitrogen, the final composites cannot present better properties.

By increasing the temperature of the iHP process, the densification of the composites are better; however reaction between the reinforcement (i.e, nano-diamonds particles) and the titanium of the matrix can take place.

6 General conclusions

Considering the starting materials (Ti base powder and reinforcing phase)

- The selection of an adequate starting matrix powder for the development of a composite is the first step to obtain the desired mechanical properties of this composite. The influence of low impurity levels is well discernible from the final properties of the compacts prepared from the different titanium starting powders.
- Compacts prepared from TiH_2 matrix powder exhibited higher oxygen, nitrogen and hydrogen content and consequently higher hardness values in comparison to the composites from CPTi matrix powder.
- The addition of reinforcement in defined concentration differently affects the mechanical properties of the composite, depending on the content. The particle size and impurity of the reinforcement particles and fibres have important consequences on the final properties and microstructure of the TiMMCs.
- There is a strong influence of the addition of reinforcement with high oxygen content on the final TiMMCs, increasing its oxygen content.
- The addition of the boron and TiB_2 reinforcements increases the hardness of the TiMMCs in spite of the decrease of the density of the specimens up to certain contents.
- Outstanding mechanical properties are observed for the composites reinforced with boron particles at 450°C for the composites from Ti6Al4V matrix and at 250°C for the composites from CPTi matrix. The reason for this surprising behaviour is however not yet clear.

Considering the manufacturing processes

- Applying a suitable sintering procedure lowers the oxygen content in the final compacts, thus having a positive effect on the final mechanical properties.
- In general, by increasing the temperature of the manufacturing process, the density and hardness of the specimens increase, and the oxygen content is slightly reduced.
- The increase of the holding time resulted in an increase of the density for all the composites. However, such longer time at higher temperature could promote reaction between the titanium matrix and the reinforcements.
- The use of different hot pressing dies caused significant differences of the final properties between composites from the same powder mixes.
- The mechanical pressure affected principally the densification of the green samples produced via cold pressing, but not really of the sintered ones.
- The good dispersion of the reinforcement materials, in particular CNFs, is

essential for improving the densification of the composites. However, eliminating the clusters present in the CNFs was not achieve because of the difficulty to disperse the CNFs.

As general conclusion for the manufacturing of a TiMMCs and Ti6Al4V-MMCs by powder metallurgy processing, the starting powders (for each matrix type) with lower impurity content are optimum to be used as matrix powder.

In this work, the most promising powder is the CPTi(2) to fabricate TiMMCs and Ti6Al4V(1) to Ti6Al4V-MMCs. Thus, the oxygen concentration in the composite will be lower. It means, the mechanical properties will be better. Each powder metallurgical route present advantages and disadvantages, however the use of one or the other technique depends on the composite requirements.

References

1. Polmear, I.J., *Titanium alloys*, in *Light Alloys (Fourth Edition)*. 2005, Butterworth-Heinemann: Oxford. p. 299-365.
2. Lütjering, G. and J.C. Williams, *Titanium*. 2nd. ed. Engineering materials and processes 2007, Berlin: Springer. 379.
3. Peters, M. and C. Leyens, *Titan und Titanlegierungen*, ed. WILEY-VCH. 2002. 16-22.
4. Campbell, F.C., *Titanium*, in *Manufacturing Technology for Aerospace Structural Materials*. 2006, Elsevier Science: Oxford. p. 119-174.
5. Leyens, C. and M. Peters, eds. *Titanium and Titanium Alloys*. 2003, Wiley-VCH GmbH & Co. KGaA: Weinheim. 513.
6. Danninger, H., et al., *Technologie der metallischen Sonderwerkstoffe(Technology of Less-CommonMetals)*. 2006, Institut für Chemische Technologien und Analytik Technische Universität WienSommersemester: Vienna.
7. Sibum, H., et al., eds. *Titanium, Titanium Alloys, and Titanium Compounds*. 2005, Wiley-VCH Verlag GmbH & Co. KGaA: Weinheim, Germany.
8. Szkliniarz, W. and G. Smolka, *Analysis of volume effects of phase transformation in titanium alloys.* Journal of Materials Processing Technology, 1995. **53**(1-2): p. 413-422.
9. Seward, G.G.E., et al., *In situ SEM-EBSD observations of the hcp to bcc phase transformation in commercially pure titanium.* Acta Materialia, 2004. **52**(4): p. 821-832.
10. U.S. Department of Transportation, F.A.A., *Metallic Materials Properties Development and Standardization (MMPDS)*. 2003, Office of Aviation Research: Washington, D.C. p. 5.1-5.145.
11. Boyer, R. and S. Lampman, *Material Properties Handbook; Titanium Alloys*, ed. A. International. 2004, O.H., USA. 1176.
12. Peters, M., C. Leyens, and J. Kumpfert, *Titan und Titanlegierungen*. 1996, Köln, Germany: Werkstoff-Informationsgesellschaft 227
13. Jaffee, R.I., *The Physical Metallurgy of Titanium Alloys.* Progress in Metal Physics, 1958. **7**: p. 65-163.
14. Jaffee, R.I., H.R. Ogden, and D.J. Maykuth, *Alloys of Titanium with Carbon, Oxygen, and Nitrogen.* Transactions of the American Institute of Mining and Metallurgical Engineers, 1950. **188**(10): p. 1261-1266.
15. Teter, D.F., I.M. Robertson, and H.K. Birnbaum, *The effects of hydrogen on the deformation and fracture of [beta]-titanium.* Acta Materialia, 2001. **49**(20): p. 4313-4323.
16. Briant, C.L., Z.F. Wang, and N. Chollocoop, *Hydrogen embrittlement of commercial purity titanium.* Corrosion Science, 2002. **44**(8): p. 1875-1888.
17. Smith, W.F., *Fundamentos de la ciencia e ingeniería de materiales*. 3rd ed, ed. S.A.U. McGraw-Hill Interamericana de España. 1998, Madrid. 717.
18. Zwicker, U., *Titan und Titanlegierungen*. 1974, Berlin, Germany: Springer. 717.
19. Conrad, H., *Effect of Interstitial Solutes on the Strengths and Ductility of Titanium.* Progres in Materials Science 1981. **26** p. 123–403
20. Lefebvre, L.P. and E. Baril, *Effect of Oxygen Concentration and Distribution on the Compression Properties on Titanium Foams.* Advanced Engineering Materials, 2008. **10**(9): p. 868-876.
21. German, R.M., *Powder Metallurgy & Particulate Materials Processing*, ed. MPIF. 2005, New Jersy. 522.

22. Danninger, H. and C. Gierl, *Pulvermetallurgie und Sinterwerkstoffe, Teil I (Pulvermetallurgische Verfahren)*. 2006, Vienna University of Technology: Vienna.
23. Danninger, H. and C. Gierl, *Pulvermetallurgie und Sinterwerkstoffe, Teil II (Werkstoffe)*. 2007, Vienna University of Technology: Vienna.
24. McGraw-Hill, ed. *McGraw-Hill Encyclopedia of Science and Technology*. 8th. ed. Vol. 14: NY, USA. 273.
25. Pease, L.F. and W.G. West, *Fundametals of Powders Metallurgy*. 2002, USA: MPIFl, Metal Powder Industry Federation.
26. Schatt, W. and K.P. Wieters, *Powder Metallurgy, Procesing and Materials*, ed. EPMA. 1997, Düsseldorf: VDI-Verlag GmbH.
27. Cocks, A.C.F., *Constitutive modelling of powder compaction and sintering*. Progress in Materials Science, 2001. **46**(3-4): p. 201-229.
28. EPMA, *Design for Powder Metallurgy*, in *PM Learning Center*. 2008, EMPA.
29. Skoglund, P., M. Kejzelman, and I. Hauer, *High density PM components by high velocity compaction*, H. AB, Editor, Höganäs AB: Sweden.
30. Hydropulsor-EPM. *High Velocity Compaction*. 2009 [cited; Available from: http://www.hydropulsor-epm.com/english/hvc_compaction.htm.
31. German, R.M. and A. Bose, *Injection Molding of Metals and Ceramics*. 1997: MPIF Publication.
32. Milberg, J. and M. Sigl, *Electron beam sintering of metal powder*. Production Engineering, 2008. **2**(2): p. 117-122.
33. ARCAM. *EBM - Rapid-manufacturing in metal*. 2008 [cited; Available from: http://www.arcam.com/index.asp.
34. Bose, A. and W. Eisen, *Hot Consolidation of Powders and Particles*. 2003, New Jersey: Metal Powder Industries Federation, MPIF.
35. German, R.M., *Sintering theory and practice*. 1996, NY, USA: Wiley-Interscience publication. 550.
36. *ASTM E-1409 Standard Test Method for determination of oxygen and nitrogen in titanium and titanium alloys by the inert gas fusion technique*. 2005, ASTM International: USA.
37. Torralba-Castelló, J.M. and M. Campos-Gómez, *Technología de Polvos*, in *Open course ware*. 2008, Dpto de Ing. de Materiales e Ing. Química, Universidad Carlos III de Madrid: Madrid,Spain.
38. Cantor, B., F. Dunne, and I. Stone, *Metal and Ceramic Matrix Composites*. Materials Science and Engineering. 2004, UK: Inst. of Physics,Publishing Ltd. 419.
39. Chawala, N. and K.K. Chawla, *Metal Matrix Composites*. 2006, NY, USA: Springer. 65-112.
40. Froes, F., et al., *Titanium in the family automobile: The cost challenge*. JOM Journal of the Minerals, Metals and Materials Society, 2004. **56**(2): p. 40-44.
41. Froes, F.H., et al., *Titanium Alloys: Properties and Applications*, in *Encyclopedia of Materials: Science and Technology*. 2001, Elsevier: Oxford. p. 9367-9369.
42. Liu, Y., et al., *Design of powder metallurgy titanium alloys and composites*. Materials Science and Engineering: A, 2006. **418**(1-2): p. 25-35.
43. Hurless, B.E. and F.H. Froes, eds. *Lowering the cost of Titanium*. The AMPTIAC Quarterly. Vol. 6, Depertament of Defense USA. 3-9.
44. Moll, J.H. and C.F. Yolton, *Production of Titanium Powder*. ASM Handbook, ed. C.R. Center. Vol. 7. 1998, USA: ASM International.

45. Moll, J., *Utilization of gas-atomized titanium and titanium-aluminide powder*. JOM Journal of the Minerals, Metals and Materials Society, 2000. **52**(5): p. 32-34.
46. Froes, F., et al., *The technologies of titanium powder metallurgy*. JOM Journal of the Minerals, Metals and Materials Society, 2004. **56**(11): p. 46-48.
47. Peter, W.H., et al. *Non-melt processing of "Low-Cost", armstrong titanium and titanium alloy powders*. in *Light Metals Technology Conference* 2007. Orlando, FL, USA.
48. Esteban, P.G., et al., *Low-cost titanium alloys? Iron may hold the answers.* Metal Powder Report, 2008. **63**(4): p. 24-27.
49. Campbell, F.C., *Metal Matrix Composites*, in *Manufacturing Technology for Aerospace Structural Materials*. 2006, Elsevier Science: Oxford. p. 419-457.
50. Eriksson, M. and M. Andersson, *Titanium-hydroxyapatite composite biomaterial for dental implants.* Powder Metallurgy, 2006. **49**: p. 70-77.
51. Vandermark, R., *Opportunities for the titanium industry in bicycles and wheelchairs.* JOM Journal of the Minerals, Metals and Materials Society, 1997. **49**(6): p. 24-27.
52. Tjong, S.C. and Z.Y. Ma, *Microstructural and mechanical characteristics of in situ metal matrix composites.* Materials Science and Engineering: R: Reports, 2000. **29**(3-4): p. 49-113.
53. Ma, Z.Y., S.C. Tjong, and L. Gen, *In-situ Ti-TiB metal-matrix composite prepared by a reactive pressing process.* Scripta Materialia, 2000. **42**(4): p. 367-373.
54. Gorsse, S., J.P. Chaminade, and Y. Le Petitcorps, *In situ preparation of titanium base composites reinforced by TiB single crystals using a powder metallurgy technique.* Composites Part A: Applied Science and Manufacturing, 1998. **29**(9-10): p. 1229-1234.
55. Yolton, C.F. and J.H. Moll, *Evaluation of discontinuously reinforced Ti-6Al-4V composite*, C. Research., Editor, Crucible Materials Corporation: Pittsburgh, PA15205-1022. p. 1-8.
56. Tjong, S.C. and Y.-W. Mai, *Processing-structure-property aspects of particulate- and whisker-reinforced titanium matrix composites.* Composites Science and Technology, 2008. **68**(3-4): p. 583-601.
57. Munro, R.G., *Material Properties of Titanium Diboride.* Journal of Research of the National Institute of Standards and Technology, 2000. **105**(5): p. 709-720.
58. Ravi Chandran, K. and D. Miracle, *Titanium-boron alloys and composites: Processing, properties, and applications.* JOM Journal of the Minerals, Metals and Materials Society, 2004. **56**(5): p. 32-33.
59. Arvieu, C., J.P. Manaud, and J.M. Quenisset, *Interaction between titanium and carbon at moderate temperatures.* Journal of Alloys and Compounds, 2004. **368**(1-2): p. 116-122.
60. Ni, D.R., et al., *Fabrication and tensile properties of in situ TiBw and TiCp hybrid-reinforced titanium matrix composites based on Ti-B4C-C.* Materials Science and Engineering: A, 2008. **478**(1-2): p. 291-296.
61. Zhang, R., J. Kruszewski, and J. Lo. *Microstructure and mechanical properties of TiC particulates reinforced titanium matrix composite made by MIM.* in *Proceedings of the Light Metals Technology Conference*. 2007. Canada.
62. Alman, D.E. and J.A. Hawk, *The abrasive wear of sintered titanium matrix-ceramic particle reinforced composites.* Wear, 1999. **225-229**(Part 1): p. 629-639.

63. Lu, J., et al., *In situ preparation of (TiB + TiC + Nd2O3)/Ti composites by powder metallurgy.* Journal of Alloys and Compounds. **In Press, Corrected Proof**.
64. Dabhade, V.V., T.R.R. Mohan, and P. Ramakrishnan, *Sintering behavior of titanium-titanium nitride nanocomposite powders.* Journal of Alloys and Compounds, 2008. **453**(1-2): p. 215-221.
65. Poletti, C., et al., *Production of titanium matrix composites reinforced with SiC particles.* Composites Science and Technology, 2008. **68**(9): p. 2171-2177.
66. Sepúlveda, R. and F. Arenas, *TiC-VC-Co: a study on its sintering and microstructure.* International Journal of Refractory Metals and Hard Materials, 2001. **19**(4-6): p. 389-396.
67. Miyoshi, K., et al., *Wear behavior of low-cost, lightweight TiC/Ti-6Al-4V composite under fretting: Effectiveness of solid-film lubricant counterparts.* Tribology International, 2008. **41**(1): p. 24-33.
68. Monticelli, C., F. Zucchi, and A. Tampieri, *Triboelectrochemical behaviour of a Si3N4-TiN ceramic composite and a titanium alloy commonly used in biomedical applications.* Wear. **In Press, Corrected Proof**.
69. Geng, L., et al., *Hybrid effect of TiBw and TiCp on tensile properties of in situ titanium matrix composites.* Journal of Alloys and Compounds, 2008. **463**(1-2): p. 488-492.
70. Panda, K. and K. Ravi Chandran, *Synthesis of ductile titanium-titanium boride (Ti-TiB) composites with a beta-titanium matrix: The nature of TiB formation and composite properties.* Metallurgical and Materials Transactions A, 2003. **34**(6): p. 1371-1385.
71. Morsi, K., et al., *Processing of titanium-titanium boride dual matrix composites.* Journal of Materials Processing Technology, 2008. **196**(1-3): p. 236-242.
72. Gorsse, S., et al., *Investigation of the Young's modulus of TiB needles in situ produced in titanium matrix composite.* Materials Science and Engineering A, 2003. **340**(1-2): p. 80-87.
73. Giannopoulos, G.I., D. Karagiannis, and N.K. Anifantis, *Micromechanical modeling of mechanical behavior of Ti-6Al-4V/TiB composites using FEM analysis.* Computational Materials Science, 2007. **39**(2): p. 437-445.
74. Thian, E.S., et al., *Ti-6A1-4V/HA composite feedstock for injection molding.* Materials Letters, 2002. **56**(4): p. 522-532.
75. Poletti, C. and S. Kremmer, *Hot formability of particle reinforced Ti-alloys,* in *European conference on Composite Materials*. 2006: Biarritz, France.
76. Cowen, C.J. and C.J. Boehlert, *Microstructure, Tensile, and Creep Behavior of Boron-Modified Ti-15Al-33Nb (at.%).* Metallurgical and Materials Transactions A, 2008. **39**(2): p. 279-293.
77. Godfrey, T.M.T., et al., *Microstructure and tensile properties of mechanically alloyed Ti-6A1-4V with boron additions.* Materials Science and Engineering A, 2000. **282**(1-2): p. 240-250.
78. Kuzumaki, T., et al., *Mechanical Characteristics and Preparation of Carbon Nanotube Fiber-Reinforced Ti Composite.* 2000. **2**(7): p. 416-418.
79. Even, C., C. Arvieu, and J.M. Quenisset, *Powder route processing of carbon fibres reinforced titanium matrix composites.* Composites Science and Technology, 2008. **68**(6): p. 1273-1281.
80. Carreño-Morelli, E., et al. *Carbon nanotube reinforced metal matrix composites*. in *EURO PM2003, European Conference on Powder Metallurgy*. 2003. Valencia, Spain: EPMA.

81. Novikov, N., et al., *Quality rating of a metal matrix-diamondcomposite from its thermal conductivity and electric resistance.* Mechanics of Composite Materials, 2006. **42**(3): p. 253-262.
82. Hanada, K., et al., *Fabrication of Ti/cluster diamond/TiC in situ composites.* Journal of Materials Processing Technology, 2003. **139**(1-3): p. 362-367.
83. Osswald, S., et al., *Increase of nanodiamond crystal size by selective oxidation.* Diamond and Related Materials, 2008. **17**(7-10): p. 1122-1126.
84. Froes, F.H., O.N. Senkov, and J.I. Qazi. *Hydrogen as temporary alloying element in titanium alloys*. in *High Performance P/M Components*. 2002. Coimbra, Portugal.
85. Eliezer, D., et al., *Positive effects of hydrogen in metals.* Materials Science and Engineering A, 2000. **280**(1): p. 220-224.
86. Bhosle, V., et al., *Dehydrogenation of nanocrystalline* TiH_2 *and comsequent consolidation to form dense Ti.* Metallurgical and materials transactions A, 2003. **34A**.
87. Calea, G., D. Drimer, and C. Ionescu, *Bearbeitbarkeit von Titan und Titanlegierungen.* Zeitschrift für industrielle Fertigung, 1985. **75**(10): p. 616-620.
88. Froes, F.H. *Cost effective synthesis, processing and applications of light-weight metallic materials using a powder approach*. in *High Performance P/M Components*. 2002. Coimbra, Portugal.
89. Cahn, R.W., P. Haasen, and E.J. Kramer, *Materials Science and Technology*. Vol. 13/14. 2005, Weinheim, Germany: WILEY-VCH. 125-127.
90. Park, J., et al., *Forming of near net shapes of Titanium Alloys by blended elemental powder metallurgy*. 1984, Los Angeles, USA: Industrial Heating. 32-35.
91. Froes, F.H. and D. Eylon, *Powder Metallogy of Titanium Alloys-a review.* Powder Metallurgy International, 1985. **17**(4): p. 163-167.
92. Friedman, G., *Titanium PM Gyro Components.* MPR, 1984(5): p. 273-281.
93. Weiss, I., et al., *Effect of isothermal forging on Microstructure and Fatigue behaviour of blended elemental Ti6Al4V powder compacts.* Metallurgical Transactions, 1986. **17A**: p. 549-559.
94. Campos, J.B., et al. *Titanium-Hidroxyapatite sintered composites processing and characterization*. in *PM2004 Powder Metall. World Congress & Exhibition*. 2004. Vienna, Austria.
95. Guden, M., et al., *Compression testing of a sintered Ti6Al4V powder compact for biomedical applications.* Materials Characterization, 2005. **54**(4-5): p. 399-408.
96. Ivasishin, O.M., et al., *Cost-effective blended elemental powder metallurgy of titanium alloys for transportation application*. Key Engineering Materials. Vol. 188. 2000. 55-62.
97. Key-to-Metal, *Casting and Powder Metallurgy Titanium Alloys.* Key to Metals, 2008. **Nonferrous**.
98. Jaffee, R.I. and I.E. Campbell, *The Effect of Oxygen, Nitrogen, and Hydrogen on Iodide Refined Titanium.* Transactions of the American Institute of Mining and Metallurgical Engineers, 1949. **185**(9): p. 646-654.
99. Shackelford, J.F. and W. Alexander, *Titanium Boride (TiB2),* in *CRC Materials Science and Engineering Handbook*. 2001. p. 46, 50.
100. Gauthier, M. and E. Baril, *High-temperature interation of titanium with ceramic materials,* National Research Council Canada: Québec. p. 127-140.

Europass Curriculum Vitae

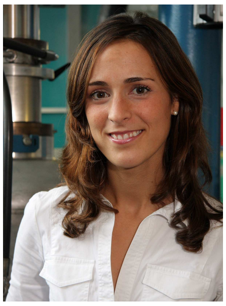

Personal information

First name/ Surnames	**Montealegre Meléndez / Isabel**
Addresses	9/13, Ziegelofengasse, 1050, Vienna, Austria 3/3D, C/Ancha de Gracia, 18002, Granada, Spain
Telephone	+34958263972 (Spain) Mobiles: +436503302962 (Austrian) +34661623296 (Spain)
E-mail	Isabel.montealegre@lycos.com
Nationality	Spanish
Date of birth	22nd August 1980
Gender	Woman

Work experience

Dates	From February 2004
Occupation or position held	PhD student and Chemical Engineer
Main activities and responsibilities	Development of a PhD about Ti based Matrix Composites via PM (from February 2006) Participation and contribution in European projects related to Nano/Micro technology: TASNANO (www.medinfo.dist.unige.it/Tasnano/) y PRONANO (www.pronano.org). Packaging of microchip by the use of ceramic parts produced by PIM. Practices in adsorption of oil on the surface of carbonaceous materials (August to December 2004).
Name and address of employer	Austrian Research Centers GmbH –ARC , (www.arcs.ac.at) Department of Advanced Materials and Aerospace Technologies. PTC (Powder Technology Center) group.
Type of business or sector	Research
Dates	From September 1999 to 2003
Occupation or position held	Conference hostess (1) Chemistry teacher (2)
Main activities and responsibilities	In parallel to the University studies: 1) Conference assistant; 2) Support Teacher of Chemistry.
Name and address of employer	1) Evens azafatas// Alhambra Azafatas, Granada. 2) Cologio Regina Mundi, Granada.
Type of business or sector	1) Evens company; 2) Education

Education and training

Dates	From February 2006 to April 2009
Title of qualification awarded	Dr. tech.
Principal subjects	Development of Titanium based Composites via Powder Metallurgy
Name and type of organisation providing education and training	Institute of Chemical Technologies and Analytics, Vienna University of Technology. Austria.

Dates	May 2007
Title of qualification awarded	Processing of advanced materials (accreditation)
Principal subjects	Composites materials
Name and type of organisation providing education and training	KMM Network of Excellence (www.kmm-noe.org), Imperial College, London, UK.
Dates	September 2005
Title of qualification awarded	Powder Metallurgy summer school (accreditation)
Principal subjects	Training in powder metallurgy
Name and type of organisation providing education and training	EPMA European Powder Metallurgy Association (www.epma.com), Aachen, Germany.
Dates	From 1998 to 2004
Title of qualification awarded	Chemical and environmental Engineer (accreditation)
Principal subjects	Chemical industry and Environmental formation and training. Quality environmental control
Name and type of organisation providing education and training	Centro Mediterráneo (www.ugr.es/~cm) Universidad de Granada, Spain.

Personal skills and competences

Mother tongue **Spanish**

Other language/ Self-assessment	**Understanding**				**Speaking**				**Writing**	
European level (*)	Listening		Reading		Spoken interaction		Spoken production			
English	C2	Mastery	C2	Mastery	C2	Mastery	C2	Mastery	C2	Mastery
German	C2	Mastery	C1	Effective Operational Proficiency	C2	Mastery	C2	Mastery	C1	Effective Operational Proficiency
French	A1	Breakthrough	A2	Waystage	A1	Breakthrough	A2	Waystage	A1	Breakthrough

(*) A1Common European Framework of Reference for Languages

Social skills and competences	Communication skills in multicultural and international contexts, ability to rapid integration into international work environments, gained after long stays in various countries of the EU. Facility to present and defend arguments in English, German and Spanish, demonstrated at various conferences and lectures (Prize for best poster presentation at the conference JUNIOREUROMAT 2008, session 2. (Www.dgm.de/past/2008/junior-euromat)).
Organisational skills and competences	Availability to travel. Ability to establish and work with networks of contacts at the international level, gained from participating in projects with more than ten European partners. Capacity to organize social events gained after working as a Conference assistant.

Additional information

Industrial and academic certificates recommendations available upon request.

Annexes

[1-5] Work presented in different conferences:

1. Montealegre-Meléndez, I. et al., Estimation of an optimizing manufacturing of Ti and Ti-6Al-4V MMCs via Hot Pressing., in Materials Science and Engineering. 2008, DGM: Nürnberg.
2. Montealegre-Meléndez, I. et al. Microstructural and mechanical properties of TiMMCs under the influence of raw powders and processing conditions in Junior Euromat. 2008. Lausanne.
3. Montealegre-Meléndez, I. et al. Influence of the Hot Pressing Parameters on Mechanical and Microstructural Properties of TiMMCs. in Euro PM2008. 2008. Mannheim: EPMA.
4. Montealegre-Meléndez, I. et al. Fabrication of Nano-reinforced TiMMCs via PM, in 17. Symposium: Verbundwerkstoffe und Werkstoffebunde. 2009, DGM: Bayreuth.

Poster presentation:

5. Montealegre-Meléndez, I. et al. Sintering behaviour and properties of TiMMCs. EUROMAT 2008, Nürnberg.